The Role of Gaf-1b in Intracellular Trafficking and Autophagy

---

Dissertation
zur
Erlangung der naturwissenschaftlichen Doktorwürde
(Dr. sc. nat)

vorgelegt der
Mathematisch-naturwissenschaftlichen Fakultät
der
Universität Zürich

von

Tu-My Diep

von

Bern

Promotionskomitee
Prof. Dr. Peter Sonderegger (Vorsitz)
Prof. Dr. Jack Rohrer
Dr. Uwe Konietzko

Zürich 2012

Contents

Summary

Regulated endocytosis and recycling is an essential process for cells to maintain their function and retain the composition of the plasma membrane. Recycling is involved in several cellular processes such as cell adhesion and junction formation, cell migration, cytokinesis, morphogenesis, cell fusion, cell polarity, signal transduction, nutrient uptake, learning and memory. Another important process is autophagy. This plays an essential role as a physiological system for cellular homeostasis. Many neurodegenerative diseases, such as Alzheimer's disease, Parkinson's disease or Huntington's disease, are linked to defective autophagy due to the inability to clear aggregates of mutated toxic proteins. The understanding and treatment of such diseases relies on detailed knowledge of the molecular machinery that governs and controls autophagy.

Calsyntenin-1 is a neuronal type-1 transmembrane protein of the cadherin superfamily found at postsynaptic sites in the adult mouse brain. We recently showed that amyloid precursor protein (APP) exits the *trans*-golgi network (TGN) in association with calsyntenin-1 in tubulovesicular organelles in a kinesin-1-dependent manner and that these vesicles are transported anterogradely along axons. Additionally, we found axons contained at least two distinct, non-overlapping calsyntenin-1-containing transport packages, one is characterized by the presence of APP and early-endosomal markers, the other with recycling-endosomal markers. Organelle immunoisolation and biochemical approaches indicate that calsyntenin-1 provide a protective mechanism for axonal transport of APP. Recently, Gaf-1b, a splice variant of the Rab11-interacting protein Rip11, was identified as a novel interaction partner of calsyntenin-1. Here we characterized the interaction and the physiological function of Gaf-1b and calsyntenin-1. Mutational studies showed that Gaf-1b specifically interacts with the C-terminus of calsyntenin-1 through its C2 domain. We suggested that Gaf-1b is C-terminally bound to membranes through the association with GTP-Rab11, and that the splice insert of Gaf-1b was necessary to facilitate a conformation by which the N-terminus of Gaf-1b can interact with calsyntenin-1. Overexpression of calsyntenin-1 and light chains (KLC1) of kinesin-1 impaired overall ER and Golgi structure and aggregated Gaf-1b in TGN subdomains. In addition, immunoisolation of calsyntenin-1- and Gaf-1b-containing organelles from mouse brains and colocalization studies in cultured neurons indicate that Gaf-1b/Rab11 is recruited to the TGN, leaves the TGN in a calsyntenin-1-dependent manner, and is involved in the tethering of TGN-derived tubules to recycling endosomes. Biochemical approaches showed a direct interaction of Gaf-1b with Rab11 and a potential interaction between calsyntenin-1 and syntaxin 13, suggesting that calsyntenin-1 links SNARE complexes containing syntaxin 13 to Gaf-1b, which in turn recruits the small GTPase Rab11. This complex may play a role in the accurate tethering and fusing of recycling vesicles with other organelles or with the plasma membrane. Interestingly, high expression of Gaf-1b and calsyntenin-1 in HeLa cells resulted in an alteration of the cell shape and in extensive outgrowth of the plasma membrane. Thus, we assumed that calsyntenin-1 and Gaf-1b/Rab11 have a specific function in regulating plasma membrane expansion, cytoskeleton rearrangement and/or receptor recycling in axonal growth cones or spine growth at postsynaptic sites. We further demonstrated that Gaf-1b interacts specifically and directly with the two MAP1LC3A/Atg8 family members GABARAPL1 and GABARAPL2. Members of the MAP1LC3/Atg8 family are associated with the process of autophagy. In HeLa cells we found that Gaf-1b associates with subcompartments of the autophagosomal pathway. Induction of autophagy by starvation mediates perinuclear aggregates positive for Gaf-1b and the autophagosomal marker LC3. Downregulation of Gaf-1b affected the level of autophagosomes in HeLa cells. Furthermore,

pharmacological studies indicated that Gaf-1b may play a role in the downstream steps of the autophagosomes formation.

In summary, our data indicated a direct relation between endosomal organelles in the autophagic pathway. Gaf-1b may regulate the recruitment of multivesicular bodies (MVBs) masked with Rab11 and GABARAPL1 and GABARAPL2 to autophagosomal membrane to induce the fusion of MVBs with lysosomes.

Zusammenfassung

Regulierte Endozytose und Recycling von Membranbestandteilen ist ein essentieller Prozess für Zellen, um ihre Funktion aufrecht zu erhalten. Recycling nimmt Teil an verschiedenen zelluläre Prozessen, wie die Bildung von Zellkontakten und Zelladhäsion, Zellwanderung, Zellteilung, Morphogenese, Zellfusion, Zellpolarität, Signaltransduktion und Nahrungsaufnahme. Ein anderer wichtiger zellulärer Prozess ist die Autophagie, welche eine essentielle Rolle für die zelluläre Homöostase spielt. Gestörte Autophagie kann zu diversen neurodegenerativen Erkrankungen, wie z.B. Alzheimer, Parkinson und Huntington führen, da die Zelle Aggregate von mutierten toxischen Proteinen nicht entfernen kann. Das Verständnis der molekularen Grundlagen dieser Erkrankungen und deren Behandlung sind daher abhängig von einer detaillierten Aufklärung der molekularen Maschinerie, welche Autophagie vermittelt und kontrolliert.

Calsyntenin-1 ist ein neuronales Typ-1-Transmembranprotein der Cadherin-Superfamilie, das an der postsynaptischen Seite im adulten Nervensystem vorkommt. Wir haben kürzlich gezeigt, dass Amyloid-Precursor-Protein zusammen mit Calsyntenin-1 das Trans-Golgi-Netzwerk in tubulär-vesikulären Organellen mittels eines Kinesin-1-abhängigen Prozesses verlässt. Diese Vesikel werden anterograd entlang der Axone transportiert. Zusätzlich haben wir herausgefunden, dass Axone mindestens zwei verschiedene, nicht überlappende Calsyntenin-1-enthaltende Transportvesikel besitzen. Die einen sind durch die Anwesenheit von Amyloid-Precursor-Protein und early-endosomalen Markern charakterisiert und die anderen durch die Marker der Recyclingendosomen. Immunoisolierung von Organellen und biochemische Studien weisen darauf hin, dass Calsyntenin-1 einen schützenden Mechanismus für den axonalen Transport von Amyloid-Precursor-Protein bietet. Neulich wurde Gaf-1b, eine Splice-Variante des Rab11-bindenden Proteins Rip11, als neuer Interaktionspartner von Calsyntenin-1 identifiziert. Wir haben hier die Interaktion und physiologische Funktion von Gaf-1b und Calsyntenin-1 charakterisiert. Mutationsstudien zeigten, dass Gaf-1b über die C2-Domäne spezifisch mit dem Carboxy-Terminus von Calsyntenin-1 interagiert. Wir nehmen an, dass der Carboxy-Terminus von Gaf-1b über die Wechselwirkung mit GTP-Rab11 an die Plasmamembran bindet und der Splice-Einschub von Gaf-1b notwendig ist, damit Gaf-1b eine Konformation annehmen kann, in welcher der Amino-Terminus von Gaf-1b mit Calsyntenin-1 interagieren kann. Überexpression von Calsyntenin-1 und die leichte Untereinheit von Kinesin-1 veränderte die Struktur des endoplasmatischen Retikulums und des Golgi-Apparates und reicherte Gaf-1b in Subdomänen des Trans-Golgi-Netzwerkes an. Zusätzlich zeigten die Immunoisolierung von Calsyntenin-1- und Gaf-1b-enthaltenden Organellen aus Maushirn und Co-Lokalisations-Experimente in Neuronenkulturen, dass Gaf-1b/Rab11 ins Trans-Golgi-Netzwerk rekrutiert werden, und dieses dann in einer Calsyntenin-1-abhängigen Art verlassen. In der Folge sind Gaf-1b/Rab11 am Anbinden von tubulären Organellen, die aus dem Trans-Golgi-Netzwerk entsprangen, an Recyclingendosomen beteiligt. Biochemische Experimente zeigten eine direkte Interaktion von Gaf-1b mit Rab11. Wir fanden auch Hinweise für eine Interaktion zwischen Calsyntenin-1 mit Syntaxin 13. Solche Interaktionen könnten in Anbindungs- und Fusionsprozessen von Recyclingvesikeln mit anderen Organellen oder der Plasmamembran eine Rolle spielen. Interessanterweise konnten wir in HeLa Zellen extreme Auswüchse der Plasmamembran beobachten, wenn Gaf-1b und Calsyntenin-1 stark überexprimiert wurden. Daraus folgerten wir, dass Calsyntenin-1 und Gaf-1b/Rab11 eine Funktion in der Regulation von Plasmamembranexpansion, Cytoskelett-Reorganisation und/oder Rezeptor-Recycling in axonalen Wachstumskegeln oder dendritischen Dornen haben. Weiter haben wir gezeigt,

dass Gaf-1b spezifisch und direkt an zwei Mitglieder der MAP1LC3A/Atg8-Familie, nämlich GABARAPL1 und GABARAPL2, bindet. Mitglieder der MAP1LC3A/Atg8-Familie sind in Prozesse der Autophagie involviert. In HeLa Zellen ist Gaf-1b mit Subkompartimenten des autophagosomalen Pfads assoziiert. Induktion von Autophagie durch Nährstoffentzug förderte die Bildung von perinukleären Aggregaten, die Gaf-1b und den autophagosomalen Marker LC3 enthalten. Verminderte Expression von Gaf-1b beeinflusste die Zahl der Autophagosomen in HeLa Zellen. Weitere pharmakologische Studien weisen darauf hin, dass Gaf-1b eine Rolle in weiteren Schritten der Autophagosomenbildung spielt. Zusammengefasst deuten unsere Daten auf einen direkten Zusammenhang zwischen endosomalen Organellen des autophagosomalen Pfads hin. Gaf-1b könnte dabei die Rekrutierung von multivesikulären Strukturen, die mit Rab11 dekoriert sind, und GABARAPL1/GABARAPL2 an autophagosomale Membranen regulieren und dann die Fusion von multivesikulären Strukturen und Lysosomen induzieren.

Abbreviations

aa	amino acid
ADAM	a disintergrin and metalloproteinase
AICD	APP intracellular domain
AMPA	alpha-**a**mino-3-hydroxy-5-**m**ethyl-4-isoxazole**p**ropionic **a**cid
APP	amyloid β-protein precursor
ATP	adenosintriphosphate
BACE	β-site APP cleavage enzyme
CAM	cell adhesion molecule
CCP	clathrin-coated pit
CCV	clathrin-coated vesicles
CD-M6PR	cation-dependent mannose-6-phosphat receptor
CNS	central nervous system
COPI/II	coat protein complex I/II
Cst	calsyntenins
CTF	C-terminal fragment
Cy3	cyanine 3
Cy5	cyanine 5
DAPT	*N*-[N-(3,5-difluorophenacetyl)-L-analyl]-S-phenylglycin t-butyl ester
DIV	days *in vitro*
DMEM	Dulbecco's modified eagle medium
DMSO	dimethyl sulfoxide
cDNA	complementary deoxyribonucleic acid
pcDNA	plasmid deoxyribonucleic acid
DTT	DL-dithiothreitol
ed	ectodomain
EDTA	ethylene diamine tetracetic acid
EEA1	early endosome antigen 1
EGFP	enhanced green fluorescence protein
EGFR	epidermal growth factor receptor
EHD3	Eps 15 homology domain-containing protein 3
ER	endoplasmatic reticulum
Erb	type 1 transmembrane receptor tyrosine kinase
ERC	endosomal recycling compartment
ERM	ezrin-radixin-moesin
ERGIC	ER-Golgi intermediate compartment
EtBr	ethidium bromide
EtOH	ethanol
FCS	fetal calf serum
FIPs	Rab-family interacting proteins
FITC	fluorescein isothiocyanate
fl	full-length
GABA	Gamma-aminobutyric acid

GABARAP	$GABA_A$ receptor associated protein
GABARAPL 1/2	$GABA_A$ receptor associated protein ½
Gaf-1b	γ-SNAP-associated factor 1b
GAP	GTPase-activating protein
GATE-16	Golgi-associated ATPase Enhancer of 16 kDa
GDI	GDP dissociation inhibitor
GDP	guanidinediphosphate
GEC1	glandular epithelial cells
GEF	GDP/GTP exchange factor
GFP	green fluorescence protein
GM130	Golgi martrix protein of 130kD
GST	Glutathione S-Transferase
GTP	guanidinetriphosphate
HA	hemagglutinin
$HBSS^{++}$	Hanks Balanced Salt Solution (1 mM $MgCl_2$, 1 mM $CaCl_2$, and 1% vol/vol human serum albumin)
HRP	horseradish peroxidase
IC	ER-Golgi intermediate compartment
ICC	immunocytochemistry
IgG	immunoglobulin G
IP	immunoprecipitation
KBS	KLC-1 binding segment
kD	kilo Dalton
KHC	kinesin-heavy chain
KLC	kinesin-light chain
LAMP	lyosome associated membrane protein
LC	light chain
LDL	low density lipoprotein
LTP	long-term potentiation
LB	Luria-Bertani broth
MAP	microtubule-associated protein
MDCK	Madin-Darby canine kidney
mRFP	monomeric red fluorescence protein
MS	mass spectormetry
MTOC	microtubule-organizing centre
NA	numerical aperture
NMDA	*N*-methyl-d-aspartate
NSF	*N*-ethylmaleimide-sensitive factor
NTP	nucleoside triphosphate
dNTP	deoxynucleoside triphosphate
PA	phosphatidic acid
PBS	phosphate-buffered saline
PCR	polymerase chain reaction
PEI	polyethylenimine
PFA	paraformaldehyde

PLL	poly-L-lysine
PM	plasma membrane
PMA	phorbol 12-myristate 13-acetate
PNS	postnuclear supernatant
POD	peroxidase
PSD	postsynaptic density
PI(3)P	phosphatidylinositol (3)-phosphate
PtdIns(3,4,5)P_3	phosphatidylinositol-(3,4,5)-triphosphate
PVDF	polyvinylidene fluoride
RBD	Rab11/25 binding domain
RCP	Rab11 coupling protein
REP	Rab escort protein
RFP	red fluorescence protein
Rip11	Rab11 interacting protein
RNA	ribonucleic acid
RNAi	RNA interference
mRNA	messenger ribonucleic acid
rpm	revolutions per minute
RT	room temperature
RT-PCR	reverse transcriptase poly chain reaction
SDS-PAGE	sodium dodecyl sulfate polyacrylamide gel electrophoresis
SE	sorting endosome
siRNA	small interfering RNA
SNAP	soluble NSF association protein
SNARE	SNAP receptor
STEM	surface-connected tubules entering macrophage
Stx	syntaxin
TAE	Tris-acetate EDTA (ethylene diamine tetracetic acid)
TBST	Tris-buffer saline Tween
Tf	transferrin
TfR	transferrin receptor
TGN	*trans*-golgi network
TM	transmembrane
TPR	tetratricopeptide repeat
UV	ultra violet
VAMP	vesicle associated membrane protein
WB	Western blot
wt	wild-type

Publications

The following publications have been obtained during my PhD thesis:

Original articles:

05/2012 Steuble, M., Diep, T. M., Schatzle, P., Ludwig, A., Tagaya, M., Kunz, B. and Sonderegger, P. (2012). Calsyntenin-1 vesicles shelter APP from proteolytic processing during anterograde axonal transport. *Biology Open* 000, 1-14.

08/2010 Steuble, M., Gerrits, B., Ludwig, A., Mateos, J. M., Diep, T. M., Tagaya, M., Stephan, A., Schatzle, P., Kunz, B., Streit, P. et al. (2010). Molecular characterization of a trafficking organelle: dissecting the axonal paths of calsyntenin-1 transport vesicles. *Proteomics* 10, 3775-88.

01/2009 Ludwig, A., Blume, J., Diep, T. M., Yuan, J., Mateos, J. M., Leuthauser, K., Steuble, M., Streit, P. and Sonderegger, P. (2009). Calsyntenins mediate TGN exit of APP in a kinesin-1-dependent manner. *Traffic* 10, 572-89.

Selected Meeting Abstracts:

10/2012 Diep, T. M., Steuble, M., Schatzle, P., Ludwig, A., Tagaya, M., Kunz, B. and Sonderegger, P. (2012). Calsyntenin-1 vesicles shelter APP from proteolytic processing during anterograde axonal transport. *Society for Neuroscience,* New Orleans. Abstract submitted and accepted.

06/2012 Steuble, M., Diep, T. M., Schatzle, P., Ludwig, A., Tagaya, M., and Sonderegger, P. (2012). Calsyntenin-1 vesicles shelter APP from proteolytic processing during anterograde axonal transport. *ZNZ and NCCR Neuro Joint Symposium,* Zurich.

05/2011 Diep, T. M., Steuble, M. and Sonderegger, P. (2011). The role of Gaf-1b in vesicular transport of calsyntenin-1 in neurons. *ZNZ PhD Retreat*, Valens.

02/2011 Steuble, M., Diep, T. M., Kunz, B., and Sonderegger, P. (2011). A role of calsyntenin-1 for sheltered APP transport along axons. *NCCR Neuro (National Center of Comptence in Research Neural Plasticity and Repair)*, Warth.

03/2009 Diep, T. M., Ludwig, A., Blume, J., Yuan, J., Mateos, J. M., Leuthauser, K., Steuble, M., Streit, P. and Sonderegger, P. (2009). Calsyntenins mediate TGN exit of APP in a kinesin-1-dependent manner. *Swiss Society of Neuroscience*, Fribourg.

03/2008 Diep, T. M., Steuble, M., Ludwig, A. and Sonderegger, P. (2008). APP and calsyntenin-1: differently regulated proteolytic processing and trafficking in axonal endosomal subcompartments. *NCCR Neuro (National Center of Comptence in Research Neural Plasticity and Repair)*, Berlingen.

1. Introduction

1.1 Intracellular Transport

Eukaryotic cells have developed an elaborate endomembrane system that compartmentalizes biochemical pathways and biosynthetic processes. Each organelle is characterized by a specific protein composition that needs to be sustained. Intracellular transport plays an important role in the maintenance of the specific protein composition of distinct compartments. There are two major pathways in the intracellular trafficking: the secretory pathway and endocytic pathway. The secretory pathway involves the transport of molecules from the endoplasmic reticulum (ER), through the Golgi apparatus, toward the cell periphery. The distinct membrane-bound compartments are interconnected by vesicular traffic for secretion of newly synthesized proteins, carbohydrates and lipids. On their way to the extracellular space, newly synthesized secretory proteins pass through several membrane-enclosed organelles until they reach their maturation. This process includes the translation and folding at the endoplasmatic reticulum, the package into COPII coated vesicles for transport to the Golgi complex where they undergo modifications, and, as a last step, leaving the *trans*-Golgi network (TGN) through the secretory granules (Figure 1.1) [2]. The endocytic pathway involves the internalization of molecules from the plasma membrane or the extracellular space into endosomes. The fate of proteins is determined by sorting processes in endosomes. This pathway comprises of several distinct endocytic organelles, including sorting endosomes for protein sorting, late endosomes and lysosomes for protein degradation. Additionally, the endocytic recycling describes the pathway through which endocytosed proteins (such as receptors) are recycled back to the plasma membrane through the recycling endosomes. Endocytic and exocytic organelles communicate constantly with each other through the aid of the transport vesicles. These vesicles continually bud from one membrane and fuse with another membrane, thereby transporting membrane components and soluble cargo [3].

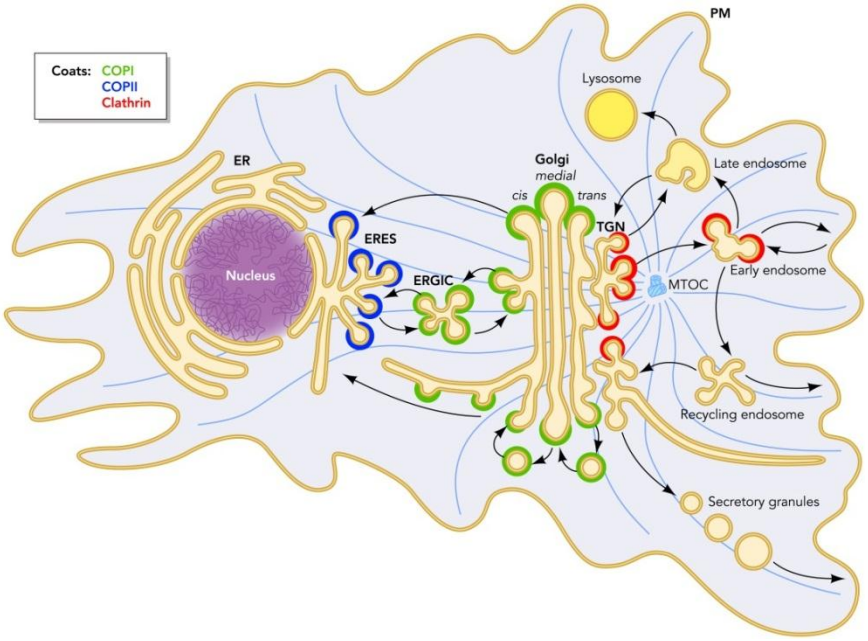

Figure 1.1: Intracellular transport pathways.
The compartments of secretory and endocytic pathways are shown. The location of the different coats is indicated: COPII (blue), COPI (green) and clathrin (red). ER, endoplasmatic reticulum; ERES, ER exit site; ERGIC, ER-Golgi intermediated compartment; MTOC, microtubule-organizing center; TGN, *trans*-Golgi network (adapted from [4]).

Intracellular trafficking, cell movement and subcellular localization of organelles are dependent on the cytoskeleton. Microfilaments, intermediate filaments and microtubule are the three main types of cytoskeletal filament. The actin filaments are the thinnest filaments of the cytoskeleton. They are composed of two coiled strands of chains of actin subunits [5]. Their orientation is more random throughout the cell, but there are bundles of actin filaments that are mainly concentrated directly beneath the plasma membrane for the maintenance of cellular shape and formation of cytoplasmic protrusions, such as pseudopodia or microvilli. Actin filaments are polar structures with a barbed end and a pointed end [5]. Actin filaments are involved in the participation of cell-to-cell or cell-to-matrix junctions. They also function in vesicle endocytosis, cell migration, cytokinesis and, along with myosin, in muscular contraction. During vesicle biogenesis actin filament dynamics promote membrane deformation, such as creation of tubular bud on nascent transport carriers during post-Golgi transport, or the production of spherical carriers during endocytosis [6]. Intermediate filaments are more stable than actin filaments and, like actin filaments, they participate in the maintenance of cell-shape and in the cell-to-cell and cell-to-matrix junctions. Intermediate filaments are also involved in the organization of internal three-dimensional structure of the cell and anchoring organelles. Microtubules are hollow cylindrical filaments comprising of protofilaments. Protofilaments are polymers of alpha and beta tubulin. Tubulin polymerizes end-to-end with an alpha-subunit of one tubulin dimer contacting the beta-subunit of the next [7]. Therefore, in a protofilament one end will have the alpha-subunit exposed and the other end will have the beta-subunit exposed, referred to as minus and plus end, respectively. This polarity is an important feature of the microtubule structure. Microtubules are involved in many cellular processes, including vesicular transport, determination of cell shape, cytoplasm organization, mitosis, and cytokinesis [7]. Microtubules are nucleated and they are organized by microtubule-organizing centres (MTOCs), such as centrosomes. The plus end of the microtubule is pointed toward the cell periphery and the minus end is pointed toward the centrosome [8]. Microtubule-associated proteins (MAPs) regulate the microtubule dynamics. Membranous carriers are transported within the cell through motor proteins moving along microtubules in a defined direction. Kinesin and dynein are the major motor protein of the microtubule. Kinesin moves toward the plus end of the microtubule, therefore transports cargos from the centre of the cell towards the periphery. This form of transport is referred to as anterograde transport. In contrast, dynein normally moves toward the minus end of the microtubule. The movement of transport packages from the periphery toward the centrosome is defined as retrograde transport. Thus, motor proteins link the cargo to the microtubule by interacting directly with a transmembrane protein, or indirectly, via adaptor proteins.

Organelles communicate with each other through transport of vesicles. The size and form of the vesicle varies from small and round (40 nm - 100 nm), to large and irregular tubulovesicular (≥200 nm). The transfer of cargo between compartments involves different proteins and contains distinct steps, namely vesicle budding, protein sorting, vesicle targeting and vesicle fusion (Figure 1.2). Firstly, coat proteins are assembled to induce membrane curvature and to promote budding of new vesicle from a donor organelle [9, 10]. Then, cargo proteins are selectively sorted into the forming vesicles, while resident proteins are retained in the donor compartment. The cargo selection is then mediated by coat proteins recognizing sorting signals present in the cytosolic domains of transmembrane cargo proteins. In a next step, the formed vesicle dissociates from the donor membrane by a mechanism called scission. Subsequently, vesicles lose their coat on the way to the acceptor membrane. Targeting and fusion to a specific acceptor compartment is strictly regulated by specific proteins. Tethering is mediated by Rab proteins and SNAREs are involved in membrane fusion.

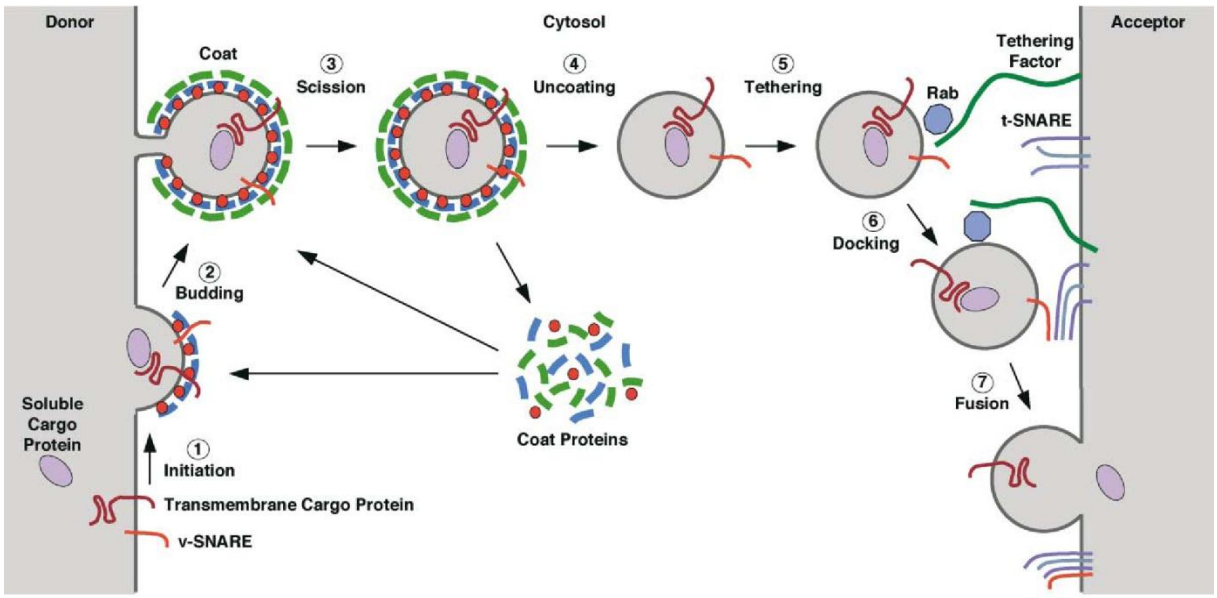

Figure 1.2: Vesicular transport.
1) Coat proteins are assembled from the cytosol to initiate budding. 2) COPI, COPII or clathrin mediate the budding of transport carriers and the uptake of cargo into transport vesicles. 3) The newly formed vesicle dissociates from the donor membrane with different coats using different mechanisms for the scission. 4) The vesicle loses its coat on the way to their destination. 5) The vesicle is transported to the acceptor membrane. The vesicle is guided by the cytoskeleton and is tethered to the acceptor compartment by Rab GTPases and tethering factors. 6) Docking is mediated by SNARE complex formation where v-SNARE and t-SNARE assemble into a four-helix bundle. 7) The assembled four-helix bundle drives the fusion of the vesicle with its target compartment. The cargo is subsequently depleted into the acceptor compartment (adapted from [3]).

1.2 Secretory Pathway

The secretory pathway involves the delivery of various transmembrane and secretory proteins to their target location and is essential for the cellular function. The secretory pathway comprises of structurally distinct membrane-bound compartments and transport intermediates trafficking between these compartments. The compartments of the secretory pathway include the ER, the ER exit sites (ERES), the ER-Golgi intermediate compartment (ERGIC), the Golgi complex, and the *trans*-Golgi network (TGN) [4].

The first station of the secretory pathway is the endoplasmatic reticulum, the site of protein synthesis. The ER originally evolved through the invagination of the plasma membrane. Therefore, the internal lumen of the ER is topically equivalent to the outside of the cell [11]. Its immense reticular membranous structure is contiguous with the nuclear membrane. Almost the entire cytoplasm is captured by the ER, and the ER consists of more than half of the total membrane in eukaryotic cells [12]. The ER is involved in different important functions such as protein translation, folding and modification, lipid synthesis, calcium homeostasis, and production and storage of glycogen, steroids and other macromolecules. The ER can be distinguished from the nuclear envelope, and from smooth (ribosome-free) and rough (ribosome-coated) membranes. Transmembrane or secreted proteins are initially translated at ribosomes in the cytosol, and they enter the ER by the recognition of a signal peptide found at the N-terminus of the protein. The signal recognition particle (SRP) recognizes the signal peptide and forms a ribosome/nascent protein/SRP complex that binds to the ER membrane through the SRP receptor [13]. At the ER membrane the nascent protein chain enters the ER lumen through a proteinaceous pore in the membrane, namely the Sec61 translocon [11]. The translation

proceeds and the newly synthesized proteins are released in the lumen of the ER, where protein chaperons and lectins assure proper protein folding. Posttranslational modifications may take place during this process. The nascent secretory proteins leave the ER at the ER exit sites (ERES). ERES are specialized areas of the smooth ER that form buds on the nuclear envelope, and form tubulovesicular networks in the periphery of the cell [14]. The ERES are coated with COPII coat components. Soluble cargo proteins are sorted to the ERES by binding with cargo receptors that belong to the ERGIC-53 family [15], the p24 family [16, 17] or the Erv family [18]. The lumen-exposed domain of the receptors binds to the cargo proteins, while the cytoplasmic domain interacts with COPII components [4]. COPII coat assembly starts with the recruitment of the small GTPase Sar1-GTP and two sub-complexes consisting of Sec23/Sec24 and Sec13/Sec31 [14]. After budding, the COPII coated transport vesicles are transported to the next compartment in the secretory pathway, a network of tubulovesicular clusters, also known as ER-Golgi intermediate compartment (ERGIC) [19]. The ERGIC is the major sorting station where ER residing proteins are recycled back to the ER via COPI-mediated retrograde transport, and secretory cargos are delivered to the *cis*-Golgi [20] by forming a new *cis*-Golgi or by fusing with an already existing *cis*-Golgi [19]. In the ER-to-Golgi transport the microtubules play an important role because they associate with the ERGIC and mediate dynein-dependent anterograde transport to the Golgi [21] and kinesin-dependent retrograde transport [22].

The Golgi apparatus is a multifunctional organelle next to the nucleus and closely associated with the microtubule-organizing centre [23]. The Golgi in mammals is composed of a single ribbon of stacked cisternae with a defining *cis*-to-*trans* asymmetry [24]. It has been shown in neurons that the Golgi complex also adapts a ribbon-like network to a perinuclear position, but there is also Golgi outposts observed in dendrites. These Golgi outposts represent many highly localized stations of the secretory pathway [25]. Overall, the Golgi apparatus is the central station in the secretory pathway. The Golgi apparatus is the place where post-translational modifications of secretory and transmembrane proteins take place, such as glycosylation, sulfation and proteolytic processing. These modifications in the Golgi are crucial for protein localization, stability and specificity of interactions [26]. Additionally, protein sorting is a major function of this organelle. Cargos approaching the Golgi from the ER, fuse at the *cis*-side to form the *cis*-Golgi network (CGN), and are then transported and further processed through the Golgi, to reach their final functional form at the *trans*-Golgi network (TGN). For the traverse of proteins through the Golgi apparatus, several models have been proposed, such as the anterograde vesicular transport and the cisternal maturation model. The anterograde vesicular transport suggests that each individual cisterna is stable and immobile while cargo is transported anterogradely in COPI coated vesicles that bud from one cisterna and fuse with the next one [20]. The fact that COPI was shown to be responsible for retrograde transport, and that COPI vesicle only transport small cargo molecules, render the anterograde vesicular transport model for intra-Golgi transport questionable. In comparison, the cisternal maturation model is the most accepted model up to date [27]. This cisternal maturation model states that cargo is kept within the same cisterna and traverses from the *cis*- to the *trans*-face together with the cisterna. During this process, the cisterna changes its composition by packaging of specific cisternal components, such as enzymes and lipids, into COPI vesicles that move in the retrograde direction from the *trans*- to the *cis*-Golgi cisterna [28].

Secretory proteins reach the *trans*-Golgi network (TGN) after traversing the Golgi complex. The TGN, a series of interconnected tubules that arise from three *trans*-Golgi cisternae [24], is the major sorting centre of the secretory pathway. The size and structure of the TGN is very dynamic and depends on the ratio of trafficking, the ratio of cargo input and output to the TGN along various trafficking routes [26]. It was shown that trafficking blockage, induced by low temperature, results in an

increased membrane surface area of the TGN [29]. The TGN does not only receive secretory proteins from the *trans*-Golgi cisternae, but also recycling proteins from the endocytic pathway traverse through the TGN [30, 31]. Therefore, the TGN is also an important node point for the communication between the secretory and the endosomal system [1]. In the TGN, secretory proteins pass through their final modification and then achieve their maturation through protease cleavage [20]. At the TGN, the newly synthesized proteins are sorted to distinct pleiomorphic carriers that target different final destinations: apical or basolateral membranes, recycling endosomes, early/sorting endosomes, late endosomes, and specialized compartments, such as secretory granules in secretory cells (Figure 1.3) [1]. Vesicles destined for the endosomal/lysosomal system are coated with clathrin coats. Only the tubules from the last cisterna show clathrin-coated buds [32].

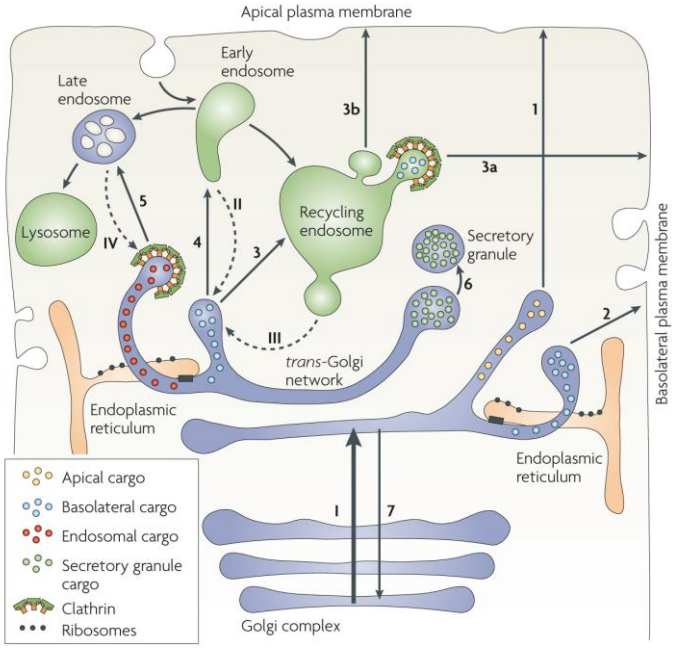

Figure 1.3: The TGN is a major sorting centre for endocytic and exocytic pathways.
Secretory proteins traverse through the Golgi complex to distinct domain of the TGN (I), where they are transported to different destinations (1-5). The TGN sorts proteins to apical plasma membrane (1), the basolateral plasma membrane (2), recycling endosome (3), early/sorting endosome (4), late endosome (5) and specialized compartments, such as secretory granules (6) in secretory cells. The TGN also receives cargos from the endocytic pathway (II-IV) and sends Golgi-resident proteins back to the earlier Golgi complex (7). Only tubules from the last cisterna are clathrin-coated. The ER is in close contact with the tubules of the last two cisternae for the exchange of lipids. Some apical or basolateral proteins pass through the recycling endosome before they reach the apical plasma membrane (3, 3b) or basolateral plasma membrane (3, 3a), respectively (adapted from [1]).

1.3 Endocytic Pathways

The endocytic pathways are used for internalization of molecules from the cell surface, such as receptor-associated ligands, plasma membrane proteins, soluble molecules from the plasma membrane, or the extracellular space and lipids. The removal of membrane from the cell surface is balanced by endosomal recycling of the endocytosed proteins and lipids back to the plasma membrane. The balance between endocytosis and recycling maintains the composition of the plasma membrane, and is important for several cellular processes such as cell adhesion and junction formation, cell migration, cytokinesis, cell polarity, signal transduction and nutrient uptake [33].

There are various mechanisms of endocytosis that can be distinguished on the level of clathrin-dependent and clathrin-independent endocytosis [34]. In the last few years increased interest in clathrin-independent endocytic pathways has arose. The best-known non-clathrin-coated pit mechanism is caveolae formation. Caveolae are invaginations of the plasma membrane that are coated with caveolin and the associated cavins [35, 36]. Other mechanisms of clathrin-independent endocytosis include phagocytosis and pinocytosis. Phagocytosis refers to the uptake of large particles like microorganisms or dead cells into phagosomes. This mode of internalization is induced by an

actin-dependent process. This process usually occurs in specialized cells, such as macrophages, but other cell types are also able to use phagocytosis [37]. Pinocytosis is the uptake of fluids into small vesicles of about 100 nm. So far, the best characterized endocytic mechanism is receptor-mediated endocytosis that involves the internalization of receptors and their ligands by clathrin-coated pits. Clathrin is composed of three heavy and three light chains. They assemble to form three-legged cage-like structures, referred to as a triskelion. The assembly of triskelia induces curvature in the membrane [38]. Since triskelia do not directly interact with the membrane, a multiprotein complex, called adaptor proteins (AP), is needed to recruit triskelia to the membrane [39]. AP-1 functions as clathrin-coated vesicle (CCV) formation at the TGN, and AP-2 is responsible for the CCV formation at the plasma membrane [40]. Alongside the recruitment of triskelia to the membrane and organization of CCP formation, the APs also function as cargo docking proteins for molecules inside vesicles. To complete the formation of clathrin-coated vesicles additional accessory proteins are needed. Epsins and endophilin induce the bending of the membrane for vesicle budding [41], GTPase dynamin is required for the fission of the vesicle from the donor membrane [42], and amphyphisin binds to endophilin, clathrin, AP and dynamin [43].

Ligands and their plasma membrane receptors (e.g. TfR and LDLR) are internalized through clathrin-coated pits, and the newly formed vesicles in the cell shed their clathrin coats. After the clathrin coat disassembly the vesicles fuse with other newly formed vesicles, or with pre-existing sorting endosomes. Sorting endosomes show a tubulovesicular structure with a light acidic luminal pH of about 6.0, and they are located in the periphery of the cell [44]. Sorting endosomes allow fusion with newly endocytosed vesicles for about 5-10 minutes. Afterwards, they start to move along microtubules toward the cell centre, stop fusing with other endocytosed vesicles, and the lumen of the sorting endosome becomes more acidic. Molecules in sorting endosomes are delivered to either one of the four destinations, namely the TGN, the late endosome, the plasma membrane, or the endosomal recycling compartment (ERC) (Figure 1.4). The low pH of sorting endosomes facilitates conformational changes in proteins that can lead to the release of ligands from their receptors. The molecules destined for degradation in lysosomes are first delivered to late endosomes. The sorting endosome retains soluble ligands and membrane proteins in their lumen. Acidic hydrolases start to accumulate in sorting endosomes, thus the sorting endosomes begin to mature to late endosomes, resulting in a pH drop of about 0.5 units. Newly synthesized lysosomal proteins bound to mannose-6-phosphate receptors (M6PR) are delivered from the TGN to late endosomes [45]. The luminal pH plays an important role in the maturation of sorting endosomes. It was demonstrated that Bafilomycin A1, which is a vacuolar H^+-ATPase inhibitor, decreases the maturation process of sorting endosomes to late endosomes and lysosomes [46, 47]. A goal of sorting signalling receptors to late endosomes is to terminate receptor signalling, and to suppress cell responses to further signal input until new receptors are synthesized [48]. Membrane receptors (e.g. EGFR, Erbs) are ubiquitylated in order to assign them for downregulation. Ubiquitylated receptors are recognized by endosomal sorting complexes required for transport (ESCRTs), that are also required for the biogenesis of endosomal multivesicular bodies (MVB) [49]. The receptors are ubiquitylated at the cytoplasmic side. The ESCRTs recognize this domain and induce inward-budding and the generation of intraluminal vesicles [50]. This separates the cytoplasmic part of the receptor from the rest of the cell, and therefore suppresses their signalling capability. Furthermore, MVBs fuse with lysosomes to degrade their luminal content.

While the sorting endosomes translocate to the centre of the cell before maturation to late endosomes, most recycling proteins rapidly leave the sorting endosome by the budding of narrow-diameter tubules [51, 52]. Sorting endosomes are separated in two distinct domains, namely the

vacuolar domain and the network of tubules. Proteins that are retained in the vacuolar domain are destined for degradation. Recycling proteins are accumulated in the network of tubules. Over 95% of endocytosed proteins in sorting endosomes are removed before the maturation to late endosomes can take place, and the $t_{1/2}$ of endosome exit is 2 minutes or less [51, 52]. Thus, generating a tubular geometry, where recycling proteins are translocated, is the first step of endocytic sorting (Figure 1.4; right panel).

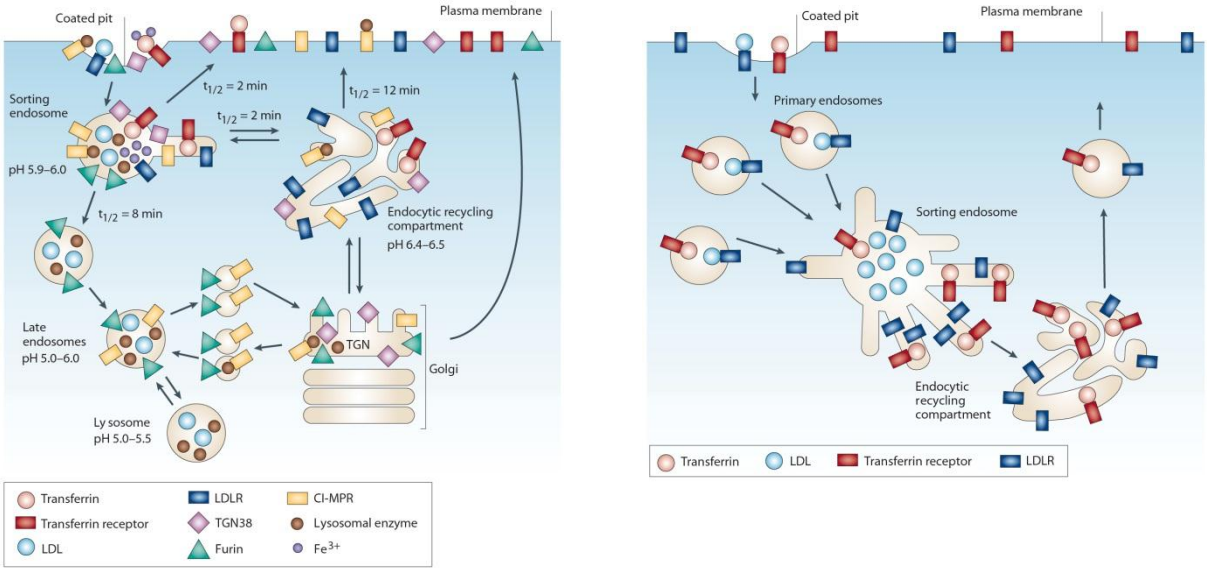

Figure 1.4: Model of receptor-mediated endocytic trafficking.
Left: Ligands bind at the plasma membrane to their receptors. The receptor-ligand complex is endocytosed mediated by clathrin coats and transported to sorting endosomes. Vesicles can fuse with other newly formed vesicles or with pre-existing sorting endosomes. Proteins destined for degradation are retained in sorting endosomes that mature into late endosomes and lysosomes. Recycling proteins are recycled back to the plasma membrane either directly from the sorting endosomes or through the endocytic recycling compartment (ERC). The ERC can receive proteins from the TGN and from endosomes. Proteins in recycling endosomes are either sorted back to sorting endosomes, to the cell surface, or to the TGN. Some receptors and molecules traffic between late endosomes and the TGN. Right: Recycling proteins are accumulated in the tubular domain of sorting endosomes. From the tubular domain they are transported further to the endocytic recycling compartment. The vacuolar domain matures to late endosomes and lysosomes and contains proteins destined for degradation. LDLR, Low-density-lipoprotein receptor; LDL, low-density-lipoprotein; CL-MPR, cation-independent mannose-6-phophate receptor; TGN; *trans*-Golgi network (adapted from [53]).

Recycling proteins are sorted back onto the cell surface through two main pathways: the fast recycling route or the slow recycling route. One part of the recycling proteins in the sorting endosome returns to the cell surface through the fast recycling pathway. In this pathway they are directly recycled back to the plasma membrane from the sorting endosome. The other part takes the slow recycling route through the endosomal recycling compartment [54]. Clathrin and its adaptor proteins have been found on recycling endosomes, indicating that recycling endosomes may also form vesicles in a clathrin-dependent manner [55, 56]. Therefore, recycling endosomes use similar mechanisms for vesicle formation as do other transport intermediates forming compartments. The ERC (pH 6.4) is slightly less acidic than the sorting endosomes (pH 6.0) and represents a heterogeneous and tubulovesicular morphology. In some cells the ERC are distributed widely throughout the cytoplasm. However, most of the ERC are typically localized juxtanuclear around the microtubule-organizing centre next to the TGN, and they are associated with microtubules [55-57]. The ERC targets

molecules to three different destinations: to the plasma membrane, to the sorting endosomes, or to the *trans*-Golgi network. The transport from the ERC to either one of the destinations depends on the generation of transport intermediates, vesicles or tubules. Different ERC residing proteins regulate the transport from the ERC, such as Rab11 and the Eps15-homology-domain protein EHD1/Rme1 because the transport of various proteins to the TGN and to the plasma membrane is affected when the activities of these proteins are altered [58]. Many plasma membrane proteins, such as Tac-TGN38, which are destined for the TGN, pass through the ERC before reaching the TGN. It was shown that TGN resident proteins can recycle several times between the plasma membrane and ERC until they are delivered to the TGN [59]. The equilibrium of the protein distribution is maintained because endocytic recycling is fast, compared to the exit rate from the Golgi. Many proteins, which are not destined for the ERC, are still transported through the ERC on the way to their destination. Hence, the ERC is an important sorting centre for molecules with distinct cellular locations.

1.4 Endocytic Pathways in polarized cells

Recycling pathways are essential for sorting molecules to their appropriate cellular locations, and for the homeostasis of proper membrane and lipid distribution in secretory and endocytic compartment. Many cell types display a polarized morphology by developing discrete functional domains. Especially epithelial cells have distinct apical and basolateral domains defined by different protein composition and separated by tight junctions. Neurons are highly polarized cells with two structurally and functionally distinct domains, the axon and the dendrites [60-62]. Furthermore, dendrites can be polarized into apical versus basolateral dendrites [63]. The establishment of neuronal polarity begins early in the development of neurons. The maintenance and establishment of neuronal polarity requires tightly coordinated regulation of the cytoskeleton and the cellular transport machinery [64, 65]. The first step to establish a polarized neuron is the determination of a single axon, the axon specification [66]. During axon specification, the cytoskeletal of one of the nascent neurites undergoes prominent changes and the membrane composition is rearranged. The result is a neuritic process that possesses different morphology and function from other neurites that are developing into dendrites [67, 68]. The axonal growth cone is different from the dendritic growth cone in their protein composition and development [69]. In the axon of mature neurons the microtubule has a polarized orientation. The plus end points towards the distal part of the axon, away from the cell body. In dendrites the microtubules possess mixed polarity [70]. The Rho family GTPases (Rho, Rac and Cdc42) control cellular functions by regulating the actin cytoskeleton [71]. It was shown that the Rho GTPases are important in establishing cell polarity [72] and influencing the neuronal morphology [73]. Reorientation of organelles of the secretory pathway during polarization is a result of a rearrangement of the cytoskeleton. This creates a polarized secretory pathway with an orientation that supports directional and selective membrane trafficking [74]. In epithelial cells, the Golgi apparatus is relocated in the apical region of the cytoplasm, and protein delivery is directed towards the apical part of the lateral plasma membrane [75]. In neurons, the Golgi is located in the soma prior to polarization, during polarization it extends into larger dendrites [63].

To maintain the polarity of a cell, sustainment of the proper protein, lipid and cytoskeletal composition within the distinct membrane subdomains is required. Several mechanisms have to be coordinated to support polarization within cells. Barriers to control protein diffusion and stabilization of protein complexes at the membrane by scaffolding proteins are necessary. Additionally, polarized

trafficking through the endocytic and secretory pathways must occur [63]. Membrane trafficking in polarized cells is best understood and described in epithelial cells. Proteins assigned for either the apical or the basolateral membrane domain are directly sorted in the TGN into two distinct vesicle species, in epithelial Madin-Darby canine kidney (MDCK) cells [76]. Another pathway, in which proteins are sorted via transcytosis, was demonstrated for hepatocytes. In this pathway, membrane proteins are first transported to the cell surface at the basolateral site. After internalization into endosomes, proteins are sorted to the apical or basolateral membrane. Therefore, all the proteins are first transported to the basolateral membrane, even if they are destined for the apical membrane [77]. It was suggested that basolateral and apical domains of MDCK cells correspond to the somatodendritic and axonal domains of neurons, respectively [60]. The function of neurons is crucially dependent on the morphological and functional differences between their axonal and dendritic domains [60-62]. In addition to the distinction of axonal and dendritic domains, the neuronal polarity is much more complex, as the dendritic and the axonal surface area are further polarized and specialized into distinct subdomains [78]. Three different models have been proposed for the polarized sorting of proteins to axonal and somatodendritic domains in neurons (Figure 1.5) [63]. The selective pathway suggests that, at the TGN, axonal and dendritic proteins are sorted into separate transport packages and selectively transported to axons or dendrites. Extensive studies showed that NgCAM reach the axonal membrane through the selective delivery pathway [61, 79]. The FnIII domain at the ectodomain of NgCAM is a sufficient sorting signal to assign NgCAM to the axon [61]. The selective fusion route states that axonal and dendritic carriers are transported to both domains, but the fusion is restricted to either one or the other target membrane [61]. The selective retention pathway postulates that axonal proteins (such as VAMP2) are unselectively transported to axonal and somatodendritic domains. At the dendritic membrane the proteins are not accumulated but rapidly endocytosed into sorting/recycling endosomes and further sorted to the axon via transcytosis [61, 79, 80]. Thus, endocytic recycling plays an important role in the establishment and maintenance of cellular polarity.

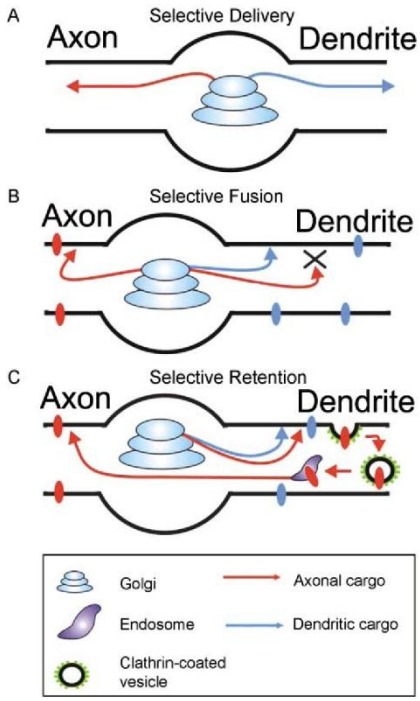

Figure 1.5: Three possible pathways for the polarized sorting of axonal and dendritic plasma membrane proteins.
Three models have been proposed for polarized sorting of axonal and dendritic plasma membrane proteins: (A) Selective delivery describes that axonal and dendritic proteins are sorted directly at the TGN to their target destination. (B) Selective fusion states that axonal proteins are delivered to both domains but can fuse only with the axonal plasma membrane and not with the somatodendritic membrane. (C) In selective retention, proteins are first transported to the dendritic surface and after internalization, proteins are sorted in endosomes to the axonal membrane (adapted from [63]).

1.5 Autophagy

Autophagy is an evolutionary conserved and strictly regulated lysosomal degradation pathway that is used by eukaryotes for the degradation of cytoplasmic components, such as long-living proteins, entire organelles, and RNA. Therefore, autophagy plays an essential role as a physiological system for cellular homeostasis. Autophagy occurs in virtually all cells at a low basal level. There are three types of autophagy, namely macroautophagy, microautophagy and chaperone-mediated autophagy [81, 82]. Microautophagy and chaperone-mediated autophagy take place directly at the lysosomal membrane. Microautophagy involves direct engulfment of a small fraction of cytoplasm into lysosomes by inward inversion of the lysosomal membrane. In Chaperone-mediated autophagy, cytosolic proteins are unfolded by chaperone proteins and are translocated across lysosomal membranes [83]. Among the three forms of autophagy, the most studied one is macroautophagy. Macroautophagy (hereafter referred to as autophagy) involves the formation and expansion of a cup-shaped structure, termed as isolation membrane or phagophore, that engulfs fractions of the cytoplasm or organelles into a double membrane-bound vacuole, the autophagosome [84-86].

It has been demonstrated that autophagy plays an important role in vertebrate development. Specific cytosolic rearrangements are required for proliferation, death and differentiation during embryogenesis and postnatal development in mammals [86]. During embryogenesis there are enhanced metabolisms or phases of silence in cells. Therefore, cells need to modify their organelle or protein content quickly to rapidly adapt and respond to adverse conditions. Autophagy could fulfil these requirements and be the dynamic tool to revive cells or modify their external appearance within a few hours [86]. Autophagy is also involved in neurodegenerative diseases, aging, cancer, cell death, antigen presentation and bacterial invasion [87]. Many neurodegenerative diseases, such as Alzheimer's disease, Parkinson's disease, amyotrophic lateral sclerosis, or Huntington's disease, are linked to defective autophagy due to the failure to clear aggregates of mutated toxic proteins [88]. In insects it was shown that increased autophagy is related to the nonapoptotic programmed cell death, the type II cell death, where increased lysosomal activity and formation of a large number of autophagosomes can be observed [89]. Such a death pathway was only found in the developing nervous system of higher eukaryotes [90].

Autophagy is also an adaptive catabolic response to metabolic stresses, including starvation, growth factor depletion or hypoxia. A key molecule in regulating autophagy is the kinase mammalian target of rapamycin (mTOR). When mTOR is phosphorylated, autophagy is inhibited until it is dephosphorylated [86]. mTOR functions as a sensor for the cellular nutrient level. Nutrient deprivation in cells leads to inhibition of mTOR by dephosphorylation. mTOR inhibition results in activation of the ULK1/ULK2 (Atg1 in yeast) complex which initiates a cascade of events that lead to the formation of autophagosomes [91].

Most of the genes involved in autophagy were first studied and characterized in yeast. These autophagy-related (Atg) genes are involved in regulating autophagosome formation and they also function in other stages of autophagy. Around thirty-three Atg genes have been identified in yeast and homologues of many of these genes have been described in higher eukaryotes [92]. Two major steps are responsible for the process of autophagosome formation: nucleation and elongation of the isolation membrane (Figure 1.6). Formation of autophagosomes starts with the nucleation process, the generation of isolation membranes. The nucleation process is activated by phosphatidylinositol (PI) phosphorylation and involves lipid kinase signalling complex comprising of the ULK1/Atg1 kinase complex, the autophagy specific class III phosphatidylinositol-3-OH kinase (PI(3)K/hVps34), Beclin 1

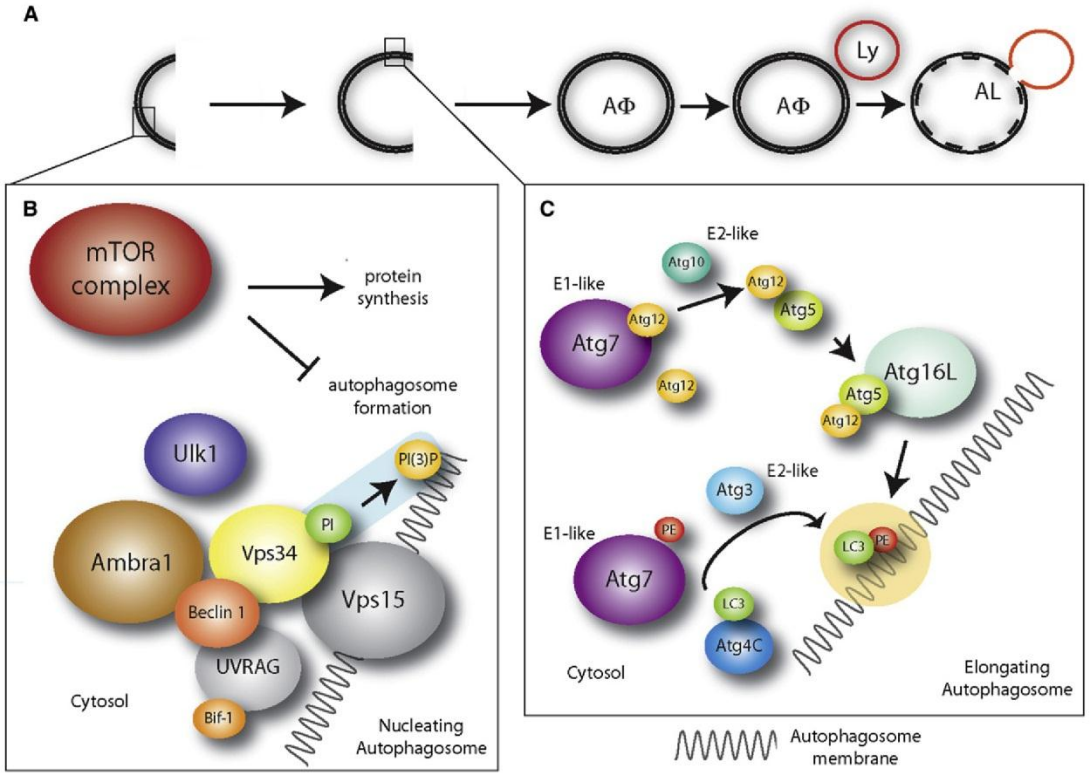

Figure 1.6: The formation of autophagosomes in mammalian cells.
(A) Autophagy is induced by the formation (nucleation) and expansion (elongation) of an isolation membrane (phagophore). Phagophore closes to form the autophagosome (Aϕ), a double-membrane vesicle that engulfs cytoplasmic components and organelles. Autophagosomes fuse with lysosomes (Ly) to form autolysosomes (AL). (B) The nucleation step is shown involving the ULK1/Atg1 kinase complex, the autophagy specific PI3-kinase complex (Beclin 1, Vps15, Vps34) and PI(3)P effectors and their related proteins. Ambra 1 promotes Beclin 1/Vps34 interaction. Additionally, UVRAG and Bif-1 are two regulators of the Beclin 1/Vps34 complex. (C) Atg12- and LC3/Atg8-conjugation systems are responsible for the elongation step. Atg7 activates LC3, LC3 is then transferred to Atg3 and modified with a lipid attachment molecule phospatidylethanolamine (PE). The complex Atg12/Atg5/Atg16L mediates the LC3-PE binding to the autophagosome membrane (adapted from [86]).

(Atg6 or Vps30 in yeast), and the coiled-coil tether p150 (hVps15 or Vps15 in yeast). p150 is important for the attachment of the complex with the isolation membranes. Phosphatidylinositol-3-phosphate recruits other effector proteins to the isolation membrane, which in turn promote expansion of the pre-autophagosomal membrane [84]. There are two major models proposed for the origin of the isolation membranes, the maturation model and the assembly model [93]. The maturation model states that the isolation membrane is derived from pre-existing cytoplasmic organelle such as the ER. The assembly model suggests that the autophagosomal membrane is established anew from localized lipid synthesis (Figure 1.7) [93].

Elongation of the Isolation membrane is induced by phosphatidylethanolamine (PE) modification of LC3/Atg8 [86], a light chain of MAP1 (MAP1LC3/LC3) (Figure 1.6) [94]. They were first identified in neurons and there are three paralogues in mammals: LC3A, LC3B and LC3C [95]. GABARAP, GEC1/GABARAPL1, GATE16/GABARAPL2 and GABARAPL3 are four additional Atg8 homologues [96]. LC3 is cleaved by the cysteine protease Atg4/autophagin to form the cytosolic LC3-I. HsAtg4B cleaves the LC3 precursor after a conserved glycine residue (Gly120), to which the amino group of PE is then conjugated [97, 98]. Thus, the modification of LC3-I to membrane-bound form

LC3-II involves two conserved ubiquitin-like conjugation systems that are arranged in a coordinated way. First, Atg12 is associated to Atg5, and then the complex formation of LC3-PE, prior to their conjugation to the isolation membrane. Atg7 acts as an E1-like ubiquitin conjugating enzyme in both cases, whereas Atg10 and Atg3 function as E2-like ubiquitin conjugating enzymes for Atg12 and LC3-I, respectively. The Atg12-Atg5 complex is localized together with Atg16 to the isolation membrane acting as an E3-like ubiquitin conjugating enzyme for the PE attachment to LC3 [99, 100].

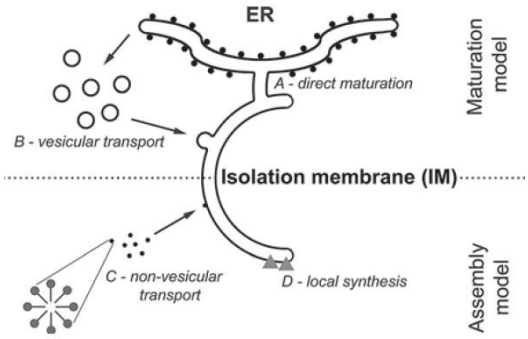

Figure 1.7: Models of the origin of the isolation membrane. The maturation modal states that the membrane may be derived directly from the ER (A), or in form of vesicular transport (B). The assembly model states that the membrane may be assembled de novo at the site of phagophore formation, originating from nonvesicular transport such as micellar (C) or local synthesis (D) (adapted from [93]).

After forming the double-membrane vacuole, the autophagosomes undergo extensive remodelling. This remodelling process, also known as autophagosome maturation, includes fusion with early and late endosomal vesicles, such as the MVBs, to form the amphisome hybrid organelle. Finally, amphisomes acquire hydrolytic enzymes through the fusion with lysosomes forming autolysosomes to degrade intraluminal components and the inner membrane [101, 102]. The digested components are then recycled to the cytosol and reused. There is a close relation between the endocytic and autophagic pathway at the molecular level as it was shown that many proteins of the endosomal pathway are involved in autophagosome maturation steps in yeast and mammalian cells, such as Rab5 [103], Rab7 [104, 105], Rab11 [106], Vam3p, SKD1 and the SNARE protein Vti1p (Figure 1.8).

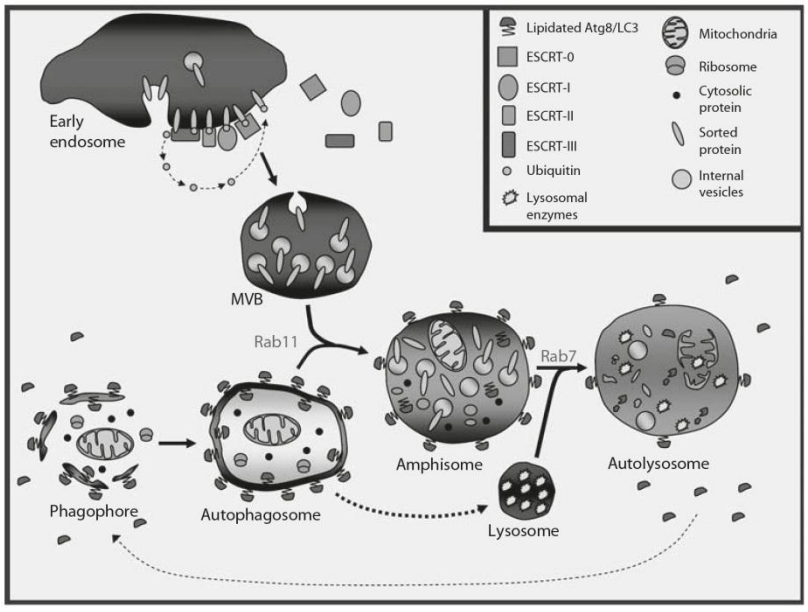

Figure 1.8: Autophagosome and MVB maturation to autolysosome. Cytosolic proteins and organelles destined for degradation are engulfed in phagophore forming autophagosome. In the endocytic pathway, proteins targeted for degradation are sorted into luminal vesicles of MVBs. Mature MVBs fuse with autophagosome to form amphisome. Finally, amphisomes fuse with lysosome to generate autophagolysosome (adapted from [87]).

1.6 SNAREs

Membrane docking and fusion are fundamental processes in cells with regard to the secretory and endocytic pathway. One of the key mediators in this processes are the soluble NSF-attachment protein receptor (SNARE) proteins [3, 107]. SNARE proteins represent a superfamily of the type II transmembrane proteins, with nine subfamilies, in which totally 36 members were identified in human [108]. The C-terminal domain of most SNAREs is attached to the membrane, while the N-terminus points toward the cytosol. The SNAREs possess a single transmembrane domain at their C-terminal ends that is bound to the SNARE motif by a short linker. The SNARE motif consists of a characteristic, conserved, and reactive heptad 60-70 residue repeat domain. Between the subgroups of SNAREs, there are differently folded domains in many SNAREs that are found between the N-terminus and SNARE motif [109, 110]. SNAREs are grouped according to their domain structure and sequence homology, as members of the vesicle associated membrane protein (VAMP), syntaxin or synaptosomal associated protein of 25 kD (SNAP-25) families [111]. Further, SNAREs are classified according to their localization, into v-SNAREs (vesicle-associated) and t-SNAREs (target membrane-associated), or, based on a conserved residue in the centre of the SNARE motif, into R- and Q-SNAREs [112]. The R- and Q-SNAREs terminology is more convincing than the v- and t-SNAREs as the latter terminology is not persuasive in describing homotypic fusion events, e.g. those between endosomes. In some respects, there is a rough correspondence of R-SNAREs to v-SNAREs and Q-SNAREs to t-SNAREs that is only true for fusion events between secretory vesicles and the plasma membrane. The Q-SNAREs can be further classified into Qa-, Qb- and Qc-SNAREs. The QabcR-rule states that all functional SNARE complexes contain one member of each subfamily [112].

Membrane fusion starts with the docking of the donor membrane to the target membrane (Figure 1.9). The first step is the nucleation that describes the formation of a *trans*-SNARE complex, consisting of one R-SNARE and three Q-SNAREs. These proteins form an extremely stable four-helix bundle that brings the lipid bilayers close together and pushes water molecules away from the fusion site, resulting in membrane fusion. The fusion event is initiated by using the free energy that is released during the formation of the extraordinary stable four-helix bundle [113, 114]. After membrane fusion, the *trans*-SNARE complex becomes the *cis*-SNARE complex because the SNARE complex now resides in the same membrane [115]. The SNARE complex needs to be dissociated to allow the SNAREs to be recycled back to their original location. The recycling of SNAREs is mediated by the AAA+ protein NSF (*N*-ethylmaleimide-sensitive factor) and the cofactor α-SNAP. α-SNAP binds to the *cis*-SNARE complex and recruits NSF, which leads to ATP hydrolysis and to the dissociation of the complex. The released SNAREs are subsequently recycled back to their resident compartment [116].

Up to date, the neuronal SNARE complex is the best studied among the SNARE complexes. The R-SNARE VAMP2 resides on the synaptic vesicle membrane, and the two Q-SNAREs syntaxin 1 (Qa) and SNAP-25 (Qbc) are located on the presynaptic plasma membrane. Membrane fusion is driven by the formation of the stable four-helix bundle that is referred to as the SNARE core complex [117, 118]. The crystal structure of the neuronal SNARE core complex resolved that the four-helix bundle consists of one coil of syntaxin 1 and VAMP2, and two coils of SNAP-25 [119]. This coiled-coil structure is kept together by 15 hydrophobic interaction-planes and a central ionic layer, in which the arginine and three glutamine of the core motif form strong hydrogen bonds [111]. The neuronal SNARE complex was first observed in fusion events of synaptic vesicles, with the active zone of presynaptic membrane. Therefore, the interaction of these three proteins is essential for synaptic transmission (Squire et al., Fundamental Neuroscience, 2003).

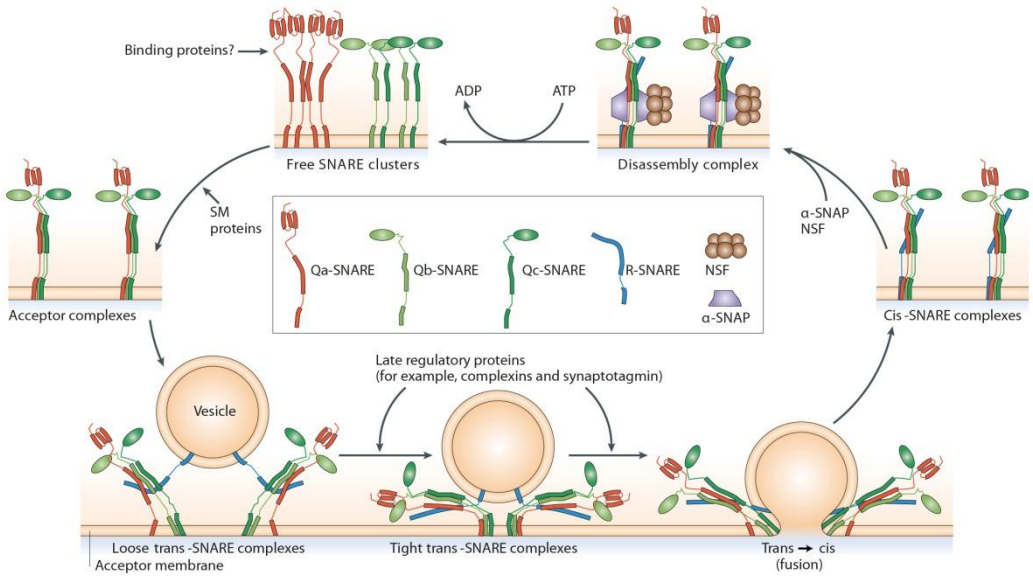

Figure 1.9: Membrane fusion is mediated by SNAREs.
One monomeric R-SNARE from the donor membrane assembles with the oligomeric Q-SNAREs at the target membrane to form a four-helix bundle, the *trans*-SNARE complex. The four-helix bundle initiates membrane fusion leading to the formation of a *cis*-SNARE complex at the target membrane. In order to recycle SNAREs, α-SNAP binds to the *cis*-SNARE complex and recruits NSF. ATP hydrolysis leads to the dissociation of the SNARE complex. The released R-SNARE can bud into vesicles to recycle back to its resident compartment (adapted from [107]).

Different SNARE complexes are necessary to perform fusion events between distinct cellular membranes and each SNARE functions in specific intracellular fusion steps that are localized in different compartments. Syntaxin 1, -2, -4, SNAP-23 and SNAP-25 are localized at the plasma membrane, VAMP2 is found on synaptic and neurosecretory vesicles, syntaxin 5 and VAMP4 in the Golgi apparatus, syntaxin 6 at the TGN, syntaxin 7 in late endosomes and lysosomes, and VAMP2/3 and syntaxin 13 in recycling endosomes [107].

In non-polarized cells, syntaxin 13 is localized to sorting endosomes and tubulovesicular recycling endosomes, in which it is involved in early endosome trafficking and in endosomal recycling of plasma membrane components [120, 121]. In neurons, syntaxin 13 is also found in tubular sorting and recycling endosomes, where it colocalizes with transferrin receptor (TfR). Syntaxin 13 is associated with recycling endosomes that are localized in both dendrites and axons [62]. Neurotransmitter receptor trafficking at dendritic spines from excitatory synapses is regulated by recycling endosomes containing syntaxin 13 [122-124]. Syntaxin 13 also plays specific roles in neurite growth [125]. Hence, recycling endosomes may be the source of membrane and protein material for activity-dependent spine potentiation and growth.

SNAREs ensure specific membrane docking and fusion, but additional specificity is mediated by tethering proteins that dock the membranes prior to SNARE complex formation. One of the regulatory proteins determining membrane association is the Rab family of small GTPases. Rab tethers collaborate with SNAREs to ensure correct fusion between membranes.

1.7 Rab proteins

Rab GTPases are members of the Ras-like small GTP-binding protein superfamily, which function as molecular switches that cycle between GTP- (active) and GDP-bound (inactive) conformations. This family also includes Ras, Ran, ARF and Rac/Rho GTPases. More than 60 different Rab family members were identified in humans and 11 were found in yeast [126, 127]. Different Rab GTPases are localized to the cytosolic face of distinct intracellular membranes, where they regulate intracellular membrane trafficking [126]. Rab GTPases undergo cycles of membrane association and cytosolic localization, which is tightly coupled to the guanine nucleotide cycle. This process is strictly regulated by a large number of Rab associated proteins (Figure 1.10). Rab GTPases associates with the membrane through a hydrophobic geranylgeranyl tail that is the result of post-translational modification at the C-terminus. Newly synthesized Rab proteins in the cytosol, in their GDP-bound state, are recognized and bound by a Rab escort protein (REP), that targets Rab proteins to Rab prenyltransferase (RGGT) [128]. RGGT prenylates Rab proteins by addition of geranylgeranyl isoprenoids on one or two C-terminal cysteine residues, present in CC or CXC motifs. The cytosolic GDP dissociation inhibitor (GDI) forms a complex with GDP-bound Rab proteins, shields the geranylgeranyl tail from the hydrophilic environment, and therefore maintains Rab soluble in the cytosol. At the membrane, GDI is then replaced by the GDI displacement factor (GDF) to liberate the prenyl groups promoting membrane association. Rab proteins are subsequently activated by the release of GDP, and through the loading of GTP, promoted by guanidine nucleotide exchange factor (GEF). In the GTP-bound form, Rab is then free to interact with downstream effector proteins. The active state of Rab proteins is terminated by GTP hydrolysis catalyzed by GTPase activating proteins (GAPs) [129]. The cycle of membrane association and membrane extraction can then be restarted.

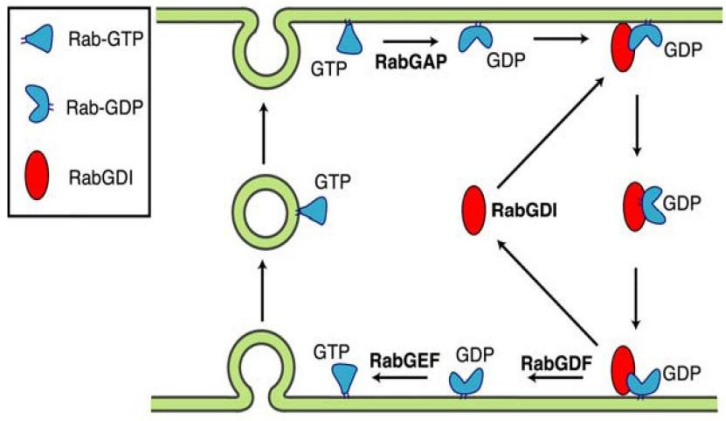

Figure 1.10: Rab GTPase undergoes a cycle of membrane association and membrane extraction. Rab forms a complex with cytosolic GDP-dissociation inhibitor (RabGDI) after GTP hydrolysis. GDI displacement factor (GDF) replaces GDI that promotes association of Rab to the membrane. GDP is exchanged by GTP promoted by guanidine nucleotide exchange factor (RabGEF). In the GTP-bound form, Rab is then free to interact with downstream effector proteins. The active state of Rab proteins is terminated by GTP hydrolysis catalyzed by GTPase activating proteins (RabGAP).

In the activated and GTP-bound state, Rab proteins recruit and interact with Rab effector proteins that represent a very heterogeneous group of proteins. Rab effector proteins cover a variety of functions. They are involved in the sorting during vesicle formation (e.g. TIP47) [130], in the regulation of intracellular transport, in which they function as motor or motor adapters (e.g. Rabkinesin-6, myosinVa) [131, 132], and in vesicle tethering (e.g. EEA1, Golgins, TRAPP-I, TRAP-II, HOPS, VPS) [133]. Rab proteins also play a role in membrane fusion, where they indirectly regulate SNARE functions through Rab effectors. Therefore, Rab proteins are crucial in tethering and docking

processes between organelles, which then lead to membrane fusion. Thus, it has been proposed that the Rab domain is a prerequisite for the appropriate *trans*-SNARE pairing upon tethering or docking. Different Rab GTPases are localized to the cytosolic face of distinct intracellular membranes, where they regulate endocytic membrane traffic. For example, Rab1 is located at the ER exit sites, and in the pre-Golgi intermediate compartment (IC), and it is involved in the tethering of ER-derived vesicles to the Golgi complex. Rab6, Rab33 and Rab40 are localized to the Golgi and mediate intra-Golgi trafficking. Rab6 also regulates the movement of vesicles and organelles along microtubules by direct interaction with Rabkinesin-6 [131, 134]. Rab33, together with Rab24, regulate the formation of autophagosomes. Rab3 is present on the synaptic vesicle surface, and regulates vesicle availability or docking to release sites. Rab5 is localized to sorting endosomes and plasma membrane, and it mediates endocytosis and homotypic early endosome fusion of clathrin-coated vesicles [135, 136]. Rab11 is involved in the slow endocytic recycling pathway through recycling endosome, whereas Rab4 regulates the fast endocytic recycling pathway directly from sorting endosomes. The late endosome-associated Rab7 plays a role in the maturation of late endosome and their fusion with lysosomes. Rab9 also resides in late endosomes and mediates trafficking from late endosomes to the TGN (Figure 1.11) [137].

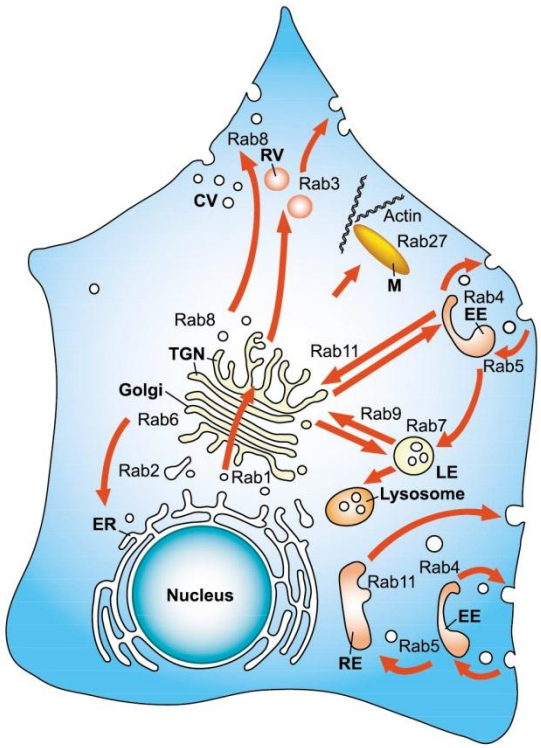

Figure 1.11: Subcellular localization of selected Rab proteins. The biosynthetic and endocytic circuits (arrows) are shown. ER, endoplasmatic reticulum; TGN, *trans*-Golgi network; CV, constitutive secretory vesicles; RV, regulated secretory vesicles; M, melanosomes; EE, early endosomes; LE, late endosomes; RE, recycling endosomes (adapted from [127]).

Different Rab proteins are localized to distinct organelles, and it has been shown, that different Rab proteins localized on the same organelle are clustered in distinct membrane microdomains called the Rab domains [138]. The sorting endosomes comprise only of Rab5, or of a combination of Rab4 and Rab5, whereas recycling endosomes contain distinct domains of Rab4 and Rab11. Exogenously applied transferrin as endocytic marker was found to pass these domains. Rab5 seems to be responsible for the delivery of endocytic vesicles to early endosomes, where Rab4 and Rab11 take over and recycle receptors back to the cell surface. Late endosomes comprise of distinct membrane domains that carry Rab7 or Rab9, respectively. M6PRs are strongly accumulated at Rab9

microdomains [139]. These Rab domains are dynamic but seem to keep a relatively stable distribution over time.

1.8 Rab11 and Rab11-interacting proteins

There are three members of the Rab11 subfamily, namely Rab11a, Rab11b and Rab25. Rab11a and Rab11b are expressed ubiquitously and Rab25 is expressed almost only in epithelial cells. Rab11 is localized to the TGN, post-Golgi vesicles and recycling endosomes [140]. In MDCK cells, Rab11 is involved in apical recycling and targeting [141]. In parietal epithelia cells, Rab11 is enriched in tubulovesicular structures containing H^+/K^+ ATPase where it regulates the delivery of H^+/K^+ ATPase to the apical membrane [142]. Rab11 is involved in the exit of the membrane from the ERC [143]. It was shown in CHO cells that Rab11 regulates the late recycling of TfR form ERC to the plasma membrane [140, 144], as the dominant-negative mutant of Rab11 did not block the access of transferrin to tubular endosomes. It has also been shown that Rab11 plays a role in biosynthetic exocytic membrane trafficking [145] because Rab11 is involved in post-Golgi trafficking of rhodopsin to the photosensitive apical membrane of Drosophila photoreceptors [146], or the trafficking and basolateral targeting of E-cadherin [147]. Therefore, Rab11 is responsible for the polarized sorting of various proteins.

Different Rab11-effector proteins have been identified such as FIPs, Rabphilin-11/Rab11BP [148], myosin Vb [149], phosphoinositide 4-kinase β and Sec15 [150]. There are five members of the family of Rab11-interacting proteins (FIPs), Rip11/Gaf-1, FIP2, RCP/FIP1C, FIP3/Efrin and FIP4/Arfophilin-2 that are predominantly membrane-bound and localize to the endosomal recycling compartment. Even though the degree of sequence homology between the FIPs is low, they all share a highly conserved 20-amino acid motif at the C-terminus of the protein, referred to as the Rab11/25 binding domain (RBD). Crystal structure of Rab11 in complex with FIPs shows that the RBD of the FIPs forms an α-helical parallel coiled-coil homodimer, creating two hydrophobic Rab11-binding patches, that interact with the switch I and switch II regions of two Rab11 proteins [151]. FIPs have the ability to self-interact in order to form a homodimeric complex. Furthermore, FIP2, Rip11 and FIP3 can interact with each other, indicating a hetero-binding ability [152]. Hence, Rab11 and FIPs form a heterotetrameric complex, arranged in a Rab11-$(FIP)_2$-Rab11 conformation. Based on the primary structure of the FIPs, there are two different types of putative calcium-binding domains at their N-termini that form the basis to divide the FIPs in two classes (Figure 1.12). Rip11, FIP2 and RCP belong to the class I FIPs. The characteristic hallmark of this class is a C2 domain at the N-terminus. C2 domains are approximately 130 amino acid motifs known to act as binding modules for protein-protein and protein-phospholipid interactions [153]. The C2 domain of the class I FIPs plays a crucial role in subcellular localization of the FIPs. The FIPs preferentially bind to phosphatidylinositol-(3, 4, 5)-trisphosphat [PtdIns(3,4,5)P_3] and the second messenger phosphatidic acid (PA). It was suggested that the C2 domains of the FIPs mediate the targeting of these proteins to docking sites at plasma membranes enriched in PtdIns(3,4,5)P_3 and PA [153]. The class II FIPs include FIP3 and FIP4. They possess an ezrin-radixin-moesin (ERM) domain, EF hands and a prolin-rich domain.

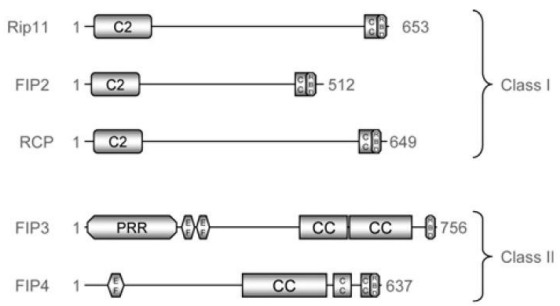

Figure 1.12: The two classes of Rab11-FIPs. There are five members of the Rab11-FIPs. Based on sequence homology, FIPs are divided into two distinct classes. Class I FIPs consists of Rip11, FIP2 and RCP, whereas class II FIPs contain FIP3 and FIP4 (adapted from [154]).

In the last decade, Rab11-FIPs were extensively studied and tremendous progress was achieved regarding the functional aspect of Rab11-FIPs. It was proposed that different Rab11-FIPs form mutually exclusive complexes with Rab11, therefore directing Rab11 to different membrane trafficking pathways [155]. The Rab11-FIPs have been identified as key players in the regulation of several distinct intracellular membrane trafficking events [154]. Their cellular functions are grouped into three categories: recycling of cargo to the cell surface, delivery of the membrane to the cleavage furrow/midbody during cell division, and linkers between Rab11 and molecular motor proteins [154]. Other than the remaining FIPs of the class I, RCP can also bind the Rab4 GTPase [156], and RCP has been associated with regulating protein recycling from the sorting and recycling endosome to the plasma membrane. It was shown that RCP, in complex with Rab11, is involved in the sorting of TfR into the recycling pathway and not into the degradative pathway [157]. RCP is also involved in recycling $\alpha 5\beta 1$ integrin and EGFR1, and in regulating $\alpha 5\beta 1$ integrin-dependent cell motility by increasing fibronectin-dependent migration of tumour cells into three-dimensional microenvironments [158]. FIP2 is also responsible for the recycling of cargo molecules to the cell surface, such as aquaporin-2 and CXC chemokine receptor 2 [159, 160]. Additionally, there is a FIP2 function in LTP because disruption of FIP2 function blocks the recycling of AMPA receptors and dendritic spine growth in postsynaptic neurons [161]. The recycling and trafficking of all these proteins are regulated by the complex composed of myosin Vb, Rab11 and FIP2 [159, 161, 162]. Rip11 was shown to interact with kinesin II, and this complex regulates the sorting of internalized receptors to the slow recycling pathway [163]. Rip11 has also been associated with the translocation of GLUT4 transporter-containing vesicles to the cell surface of adipocytes in response to insulin treatment [164]. Rip11 and Rab11 localize to apical organelles and the apical plasma membrane in MDCK cells [165]. The cytosolic fraction of Rip11 showed higher phosphorylation levels than membrane associated with Rip11, suggesting that membrane association might be regulated by certain kinases. Another study showed that Rip11 interacts with γ-SNAP [166]. γ-SNAP is a member of the SNAP family and is involved in intracellular membrane trafficking [167].

The γ-SNAP-associated factor (Gaf-1b) was recently identified as a new splice variant of Rip11. An additional 565 amino acid splice insert of Gaf-1b differ Gaf-1b from Rip11. The human Rip11/Gaf-1b gene is located on chromosome 2, spans roughly 40 kb and contains 6 exons [168]. Rip11 is encoded by exons 1, 2, 3, 5 and 6. Exons 5 and 6 encode for the C-terminal region that is common to Rip11 and Gaf-1b. Exon 4 encodes the specific splice insert of Gaf-1b. Kawase *et al.,* (2003) showed that Rip11 and Gaf-1b are localized to microsomes and recycling endosomes.

We recently identified an interaction between Gaf-1b and the neuronal transmembrane protein calsyntenin-1 in immunoprecipitation from mouse brain membranes. Using organelle immunoisolation with anti-calsyntenin-1 antibody, we isolated organelles that contained Gaf-1b/Rip11, Rab11, syntaxin

13 and many other proteins that link Gaf-1b and calsyntenin-1 to recycling-endosomal functions. Additionally, in a yeast two-hybrid screen approach, we identified GABRAPL2 as a new interaction partner of Gaf-1b. Starvation experiments indicate that Gaf-1b is associated with autophagy.

1.9 The calsyntenin family

Calsyntenin-1 (Cst1) belongs to the cadherin superfamily and is a neuronal type I transmembrane protein that is localized to the postsynaptic membrane in the adult mouse brain [169]. Vogt *et al.,* 2001, originally identified calsyntenin-1 in an *in vitro* screen for target protein extracellular proteases, and suggested that calsyntenin-1 played a role in postsynaptic calcium signalling. The mature calsyntenin-1 protein is composed of an extracellular N-terminal part of 831 amino acids (115 kD), a transmembrane moiety of 19 amino acids, and a cytoplasmic segment of 100 amino acids. Calsyntenin-1 contains two cadherin-like domains, and a laminin G-like domain at the N-terminus, and a highly acidic region in the cytoplasmic C-terminus. The acidic stretch of thirty-nine amino acids is flanked by two highly conserved sequence motif with the core sequence “WDDS”. Such long acidic stretches were shown to have a calcium-binding property, and calsyntenin-1 has been demonstrated to bind calcium with low affinity but high capacity [169]. Besides calsyntenin-1, other members of the calsyntenins family have been identified in humans and mice, namely calsyntenin-2 (Cst2) and calsyntenin-3 (Cst3) [170]. Calsyntenin-1 contains an amino acid sequence identity to calsyntenin-2 and calsyntenin-3 of 58% and 94% in human, and 56% and 51% in mouse, respectively. The three calsyntenins are highly homologue in their extracellular segments but differ significantly from each other in the central and distal parts of the cytoplasmic segments (Figure 1.13). In the extracellular moiety they all form a cleavegeable signal peptide in their first 20 amino acid sequence. The two cadherin-like repeats, the laminin G-like domain and the single transmembrane domain, are all located at the same positions. The central part of the cytoplasmic moiety in calsyntenin-2 is still rich in acidic

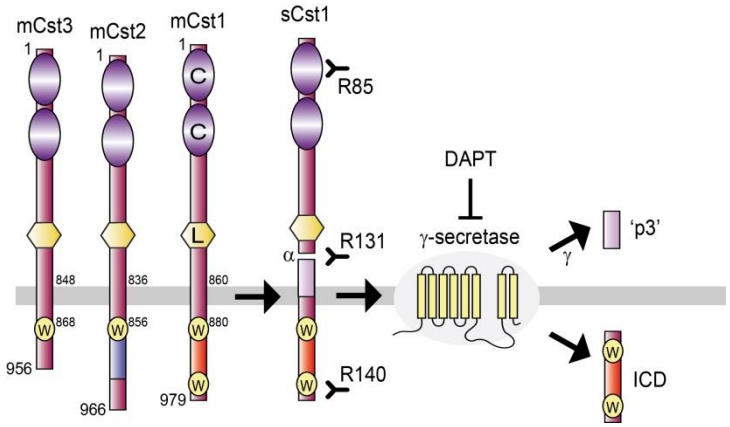

Figure 1.13: Schematic representation of the domain structure and proteolytic processing of the calsyntenin family members.

Calsyntenins are type I transmembrane proteins containing two N-terminal cadherin-like domains (C) , a laminin G-like domain (L), a transmembrane domain and a cytoplasmic domain. The cytoplasmic segment of calsyntenin-1 contains much more acidic residues compared to calsyntenin-2. The cytoplasmic domain of calsyntenin-3 is less acidic and much shorter than those of calsyntenin-1 and calsyntenin-2. All three calsyntenins possess the kinesin-binding segment with a WDDS core motif (W), two in calsyntenin-1 and calsyntenin-2 and one in calsyntenin-3. All three calsyntenins undergo ectodomain shedding by α-secretases. The transmembrane stump is subsequently cleaved in the transmembrane domain by γ-secretase. Activity of γ-secretase can be inhibited by DAPT. Cst1, calsyntenin-1; Cst2, calsyntenin-2; Cst3, calsyntenin-3.

amino acids, but the total number of acidic amino acids and the size of contiguous acidic amino acids clusters are lower than in calsyntenin-1. The C-terminus of human and murine calsyntenin-2 differs significantly from calsyntenin-1. The cytoplasmic part of calsyntenin-3 is obviously shorter and lacks most of the acidic stretch found in calsyntenin-1 and calsyntenin-2 (Figure 1.14). All three calsyntenins are predominantly expressed in the brain. Additionally, low expression level for calsyntenin-1 was found in the kidney, the lung, the skeletal muscle, the heart, and the testis [170]. In neurons, calsyntenins are located in the postsynaptic membrane of asymmetric synapses. The neuronal expression pattern for each calsyntenin member is different. Calsyntenin-1 is especially expressed in CNS neurons, while the expression level of calsyntenin-2 and calsyntenin-3 is obviously variable across distinct neuronal subpopulations. Different neuronal expression patterns of the calsyntenin members suggest a specific function of the calsyntenin-1, calsyntenin-2, and calsyntenin-3 in distinct neuronal subpopulations [170].

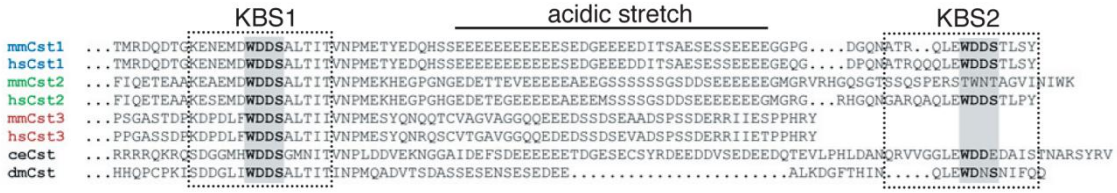

Figure 1.14: Sequence alignment of the cytoplasmic segment of calsyntenins.
Note, the acidic stretch is less acidic in calsyntenin-2 and calsyntenin-3 compared to calsyntenin-1. Cst1, calsyntenin-1; Cst2, calsyntenin-2; Cst3, calsyntenin-3 (adapted from [171]).

We recently identified the kinesin-light chain 1 (KLC1), the light chain subunit of the microtubule-dependent motor complex kinesin-1, as an interaction partner of calsyntenin-1 [171]. The two conserved WDDS motifs in the cytoplasmic moiety of calsyntenin-1 were shown to be involved in the direct interaction with the TPR domains of KLC1. Therefore, they were termed kinesin-binding segment 1 and 2 (KBS1 and KBS2). Mutations in the conserved KBS1 and KBS2 almost completely disrupted the binding to KLC1 *in vitro,* but also impaired vesicular transport of calsyntenin-1 containing organelles along axons. These data indicate calsyntenin-1 functions in the anterograde and kinesin-1-mediated transport of tubulovesicular organelles along axons [171].

Calsyntenin-1 undergoes a two-step proteolytic processing that is very similar to the processing step of the amyloid precursor protein (APP) (Figure 1.13). Firstly, calsyntenin-1 is cleaved in the juxtamembrane region of its extracellular segment to yield the soluble ectodomain that is enriched in the cerebrospinal and vitreous fluid [169]. Secondly, the C-terminal fragment is further cleaved within the transmembrane domain by γ-secretase [172]. Recently, it was shown that the extracellular segment of calsyntenin-1 is cleaved by the α-secretase ADAM10 and ADAM17, but not the β-secretase BACE1 [173]. The C-terminal product appears to degrade rapidly, but it was also demonstrated that the intracellular domain fragment (ICD) of calsyntenin-1 inhibits the AICD/Fe65/Tip60-mediated nuclear transactivation activity of APP, probably through the competition with calsyntenin-1 ICD and AICD for binding to Fe65 [174].

Calsyntenins and APP share many features. They are both neuronal type I transmembrane proteins, and they undergo similar proteolytic processing steps; ectodomain shedding followed by regulated intramembrane proteolysis [172, 174]. Additionally, both proteins are transported by kinesin-1 in axons [175]. Calsyntenins (also termed as alcadeins) were shown to form a tripartite complex with APP and the adaptor protein Mint2 (also termed as X11L) that stabilizes the intracellular full-length

APP by inhibiting ectodomain shedding and adjacent presenilin-dependent cleavage. Mint2, as well as Fe65, interact with the cytoplasmic domain of APP through a conserved NPTY motif, whereas calsyntenin-1 binds to both adaptor proteins through a similar motif (NPMETY), and was shown to stabilize full-length APP by a mechanism dependent on Mint2 [174]. These data indicate that calsyntenin-1 might have a protector function in the APP metabolism that is misregulated in Alzheimer's disease.

We recently showed that APP exits the TGN in association with calsyntenin-1 in tubulovesicular organelles in a kinesin-1-dependent manner [176], and that these vesicles are transported anterogradely along axons [171, 177]. Using organelle immunoisolation and proteomics, we then found that axons contained at least two distinct, non-overlapping calsyntenin-1-containing transport packages. One is characterized by the presence of APP and early-endosomal markers, the other contains recycling-endosomal markers as well as Rip11/Gaf-1b (Figure 1.15) [178]. The calsyntenin-1/APP organelles that are co-transported anterogradely along axons, contain BACE1, but not ADAM10. Interestingly, incubation studies with immunoisolated vesicles indicated that APP contained in calsyntenin-1/APP organelles was stable against BACE1 premature cleavage. This result indicates that calsyntenin-1 provide a protective mechanism for axonal transport of APP [177].

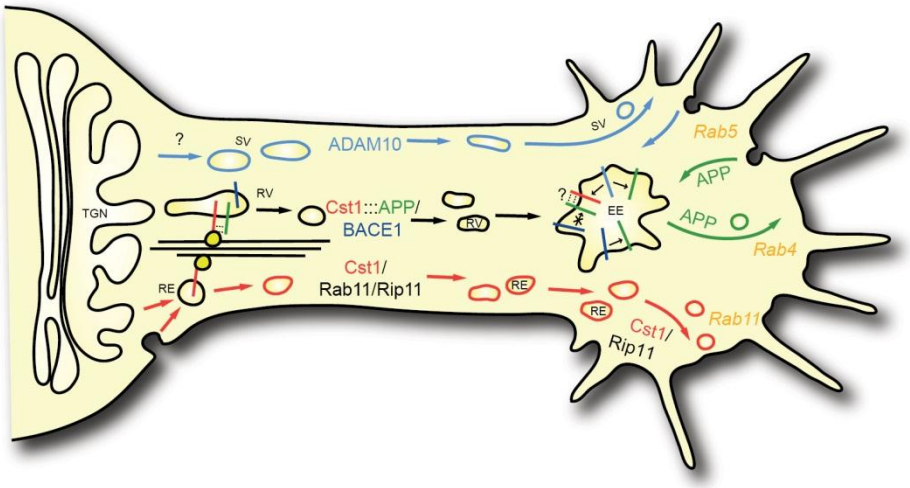

Figure 1.15: Model of the itinerary of vesicular calsyntenin-1/APP and calsyntenin-1/Rab11 forming distinct transport packages for anterograde axonal transport to the growth cone.

Axons contained at least two distinct, non-overlapping calsyntenin-1-containing transport packages. The calsyntenin-1/APP/BACE1 transport packages (black) transport full-length APP to EEs in the C-domain of growth cones. The calsyntenin-1/Rab11/Rip11 transport packages (red) deliver recycling proteins to the RE in an independent APP-free anterograde transport route. ADAM10 is transported to the plasma membrane on a calsyntenin-1-independent transport route. Cst1, calsyntenin-1; TGN, *trans*-Golgi network; SV, secretory vesicle; RV, calsyntenin-1-containing early-endosomal replenishment vesicle; RE, calsyntenin-1-containing recycling-endosomal vesicle; EE, early endosome (adapted from [177]).

1.10 GABARAP-likes and MAP1LC3 family

In yeast, the autophagy-related protein 8 (Atg8) functions in the formation step of autophagosomes [179]. In mammals, at least eight Atg8 orthologues have been identified, and, based on their amino acid sequence homology, they are divided into LC3 (LC3A-C) and the GABARAP/GATE-16 (GABARAP, GATE-16/GABARAPL2, GEC1/GABARAPL1) subfamilies [180, 181]. GABARAP, GABARAPL1, GABARAPL2 and LC3 are all expressed in the whole brain. GABARAP is expressed differently throughout the rat brain, with strongest expression in the pituitary gland and weaker expression in the cerebellum, the pons, the olfactory bulb, the cortex, the hippocampal formation, and the diencephalon. The highest mRNA levels of GABARAPL1 are in the pons and diencephalon, and there is a weaker expression in the cerebellum, the olfactory bulb, the cortex, the pituitary gland, the hippocampal formation, and the cerebral nuclei. LC3 shows a similar expression pattern to that of GABARAPL1, but the expression level is lower in all the brain subregions compared to GABARAPL1. GABARAPL2 is very weakly expressed in all the subregions of the brain. It was shown in rat brains, that GABARAPL1 is expressed the strongest, followed by LC3, GABARAP, and GABARAPL2 [182].

LC3 was first identified in neurons as one of the three light chains (LC1, LC2 and LC3) of the microtubule-associated protein 1A and 1B (MAP1A and MAP1B) [95]. Three paralogue genes encode for LC3 in human, namely LC3A, LC3B and LC3C, and they show different expression patterns in distinct tissues. Also, the subcellular location patterns vary slightly [181]. Post-translational modification of LC3 results in the conversion of the C-terminally truncated, cytosolic form-I of LC3 to its lipidated, membrane-bound form-II. LC3 is associated with lysosomal transport and degradation via autophagy. The conversion of LC3-I to LC3-II is highly enhanced in cells under starvation condition that efficiently induce autophagy, and the association of LC3 with autophagosomal and pre-autophagosomal membranes was found to depend on form-II. The amount of LC3-II correlates well with the number of autophagosomes. Therefore, LC3 is a reliable autophagosomal marker [83, 98].

GABARAP ($GABA_A$ receptor associated protein) was identified as an interaction protein of the γ2-subunit of the $GABA_A$ receptor that links the receptor with microtubules [183, 184]. It was shown that GABARAP is involved in the targeting of the γ2-subunit of the $GABA_A$ receptor to the plasma membrane [185]. The fact that GABARAP is preferentially expressed in the pituitary gland suggests that GABARAP may play a role in vesicle transport specifically in glandular tissues [182]. With the increasing number of identified interaction partners of GABARAP, GABARAP may play a wider role in a variety of different cellular processes, such as autophagy, apoptosis, vesicular transport, fusion events, synaptic plasticity, calcium homeostasis, and cell adhesion [186].

GABARAPL2 and GABARAPL1 are also termed as Golgi-associated ATPase Enhancer of 16 kD (GATE-16) and GEC1 (derived from glandular epithelial cells), respectively. They are both small 117 residue globular proteins, and belong to the ubiquitin-like superfamily. Crystal structure analysis and homology modelling showed that they possess a central ubiquitin-like fold with two additional N-terminal α-helices that are highly positively charged and are involved in tubulin binding. The ubiquitin-like core domain comprises of two parallel β-strands that are flanked by two anti-parallel β-strands [187, 188]. GABARAP has two hydrophobic pockets on one face of the core domain that are highly conserved among the other GABARAP homologues, including GABARAPL1 and GABARAPL2. These pockets exhibit high binding affinity for indole derivates, thus indicating an important role for protein-protein interaction [189].

GABARAPL1 was identified as a linker between the $GABA_A$ receptor and microtubules where it directly interacts with them [183, 184]. Additionally, through the interaction of GABARAPL1 and tubulin, it was shown that GABARAPL1 promotes tubulin assembly and microtubule bundling. GABARAPL1 interacts with another receptor, the human κ-opioid receptor (hKOR) [190]. The interaction of GABARAPL1 with the $GABA_A$ receptor and hKOR suggests that GABARAPL1 plays a role in the signal transmission by targeting these membrane receptors to the cell surface. The interaction of GABARAPL1 with tubulin and NSF may contribute to the intracellular transport of $GABA_A$ receptor and hKOR [184, 191]. Recent studies also associate GABARAPL1 with autophagy. It was demonstrated that GABARAPL1 localizes to autophagic vacuoles upon inhibition of lyosomal enzyme activity in MCF7 and HEK293 cells [192]. GABARAPL1 accumulates in punctuated structures in the cytoplasm upon starvation in wild-type mouse embryonal fibroblasts (MEFs), while in Atg4B deficient MEFs this effect is abolished [193].

GABARAPL2 was shown to localize at the Golgi complex and to regulate docking and fusion processes in intra-Golgi traffic and Golgi assembly form mitotic fragments through the interaction with NSF and the Golgi v-SNARE GOS-28 [194, 195]. The interaction with NSF was reported to stimulate the ATPase activity of NSF, and thereby enhance NSF-driven *trans*-SNARE complex disassembly. The interaction of GABARAPL2 with GOS-28 prevents the binding of GOS-28 to its cognate t-SNARE component syntaxin 5, and it protects the labile, unpaired GOS-28 from proteolysis upon NSF-driven SNARE disassembly [196, 197]. This data suggest that GABARAPL2 acts as a regulator of SNARE pairing. It was reported that Atg8 can partially replace GABARAPL2 in the intra-Golgi transport assay [195], and that Atg8 mediates tethering and hemifusion of membranes in *in vitro* fusion experiments with liposomes [198], hence suggesting that GABARAPL2 and its homologues have a conserved role as regulators of membrane fusion events and SNARE activity. Furthermore, GABARAPL2 has been associated with autophagic processes. The membrane-bound form-II of GABARAPL2 is upregulated and relocalized to LC3-positive structures upon starvation [98]. It was also shown that GABARAPL2 is essential for autophagosome biogenesis [199].

1.11 Aims

During my master thesis we showed a specific interaction between the very C-terminus of the cytoplasmic tail of calsyntenin-1 and Gaf-1b. Immunoprecipitation experiments and immunocytochemistry showed that calsyntenin-1 and Gaf-1b are associated with the recycling-endosomal protein syntaxin 13. We thus suggest that calsyntenin-1 links a certain type of SNARE complex containing syntaxin 13 to Gaf-1b, which in turn recruits the small GTPase Rab11. Altogether, we suggested that calsyntenin-1 plays a role in the transport and/or the appropriate docking and fusion of recycling endosomes by recruiting kinesin-1, SNAREs and Rab GTPases.

The ultimate aim of this PhD thesis was to continue characterizing the function and the physical and spatial interaction of Gaf-1b and calsyntenin-1, in particular of the Gaf-1b and calsyntenin-1 interaction in the endosomal recycling pathway. Because calsyntenin-1 mediates APP exit in a kinesin-1-dependent manner, we wondered whether Gaf-1b is also associated with this process. Overexpression and immunocytochemistry studies revealed that Gaf-1b trafficking is disrupted upon blockage of calsyntenin-1 and KLC1 TGN exit. Furthermore, we were interested in the biochemical, functional, and dynamic properties of calsyntenin-1-containing organelles, and in their cargo content. The organelle population containing endosomal recycling protein, as well as Gaf-1b/Rip11, was in the focus of our interest. Therefore, we wanted to know how Gaf-1b and calsyntenin-1 are related to the endosomal recycling pathway, and we asked whether Rab11 was able to interact with Gaf-1b and calsyntenin-1. To this end, we performed GST pull-down experiments from mouse brain homogenates and transfected HeLa cells to characterize the interaction of Gaf-1b and calsyntenin-1 with different Rab proteins. Next, we characterized the involvement of Gaf-1b in receptor recycling, such as TfR, EGFR and Erbs, by using siRNA knock-down assay and Western blot analysis. Gaf-1b overexpression and downregulation experiments showed a notable effect on the cell morphology and cell viability, respectively, which prompted us to investigate the cytoskeleton in more detail in relation to Gaf-1b. In order to get more insight into the function of Gaf-1b, we searched for a new interaction partner of Gaf-1b, using a yeast two-hybrid screen. The newly identified interaction partner of Gaf-1b was then characterized and associated Gaf-1b with autophagy. Altogether, we performed a combinatorial approach to reach our aim, applying biochemical, cell-biological and immunocytochemical techniques on primary neuronal cultures, *in vivo* material isolated from mouse brains, and from heterologous cell culture systems. Conventional protein-protein interaction assays, pharmacological approaches, downregulation assays, confocal and live cell imaging were used to unriddle the function of Gaf-1b in intracellular processes.

2. Results

2.1 Gaf-1b is a novel interaction partner of calsyntenin-1

Previously we elucidated the function of calsyntenin-1 in the transport of kinesin-1-dependent post-Golgi vesicular carriers to axonal growth cones [176]. These carriers represented two distinct, non-overlapping transport packages of calsyntenin-1, the calsyntenin-1/APP/BACE1 and calsyntenin-1/Rab11 organelles [200]. Calsyntenin-1 as an one-way cargo-docking molecule was shown to be an essential element for sheltered anterograde transport of APP. It has been demonstrated to protect the APP cargo from premature proteolytic degradation by ADAM10 and BACE1 during transport [177].

In order to gain more information on the function of calsyntenin-1, we aimed at identifying new interaction partners of calsyntenin-1. A former lab member (A. Konecna) performed immunoprecipitations (IP) from solubilized V1 membranes of P6 mice. The different membrane fractions were prepared by differential centrifugation as described previously [171, 201, 202] and solubilized in IP-buffer. The cell lysate was subjected to immunoprecipitations using the affinity-purified anti-calsyntenin-1 antibodies R85, R140, or the protein-A-purified R140 pre-immune IgGs as a control. Immunoprecipitates were loaded on a 4-12% Bis-Tris gel and proteins were stained with Coomassie dye that was compatible with mass spectrometry (MS). Stained gel bands that specifically co-immunoprecipitated in R85 and R140 IPs were cut out of the gel, digested with trypsin and subjected to MS analysis. As anticipated, R140 precipitated full-length calsyntenin-1, while R85 immunoprecipitated full-length calsyntenin-1 and the ectodomain of calsyntenin-1 (Figure 2.1 A). Only R85 co-immunoprecipitated a major band with a molecular weight of about 300 kD, which was identified as microtubule-associated protein 2 (MAP2). On the contrary, only R140 co-immunoprecipitated a major band with an apparent molecular weight of about 200 kD and a minor band running slightly below 200 kD. Both bands and a third band running at about 150 kD were identified as Gaf-1b (KIAA0857). Altogether, twelve peptide fragments could be clearly assigned to the mouse Gaf-1b sequence. Gaf-1b was recently identified as a splice variant of Rip11, a Rab11-interacting protein, and has been implicated in endosomal recycling function [165, 168]. The domain structure of Rip11 and its splice variant Gaf-1b has been illustrated in Figure 2.1 B. Gaf-1b and Rip11 belong to the class 1 family of Rab11-interacting proteins (Rab11-FIPs). The hallmark of this class is the N-terminal C2 domain and all Rab11-FIPs contain a C-terminal Rab11/Rab25-binding domain (RBD) [154]. Gaf-1b differs from Rip11 by the presence of an alternative and large 565 amino acid splice insert.

To confirm the previous result by Western blotting, we performed IPs from solubilized V1 membranes of P6-P8 mice using the antibodies R85 and R140 for precipitating calsyntenin-1 and anti-Gaf-1b antibody A and C for precipitating Gaf-1b and Rip11. The polyclonal antibodies R140 co-immunoprecipitated Gaf-1b, but R85 did not (Figure 2.1 C). Interestingly, none of the calsyntenin-1 antibodies co-immunoprecipitated Rip11. The anti-Gaf-1b antibody A and C immunoprecipitated Gaf-1b and Rip11, but did not co-immunoprecipitate calsyntenin-1. Neither calsyntenin-1 nor Gaf-1b was precipitated with non-immune IgG and all immunoprecipitates were exempt of APP, indicating a specific interaction between calsyntenin-1 and Gaf-1b in V1 mouse brain membranes. Further, we verified the presence of calsyntenin-1/Gaf-1b complex by immunoprecipitations from cultured cortical neurons (data not shown), clearly showing that calsyntenin-1 and Gaf-1b form a complex in neurons.

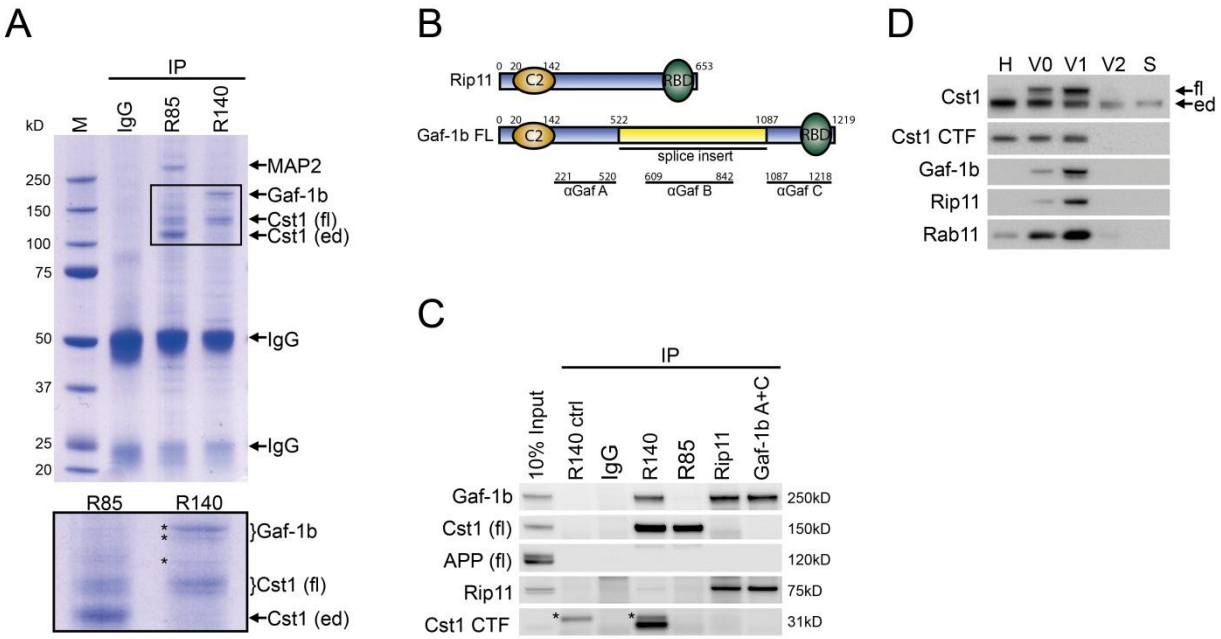

Figure 2.1: Gaf-1b is a novel interaction partner of calsyntenin-1.
(A) V1 brain fraction were prepared from P6 mouse brains by subcellular fractionation, solubilized and subjected to immunoprecipitations (IPs) using the indicated antibodies. Immunoprecipitates were separated on a 4-12% Bis-Tris gel and analysed by Coomassie blue staining. The molecular weight marker and the IgG heavy and light chains are indicated. Full-length calsyntenin-1 and its ectodomain were precipitated and are indicated. Interaction partners of calsyntenin-1 were identified by mass spectrometry of in-gel digested protein. Two major proteins co-immunoprecipitated with antibodies R140 or R85 were identified as Gaf-1b and MAP2, respectively. Three distinct bands belong to Gaf-1b (see asterisks, magnification of the boxed area). (B) Schematic drawing showing the domain structure of the splice variant Rip11 and Gaf-1b. Both protein contain a N-terminal C2 domain and a C-terminal Rab11/25 binding domain (RBD). Gaf-1b possesses a 564 amino acid splice insert in the central region of the protein (yellow). Antigens used to produce antibodies anti-Gaf1b A, B and C against Rip11/Gaf-1b are shown. (C) V1 brain fraction were prepared from P8 mouse brains by subcellular fractionation, solubilized and subjected to immunoprecipitations using the indicated antibodies. Immunoprecipitates were separated on a 10-20% Tricine gel and blotted onto PVDF membrane. The polyclonal antibody R140 co-immunoprecipitated Gaf-1b, but R85 did not. The anti-Rip11 and anti-Gaf-1b A antibodies precipitated Rip11 and Gaf-1b, but not calsyntenin-1. APP was not co-immunoprecipitated by any of the used antibodies. Neither calsyntenin-1 nor Gaf-1b was precipitated with non-immune IgG. R140 control (ctrl) served as a reference to discriminate between IgG light chains (asterisks) and the calsyntenin-1 C-terminal fragments (CTF). (D) Different membrane fractions (V0, V1, V2) and the final supernatant (S) of P7 mice were prepared by differential centrifugation. 30 µg of each fraction was separated on a 4-12% Bis-Tris gel and blotted onto PVDF membrane. Immunoblot was analysed with the following antibodies: anti-Gaf-1b C for Gaf-1b and Rip11, R85 for full-length calsyntenin-1 and calsyntenin-1 ectodomain, R140 for C-terminal fragment of calsyntenin-1 and anti-Rab11. Gaf-1b, Rip11, Rab11, full-length calsyntenin-1 and the calsyntenin-1 C-terminal fragments are mainly enriched in the V1 fraction. Cst1, calsyntenin-1; IgG, immunoglobulin G; IP, immunoprecipitation; fl, full-length; ed, ectodomain; CTF, C-terminal fragment (adapted from Master thesis of Tu-My Diep, 2007).

Next, we analysed the subcellular distribution of Gaf-1b in mouse brain by comparing the V1 membrane fraction with other membrane fractions produced during the differential centrifugation protocol. The brain homogenate, three different membrane fractions (V0, V1 and V2) and the final supernatant (S) were analysed by immunoblotting. The V0 pellet was enriched in light mitochondria, ER- and Golgi-derived membranes. V1 and V2 fractions contained heavy and light microsomal vesicles, respectively. As shown in Figure 2.1 D, Gaf-1b, Rip11 and the recycling-endosomal protein Rab11 were enriched in the V1 fraction. The full-length form of calsyntenin-1 and the stump were

predominantly found in V0 and V1. The ectodomain of calsyntenin-1 was present in all fractions, but was most notably enriched in V1, V0 and homogenate. Our results were in accord with those of Kawase *et al.,* (2003) who showed that Gaf-1b and Rip11 are mainly localized in microsomes. The enrichment of calsyntenin-1 and Gaf-1b in identical brain vesicle fractions supported further their functional interaction.

In summary, Gaf-1b was identified as a novel interaction partner of calsyntenin-1 by IPs of mouse brain. Based on the fact that Gaf-1b belonged to the Rab11-FIPs and Rab11 is a recycling-endosomal marker, we have found an interaction partner of calsyntenin-1 which might function in the endosomal recycling pathway. This led us to the calsyntenin-1 organelle populations which are comprised of proteins of the endosomal recycling pathway and were different from those calsyntenin-1 organelles containing calsyntenin-1, APP and BACE1. Therefore, this prompted us to investigate the function of the calsyntenin-1 pathway which was involved in endosomal recycling.

2.2 Study of the interaction of Gaf-1b and calsyntenin-1

2.2.1 Calsyntenin-1 interacts specifically with Gaf-1b

Previous data demonstrated the existence of two distinct, non-overlapping transport packages of calsyntenin-1. Previously, we focused on and characterized primarily the calsyntenin-1/APP/BACE1 organelles [176-178]. Gaf-1b represented a new interaction partner of calsyntenin-1 and as it belonged to the recycling pathway, this motivated us to characterize the second calsyntenin-1 organelle population, namely the vesicle population with recycling-endosomal characteristics, and thoroughly investigated the interaction between Gaf-1b and calsyntenin-1. We turned to a heterologous cell culture system which is easier to culture compared to neuronal cell lines and which can be transfected with high efficiency. Different cell lines were analysed by immunoblotting in order to identify suitable cell lines for our purpose. As shown in Figure 2.2 A, of heterologous cells tested so far, endogenous Rip11 was expressed strongest in HeLa cells. Gaf-1b expression was generally weaker than Rip11, but was also expressed in HeLa cells. Thus, we used HeLa cells for further experiments.

Next, we aimed to roughly map the interaction site on Gaf-1b and calsyntenin-1. Cell lysates of HeLa cells co-transfected with FLAG-Gaf-1b and wild-type calsyntenin-1-myc were subjected to immunoprecipitations (IPs). The polyclonal antibody R85 strongly co-immunoprecipitated FLAG-Gaf-1b together with calsyntenin-1, but the anti-myc antibody did not (Figure 2.2 B, upper panel). Neither calsyntenin-1-myc nor FLAG-Gaf-1b were precipitated with non-immune IgG.

To answer the question whether the splice variant of Gaf-1b, i.e. Rip11, was also able to interact with calsyntenin-1, HeLa cells were co-transfected with calsyntenin-1-myc and Rip11-EGFP and subjected to IPs. R85 and anti-myc antibodies did not co-immunoprecipitate Rip11-EGFP (Figure 2.2 B, middle panel). On the other side, anti-Gaf-1b antibodies A and C also did not co-immunoprecipitate calsyntenin-1-myc. Concluding, it seemed that the splice insert of Gaf-1b was necessary for the interaction with calsyntenin-1.

Further, we tested whether calsyntenin-3 might interact with Gaf-1b. Calsyntenin-3 lacks both the very C-terminus and the KBS2 motif compared to calsyntenin-1. Furthermore, calsyntenin-3 lacks the cytoplasmic acidic stretch characteristic for calsyntenin-1. We co-transfected HeLa cells with calsyntenin-3-myc and FLAG-Gaf-1b und performed co-immunoprecipitations. R85 and anti-myc antibodies did not co-immunoprecipitate FLAG-Gaf-1b (Figure 2.2 B, lower panel). This result

suggested the distal C-terminus, the KBS2 or the acidic stretch of calsyntenin-1 to be crucial for the binding to Gaf-1b.

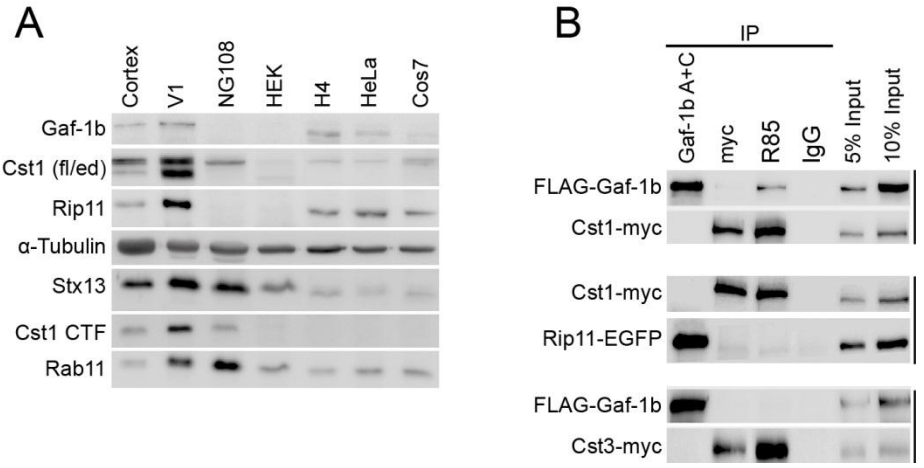

Figure 2.2: Gaf-1b specifically interacts with calsyntenin-1.
(A) The expression levels of endogenous calsyntenin-1 and Gaf-1b were tested in different cell lines (cortical neurons, V1 membranes of P7 mouse brains, NG108 cells, HEK293T cells, H4 cells, HeLa cells and Cos7 cells) by Western blotting. Cells were solubilized in lysis buffer. 30 µg protein was precipitated by Wessel-Flügge, separated by 10% SDS-PAGE and transferred onto PVDF membrane. The membrane was probed for endogenous full-length calsyntenin-1, calsyntenin-1 ectodomain, calsyntenin-1 C-terminal fragment, Gaf-1b, Rip11, Rab11, syntaxin 13 and α-tubulin. Gaf-1b and Rip11 are not expressed in NG108 and HEK cells, but weakly in Cos7 cells and stronger in H4 and HeLa cells. Calsyntenin-1 is weakly expressed in H4, HeLa and Cos7 cells, while there is almost no expression in HEK cells. (B) HeLa cells were co-transfected with FLAG-Gaf-1b and calsyntenin-1-myc (upper panel), Rip11-EGFP and calsyntenin-1-myc (middle panel) or FLAG-Gaf-1b and calsyntenin-3-myc (lower panel). Twenty-four hours post-transfection cells were solubilized and subjected to immunoprecipitations using the indicated antibodies. Immunoprecipitates were separated by 10% SDS-PAGE and blotted onto PVDF membrane. The membrane was probed with anti-Gaf-1b C, anti-GFP, anti-myc or R140. Calsyntenin-1-myc co-immunoprecipitated with FLAG-Gaf-1b (upper panel), but not with Rip11-EGFP (middle panel). FLAG-Gaf-1b co-immunoprecipitated with calsyntenin-1-myc (upper panel), but not with calsyntenin-3-myc (lower panel). Cst1, calsyntenin-1; Cst3, calsyntenin-3; IgG, immunoglobulin G; IP, immunoprecipitation; fl, full-length; ed, ectodomain; CTF, C-terminal fragment (adapted from Master thesis of Tu-My Diep, 2007).

2.2.2 The C2 domain of Gaf-1b is involved in the interaction with calsyntenin-1

We performed immunoprecipitations of calsyntenin-1 with different truncation constructs of Gaf-1b in order to identify the binding domain of Gaf-1b with calsyntenin-1 in more detail (Figure 2.3 A). First, we were interested whether the splice insert alone, the C-terminus after the splice insert or the N-terminus before the splice insert were necessary for the binding to calsyntenin-1. HeLa cells were co-transfected with EGFP-calsyntenin-1 and either with full-length FLAG-Gaf-1b, FLAG-Gaf-1b_ins, FLAG-Gaf-1b_ΔC or FLAG-Gaf-1b_ΔN (Figure 2.3 B) and subjected to IPs. As shown in Figure 2.3 B, EGFP-calsyntenin-1 strongly co-immunoprecipitated with full-length FLAG-Gaf-1b and FLAG-Gaf-1b_ΔC using the anti-Gaf-1b antibody B. As control, EGFP-calsyntenin-1 was single transfected in HeLa cells and the same co-IP was performed. Interestingly, the anti-Gaf-1b antibody B co-immunoprecipitated EGFP-calsyntenin-1, although no Gaf-1b was overexpressed. This co-immunoprecipitation might depend on endogenous Gaf-1b in HeLa cells. Therefore, the co-immunoprecipitations signals in FLAG-Gaf-1b_ΔN and FLAG-Gaf-1b_ins might also depend on endogenous Gaf-1b because the signals were of similar intensity compared to those of the control (asterisks). Neither calsyntenin-1 nor the Gaf-1b constructs were precipitated with non-immune IgG

(data not shown). This result indicated that the N-terminus was necessary for the interaction with calsyntenin-1 and the splice insert alone was not sufficient for the binding.

We next aimed at examining which part of the N-terminus of Gaf-1b was required for the interaction with calsyntenin-1. For this reason deletion mutants of the N-terminus of Gaf-1b were designed (Figure 2.3 A). HeLa cells co-transfected with EGFP-calsyntenin-1 and either with full-length

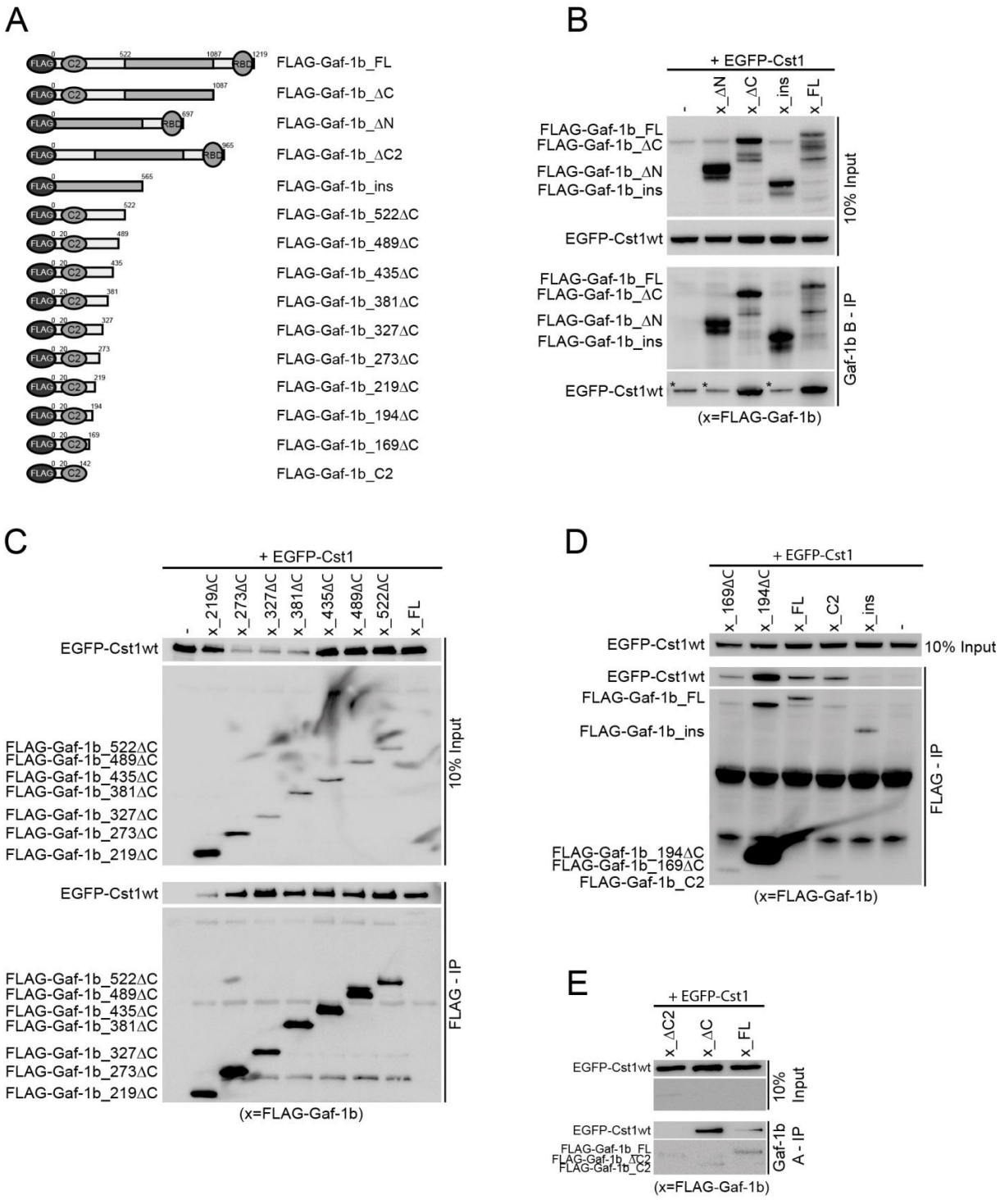

◄ Figure 2.3: The splice insert of Gaf-1b is necessary but alone not sufficient for the interaction with calsyntenin-1.
(A) Schematic drawings of the used truncated mutant constructs of the FLAG-tagged Gaf-1b. (B-E) Transfected HeLa cells were solubilized twenty-four hours post-transfection and subjected to immunoprecipitations using the indicated antibodies. Immunoprecipitates were separated by 10% SDS-PAGE and blotted onto PVDF membrane. (B) HeLa cells were co-transfected with EGFP-calsyntenin-1 and either with FLAG-Gaf-1b full-length, FLAG-Gaf-1b_insert, FLAG-Gaf-1b_ΔC, FLAG-Gaf-1b_ΔN or alone as control. EGFP-calsyntenin-1 was only co-precipitated with Gaf-1b full-length or Gaf-1b_ΔC by Gaf-1b B antibody. Note that EGFP-calsyntenin-1 was co-precipitated by Gaf-1b B in the sample without FLAG-Gaf-1b transfection, indicating that endogenous Gaf-1b may co-precipitated with EGFP-calsyntenin-1. Gaf-1b_insert and Gaf-1b_ΔN co-transfection showed a similar co-immunoprecipitation pattern as EGFP-calsyntenin-1 transfection alone, which indicate that also here endogenous Gaf-1b is responsible for the co-immunoprecipitation. Asterisks indicate EGFP-calsyntenin-1 co-precipitation by endogenous Gaf-1b in the Gaf-1b B-IP. (C) HeLa cells were co-transfected with EGFP-calsyntenin-1 and the indicated truncation mutants of FLAG-Gaf-1b. EGFP-calsyntenin-1 was co-immunoprecipitated with all truncation mutants lacking the very C-terminus of Gaf-1b and splice insert by anti-FLAG. (D) HeLa cells were co-transfected with EGFP-calsyntenin-1 and the indicated truncation mutants of Gaf-1b. EGFP-calsyntenin-1 did not co-immunoprecipitate with Gaf-1b_insert, but co-immunoprecipitated with FLAG-Gaf-1b full-length, FLAG-Gaf-1b_Δ194, FLAG-Gaf-1b_Δ169 and FLAG-Gaf-1b_C2. (E) HeLa cells were co-transfected with EGFP-calsyntenin-1 and the indicated truncation mutants of Gaf-1b. EGFP-calsyntenin-1 co-immunoprecipitated with FLAG-Gaf-1b full-length and FLAG-Gaf-1b_ΔC but did not co-immunoprecipitate with FLAG-Gaf-1b_ΔC2. These results indicate that the C2 domain in the N-terminus is involved in the binding with calsyntenin-1. Cst1, calsyntenin-1; FL, full-length.

FLAG-Gaf-1b, FLAG-Gaf-1b_522ΔC, FLAG-Gaf-1b_489ΔC, FLAG-Gaf-1b_435ΔC, FLAG-Gaf-1b_381ΔC, FLAG-Gaf-1b_327ΔC, FLAG-Gaf-1b_273ΔC or FLAG-Gaf-1b_219ΔC were subjected to IPs. All truncation constructs of Gaf-1b lacking the C-terminus from amino acid (aa) 522 to aa 219ΔC as well as full-length Gaf-1b co-immunoprecipitated with EGFP-calsyntenin-1 using the anti-FLAG antibody (Figure 2.3 C). Additional truncation mutants were designed and tested by co-immunoprecipitations. Protein extracts of HeLa transfected with EGFP-calsyntenin-1 and either full-length FLAG-Gaf-1b, FLAG-Gaf-1b_ins, FLAG-Gaf-1b_194ΔC, FLAG-Gaf-1b_169ΔC or FLAG-Gaf-1b_C2 were subjected to IPs. FLAG-Gaf-1b_194ΔC, FLAG-Gaf-1b_169ΔC and FLAG-Gaf-1b_C2 still co-immunoprecipitated with EGFP-calsyntenin-1 (Figure 2.3 D). The co-immunoprecipitation of full-length FLAG-Gaf-1b with EGFP-calsyntenin-1 was used as a positive control and FLAG-Gaf-1b_ins with EGFP-calsyntenin-1 as a negative control. Therefore, the binding domain of Gaf-1b and calsyntenin-1 could be located to the very beginning of the N-terminus of Gaf-1b.

The N-terminus of Gaf-1b contains the C2 domain, which was shown to serve as protein-protein or protein-phospholipid binding module [153]. We were interested whether the C2 domain alone is sufficient for the interaction with calsyntenin-1. For this reason, HeLa cells were co-transfected with EGFP-calsyntenin-1 and FLAG-Gaf-1b_ΔC2, which lacks the C2 domain, and the cell lysate was subjected to IPs. FLAG-Gaf-1b_ΔC2 did not co-immunoprecipitate with EGFP-calsyntenin-1 (Figure 2.3 E). As positive control, the same co-immunoprecipitation experiment was performed with lysate from HeLa cells co-transfected with EGFP-calsyntenin-1 and full-length FLAG-Gaf-1b or FLAG-Gaf-1b_ΔC. As previously shown, full-length FLAG-Gaf-1b and FLAG-Gaf-1b_ΔC co-immunoprecipitated with EGFP-calsyntenin-1. In summary our results demonstrated that the C2 domain at the N-terminus of Gaf-1 was involved in the binding of Gaf-1b to calsyntenin-1. Furthermore, the splice insert of Gaf-1b was necessary for the interaction with calsyntenin-1 but alone is not sufficient.

2.2.3 The acidic stretch of calsyntenin-1 is crucial for the interaction with Gaf-1b

To study the interaction of Gaf-1b and calsyntenin-1 in more detail, we performed immunoprecipitations of Gaf-1b with different truncation or mutation constructs of calsyntenin-1 (Figure 2.4 A). We were interested whether the cytoplasmic domain of calsyntenin-1 alone was

necessary and sufficient for the interaction with Gaf-1b. The co-immunoprecipitation result from V1 membranes (Figure 2.1 C) led us to the presumption that the cytoplasmic domain of calsyntenin-1 was crucial for the interaction with Gaf-1b because only antibody R140 was able to co-immunoprecipitate with Gaf-1b. However, IPs form heterologous cells showed that antibody R85 precipitates Gaf-1b more efficiently than R140 antibody. A potential explanation might be that the stump of calsyntenin-1 was more stable or enriched in mouse brains than in heterologous cell lines. HeLa cells were co-transfected with FLAG-Gaf-1b and the cytoplasmic domain of calsyntenin-1 fused N-terminally to EGFP and subjected to IPs. The polyclonal antibody R140 co-immunoprecipitated FLAG-Gaf-1b (Figure 2.4 B, lower panel). The anti-Gaf-1b antibodies A and C weakly co-immunoprecipitated EGFP-calsyntenin-1 cyto. The R85 antibody did not precipitate the cytoplasmic domain of calsyntenin-1 and therefore did not co-immunoprecipitate with FLAG-Gaf-1b. As control, the same co-immunoprecipitation experiment was performed with lysate from HeLa cells co-transfected with FLAG-Gaf-1b and EGFP cDNA. The antibodies R140, R85 and anti-GFP did not co-immunoprecipitate FLAG

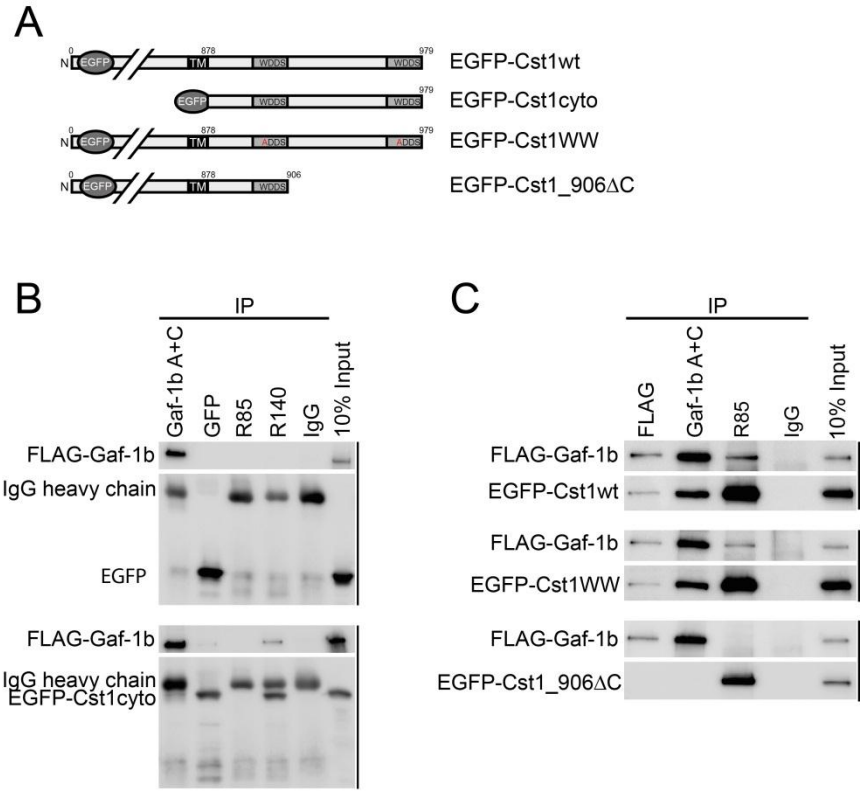

Figure 2.4: The C-terminus of calsyntenin-1 is involved in the interaction with Gaf-1b.
(A) Schematic drawings of the used truncation or mutated constructs of the EGFP-fused calsyntenin-1. (B and C) Transfected HeLa cells were solubilized twenty-four hours post-transfection and subjected to immunoprecipitations using the indicated antibodies. Immunoprecipitates were separated by 10% SDS-PAGE and blotted onto PVDF membrane. (B) HeLa cells were co-transfected with FLAG-Gaf-1b and EGFP cDNA (upper panel) or with FLAG-Gaf-1b and EGFP-calsyntenin-1_cyto (lower panel). The immunoblots were probed with anti-Gaf-1b antibody B or anti-GFP. FLAG-Gaf-1b co-immunoprecipitated with EGFP-calsyntenin-1_cyto (lower panel), but not with EGFP (upper panel). (C) HeLa cells were co-transfected with FLAG-Gaf-1b and either wild-type EGFP-calsyntenin-1 (upper panel), double mutant EGFP-calsyntenin-1_WW (middle panel) or the truncated mutant EGFP-calsyntenin-1_906ΔC (lower panel). The membranes were probed with anti-Gaf-1b antibody B or anti-GFP. FLAG-Gaf-1b co-immunoprecipitated with wild-type EGFP-calsyntenin-1 (upper panel) and with double mutant EGFP-calsyntenin-1_WW (middle panel), but not with the truncation mutant EGFP-calsyntenin-1_906ΔC (lower panel). Cst1, calsyntenin-1; IgG, immunoglobulin G; IP, immunoprecipitation; wt, wild-type; TM, trans membrane (adapted from Master thesis of Tu-My Diep, 2007).

-Gaf-1b, indicating that anti-calsyntenin-1 antibodies did not recognize Gaf-1b non-specifically (Figure 2.4 B, upper panel). Thus, the cytoplasmic domain of calsyntenin-1 was necessary and sufficient for the interaction with Gaf-1b.

Calsyntenin-1 contains two conserved kinesin-binding segments (KBS1 and KBS2) in its cytoplasmic domain. It was shown that KBS1 and KBS2 were responsible for the interaction with kinesin-light chain 1 (KLC1) *in vitro* and *in vivo* [171]. A WDDS core motif was contained in KBS1 and KBS2 which was conserved in most calsyntenins. In order to determine whether KBS1 and KBS2 were also required for the interaction with Gaf-1b, we carried out co-immunoprecipitations from HeLa cell lysates which were co-transfected with FLAG-Gaf-1b and double mutant EGFP-calsyntenin-1_WW. Both tryptophanes of the KBS1 and KBS2 were mutated to alanine in double mutant calsyntenin-1_WW. The polyclonal antibody R85 still co-immunoprecipitated FLAG-Gaf-1b and the anti-Gaf-1b antibodies A and C as well as anti-FLAG co-immunoprecipitated EGFP-calsyntenin-1_WW (Figure 2.4 C, middle panel). This result indicated that KBS1 and KBS2 were not involved in the interaction of Gaf-1b and calsyntenin-1.

Next, we were interested in the question which part of the cytoplasmic domain of calsyntenin-1 was required for the binding to Gaf-1b. HeLa cells were co-transfected with FLAG-Gaf-1b and EGFP-calsyntenin-1_906ΔC, the truncation mutant of EGFP-calsyntenin-1 lacking the C-terminal part after KBS1. R85 antibody did not co-immunoprecipitate FLAG-Gaf-1b and none of the Gaf-1b antibodies co-immunoprecipitated with EGFP-calsyntenin-1_906ΔC (Figure 2.4 C, lower panel). Further, we performed co-immunoprecipitations with FLAG-Gaf-1b and EGFP-calsyntenin-1_902ΔC which lacks the C-terminus starting before the KBS1. FLAG-Gaf-1b did also not co-immunoprecipitate with EGFP-calsyntenin-1_902ΔC (data not shown). As control the same co-immunoprecipitation experiments were carried out with EGFP-calsyntenin-1 and FLAG-Gaf-1b (Figure 2.4 C, upper panel). As previously shown, FLAG-Gaf-1b co-immunoprecipitated with EGFP-calsyntenin-1. In summary, our result showed that the cytoplasmic domain starting from the transmembrane domain to the KBS1 motif was not involved in the binding to Gaf-1b, as well as the KBS1 and KBS2 motifs were not. In contrast, the acidic stretch of calsyntenin-1 was crucial for the interaction with Gaf-1b.

2.2.4 The formation of Gaf-1b/Rip11 complex disrupts the interaction of calsyntenin-1 and Gaf-1b

FIP2 belongs to the class I Rab11-FIPs and is able to interact with Rab11 to form a heterotetrameric complex. The conformation of this complex is arranged in a Rab11-$(FIP2)_2$-Rab11 manner [151]. Gaf-1b and Rip11 both belong to the class I Rab11-FIPs, which suggested a similar heterotetrameric complex between Gaf-1b and Rip11 that might also influence the binding to calsyntenin-1. We carried out co-immunoprecipitation experiments form HeLa cells triple-transfected with wild-type calsyntenin-1, FLAG-Gaf-1b and Rip11-EGFP using the R140 and R85 antibodies for calsyntenin-1, anti-FLAG and anti-Gaf-1b antibody B for FLAG-Gaf-1b and anti-GFP for Rip11-EGFP. Anti-FLAG, anti-Gaf-1b antibody B and anti-GFP antibodies co-immunoprecipitated both FLAG-Gaf-1b and Rip11-EGFP (Figure 2.5). Interestingly, FLAG-Gaf-1b did not co-immunoprecipitate with calsyntenin-1 anymore. This result indicated that only a homotetrameric complex of Gaf-1b could interact with calsyntenin-1.

Note that parts of the interaction study between Gaf-1b and calsyntenin-1 were performed during my master thesis in 2007 [203].

Figure 2.5: Rip11 sequester Gaf-1b from calsyntenin-1.
HeLa cells were co-transfected with FLAG-Gaf-1b, Rip11-EGFP and wild-type calsyntenin-1. Twenty-four hours post-transfection cells were solubilized, subjected to immunoprecipitations using the indicated antibodies, immunoprecipitates were separated by 10% SDS-PAGE and blotted onto PVDF membrane. The membranes were probed with anti-Gaf-1b C or R140. FLAG-Gaf-1b co-immunoprecipitated with Rip11-EGFP, but did not co-immunoprecipitate with calsyntenin-1 anymore. Neither calsyntenin-1, Rip11 nor Gaf-1b were precipitated with non-immune IgG. Non-immune IgG served as a reference to discriminate between IgG light chains (asterisks) and the calsyntenin-1 C-terminal fragments. Cst1, calsyntenin-1; IgG, immunoglobulin G; IP, immunoprecipitation; wt, wild-type; CTF, C-terminal fragment (adapted from Master thesis of Tu-My Diep, 2007).

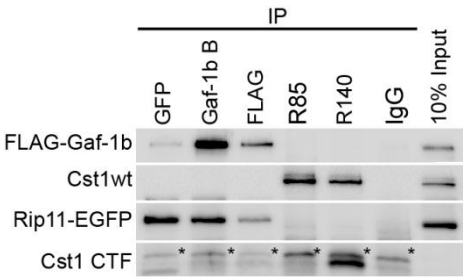

2.3. Gaf-1b and calsyntenin-1 are proteins of recycling endosomes

2.3.1 Gaf-1b and Rip11 exclusively interacts with GTP-Rab11

Rip11 and Rab11 interact in a GTP-dependent manner [165, 204]. In contrast, it was not known whether Gaf-1b, the splice variant of Rip11, could interact with Rab11 in a GTP-dependent manner. Gaf-1b and Rip11 contain the RBD domain, suggesting that Gaf-1b behaves similarly as Rip11. We generated GST-fusion proteins of wild-type Rab4, Rab5, and Rab11, as well as their constitutively active, GTPase-deficient mutant, Rab4Q72L, Rab5Q79L, and Rab11Q70L and applied these to pull-down assays. The proteins were expressed in *E.coli* and purified using glutathione sepharose [205]. Upon coupling to glutathione sepharose, wild type Rab11 and Rab11Q70L were loaded with GDP or GTP and incubated with brain lysates of P9 mice for one hour. Beads were washed, proteins eluted in SDS sample buffer, separated by SDS-PAGE and analysed by immunoblotting. Gaf-1b and Rip11 were pulled down in a GTP-dependent manner (data not shown) [205]. In contrast to Rip11, Gaf-1b was pulled down with much a lower efficiency, suggesting that Rip11 interacted with Rab11 with higher affinity. Therefore, the same experiment was performed with lysate of HeLa cells single-transfected with FLAG-Gaf-1b or co-transfected with FLAG-Gaf-1b and Rip11-EGFP. GST pull-downs were performed with GDP- or GTP-coupled wild-type Rab11 and GTPase deficient Rab11Q70L. As shown in Figure 2.6 A, FLAG-Gaf-1b was efficiently pulled down with GTP-bound Rab11 or with Rab11Q70L. Endogenous Rip11 was also pulled down in a GTP-dependent manner of Rab11, albeit weaker. GST alone or GDP-bound Rab11 did not interact with FLAG-Gaf-1b. GST pull-downs from cell lysates of HeLa cells overexpressing both FLAG-Gaf-1b and Rip11-EGFP showed that endogenous Rip11, Rip11-EGFP and FLAG-Gaf-1b were pulled down with GTP-bound Rab11 (Figure 2.6 B). Again, with lysates from heterologous cell lines, a higher amount of pulled down Rip11 was observed compared to Gaf-1b, supporting the assumption that Rip11 bound to Rab11 with a higher affinity.

Next, we investigated whether Gaf-1b could interact with other endosomal Rab proteins such as Rab4 and Rab5. GST pull-downs using wild-type Rab4, Rab5, Rab11 and their corresponding GTPase-deficient mutants Rab4Q72L, Rab5Q79L and Rab11Q70L were performed. HeLa cell lysate transfected with FLAG-Gaf-1b was incubated with the different Rab proteins. FLAG-Gaf-1b was exclusively pulled down by Rab11Q70L (Figure 2.6 C). In summary, these results showed that Gaf-1b and Rip11 interacted exclusively with Rab11 and indeed in a GTP-dependent manner [205].

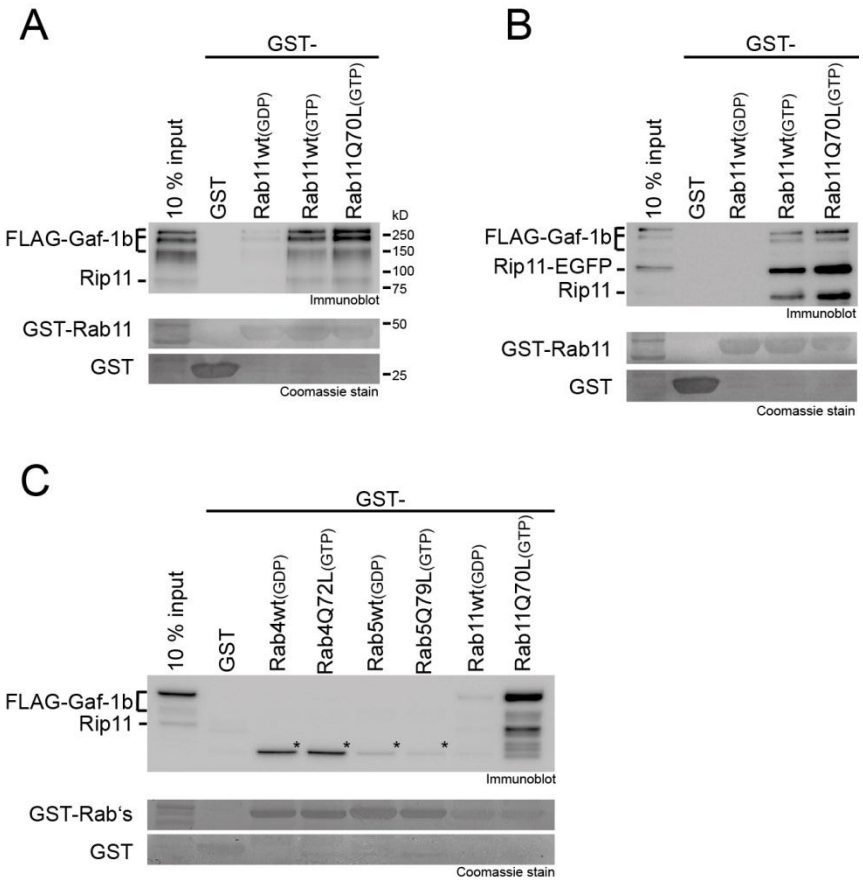

Figure 2.6: Gaf-1b interacts with Rab11.

(A and B) 10 µg of GST-fusion proteins were coupled to glutathione sepharose beads followed by guanine-nucleotide exchange at 37 °C for 30 minutes. Beads were incubated with 200 µg HeLa cell lysates supplemented with 100 µM GTP or GDP for one hour at 4 °C. Beads were washed, proteins were eluted with SDS sample buffer and separated by 10% SDS-PAGE followed by immunoblotting using the anti-Gaf-1b antibody C. The bottom panel shows the PVDF membrane stained with Coomassie brilliant blue, indicating equal loading of GST-Rab11 proteins. (A) GST pull-down from FLAG-Gaf-1b transfected HeLa cell lysate. FLAG-Gaf-1b was pulled down by GTP-bound Rab11 and Rab11Q70L. Endogenous Rip11 weakly interacted with GTP-bound Rab11 and Rab11Q70L. (B) GST pull-down from FLAG-Gaf-1b and Rip11-EGFP co-transfected HeLa cell lysate. Rip11 and Rip11-EGFP were pulled down very efficiently. FLAG-Gaf-1b was pulled down by GTP-bound Rab11 and Rab11Q70L much less compared to Rip11. (C) 8 µg of GST-Rab4, GST-Rab5 and GST-Rab11 were coupled to glutathione sepharose beads. After nucleotide exchange with 1 mM GDP (wild-type Rabs) or 1 mM GTP (Q-L mutants) for 30 minutes at 37 °C, beads were incubated with 100 µg HeLa lysate overexpressing FLAG-Gaf-1b for one hour at 4 °C. Proteins were eluted and separated on a 10-20% Tricine gel followed by immunoblotting with anti-Gaf-1b antibody C. FLAG-Gaf-1b and endogenous Rip11 were pulled down exclusively by Rab11Q70L. GST, glutathione S-transferase (adapted from Master thesis of Mauro Serricchio, 2008).

It was shown that Rip11 colocalizes with Rab11 to apical recycling endosomes in polarized epithelial cells [165] and MDCK cells [206]. In HeLa cells, Rip11 also localizes with Rab11 and other Rab11-FIPs to recycling endosomes [206]. At this stage little was known about the subcellular distribution of Gaf-1b. To gain more insight into the localization of Gaf-1b, immunofluorescence analysis was performed in HeLa cells. HeLa cells were cultured on coverslips, fixed with 4% PFA and processed for immunofluorescence using the anti-Gaf-1b antibody B and the anti-TfR antibody. The majority of cells showed a vesicular staining pattern of endogenous Gaf-1b. In these vesicles, Gaf-1b

and TfR sparsely colocalized with each other (Figure 2.7 A). In some cells Gaf-1b accumulated in structures next to the nucleus, beside the vesicular distribution. These perinuclear compartments were positive for TfR suggesting that these organelles represent the pericentriolar recycling endosome (Figure 2.7 B) [207]. We also observed that Gaf-1b colocalized partially with TfR close to the plasma membrane at the cell periphery or at the tips of plasma membrane protrusions (Figure 2.7 C). These protrusions were described as a site of membrane outgrowth and it was shown that TfR accumulates

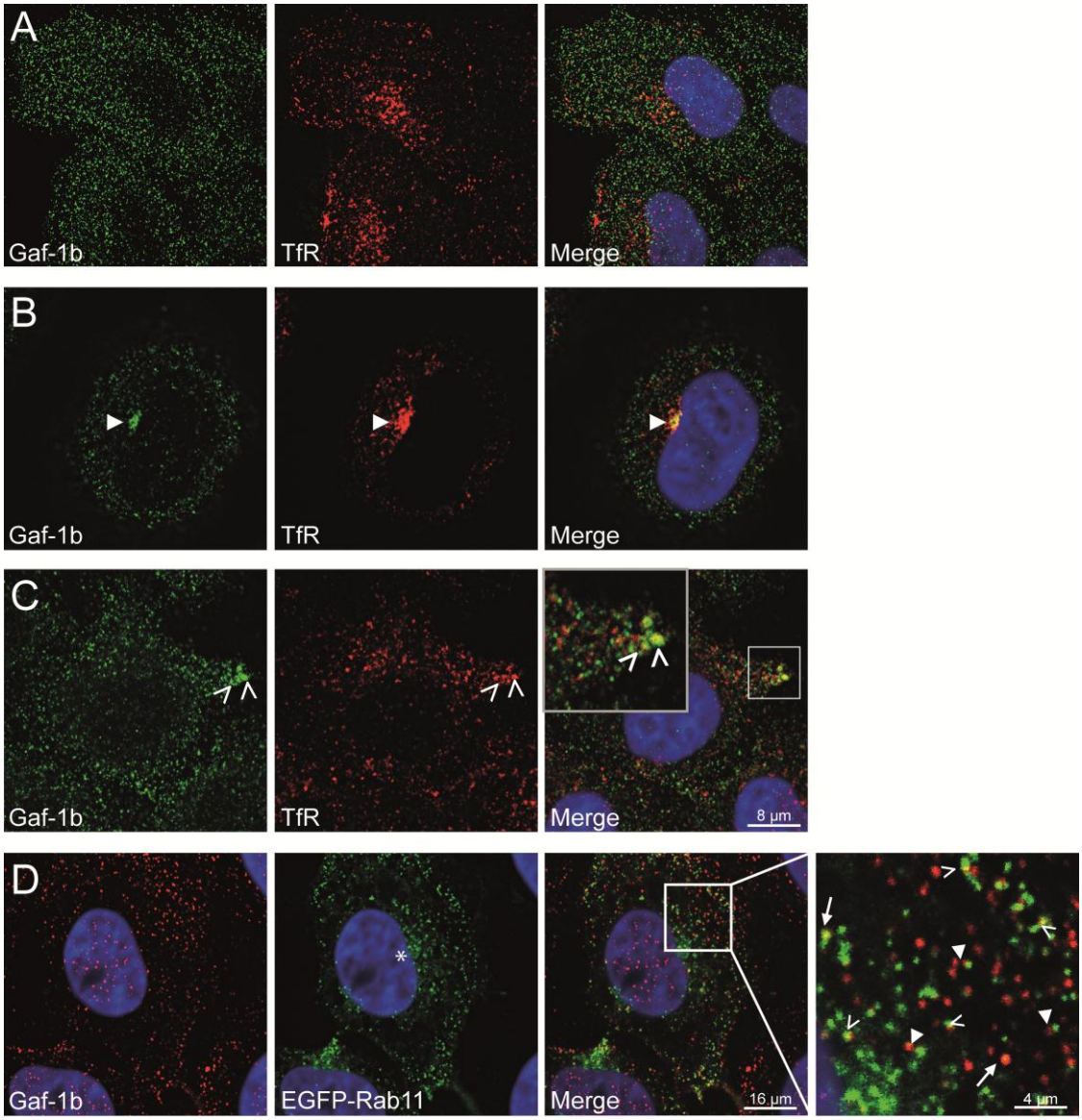

Figure 2.7: Gaf-1b localizes to cytoplasmic vesicles, perinuclear recycling endosomes and membrane outgrowths. (A-D) HeLa cells grown on coverslips were fixed with 4% PFA and processed for immunofluorescence using antibodies against TfR and Gaf-1b. Images were captured with a confocal laser scanning microscope (Leica SP1) using a 63x objective (NA 1.32). Nuclei were visualized with Hoechst dye. (A) Most cells show a vesicular pattern of Gaf-1b. Gaf-1b positive vesicles are devoid of TfR. (B) In some cells Gaf-1b is localized at a perinuclear region (►). In these pericentriolar recycling endosomes Gaf-1b and TfR colocalized with each other. (C) Gaf-1b and TfR colocalized partially at or close to the plasma membrane (>). (D) HeLa cells were transfected with EGFP-Rab11. EGFP-Rab11 localized to the pericentriolar recycling endosome (*) and to cytoplasmic vesicles. In some vesicles EGFP-Rab11 and Gaf-1b completely overlapped (→). Other EGFP-Rab11 and FLAG-Gaf-1b labeled vesicles were very close to each other, but did not overlap (►). A few vesicles of the two proteins partially overlapped (>). TfR, transferrin receptor (adapted from Master thesis of Mauro Serricchio, 2008).

at the leading edge of migrating fibroblasts [208]. In summary, Gaf-1b localized to the perinuclear recycling endosomes and to peripheral vesicular structures.

We found that Gaf-1b and Rab11 interacted *in vitro*, thus we aimed at analysing the subcellular distribution of Gaf-1b and Rab11 in living cells. Because there was no satisfactory anti-Rab11 antibody for staining endogenous Rab11, HeLa cells were transfected with EGFP-Rab11 and Gaf-1b co-stained with anti-Gaf-1b antibody B. EGFP-Rab11 showed a vesicular staining pattern and a perinuclearly aggregated structure. Gaf-1b and EGFP-Rab11 partially colocalized in a vesicular pattern, especially at the cell periphery (Figure 2.7 D). These data showed that Gaf-1b was associated with Rab11-positive recycling endosomes. Since there was only a partial overlap with Rab11, Gaf-1b might also exhibit a function which is independent on Rab11 activity [205].

2.3.2 Calsyntenin-1 interacts with the recycling-endosomal protein Rab11 through Gaf-1b

We have demonstrated that Gaf-1b interacted with calsyntenin-1. Next, we were interested whether Gaf-1b could simultaneously interact with calsyntenin-1 and Rab11. HeLa cells were single-transfected with FLAG-Gaf-1b or co-transfected with FLAG-Gaf-1b and wild-type calsyntenin-1 or EGFP-calsyntenin-1. As a control, we transfected HeLa cells with EGFP-calsyntenin-1 alone. GST pull-downs with GST and Rab11Q70L were performed. As shown before, FLAG-Gaf-1b was pulled down with GTP-bound Rab11Q70L (Figure 2.8 A, Input 2). Cells co-overexpressing FLAG-Gaf-1b and wild-type calsyntenin-1 showed that calsyntenin-1 was pulled down together with FLAG-Gaf-1b when they were incubated with glutathione-coupled GTP-bound Rab11Q70L (Figure 2.8 A, Input 1). EGFP-calsyntenin-1 was not pulled down in the absence of FLAG-Gaf-1b (Figure 2.8 B, Input 2). However, EGFP-calsyntenin-1 was pulled down in GTP-bound Rab11Q70L together with FLAG-Gaf-1b (Figure 2.8 B, Input 1). This result indicated that calsyntenin-1 interacted with Rab11-GTP indirectly through Gaf-1b and therefore calsyntenin-1 and Gaf-1b together might carry a functional role in endosomal recycling.

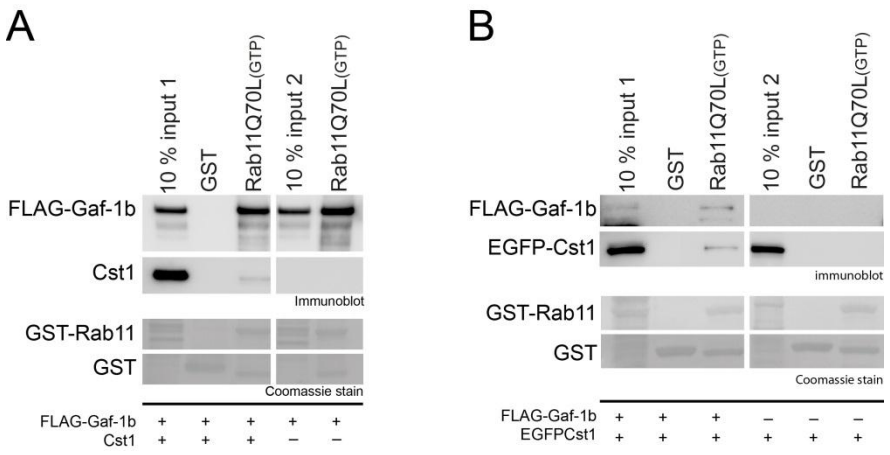

Figure 2.8: Calsyntenin-1 interacts with the recycling-endosomal protein Rab11 through Gaf-1b.
(A and B) HeLa cells were transfected with FLAG-Gaf-1b alone, FLAG-Gaf-1b and calsyntenin-1, EGFP-calsyntenin-1 alone or FLAG-Gaf-1b and EGFP-calsyntenin-1. 5 µg of GST-fusion proteins were coupled to glutathione sepharose followed by guanine-nucleotide exchange at 37 °C for 30 minutes. Beads were incubated with 200 µg HeLa cell lysates with overexpression of the indicated proteins for one hour at 4 °C. Beads were washed, proteins were eluted with SDS sample buffer and separated by SDS-PAGE (A: 10-20% Tricine gel, B: 10% SDS-PAGE) followed by immunoblotting using the anti-Gaf-1b antibody C, anti-GFP and R140. (A) Input 1 shows the lysate from FLAG-Gaf-1b and calsyntenin-1 co-transfected HeLa cells. Note that FLAG-Gaf-1b and calsyntenin-1 were pulled down with Rab11Q70L. Input 2 contains only FLAG-Gaf-1b which was pulled down with

Rab11Q70L. (B) Input 1 comprises of EGFP-calsyntenin-1 and FLAG-Gaf-1b and input 2 contains EGFP-calsyntenin-1 alone. Rab11Q70L pulled down EGFP-calsyntenin-1 together with FLAG-Gaf-1b, but EGFP-calsyntenin-1 alone was not pulled down by Rab11Q70L in absent of FLAG-Gaf-1b. Cst1, calsyntenin-1; GST, glutathione S-transferase (adapted from Master thesis of Mauro Serricchio, 2008).

2.3.3 Gaf-1b localizes with endosomal recycling and TGN marker in neurons

Previously, we showed in HeLa cells that Gaf-1b interacted with Rab11 and localized to recycling endosomes. In neurons there are distinct endosomal compartments in axons and dendrites and their function and protein content are different [63]. We were interested in the question to which endosomal compartments Gaf-1b was localized and whether Gaf-1b was associated with calsyntenin-1 in somatodendritic domains of neurons. Therefore, the degree of colocalization between Gaf-1b and calsyntenin-1 as well as between Gaf-1b and dendritic endosomes were quantified in 14 DIV hippocampal neurons (Figure 2.9). Gaf-1b and calsyntenin-1 colocalized to almost the same extent (28.9 ± 3.5% and 22.0 ± 2.4%, n=21) (Figure 2.9 A, a2). Interestingly, Gaf-1b overlapped with Rip11 to a lower extent than calsyntenin-1 (19.6 ± 2.6% and 20.3 ± 2.0%, n=23), since the anti-Gaf-1b antibody C recognizes both Rip11 and Gaf-1b. The degree of colocalization seldom exceeded 30%, although we expected a high colocalization degree for anti-Gaf-1b antibody B recognizing specifically Gaf-1b and the anti-Gaf-1b antibody C that recognizes both Rip11 and Gaf-1b. Therefore, a colocalization degree similar or higher than the degree of colocalization between Gaf-1b and Rip11 must be considered as high colocalization. Further, we determined the colocalization of Gaf-1b with the endosomal proteins TfR, EHD3, syntaxin 13, syntaxin 6 and LAMP1 (Figure 2.9 A, a4-a8). Gaf-1b colocalized well with TfR (16.7 ± 1.9% and 19.7 ± 1.4%, n=44) and syntaxin 6 (33.5 ± 1.9% and 18.9 ± 1.4%, n=19). For EHD3, syntaxin 13 and LAMP1 we had a higher degree of colocalization when we compared the endosomal marker versus Gaf-1b (15.2 ± 2.6% for EHD3, n=18; 21.8 ± 4.6% for syntaxin 13, n=15; 23.8 ± 2.9% for LAMP1, n=22). In contrast, we had a much lower colocalization degree when we quantified the overlap of Gaf-1b versus endosomal marker (8.9 ± 2.0% for EHD3, n=18; 6.3 ± 1.2% for syntaxin 13, n=15; 9.3 ± 1.2% for LAMP1, n=22). This discrepancy might be explained by the low vesicle number of the endosomal markers. It was previously shown in our laboratory that calsyntenin-1 colocalized with APP in the somatodendritic compartment of neurons. Thus, we also tested whether Gaf-1b overlapped with APP. As shown in Figure 2.9 A, a3, Gaf-1b poorly colocalized with APP (7.9 ± 1.1% and 9.3 ± 1.2%, n=43). The data sums up that Gaf-1b predominantly colocalized with recycling-endosomal markers such as TfR and syntaxin 13 and TGN marker syntaxin 6. Furthermore, Gaf-1b colocalized in dendrites about three times better with calsyntenin-1 compared to APP.

Figure 2.9: Gaf-1b colocalizes with calsyntenin-1, recycling-endosomal marker and TGN marker in dendrites. ►
(A) Cultured primary hippocampal neurons (14 DIV) were fixed, stained for Gaf-1b (anti-Gaf-1b B) and antibodies against Rip11/Gaf-1b (a1), calsyntenin-1 (a2), APP (a3), TfR (a4), EHD3 (a5), syntaxin 13 (a6), syntaxin 6 (a7) or LAMP1 (a8). To be able to use two rabbit antibodies in co-stainings, anti-Gaf-1b antibody B was masked with an excess of goat-anti-rabbit Fab-fragments (see Material and Methods). The settings were kept constant for all Gaf-1b stainings at a level where no signal appeared in the control staining. Images were captured with a confocal laser scanning microscope (Leica SP2) a 63x objective (NA 1.32) and thresholded in ImageJ. The number of particles in each channel was counted using the "count particle" tool in ImageJ. Two-color RGB images were produced in Adobe Photoshop CS3 and the number of colocalizing particles defined using the RG2B colocalization tool implemented in ImageJ. Colocalization between Gaf-1b and the endosomal markers is shown and was quantified for all costainings (B). The following number of dendrites was analysed for each costaining: a1, 23; a2, 21; a3, 43; a4, 44; a5, 18; a6, 15; a7, 19; a8, 22. Error bars indicate mean ± SEM, *p<0.05, ***p<0.001, Mann-Whitney Rank-Sum test, ###p<0.001, t-test. APP, amyloid precursor protein; Coloc, colocalization; Cst1, calsyntenin-1, Stx6, syntaxin 6; Stx13, syntaxin 13; TfR, transferrin receptor.

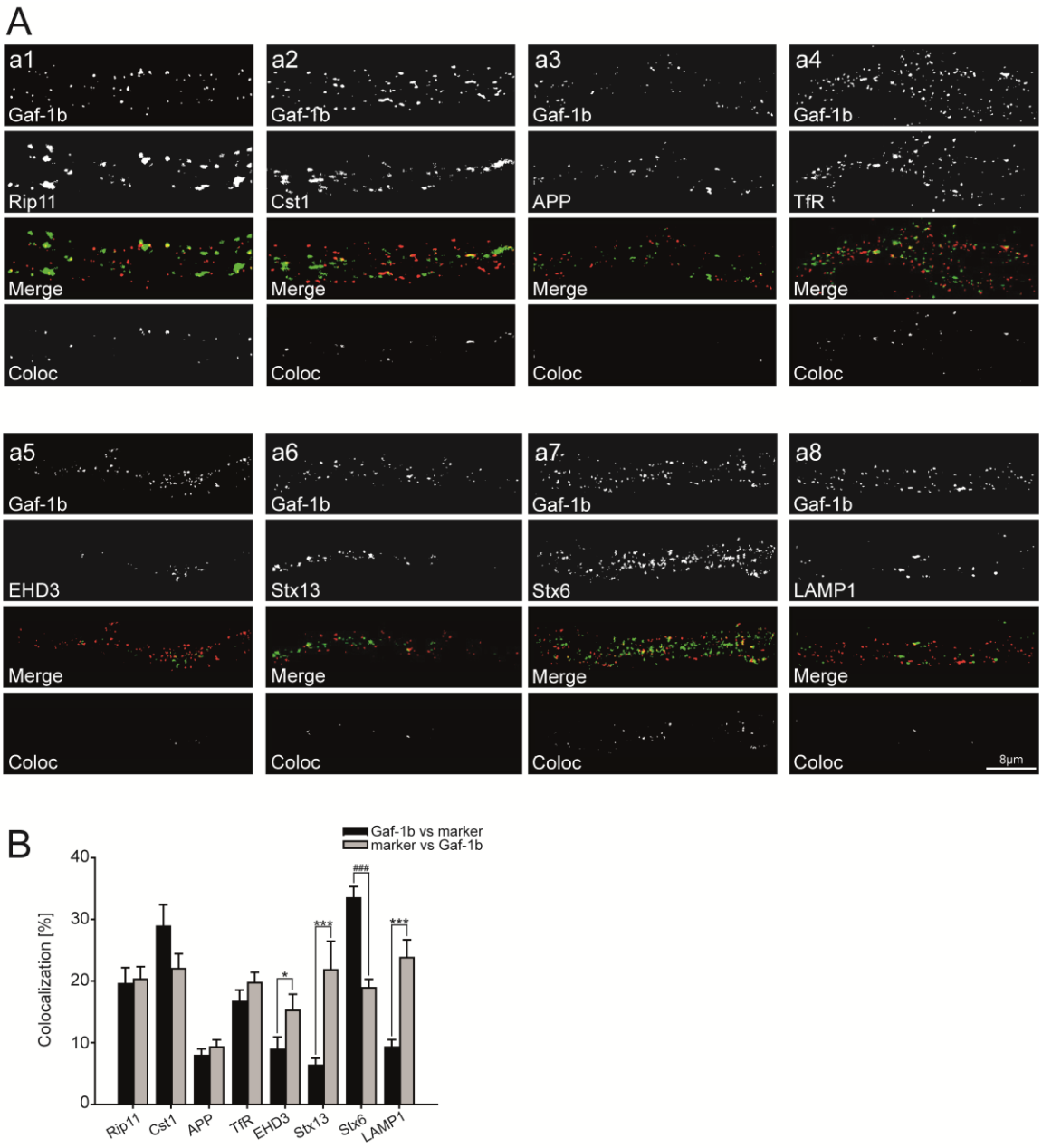

2.4 Gaf-1b is transported in calsyntenin-1 vesicles of the recycling-endosomal pathway

2.4.1 Gaf-1b and Rip11 are selectively associated with the recycling-endosomal type of calsyntenin-1 transport packages

Two distinct populations of transport organelles of calsyntenin-1 were described recently. One population of calsyntenin-1 organelles goes through recycling endosomes as they consist mainly of endosomal recycling proteins [200]. Then we showed that the Rab11-binding protein Gaf-1b was associated with calsyntenin-1, indicating that Gaf-1b might be co-transported in calsyntenin-1

organelles that go through the recycling endosome. To confirm the association of Gaf-1b and Rip11 with endosomal compartments, we immunoisolated Gaf-1b and Rip11 organelles and analysed their protein content by immunoblotting. Both organelles comprised particularly recycling-endosomal markers, such as TfR, syntaxin 13, Rab4, and Rab11, and TGN marker, such as syntaxin 16, VAMP4, mVPS45 and syntaxin 6 (Figure 2.10). Calsyntenin-1 could be also found on Gaf-1b and Rip11 organelles. Notably, the protein composition of calsyntenin-1 organelles was almost identical with those of Gaf-1b and Rip11. The calsyntenin-1 organelles additionally contained early-endosomal marker Rab5, APP and BACE1 which defined the second calsyntenin-1 organelle population with early-endosomal features [200]. We concluded that Gaf-1b was co-transported in calsyntenin-1 organelles devoid of APP to the recycling endosome.

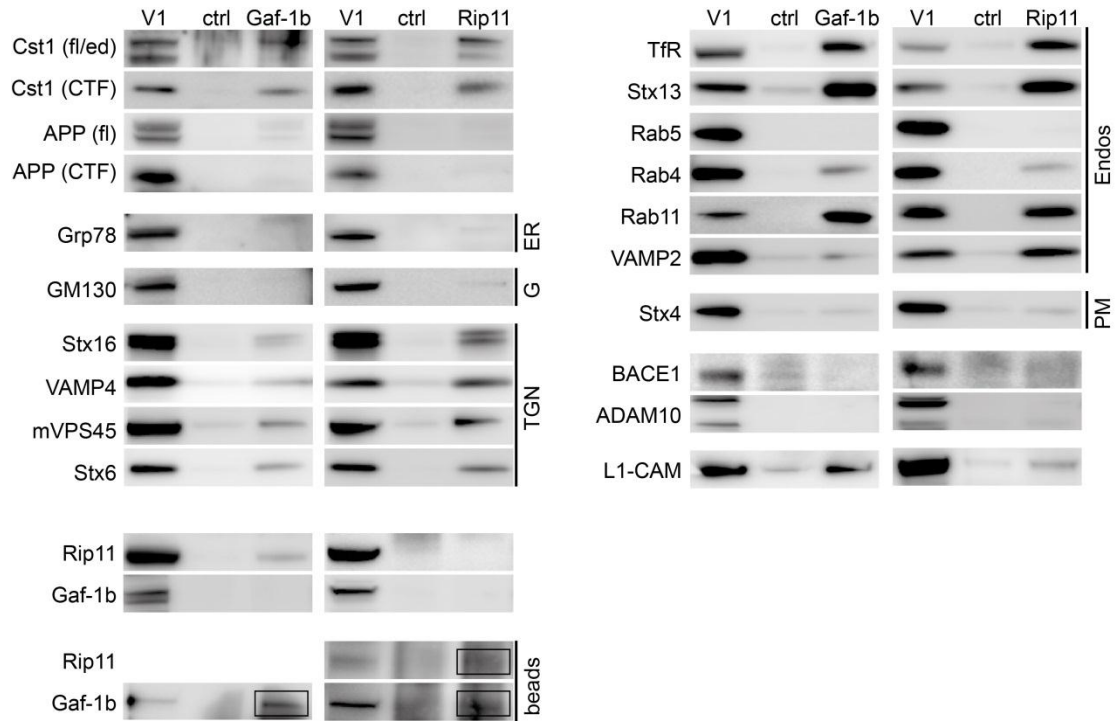

Figure 2.10: Gaf-1b and Rip11 define recycling-endosomal organelles.
Organelles were immunoisolated from V1 fractions of P7 mouse brains with Gaf-1b or Rip11 antibodies and their protein content was separated by SDS-PAGE. The immunoblot was analysed using the indicated antibodies. Note the composition of proteins in Gaf-1b and Rip11 immunoisolates is similar. The immunoisolates comprised predominantly calsyntenin-1, *trans*-Golgi markers (Stx16, VAMP4, mVPS45, Stx6) and recycling-endosomal markers (TfR, Stx13, Rab4, Rab11). The Gaf-1b and Rip11 immunoisolates were devoided of APP, BACE1, ADAM10, ER marker Grp78, Golgi marker GM130, early-endosomal marker Rab5 and plasma membrane marker syntaxin 4. Antigens used for immunoisolation were partially eluted and to some extent remained bound to the beads and were eluted with SDS (boxed bands). APP, amyloid precursor protein; Cst1, calsyntenin-1; CTF, C-terminal fragment; ctrl, control; ed, ectodomain; Endos, endosomes; ER, endoplasmatic reticulum; G, Golgi; fl, full-length; PM, plasma membrane; Stx, syntaxin; TfR, transferrin receptor; TGN, *trans*-Golgi network (data produced by Martin Steuble).

2.4.2 Gaf-1b is coupled to the calsyntenin-1/syntaxin 13 complex.

In our laboratory we recently immunoisolated calsyntenin-1 organelles that contained many endosomal proteins, especially recycling endosomes, such as syntaxin 13 and Rab11, as well as Gaf-1b and Rip11. We have shown that calsyntenin-1 was also associated with the recycling-endosomal

protein Rab11 through Gaf-1b. Further, we were interested whether calsyntenin-1 and Gaf-1b interacted with other proteins found in calsyntenin-1 organelles such as syntaxin 13. To this end, we performed IPs from HeLa cells co-transfected with wild-type calsyntenin-1 and HA-Stx13. The R140 antibodies strongly co-immunoprecipitated HA-Stx13, while the anti-HA antibodies slightly co-immunoprecipitated wild-type calsyntenin-1 (Figure 2.11 A). Next, Gaf-1b was tested whether it also interacted with syntaxin 13. IPs were performed from lysate of triple-transfected HeLa cells with FLAG-Gaf-1b, HA-Stx13 and EGFP cDNA. FLAG-Gaf-1b did not co-immunoprecipitate with HA-Stx13 (Figure 2.11 B). In addition, the antibodies R140 and R85 did not interact with HA-Stx13 in the absence of calsyntenin-1, indicating that the R140 and R85 antibodies did not unspecifically recognize syntaxin 13. We then wondered whether Gaf-1b could associate with calsyntenin-1/syntaxin 13 complex. For this purpose, the same immunoprecipitations were performed from lysate of HeLa cells triple-transfected with FLAG-Gaf-1b, HA-Stx13 and EGFP-calsyntenin-1. Interestingly, the anti-calsyntenin-1 antibody R85 co-immunoprecipitated both HA-Stx13 and FLAG-Gaf-1b, while R140 only co-immunoprecipitated HA-Stx13 (Figure 2.11 C). The anti-Gaf-1b antibodies A and C co-immunoprecipitated EGFP-calsyntenin-1 and HA-Stx13. Neither anti-HA nor anti-GFP antibodies isolated the trimeric complex. Since the cytoplasmic part of calsyntenin-1 was sufficient to interact with Gaf-1b, the cytoplasmic domain was tested whether it was also responsible for the interaction to syntaxin 13. The same experiment was performed with lysate of HeLa cells triple-transfected with EGFP-calsyntenin-1_cyto, HA-Stx13 and FLAG-Gaf-1b. Intriguingly, EGFP-calsyntenin-1_cyto still co-immunoprecipitated with HA-Stx13 and FLAG-Gaf-1b and this trimeric complex was strongly precipitated with both R140 and anti-GFP antibodies (Figure 2.11 D). R85 antibody did not co-immunoprecipitate EGFP-calsyntenin-1_cyto nor did it cross-react with syntaxin 13 or Gaf-1b. Surprisingly, EGFP-calsyntenin-1_cyto co-immunoprecipitated with FLAG-Gaf-1b much more efficiently compared to wild-type calsyntenin-1. The anti-Gaf-1b antibodies A and C also isolated the trimeric complex. Taken together, these results showed that calsyntenin-1 interacted directly with syntaxin 13, and that Gaf-1b might associate with syntaxin 13 indirectly through binding to calsyntenin-1. Additionally, the cytoplasmic part of calsyntenin-1 was sufficient to interact with both Gaf-1b and syntaxin 13. The capability of calsyntenin-1 to interact directly with syntaxin 13 and Gaf-1b and indirectly with the recycling-endosomal protein Rab11 suggested a role for calsyntenin-1 in endosomal recycling.

Figure 2.11: Gaf-1b interacts indirectly with syntaxin 13 through calsyntenin-1. ►

(A-D) Transfected HeLa cells were solubilized twenty-four hours post-transfection and subjected to immunoprecipitations using the indicated antibodies. Immunoprecipitates were separated by 10% SDS-PAGE and blotted onto PVDF membrane. (A) HeLa cells were co-transfected with wild-type calsyntenin-1 and HA-Stx13. Calsyntenin-1 was co-precipitated with HA-Stx13. (B) HeLa cells were triple-transfected with FLAG-Gaf-1b, HA-Stx13 and EGFP cDNA. The immunoblot was analysed with anti-Gaf-1b antibody C or anti-HA antibody. FLAG-Gaf-1b was not co-immunoprecipitated by anti-HA, nor the anti-Gaf-1b antibody co-immunoprecipitated HA-Stx13. (C) HeLa cells were triple-transfected with FLAG-Gaf-1b, HA-Stx13 and EGFP-calsyntenin-1. The membranes were probed with anti-Gaf-1b antibody C, anti-GFP or anti-HA. In present of EGFP-calsyntenin-1, FLAG-Gaf-1b was co-immunoprecipitated with EGFP-calsyntenin-1 and HA-Stx13. (D) HeLa cells were triple-transfected with FLAG-Gaf-1b, HA-Stx13 and EGFP-calsyntenin-1_cyto. The membranes were analysed with anti-Gaf-1b antibody C, anti-GFP or anti-HA. FLAG-Gaf-1b co-immunoprecipitated with HA-Stx13 and EGFP-calsyntenin-1_cyto. Note that both R140 and GFP antibodies strongly co-immunoprecipitated FLAG-Gaf-1b and HA-Stx13. Cst1, calsyntenin-1; HA, hemagglutinin; IgG, immunoglobulin G; IP, immunoprecipitation; Stx13, syntaxin 13; wt, wild-type (adapted from Master thesis of Tu-My Diep, 2007).

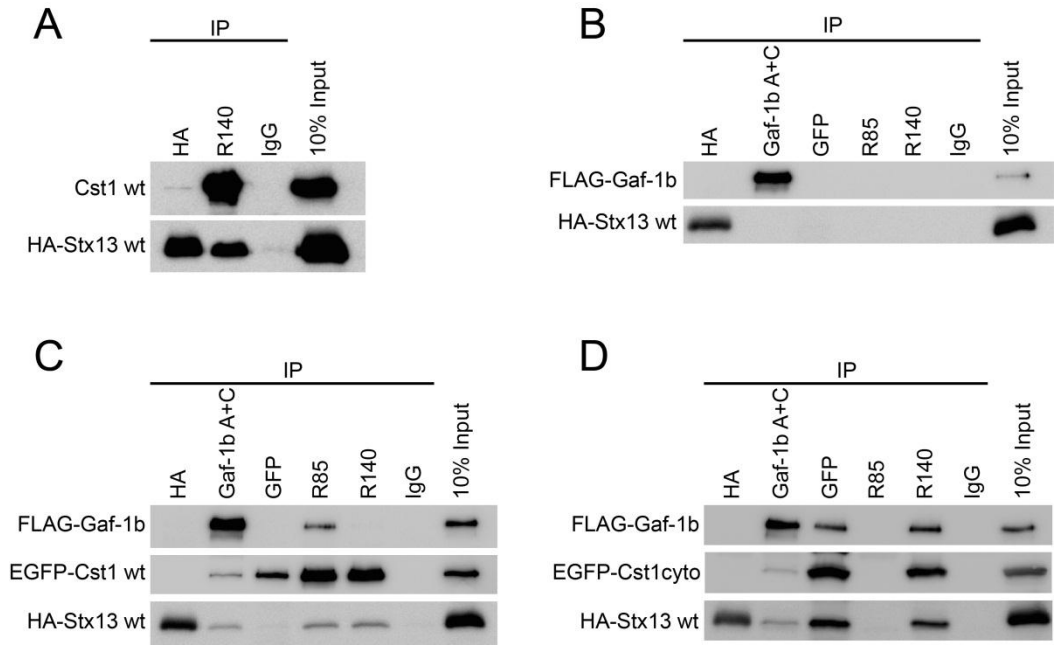

2.4.3 Gaf-1b is transported in calsyntenin-1 organelles devoid of APP

In order to provide more evidence for a co-transport of Gaf-1b with calsyntenin-1 in organelles devoid of APP, we analysed the interaction of APP with calsyntenin-1 and Gaf-1b. Previous studies showed that calsyntenin-1 and APP exit the TGN together and were co-transported in the same organelles [176, 200]. Thus, we tested whether calsyntenin-1 interacted with APP by co-transfection of HeLa cells with EGFP-calsyntenin-1 and wild-type APP and subsequent IPs. The anti-APP antibodies co-immunoprecipitated with EGFP-calsyntenin-1 (Figure 2.12 A). Then, IPs of HeLa cells co-transfected with FLAG-Gaf-1b and wild-type APP were performed. In this case neither anti-APP nor anti-Gaf-1b antibody B co-immunoprecipitated FLAG-Gaf-1b, nor APP, respectively (Figure 2.12 B). This result supported the conclusion that Gaf-1b had no relation to APP, since there were no colocalization and no interaction between these proteins. Therefore, Gaf-1b only carried a function in calsyntenin-1 organelle population which is transported through the recycling endosome.

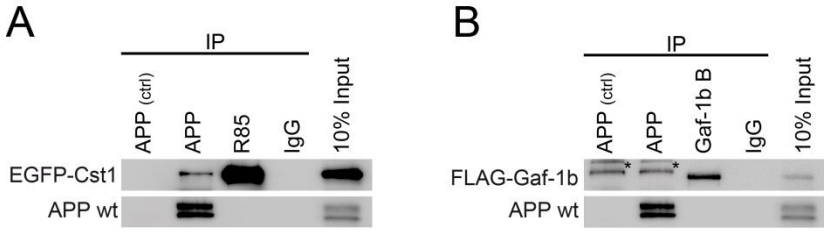

Figure 2.12: Gaf-1b is transported in calsyntenin-1 transport packages lacking APP.
(A and B) Transfected HeLa cells were solubilized twenty-four hours post-transfection and subjected to immunoprecipitations using the indicated antibodies. Immunoprecipitates were separated by 10% SDS-PAGE and blotted onto PVDF membrane. (A) HeLa cells were co-transfected with EGFP-calsyntenin-1 and wild-type APP. The anti-APP antibody co-immunoprecipitated EGFP-calsyntenin-1. (B) HeLa cells were co-transfected with FLAG-Gaf-1b and wild-type APP. Neither anti-APP antibody co-immunoprecipitated FLAG-Gaf-1b, nor anti-Gaf-1b antibody C co-immunoprecipitated APP. APP control served as a reference to discriminate between APP background staining (asterisks) and the FLAG-Gaf-1b signal. APP, amyloid precursor protein; Cst1, calsyntenin-1; IgG, immunoglobulin G; IP, immunoprecipitation; wt, wild-type; ctrl, control.

2.4.4 Gaf-1b interacts simultaneously with calsyntenin-1 and kinesin-light chain 1

Recently, our laboratory has identified the kinesin-light chain 1 (KLC1) motor protein as an interaction partner of calsyntenin-1 [171]. It was demonstrated that there is a specific interaction between the KBS1 and KBS2 domain of the calsyntenin-1 cytoplasmic part and the tetratricopeptide repeats of KLC1. Further it was shown that calsyntenins mediate TGN exit of APP in a kinesin-1-dependent manner [176]. Calsyntenin-1 was also implicated as a novel cargo-docking protein for processive, kinesin-1-mediated transport of tubulovesicular organelles along axons [171]. For Rip11 it was shown that it colocalizes at peripheral tubular endosomes where it is involved in the sorting of receptors to the slow recycling pathway. Additionally, a Rip11/kinesin II complex was identified which regulates the endocytic protein recycling [163]. Interestingly, when we examined the Gaf-1b sequence more in detail, we recognized an amino acid sequence of Gaf-1b in the splice insert, which was similar to the WDDS core motif in KBS1 and KBS2 in calsyntenin-1 (Figure 2.13 A). This prompted us to analyse whether mouse and human Gaf-1b can also interact with a kinesin motor protein, primarily with kinesin-light chain 1. For this reason, IPs with lysates of HeLa cells overexpressing mouse Gaf-1b-mCherry and HA-KLC1 were performed and a co-immunoprecipitation of the two proteins was confirmed (Figure 2.13 B). Since calsyntenin-1 interacted with KLC1, we were interested whether Gaf-1b interacted simultaneously with calsyntenin-1 and KLC1. Therefore, the same IPs were performed from lysates of HeLa cells triple-transfected with mouse Gaf-1b-mCherry, HA-KLC1 and wild-type calsyntenin-1. As shown in Figure 2.13 D, the anti-Gaf-1b antibody B co-immunoprecipitated HA-KLC1. The R140 antibody strongly precipitated calsyntenin-1 and moderately co-immunoprecipitated Gaf-1b-mCherry and HA-KLC1.

The mouse Gaf-1b sequence contained a WDDT sequence. This amino acid sequence was slightly different in human Gaf-1b, which contains a WDNT sequence. The difference of two amino acids in the human Gaf-1b compared to the WDDS core motif in KBS1 and KBS2 in calsyntenin-1 might abolish the interaction of the human Gaf-1b and KLC1. This assumption was tested by performing the same IPs with human Gaf-1b. HeLa cells were co-transfected with human FLAG-Gaf-1b and HA-KLC1. Interestingly, the human FLAG-Gaf-1b also co-immunoprecipitated with HA-KLC1 (Figure 2.13 C). When cells were triple-transfected with human FLAG-Gaf-1b, HA-KLC1 and wild-type calsyntenin-1, the trimeric complex was positively isolated by the R140 antibody (Figure 2.13 E). Taken together, it was shown that Gaf-1b interacted simultaneously with calsyntenin-1 and KLC1. Assuming that the WDDT motif in the mouse Gaf-1b and the WDNT motif in the human Gaf-1b were responsible for the interaction to KLC1, this would mean that the association with KLC1 was sufficient if the last two amino acids were acidic.

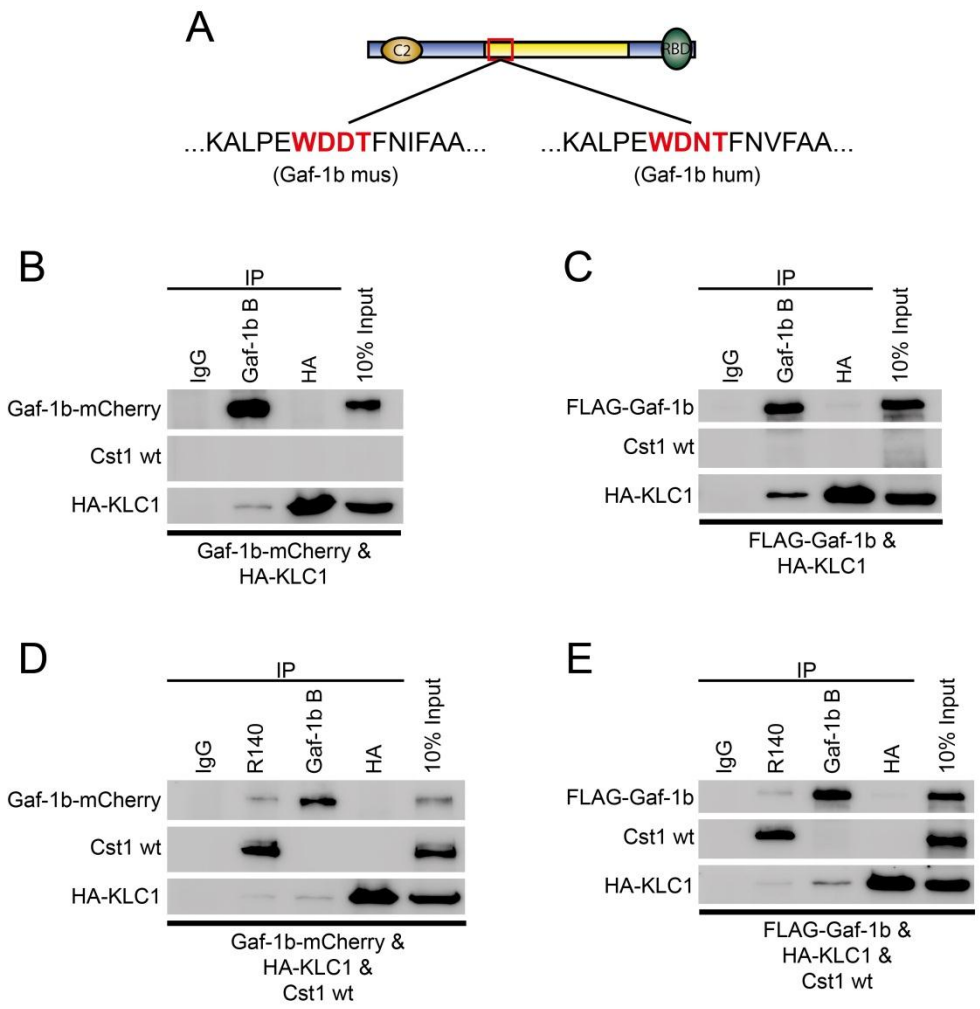

Figure 2.13: Gaf-1b interacts simultaneously with calsyntenin-1 and KLC1.
(A) Schematic drawing of Gaf-1b. Note, there is a similar sequence of mouse Gaf-1b and human Gaf-1b (highlighted in red) to the WDDS core motif in KBS1 and KBS2 (KLC1-binding segment) of calsyntenin-1. (B-E) Transfected HeLa cells were solubilized twenty-four hours post-transfection and subjected to immunoprecipitations using the indicated antibodies. Immunoprecipitates were separated by 10% SDS-PAGE and blotted onto PVDF membrane. (B) HeLa cells were co-transfected with mouse Gaf-1b-mCherry and HA-KLC1. The anti-Gaf-1b antibody B co-immunoprecipitated HA-KLC1. (C) HeLa cells were co-transfected with human FLAG-Gaf-1b and HA-KLC1. The anti-Gaf-1b antibody B co-immunoprecipitated efficiently HA-KLC1. (D) HeLa cells were triple-transfected with mouse Gaf-1b-mCherry, wild-type calsyntenin-1 and HA-KLC1. The anti-Gaf-1b antibody B co-immunoprecipitated HA-KLC1 and the anti-calsyntenin-1 antibody R140 co-immunoprecipitated with Gaf-1b-mCherry and HA-KLC1. (E) HeLa cells were triple-transfected with human FLAG-Gaf-1b, wild-type calsyntenin-1 and HA-KLC1. The anti-Gaf-1b antibody B co-immunoprecipitated HA-KLC1 and the anti-calsyntenin-1 antibody R140 co-immunoprecipitated with FLAG-Gaf-1b and HA-KLC1. Cst1, calsyntenin-1; HA, hemagglutinin; IgG, immunoglobulin G; IP, immunoprecipitation; KLC1, kinesin-light chain 1; wt, wild-type.

2.5 Gaf-1b trafficking is disrupted upon blockage of calsyntenin-1 and KLC1 TGN exit

Calsyntenin-1 recruits kinesin-light chain 1 to the TGN and post-Golgi organelles [176] and Gaf-1b colocalizes with TGN markers. Thus, we assumed that Gaf-1b might be also recruited to the TGN membranes and exit the TGN together with calsyntenin-1 and KLC1 in post-Golgi carriers.

First, the subcellular localization of Gaf-1b, calsyntenin-1 and KLC1 alone was tested. HeLa cells were single-transfected either with Gaf-1b-mEGFP, RFP-KLC1 or wild-type calsyntenin-1. All overexpressed proteins showed a vesicular staining pattern in the periphery throughout the cell (Figure 2.14 A-C). Second, RFP-KLC1 and calsyntenin-1 were overexpressed in HeLa cells. The formation of large ER membrane whorls positive for RFP-KLC1 and calsyntenin-1 was observed in cells expressing higher levels of RFP-KLC1 and calsyntenin-1 as previously described [176] (Figure 2.14 D). Because Gaf-1b also interacted with KLC1, we were interested whether Gaf-1b could also form such ER membrane whorls with KLC1. In contrast to calsyntenin-1, cells overexpressing Gaf-1b-mEGFP and RFP-KLC1 did not show any formation of ER membrane whorls (Figure 2.14 E). The staining pattern of Gaf-1b-mEGFP and RFP-KLC1 was similar to single transfected cells. In a next step, we triple-transfected HeLa cells with Gaf-1b-mEGFP, RFP-KLC1 and wild-type calsyntenin-1. Interestingly, Gaf-1b-mEGFP, RFP-KLC1 and calsyntenin-1 were largely absent from cytoplasmic vesicles, however, Gaf-1b-mEGFP and RFP-KLC1 were accumulated in giant structures close to the nucleus, and these structures were devoid of calsyntenin-1 (Figure 2.14 F, asterisk). The ER membrane whorls positive for RFP-KLC1 and calsyntenin-1 were still present (>). Additionally, some smaller structures were observed containing all three overexpressed proteins Gaf-1b-mEGFP, RFP-KLC1 and calsyntenin-1 (►). We wondered in which kind of structures Gaf-1b and KLC1 were accumulated. Therefore, the same overexpression with Gaf-1b-mEGFP, RFP-KLC1 and calsyntenin-1 was performed and the cells were co-stained with different markers, such as calnexin for ERs, GM130 for the Golgi and TGN46 for the *trans*-Golgi network. Calnexin only labeled the ER membrane whorls and colocalized with RFP-KLC1 (Figure 2.14 G, (>)). GM130 partially overlapped with Gaf-1b-mEGFP and RFP-KLC1 in the accumulated structures next to the nucleus (Figure 2.14 H, (►)), while TGN46 completely colocalized with Gaf-1b-mEGFP and RFP-KLC1 (Figure 2.14 I, (►)). Additionally, GM130 and TGN46 also labeled ER membrane whorls (>). In summary, our data indicated that Gaf-1b was also recruited to the TGN and exits the TGN in a calsyntenin-1/KLC1-dependent manner where it was then co-transported with calsyntenin-1 to recycling endosomes.

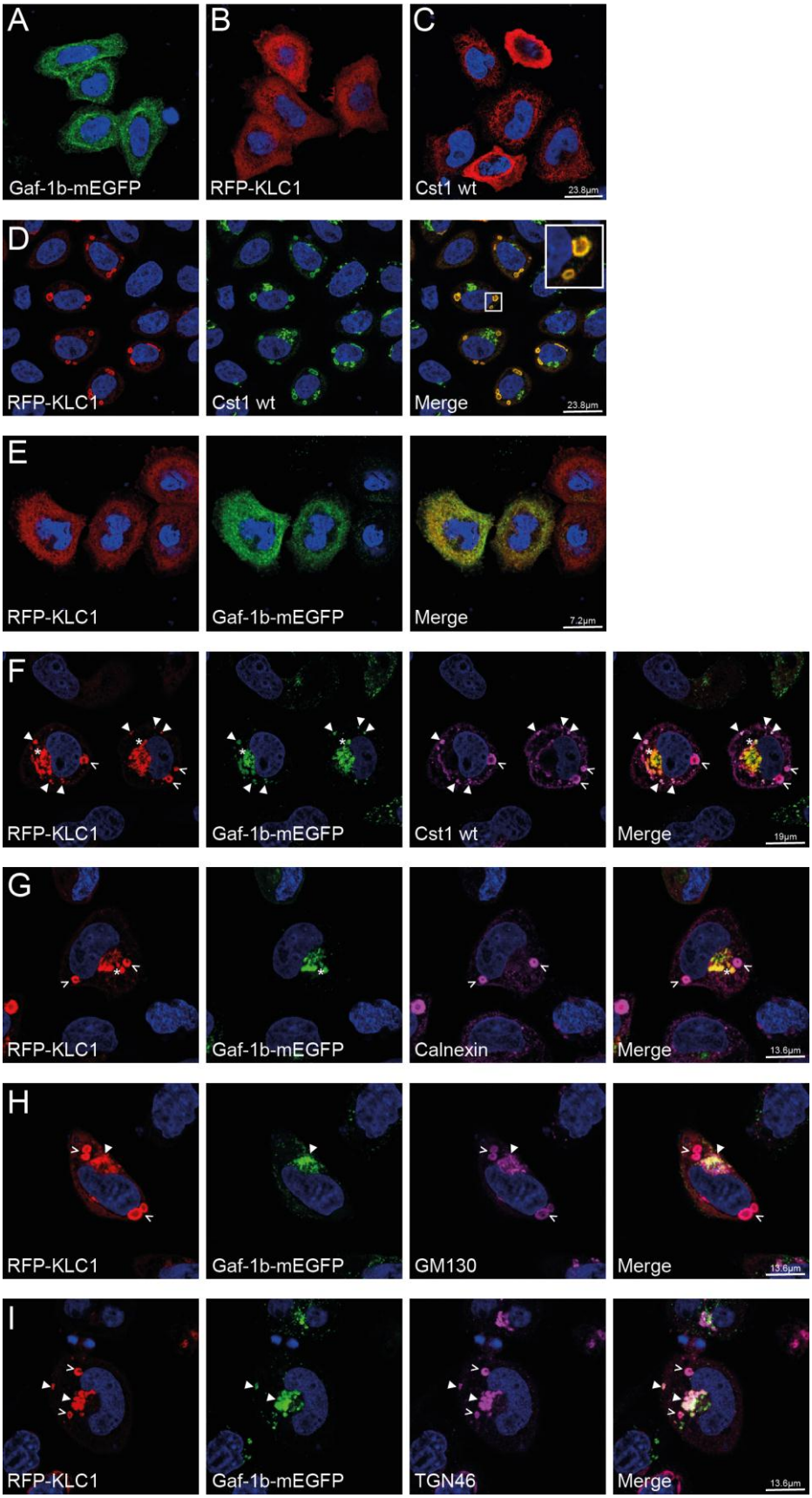
A
Gaf-1b-mEGFP
B
RFP-KLC1
C
Cst1 wt
23.8µm
D
RFP-KLC1
Cst1 wt
Merge
23.8µm
E
RFP-KLC1
Gaf-1b-mEGFP
Merge
7.2µm
F
RFP-KLC1
Gaf-1b-mEGFP
Cst1 wt
Merge
19µm
G
RFP-KLC1
Gaf-1b-mEGFP
Calnexin
Merge
13.6µm
H
RFP-KLC1
Gaf-1b-mEGFP
GM130
Merge
13.6µm
I
RFP-KLC1
Gaf-1b-mEGFP
TGN46
Merge
13.6µm

◄ Figure 2.14: Gaf-1b accumulates at the TGN upon blockage of calsyntenin-1/KLC1 TGN exit.
(A-I) Transfected HeLa cells were fixed with 4% PFA, permeabilized and processed for immunofluorescence. Single stacks were captured with a confocal laser scanning microscope (Leica SP2) using a 63x objective (NA 1.32). Nuclei were visualized with Hoechst dye. Two-color RGB images were produced in Adobe Photoshop CS3. (A-C) Single transfection of Gaf-1b-mEGFP (A), RFP-KLC1 (B) or wild-type calsyntenin-1 (C) are shown. Gaf-1b-mEGFP, RFP-KLC1 or calsyntenin-1 showed a vesicular or cytoplasmic staining pattern. (D) Co-transfection of RFP-KLC1 and wild-type calsyntenin-1. High expression of RFP-KLC1 and calsyntenin-1 lead to KLC1- and calsyntenin-1-positive giant, cylindrical structures close to the nuclear envelope (ER stacks). (E) Co-transfection of RFP-KLC1 and Gaf-1b-mEGFP showed similar localization of RFP-KLC1 and Gaf-1b-mEGFP like in single transfected cells in (A) and (B). (F-I) HeLa cells triple transfected with RFP-KLC1, Gaf-1b-mEGFP and wild-type calsyntenin-1 and stained for calsyntenin-1 (F), calnexin (G), GM130 (H) or TGN (I). (F) RFP-KLC1 and calsyntenin-1 were accumulated in ER stacks (>). In contrast to calsyntenin-1, RFP-KLC1 was accumulated in large structures at a perinuclear region which were also positive for Gaf-1b-mEGFP (*). In the periphery there were smaller accumulated structures positive for RFP-KLC1, Gaf-1b-mEGFP and calsyntenin-1 (►). (G) The ER stacks were positive for the ER marker calnexin (>), but calnexin was absent in the accumulated structure at the perinuclear region (*). (H) The Golgi marker GM130 partially overlapped with the large structure of RFP-KLC1 and Gaf-1b-mEGFP (►) and completely stained the ER stacks (>). (I) The *trans*-Golgi network marker TGN46 entirely colocalized with RFP-KLC1 and Gaf-1b-mEGFP in large accumulated structure at the perinuclear region and in smaller accumulations in the periphery (►). Additionally, TGN46 were found in ER stacks (>). Cst1, calsyntenin-1; KLC1, kinesin-light chain 1; wt, wild-type.

2.6 Gaf-1b and receptor recycling

The Rab11-FIPs have been identified as key players in the regulation of several distinct intracellular membrane trafficking events [154]. These can be grouped into three categories: recycling of cargo to cell surface, delivery of membrane to the cleavage furrow/midbody during cell division and linkers between Rab11 and molecular motor proteins [154]. RCP functions in transferrin recycling and is involved in transport of vesicles from the early sorting endosome to the recycling compartment [204]. Furthermore, RCP forms a complex with $\alpha 5\beta 1$ integrin and EGFR1 and drive their recycling to the cell surface, where RCP regulates the $\alpha 5\beta 1$ integrin-dependent cell motility [158]. It was suggested that the N-terminal C2 domains of the class I FIPs target Rab11-FIP complexes to docking sites on the plasma membrane that are enriched with phospholipids (PtdIns(3,4,5)P_3 and phosphatidic acid) [153]. FIP2 is also responsible for the recycling of cargo molecules to the cell surface, such as aquaporin-2 and CXC chemokine receptor 2 [159, 160]. Additionally, there is a FIP2 function in the synaptic LTP because disruption of FIP2 function blocks the recycling of AMPA receptors and dendritic spine growth in postsynaptic neurons [161]. The diverse functions of Rab11-FIPS in protein recycling implied that also Gaf-1b might be involved in protein recycling. To test this, Gaf-1b was down-regulated in HeLa cells by siRNA transfection and the cell lysate was analysed for deficits in recycling of EGFR, TfR, Erb3 or Erb4. As shown in Figure 2.15 A and B, the Gaf-1b siRNA efficiently down-regulated Gaf-1b by about 82.90 ± 1.2%. The Rip11 siRNA down-regulated both Gaf-1b and Rip11 by about 87.8 ± 0.9% and 88.0 ± 1.3%, respectively. In Gaf-1b and Rip11 down-regulated cells the Tf-receptor recycling was slightly decreased by 17.3 ± 1.7% for Gaf-1b knock-down and by 18.7 ± 1.3% for Rip11 downregulation. The EGFR recycling was not notably affected possessing decreased signals of 12.7 ± 2.2% and 19.8 ± 2.7% for Gaf-1b and Rip11 knock-down, respectively. Since EGFR and TfR recycle between endosomes and the plasma membrane, we wondered whether there was a difference in the presence of receptor on the surface after Gaf-1b has been down-regulated. Biotinylation experiments were performed to separate receptors bound at the plasma membrane and receptors in the cell. EGFR was mainly found at the plasma membrane and TfR was predominantly at the plasma membrane but there existed also a small fraction of TfR within the cell (Figure 2.15 C). However, we

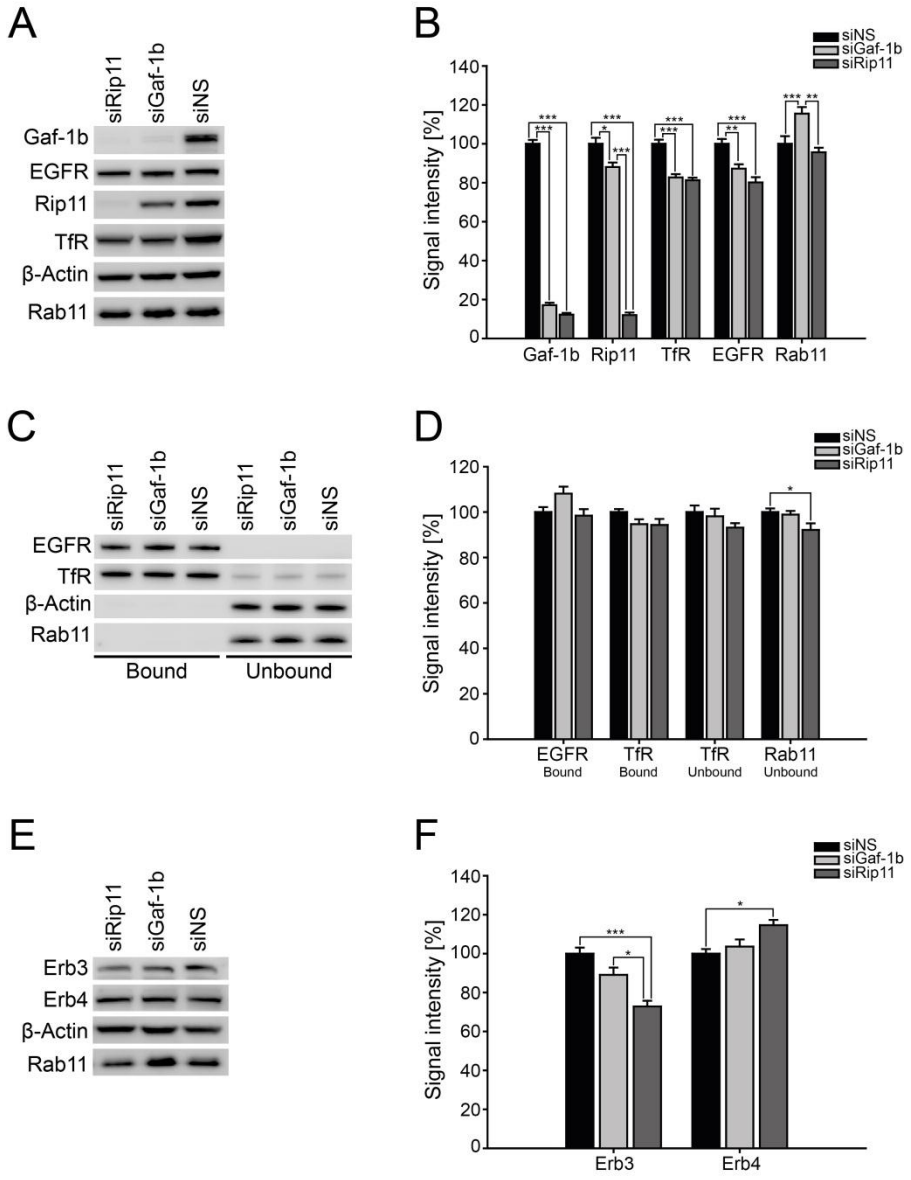

Figure 2.15: Gaf-1b and Receptor recycling.

(A, C and E) HeLa cells were transfected with nonsense, Gaf-1b or Rip11 siRNAs for 48 hours. (A) Cells were solubilized and cell lysate was separated on a 4-12% Bis-Tris gel and blotted onto PVDF membrane. Immunoblot was analysed with the following antibodies: anti-Gaf-1b C for Gaf-1b and Rip11, anti-β-actin, anti-EGFR, anti-TfR and anti-Rab11. The Gaf-1b siRNA efficiently down-regulated Gaf-1b and the Rip11 siRNA down-regulated both Rip11 and Gaf-1b. (B) Quantification of data shown in (A). Error bars indicate mean ± SEM, *p>0.05, **p>0.005, ***p>0.001, Tukey test. (C) Cells were biotinylated live at 4 °C for 15 min. After quenching residual biotin, cells were lysed and the extract added to streptavidin beads for 2 h. The unbound fraction was collected, beads were washed and bound proteins eluted with SDS-PAGE sample buffer. The bound and the unbound fraction were separated on a 4-12% Bis-Tris gel, blotted onto PVDF membrane and the immunoblots were analysed using the indicated antibodies. EGFR was only found on the plasma membrane while TfR is predominantly at the plasma membrane. (D) Quantification of data shown in (C). Error bars indicate mean ± SEM, *p>0.05, Tukey test. (E) Cells were solubilized and cell lysate was separated on a 4-12% Bis-Tris gel and blotted onto PVDF membrane. Immunoblot was analysed with the following antibodies: anti-β-actin, anti-Erb3, anti-Erb4 and anti-Rab11. (F) Quantification of data shown in (C). Error bars indicate mean ± SEM, *p>0.05, ***p>0.001, Tukey test. EGFR, epidermal growth factor receptor; NS, nonsense; TfR, transferrin receptor.

could not observe any significant difference in the receptors distribution of down-regulated Gaf-1b or Rip11 cells (Figure 2.15 D). Erb3 and Erb4 were also only slightly affected by the siRNA (Figure 2.15 E and F). Gaf-1b or Rip11 siRNA transfected cells decreased Erb3 by about 11 ± 3.7% or 17.2 ± 2.9%. This suggested that only a minor part of TfR, EGFR and Erbs (at most 20%) was affected in its recycling by the downregulation of Gaf-1b because receptor sorting could also be regulated by other Rab11-FIPs. Therefore, the main function of Gaf-1b probably did not comprise receptor recycling which could explain the minor effects observed during this study.

2.7 Overexpression of Gaf-1b and calsyntenin-1 affects the morphology of HeLa cells

Gaf-1b and calsyntenin-1 colocalized in dendrites and axons of cultured hippocampal neurons, but no significant colocalization of endogenous Gaf-1b and overexpressed calsyntenin-1 in HeLa cells could be observed. In order to analyse this more in detail, FLAG-Gaf1b was transfected in HeLa cells stably expressing mEGFP-calsyntenin-1. Interestingly, high level of FLAG-Gaf1b and mEGFP-calsyntenin-1 induced long plasma membrane extensions of the cell (Figure 2.16 F). These long membrane elongations were often broad, highly branched and oriented in a bipolar way. FLAG-Gaf-1b was found to localize at the plasma membrane, while mEGFP-calsyntenin-1 was still localized at the Golgi/TGN and to cytoplasmic vesicles. Within the branches, several bulges contained both FLAG-Gaf-1b and mEGFP-calsyntenin-1. HeLa cells stably expressing mEGFP-calsyntenin-1 but not transfected with FLAG-Gaf-1b did not show membrane extensions and the cell shape was rather round than sustained and thin (Figure 2.16 E). Transfected FLAG-Gaf-1b cells not expressing calsyntenin-1 also showed rather long plasma membrane extensions but the effect was less pronounced than in cells overexpressing both proteins (Figure 2.16 A and J). This effect was investigated with other Gaf-1b truncation constructs in the presence or absence of mEGFP-calsyntenin-1. All the truncation constructs that did not interact with calsyntenin-1, such as FLAG-Gaf-1b_ΔN, FLAG-Gaf-1b_ins and also Rip11-EGFP, did not possess any membrane elongations (Figure 2.16 B, C, G, H). In contrast, the calsyntenin-1-interacting construct FLAG-Gaf-1b_522ΔC induced again long membrane elongation but to a lesser extent compared to full-length Gaf-1b and this effect was increased in the presence of mEGFP-calsyntenin-1 (Figure 2.16 D and I). These results further supported the idea that calsyntenin-1 and Gaf-1b were co-transported in post-TGN carriers through recycling endosomes to the plasma membrane.

2.7.1 Gaf-1b knock-down induces stress fibre formation

The morphological effects observed after overexpression of Gaf-1b in HeLa cells might be caused by rearrangements of the cellular cytoskeleton. Therefore, we examined actin filaments and microtubules after downregulation of Gaf-1b in HeLa cells. Preliminary data showed the formation of robust stress fibres in siGaf-1b- and siRip11-transfected cells, while the siNS-transfected cells were of normally morphology and lacked prominent actin bundles (Figure 2.17 A).

Rho proteins are involved in the pathway that controls stress fibre formation [209] and microinjections of activated recombinant RhoA into fibroblasts leads to rapid and extensive stress fibre formation [210]. It was reported that in HeLa cells the G protein subunit βγ subunits induces stress fibre formation in a Rho-dependent manner [211]. This prompted us to analyse the actin filament-regulating proteins Cdc42 and RhoA. Preliminary immunoblotting data indicated that siGaf-1b-

transfected cells showed an increase of Cdc42 and RhoA, while the downregulation of Rip11 decreased the signal of Cdc42 and RhoA (Figure 2.17 B and C). Currently, we do not have enough data to significantly confirm this result, thus additional experiments are required. Nonetheless, these results might indicate a function of Gaf-1b in regulating Cdc42 and RhoA, possibly by being involved in the transport of these proteins to their target location.

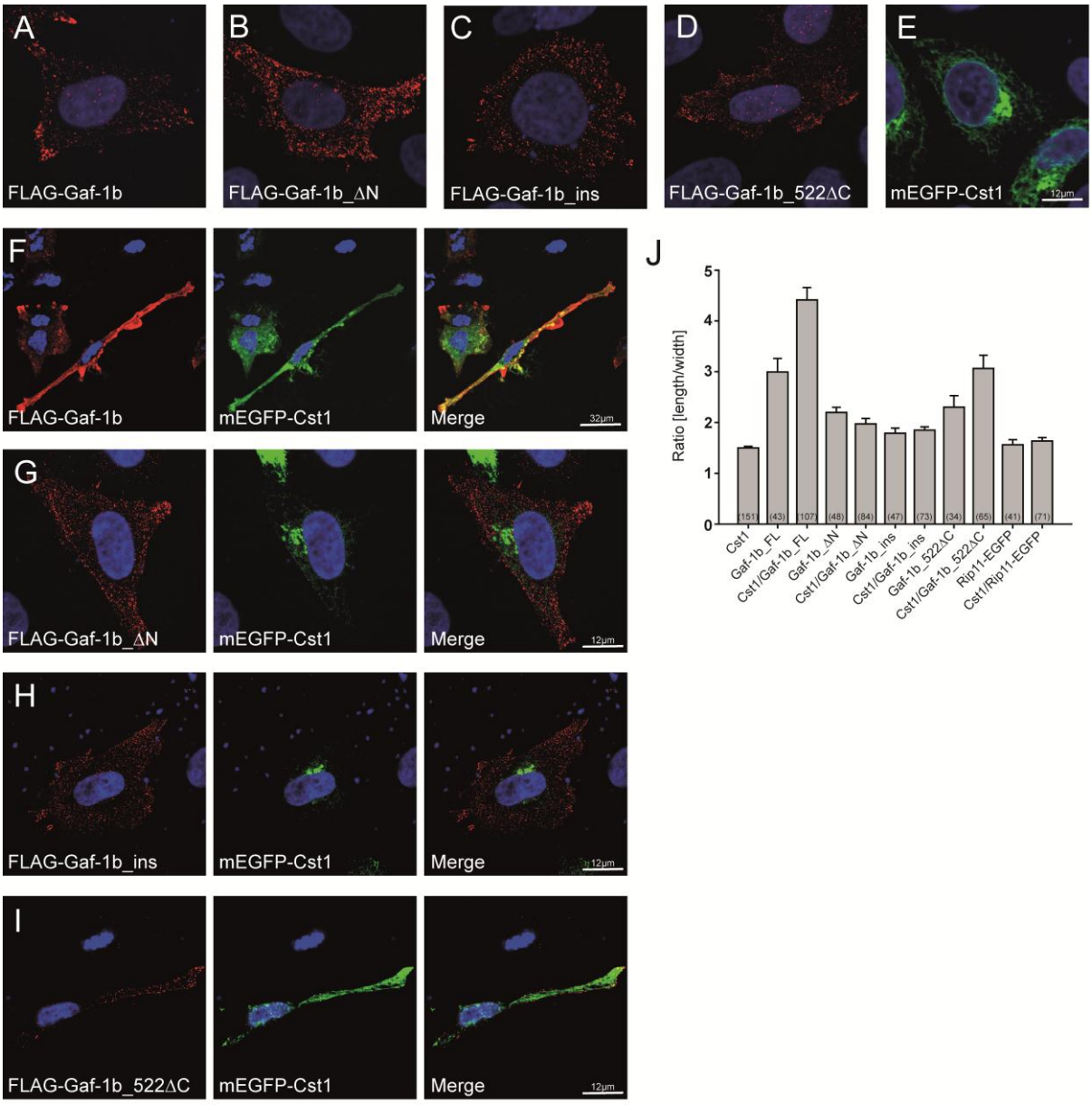

Figure 2.16: High expression of Gaf-1b affects HeLa cell morphology.
(A-I) Transfected HeLa cells were fixed with 4% PFA, permeabilized and processed for immunofluorescence. Single stacks were captured with a confocal laser scanning microscope (Leica SP2) using a 63x objective (NA 1.32). Nuclei were visualized with Hoechst dye. Two-color RGB images were produced in Adobe Photoshop CS3. (A-E) Single-transfection of FLAG-Gaf-1b (A), FLAG-Gaf-1b_ΔN (B), FLAG-Gaf-1b_ins (C), FLAG-Gaf-1b_522ΔC (D) or mEGFP-calsyntenin-1 (E). (F-I) HeLa cells were co-transfected with mEGFP-calsyntenin-1 and either full-length FLAG-Gaf-1b (F), FLAG-Gaf-1b_ΔN (G), FLAG-Gaf-1b_ins (H) or FLAG-Gaf-1b_522ΔC (I). Note, co-expression of mEGFP-calsyntenin-1 and FLAG-Gaf-1b or FLAG-Gaf-1b_522ΔC showed an altered cell shape of HeLa cells with long plasma membrane extensions. (J) Quantification of the ratio length/width of HeLa cell shape of data shown in (A-I). Error bars indicate mean ± SEM. Cst1, calsyntenin-1; ins, insert.

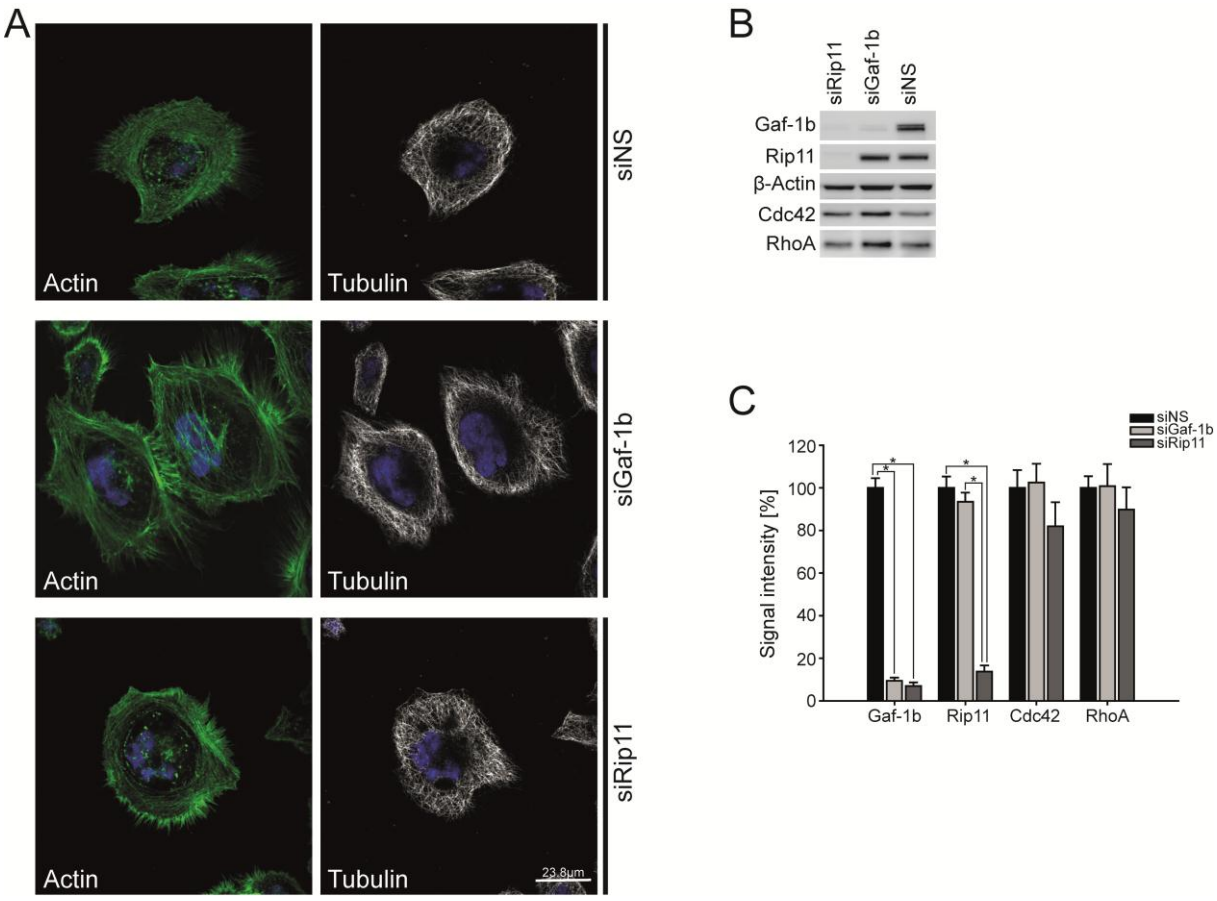

Figure 2.17: Gaf-1b knock-down induces enhanced stress fibre and filopodia formation.
(A) HeLa cells were transfected with nonsense, Gaf-1b or Rip11 siRNAs for 48 hours, fixed with 4% PFA and proteins were cross linked with 0.05% glutaraldehyde, permeabilized and processed for immunofluorescence. Actinfilaments were visualized with FITC-coupled phalloidin and tubulin was stained with anti-α-tubulin antibody. Stacks were captured with a confocal laser scanning microscope (Leica SP2) using a 63x objective (NA 1.32). Nuclei were visualized with Hoechst dye. siNS transfected cells were well spread but lacked prominent actin bundles. In siGaf-1b and siRip11 transfected cells robust stress fiber were present. (B) HeLa cells were transfected with nonsense, Gaf-1b or Rip11 siRNAs for 48 hours. Cells were solubilized and cell lysate was separated on a 4-12% Bis-Tris gel and blotted onto PVDF membrane. Immunoblot was analysed with the following antibodies: anti-Gaf-1b C for Gaf-1b and Rip11, anti-β-actin, anti-RhoA and anti-Cdc42. The Gaf-1b siRNA efficiently down-regulated Gaf-1b and the Rip11 siRNA down-regulated both Rip11 and Gaf-1b. (C) Quantification of data shown in (B). Error bars indicate mean ± SEM, *p>0.05, Tukey test. NS, nonsense.

2.8 Gaf-1b is necessary for cell viability

Calsyntenin-1 is a neuronal type-1 transmembrane protein and prominent functions of calsyntenin-1 in intracellular trafficking were identified in neurons [171, 176-178]. Because all the Gaf-1b knock-down experiments were performed in HeLa cells, we were interested how the neurons were affected when the Gaf-1b expression was down-regulated. Short hairpin RNAs down-regulating Gaf-1b and Rip11 were designed and the specificity of the shRNA was tested in HeLa cells. The shRNA of Gaf-1b specifically down-regulated Gaf-1b, while the shRip11 down-regulated both Gaf-1b and Rip11 (data not shown). Suspensions of cortical neurons were transfected with the shRNA by AMAXA nucleofection. Interestingly, we observed that neurons transfected with shRNA for Gaf-1b or Rip11 showed a very high death rate (Figure 2.18 A). After 10 DIV only a few neurons survived in Gaf-1b

and Rip11 knock-down samples, in contrast, the shNS transfected neurons exhibit a much lower death rate. This result showed that Gaf-1b was necessary for cell viability in neurons.

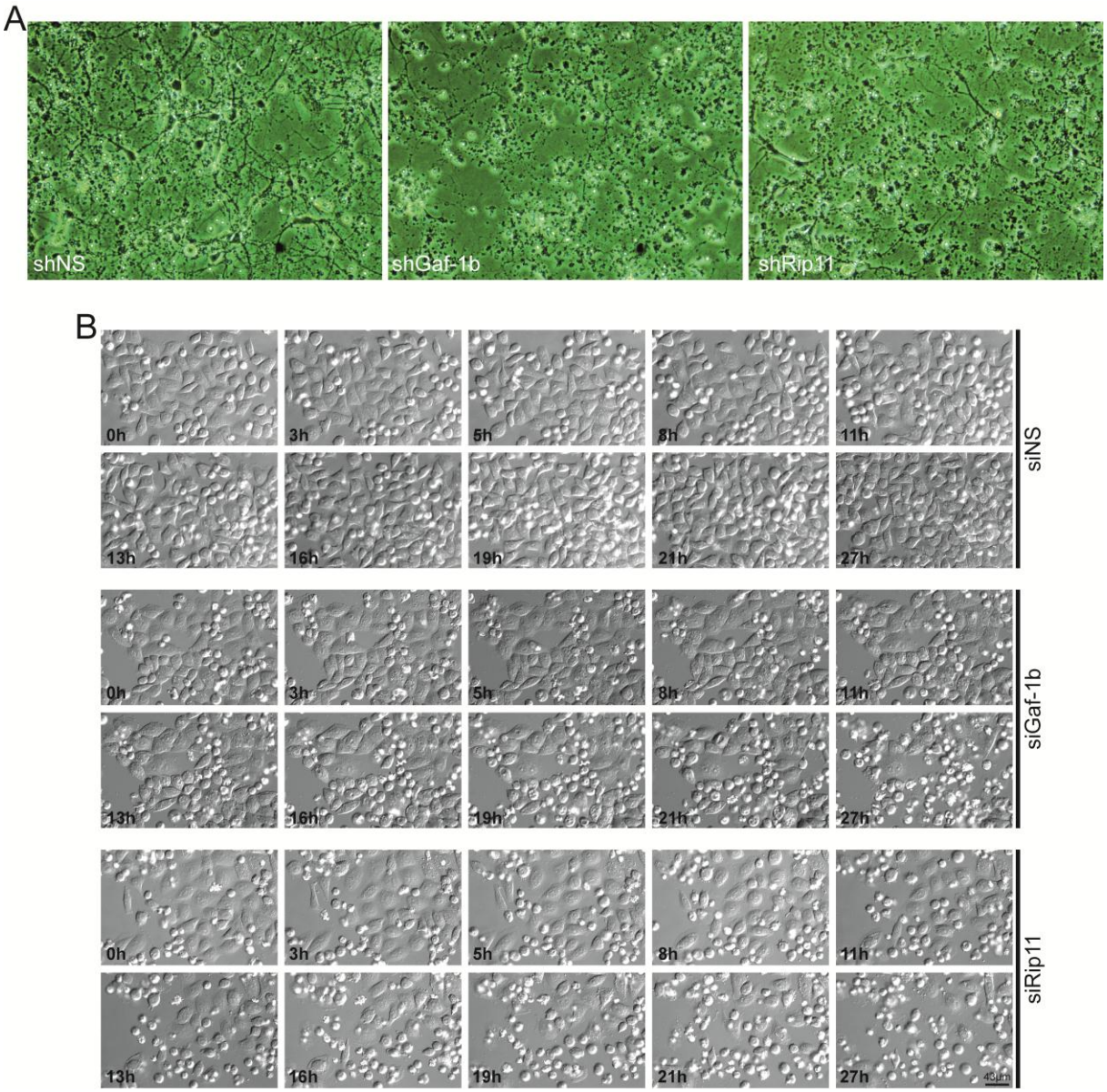

Figure 2.18: Gaf-1b is necessary for cell viability.
(A) High density cortical neurons were transfected (AMAXA) at DIV0 with the shRNA of a nonsense sequence, Gaf-1b or Rip11 and grown on PLL coated culture dishes for 10 days. Phase contrast images were captured on living neurons. Note, compared to shNS transfected neurons, there is more cell debris in shGaf-1b and shRip11 treated neurons. (B) HeLa cells were grown on PLL coated coverslips, transfected with nonsense, Gaf-1b or Rip11 siRNAs for 48 hours and imaged live at 37 °C for 27 hours using a 20x objective and frame rate of one image per 8 minutes. Time-laps sequence of siNS, siGaf-1b or siRip11 cells are shown. The siNS treated cells proliferated normally, after 27 hours the cell number were doubled. Only a few cells survived after 27 hours in siGaf-1b or siRip11 transfected HeLa cells. NS, nonsense.

In HeLa cells we usually analysed the cells 24 hours after the siRNA transfection. At this time point the cells looked healthy and siRNA-mediated knock-down was highly efficient for Gaf-1b and Rip11 (Figure 2.15 A and B). Since in neurons the long-term downregulation of Gaf-1b was lethal for

neurons, we wondered whether the Gaf-1b knock-down would also influence the HeLa cell viability over a longer time period. For this purpose, we live imaged HeLa cells 24 hours post-transfection with the indicated siRNA for 27 hours. The siNS-treated cells showed normal cellular dynamics and proliferated normally (Figure 2.18 B). In the contrary, cells transfected with siRNA against Gaf-1b or Rip11 were rather rigid, did not proliferate as usual, and died one by one over 27 hours. In summary, this result underpinned the fact that Gaf-1b was essential for cell viability.

2.9 GABARAPL1 and GABARAPL2 interact with Gaf-1b

2.9.1 GABARAPL1 and GABRAPL2 are novel interaction partners of Gaf-1b

So far little is known about the function of Gaf-1b. In order to gain more insight into the function of Gaf-1b, we performed a yeast two-hybrid screen to identify new interaction partner of Gaf-1b. A pMyc-LexA bait fusion construct of human full-length Gaf-1b was used to screen against a human fetal brain cDNA library. The screening resulted in eight positive clones. Sequence analysis showed that one of these clones corresponded to Rab11, indicating the specificity of the screen. Three clones correlated with GABARAPL2 and the other clones corresponded to OTUB1, CRIPT, farnesyltransferase and Mint2. Co-immunoprecipitation was performed from HeLa cell extracts to verify the interaction between Gaf-1b and the positive hits from yeast two-hybrid screen. Among the possible binding candidates of Gaf-1b only GABRAPL2 was positively co-immunoprecipitated with Gaf-1b (data not shown) [212, 213].

GABARAPL2 is a small globular ubiquitin-like modifier protein of the MAP1LC3/Atg8 family and has been implicated in intracellular trafficking and fusion events, as well as an interactor of NSF and the Golgi v-SNARE GOS-28 [194, 197], suggesting that it is involved in intra-Golgi transport. Additionally, members of the MAP1LC3/Atg8 family are linked to the process of autophagy [98, 192, 193, 199, 214]. Among the MAP1LC3 family members it has been described that GABARAPL1 displays 61% sequence identity and 75% sequence similarity to GABARAPL2. LC3A and LC3B are the human LC3 isoforms that are conserved in mice and are central coordinators of membrane rearrangement dynamics during autophagosome formation [85, 215]. LC3A and LC3B show a 40% and 37% sequence identity and 64% and 61% sequence similarity to GABARAPL2, respectively. In order to analyse the interaction specificity among the MAP1LC3 family members with Gaf-1b we designed HA-tagged fusion constructs of GABARAPL2 as well as of its paralogues GABARAPL1, LC3A and LC3B (Figure 2.19 A). IPs of lysate of HeLa cells co-transfected with FLAG-Gaf-1b and either HA-GABARAPL1, HA-GABARAPL2, HA-LC3A or HA-LC3B were performed. Immunoblot analysis revealed that FLAG-Gaf-1b co-immunoprecipitated with HA-GABARAPL1 and HA-GABARAPL2 (Figure 2.19 B). As a control for a specific immunoreactivity, the anti-HA antibodies were preincubated with their immunizing peptide. It was shown that neither HA-LC3A nor HA-LC3B co-immunoprecipitated with FLAG-Gaf-1b (Figure 2.19 C). Further, we were interested whether the splice variant Rip11 would interact with GABARAPL1 and GABARAPL2. The same co-immunoprecipitation experiment was performed with extracts of HeLa cells co-transfected with Rip11-EGFP and HA-GABARAPL1 or HA-GABARAPL2. Rip11-EGFP did not co-immunoprecipitate with HA-GABARAPL1 or HA-GABARAPL2 (Figure 2.19 D). These results showed that Gaf-1b specifically interacted with GABARAPL1 and GABRARAPL2. The splice insert of Gaf-1b might be crucial for the binding since Rip11 did not interact with GABARAPL1 and GABARAPL2 because the only difference between Gaf-1b and Rip11 is the additional 565 amino acid splice insert in Gaf-1b [213].

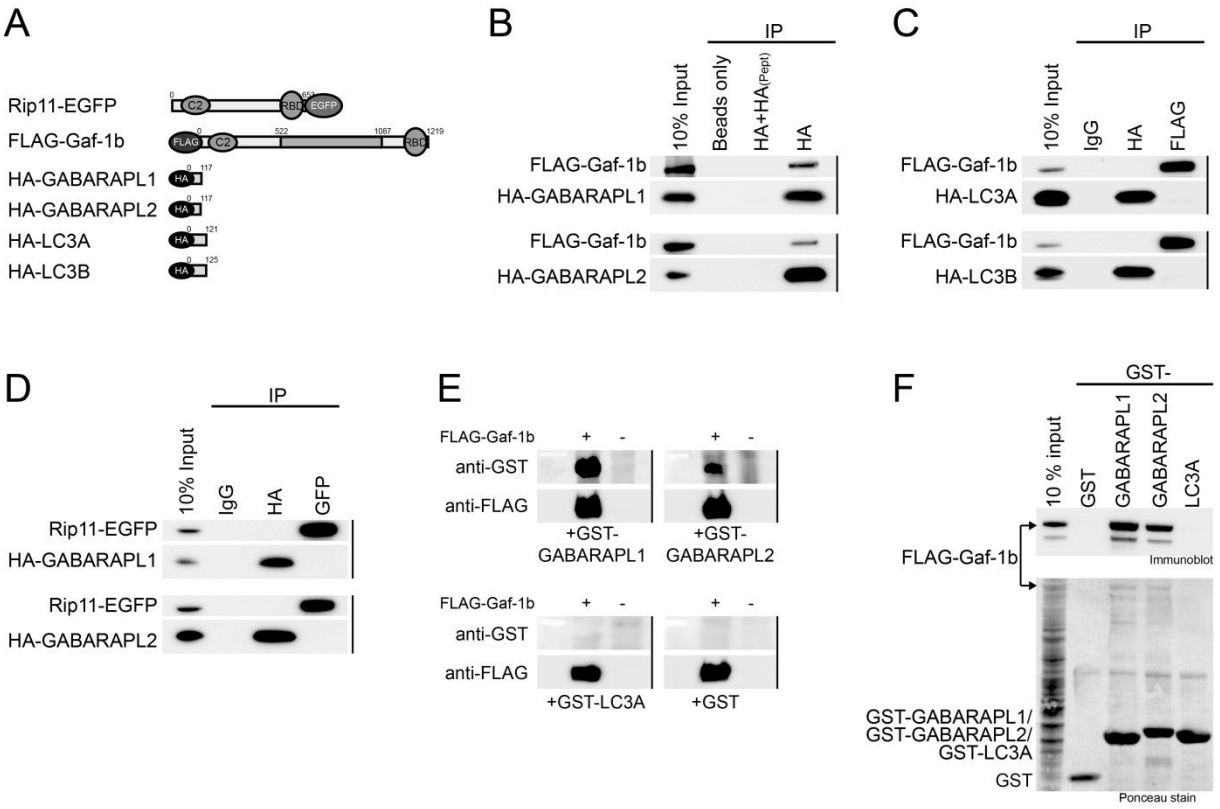

Figure 2.19: Gaf-1b interacts specifically and directly with GABARAPL1 and GABARAPL2.
(A) Schematic drawings of the used tagged fusion constructs. (B-D) Transfected HeLa cells were solubilized twenty-four hours post-transfection and subjected to immunoprecipitations using the indicated antibodies. Immunoprecipitates were separated by 12.5% SDS-PAGE and blotted onto PVDF membrane. (B) HeLa cells were co-transfected with FLAG-Gaf-1b and HA-GABARAPL1 (upper panel) or with FLAG-Gaf-1b and HA-GABARAPL2 (lower panel). The immunoblots were probed with anti-FLAG or anti-HA. Both HA-GABARAPL1 and HA-GABARAPL2 co-immunoprecipitated with FLAG-Gaf-1b. As controls for specific immunoreactivity, the precipitating anti-HA antibodies were either preincubated with their immunizing peptide ($HA_{(Pept)}$), or pre-immune mouse IgG was applied. Incubation of HeLa cell extracts with protein G-sepharose beads (beads only) served as control for unspecific sepharose matrix adsorption of FLAG-Gaf-1b. (C) HeLa cells were co-transfected with FLAG-Gaf-1b and HA-LC3A (upper panel) or with FLAG-Gaf-1b and HA-LC3B (lower panel). The immunoblots were probed with anti-FLAG or anti-HA. Neither HA-LC3A nor HA-LC3B co-immunoprecipitated with FLAG-Gaf-1b. (D) Cells were co-transfected with Rip11-EGFP and HA-GABARAPL1 (upper panel) or with Rip11-EGFP and HA-GABARAPL2 (lower panel). The immunoblots were probed with anti-Gaf-1b antibody C or anti-HA. Both HA-GABARAPL1 and HA-GABARAPL2 did not co-immunoprecipitate with Rip11-EGFP. (E) 400 µg lysate of FLAG-Gaf-1b transfected (+) or FLAG-Gaf-1b untransfected (-) HeLa cells were separated on a 5% polyacrylamide gel and blotted onto PVDF membrane. Transferred proteins were denatured and renaturated on membrane by stepwise incubation in reducing guanidine hydrochloride concentration. The membrane was blocked and incubated with 10 µg of GST-GABARAPL1, GST-GABARAPL2, GST-LC3A or GST. Unbound proteins were washed off and the membrane was probed for bound proteins with anti-GST and anti-FLAG antibodies. Only GST-GABARAPL1 and GST-GABARAPL2 (upper panel), but neither GST-LC3A nor GST (lower panel) interact directly with FLAG-Gaf-1b. (F) 400 µg cell extracts of HeLa cells transfected with FLAG-Gaf-1b were incubated with glutathione sepharose 4B beads coated with 10 µg GST or GST-fusion proteins (GST-GABARAPL1, GST-GABARAPL2, GST-LC3A). Bound proteins were analysed by Ponceau S staining and immunoblots were probed with anti-FLAG. GST-GABARAPL1 and GST-GABARAPL2, but neither GST-LC3A nor GST alone interact with FLAG-Gaf-1b under native conditions. HA, hemagglutinin; IgG, immunoglobulin G; IP, immunoprecipitation; GST, glutathione S-transferase; Pept, peptide (adapted from Master thesis of Patrick Redli, 2010).

To determine whether the interaction of Gaf-1b and GABARAPL1 and GABARAPL2 was direct, we performed Far-Western blotting. HeLa cells were transfected with FLAG-Gaf-1b or untransfected. Proteins were separated by SDS-PAGE, blotted onto PVDF membrane, renaturated directly on membrane by stepwise incubation with decreasing guanidine hydrochloride concentrations and incubated with recombinant GST-GABARAPL1, GST-GABARAPL2, GST-LC3A or GST. Bound proteins were detected by using anti-GST antibodies and FLAG-Gaf-1b was probed with anti-FLAG antibody after stripping the membrane. Our data verified a direct interaction between GABARAPL1 and GABARAPL2 with Gaf-1b (Figure 2.19 E). Probing the membrane with GST alone and GST-LC3A did not show any interaction with FLAG-Gaf-1b. The absence of bound protein in the untransfected control verified the specificity of the interaction of GST-GABARARAPL1 and GST-GABARAPL2 with Gaf-1b.

As an additional control, GST pull-down assay of Gaf-1b under native conditions with GST-fusion proteins was performed to exclude binding artefacts due to improper refolding of FLAG-Gaf-1b on membrane. GST-fusion proteins were immobilized on glutathione sepharose beads and incubated with lysates of HeLa cell transfected with FLAG-Gaf-1b. As expected, both GST-GABARAPL1 and GST-GABARAPL2 strongly pulled down FLAG-Gaf-1b, while GST alone or GST-LC3A did not (Figure 2.19 F).

In summary, our data demonstrated that Gaf-1b interacted directly with GABARAPL1 and GABARAPL2 and that both interactions required the splice insert domain of Gaf-1b [213].

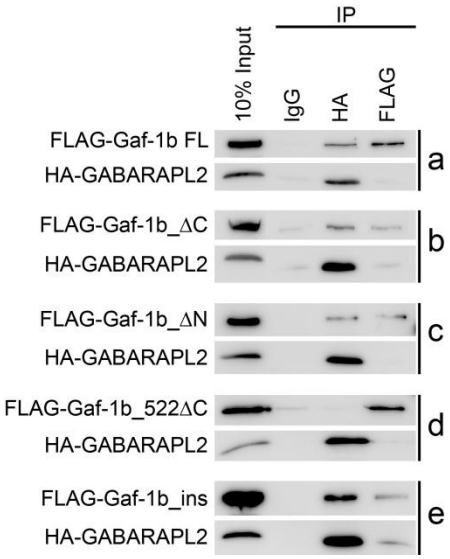

Figure 2.20: The splice insert of Gaf-1b is involved in the interaction of Gaf-1b with GABARAPL2.
(a-e) Transfected HeLa cells were solubilized twenty-four hours post-transfection and subjected to immunoprecipitations using the indicated antibodies. Immunoprecipitates were separated by 12.5% SDS-PAGE and blotted onto PVDF membrane. HeLa cells were co-transfected with HA-GABARAPL2 and either FLAG-Gaf-1b FL (a), FLAG-Gaf-1b_ΔC (b), FLAG-Gaf-1b_ΔN (c), FLAG-Gaf-1b_522ΔC (d) or FLAG-Gaf-1b_ins (e). The immunoblots were probed with anti-FLAG or anti-HA. HA-GABARAPL2 co-immunoprecipitated with FLAG-Gaf-1b FL, FLAG-Gaf-1b_ΔC, FLAG-Gaf-1b_ΔN and FLAG-Gaf-1b_ins, but not with FLAG-Gaf-1b_522ΔC. As controls for specific immunoreactivity pre-immune mouse IgG was applied. FL, full-length; HA, hemagglutinin; ins, insert; IgG, immunoglobulin G; IP, immunoprecipitation (adapted from Master thesis of Thomas Künzli, 2010).

2.9.2 Localization of the binding domain of Gaf-1b for the interaction with GABARAPL2

In the previous section, we verified the interaction of Gaf-1b with GABARAPL2 by co-immunoprecipitation. To specify the binding domain between Gaf-1b and GABARAPL2, co-IPs were performed with lysates of HeLa cells co-transfected with HA-GABARAPL2 and either full-length FLAG-Gaf-1b, FLAG-Gaf1b_ΔC, FLAG-Gaf-1b_ΔN, FLAG-Gaf-1b_522ΔC or FLAG-Gaf-1b_ins. Our result showed that all FLAG-Gaf-1b truncation constructs co-immunoprecipitated with HA-GABARAPL2, except of FLAG-Gaf-1b_522ΔC (Figure 2.20). The co-immunoprecipitation results in HeLa cells demonstrated that GABARAPL2 was able to bind to the full-length FLAG-Gaf-1b as well as to all truncation constructs of Gaf-1b containing the splice insert. In contrast, Rip11 and Gaf-1b truncation

constructs without the splice insert could not interact with GABARAPL2. This led us to the conclusion that the splice insert of Gaf-1b was necessary for binding with GABARAPL2 [212]. Here, we could show another difference between Gaf-1b and its splice variant Rip11 which indicated that Gaf-1b and Rip11 might serve different functions in HeLa cells.

2.9.3 Gaf-1b colocalizes with GABARARPL1 and GABARAPL2

The previous biochemical approach revealed that Gaf-1b interacted with GABARAPL1 and GABARAPL2 *in vitro*. Therefore, we aimed at analysing the subcellular distribution of these proteins in living cells and at confirming the physiological relevance of both interactions. HeLa cells were co-transfected with the proteins illustrated in Figure 2.21 A-F. Cells were fixed, permeabilized and processed for indirect immunofluorescence using anti-FLAG and anti-HA antibodies. Co-stainings of FLAG-Gaf-1b and HA-GABARAPL1 or HA-GABARAPL2 revealed a comparable vesicular staining pattern throughout the cell and a partial overlap of FLAG-Gaf-1b with HA-GABARAPL1 or HA-GABARAPL2 in vesicular structures in the periphery (Figure 2.21 A and B). In contrast, colocalization of FLAG-Gaf-1b with HA-LC3A or HA-LC3B was sparse (Figure 2.21 E and F). Rip11-EGFP also showed low overlap with HA-GABARAPL1 or HA-GABARAPL2 (Figure 2.21 C and D). The degree of colocalization was calculated by the linear correlation between the respective green and red channel pixel intensities from dual channel merges according to Pearson's method using the PSC colocalization tool, implemented in ImageJ [216]. The highest positive signal correlation of FLAG-Gaf-1b was found for HA-GABARAPL1 (0.50 ± 0.06) and HA-GABARAPL2 (0.42 ± 0.04) (Figure 2.21 G). The Pearson product-moment correlation coefficient was for HA-LC3A and FLAG-Gaf-1b (-0.11 ± 0.05) and HA-LC3B and FLAG-Gaf-1b (0.04 ± 0.08) close to zero. A weak negative linear correlation was calculated for Rip11-EGFP and HA-GABARAPL1 (-0.33 ± 0.03) as well as for Rip11-EGFP and HA-GABARAPL2 (-0.42 ± 0.04). These results supported our finding that Gaf-1b specifically interacted with GABARAPL1 and GABARAPL2 *in vitro* and *in vivo* [213].

Figure 2.21: Gaf-1b colocalizes with GABARAPL1 and GABARAPL2. ►
(A-F) HeLa cells were transfected with the indicated constructs, fixed with 4% PFA and processed for immunofluorescence using anti-HA and anti-FLAG antibodies. Images were captured with a confocal laser scanning microscope (Leica SP2) using a 63x objective (NA 1.32). Images were thresholded and two-color RGB images were produced in Adobe Photoshop CS3. Colocalization masks were generated by using the RG2B colocalization tool implemented in ImageJ. HA-GABRAPL1 and HA-GABRAPL2 partially colocalized with FLAG-Gaf-1b (A and B), but did not with EGFP-Rip11 (C and D). HA-LC3A and HA-LC3B sparsely colocalized with FLAG-Gaf-1b (E and F). (G) Quantification of data shown in (A-F). The linear correlation of the intensity values of the green and red pixels from unprocessed red-green-channel merges were calculated according to Pearson's method using the PSC colocalization plug-in from ImageJ. ROIs were set manually to individual cells for each image merge prior to quantification. Data represent mean value Pearson correlation coefficients (r_p) ± SEM. Coloc, colocalization; L1, GABARAPL1; L2, GABARAPL2; 3A, LC3A; 3b, LC3B; Gaf, Gaf-1b; Rip, Rip11 (adapted from Master thesis of Patrick Redli, 2010).

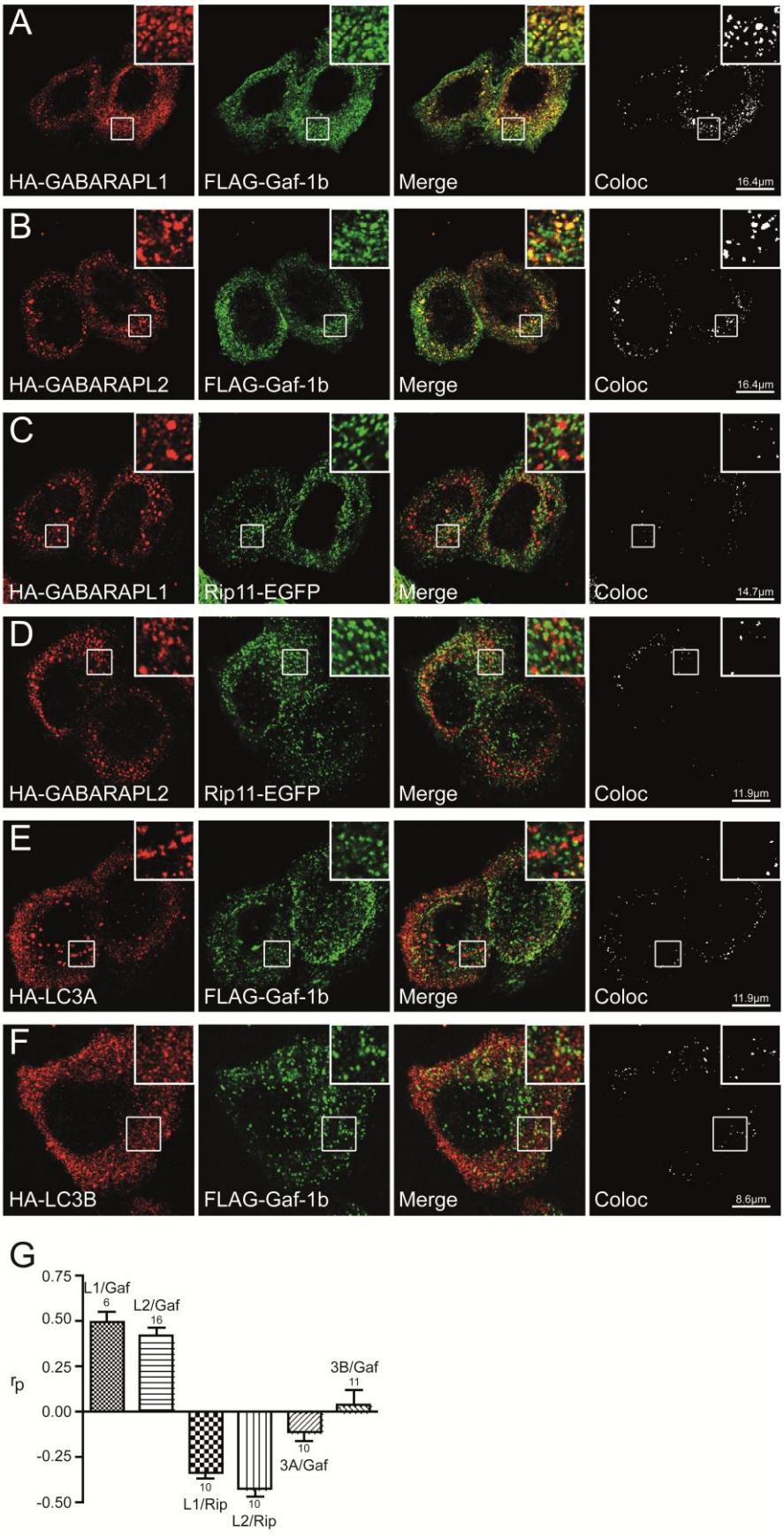
A
HA-GABARAPL1
FLAG-Gaf-1b
Merge
Coloc
16.4µm
B
HA-GABARAPL2
FLAG-Gaf-1b
Merge
Coloc
16.4µm
C
HA-GABARAPL1
Rip11-EGFP
Merge
Coloc
14.7µm
D
HA-GABARAPL2
Rip11-EGFP
Merge
Coloc
11.9µm
E
HA-LC3A
FLAG-Gaf-1b
Merge
Coloc
11.9µm
F
HA-LC3B
FLAG-Gaf-1b
Merge
Coloc
8.6µm
G
0.75
0.50
0.25
0.00
-0.25
-0.50
rp
L1/Gaf
6
L2/Gaf
16
3B/Gaf
11
10
3A/Gaf
10
L1/Rip
10
L2/Rip

2.10 Gaf-1b is involved in the autophagic pathway

2.10.1 Gaf-1b associates with membranes of the autophagosomal pathway

LC3 as well as GABARAPL1 and GABARAPL2 are described to be involved in the process of autophagy [98, 192, 193, 199, 214]. The interaction between Gaf-1b and GABARAPL1 or GABARAPL2, prompted us to investigate a potential role of Gaf-1b in the autophagic pathway. We tested whether Gaf-1b colocalized with the endogenous markers associated with the autophagosomal pathway in HeLa cells, such as Rab7, LC3A and LAMP1. Rab7 is a late endosomal marker [217] and has been described to be involved in the maturation of late autophagic vesicles [104, 105]. LC3A is regarded as the typical marker for autophagosomes [98]. LAMP1 labels lysosomal as well as late-endosomal membranes [218] and has been implicated to fusion of autophagosomes with late endosomes and lysosomes [219]. We transfected HeLa cells with FLAG-Gaf-1b and analysed the indirect immunofluorescence using the anti-FLAG antibody and the endogenous marker anti-Rab7, anti-LC3A and anti-LAMP1 antibodies. Our immunocytochemistry data showed a partial colocalization of Gaf-1b with all three markers, indicating the participation of Gaf-1b in the autophagosomal maturation pathway (Figure 2.22 A-C) [213].

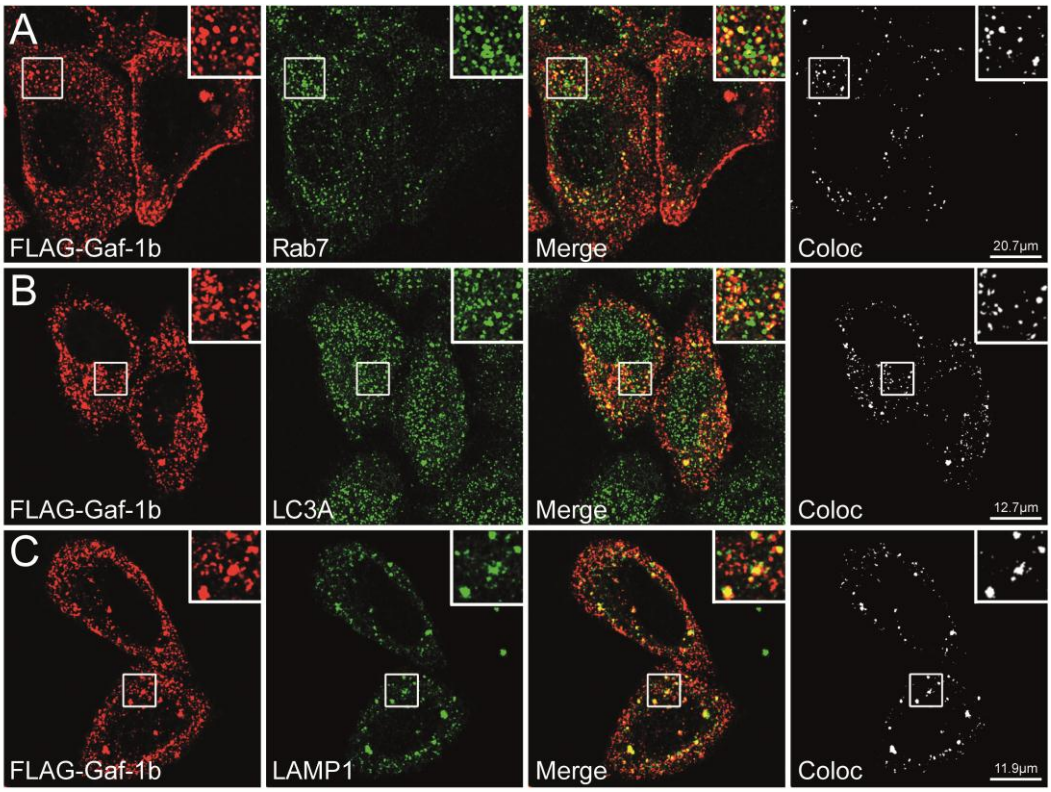

Figure 2.22: Gaf-1b associates with membranes of the autophagosomal pathway.
HeLa cells were transfected with FLAG-Gaf-1b, fixed with 4% PFA, permeabilized and stained with antibodies against FLAG-Gaf-1b, Rab7, LC3A and LAMP1. Images were captured with a confocal laser scanning microscope (Leica SP2) using a 63x objective (NA 1.32). Images were thresholded and two-color RGB images were produced in Adobe Photoshop CS3. Colocalization masks were generated by using the RG2B colocalization tool implemented in ImageJ. Gaf-1b colocalized in small vesicular pattern with Rab7 and LC3A as well as in larger structures with LAMP1. Coloc, colocalization (adapted from Master thesis of Patrick Redli, 2010).

2.10.2 Gaf-1b accumulates in perinuclear aggregates upon starvation

It was described for GABARAPL2 that it is relocalized to autophagosomes under starvation conditions [98]. Hence, we wondered whether Gaf-1b was redistributed to autophagosomal membrane upon induction of autophagy. For this reason, HeLa cells was co-transfected with FLAG-Gaf-1b and either HA-GABARAPL1, HA-GABARAPL2 or HA-LC3B. Twenty-four hours post-transfection cells were incubated for two hours in nutrient-deprived media, the Hank's balanced salt solution supplemented with magnesium and calcium. HeLa cells were subsequently fixed in 4% PFA and processed for indirect immunofluorescence using the anti-FLAG and anti-HA antibodies. As control for nonstarving conditions, HeLa cells were incubated for two hours in standard medium. Interestingly, HeLa cells highly overexpressing FLAG-Gaf-1b and either HA-GABARAPL1, HA-GABARAPL2 or HA-LC3B showed large accumulated structures next to the nucleus and smaller vesicular structures in the periphery (Figure 2.23 B, D and F). FLAG-Gaf-1b and HA-GABARAPL1, HA-GABARAPL2 or HA-LC3B colocalized in these large aggregates. In nonstarved cell, FLAG-Gaf-1b was mainly localized near the plasma membrane where it overlapped partially with HA-GABARAPL1 and HA-GABARAPL2 (Figure 2.23 A and C). In contrast, HA-LC3 showed a vesicular staining pattern in nonstarved cells (Figure 2.23 E). Upon starvation these vesicular structures in the periphery were decreased, instead a small amount of larger vesicles were observed, indicating fusion of the small vesicles to the larger aggregates. To quantify this shift we determined colocalizing puncta with a minimum diameter of 2µm (Figure 2.23 G, H, I). Upon two hours starvation cells formed significantly higher amounts of large aggregates containing Gaf-1b and either GABARAPL1, GABARAPL2 or LC3B.

Cells were live imaged upon starvation to support the observation that Gaf-1b was relocalized in large aggregates upon starvation. HeLa cells grown on coverslips were co-transfected with Gaf-1b-mCherry and HA-GABARAPL2 and the cells were starved for three hours. At the beginning of starvation Gaf-1b-mCherry showed a vesicular staining pattern in the periphery. After 40 minutes Gaf-1b-mCherry started to relocalize next to the nucleus, and from approximately one hour onwards the small vesicular structures were remarkably decreased and Gaf-1b-mCherry was accumulated in large structures at the perinuclear region (Figure 2.23 J, (>)). Altogether these results showed that Gaf-1b accumulated in GABARAPL1-, GABARAPL2- and LC3B-positive aggregates upon starvation, indicating that Gaf-1b was involved in the autophagic pathway.

Figure 2.23: Gaf-1b accumulates in perinuclear aggregated structures upon starvation. ►
(A-F) HeLa cells were transfected with the indicated constructs, twenty-four hours post-transfection starved for 2 h in $HBSS^{++}$, fixed with 4% PFA and processed for immunofluorescence using anti-HA and anti-FLAG antibodies. Images were captured with a confocal laser scanning microscope (Leica SP5) using a 63x objective (NA 1.32). Images were thresholded and two-color RGB images were produced in Adobe Photoshop CS5. Note, HeLa cells in starved conditions showed large aggregated structures positive for FLAG-Gaf-1b and HA-GABARAPL1, HA-GABARAPL2 or HA-LC3B. (G) Quantification of data shown in (A and B). (H) Quantification of data shown in (C and D). (I) Quantification of data shown in (E and F). Error bars indicate mean ± SEM, ***p>0.001, Mann-Whitney Rank Sum test. (J) HeLa cells were grown on PLL coated coverslips, transfected with Gaf-1b-mCherry and HA-GABARAPL2 for twenty-four hours. Nutrient rich media was replaced by nutrient deprived media ($HBSS^{++}$) and imaged live at 37 °C for 3 hours using a 60x objective and frame rate of one image per 2 minutes. Time-laps sequences of Gaf-1b-mCherry are shown. Note, 40 minutes after nutrient deprivation Gaf-1b-mCherry started to accumulate at the perinuclear region (>).

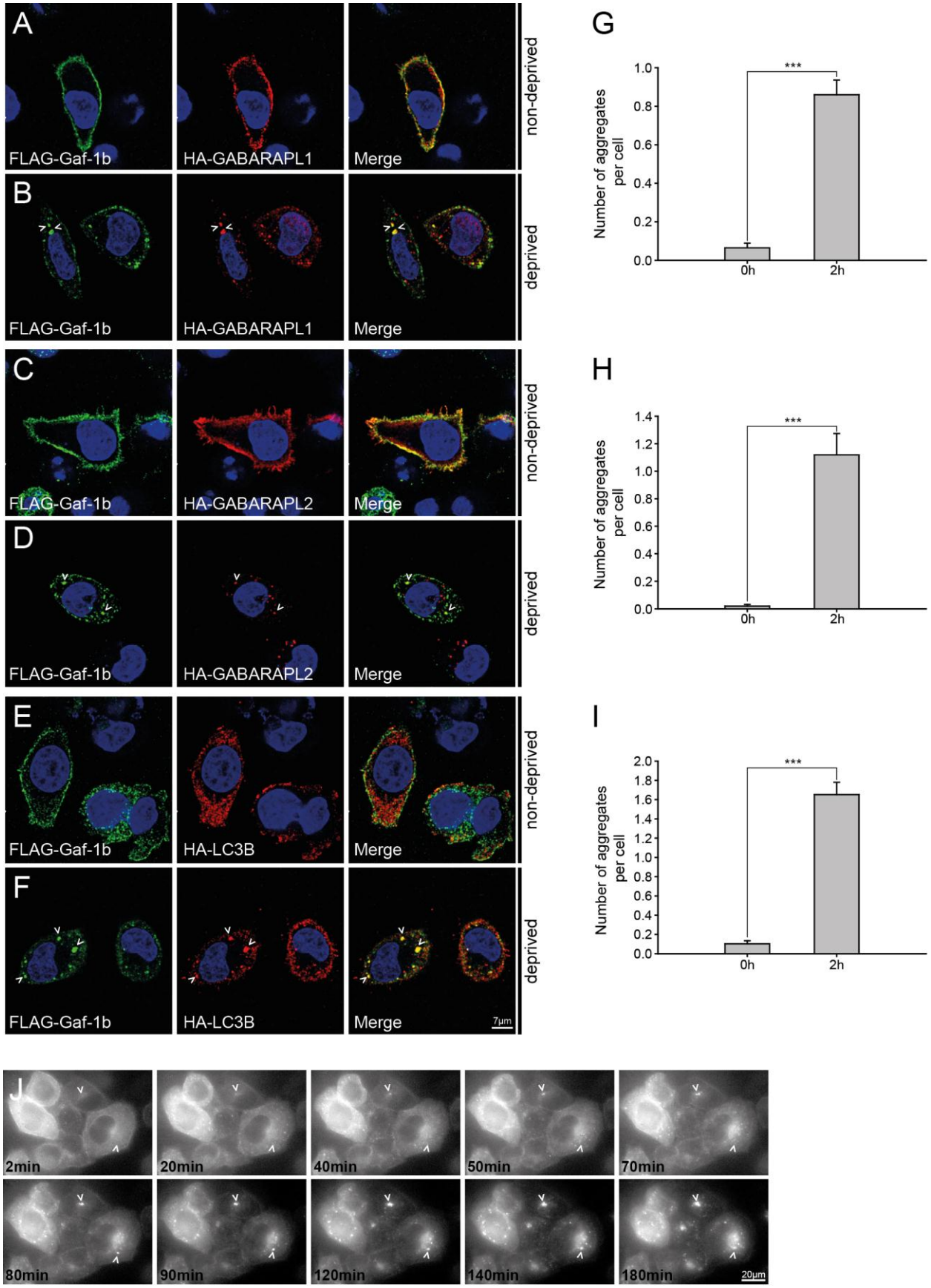
A
FLAG-Gaf-1b
HA-GABARAPL1
Merge
non-deprived
B
FLAG-Gaf-1b
HA-GABARAPL1
Merge
deprived
C
FLAG-Gaf-1b
HA-GABARAPL2
Merge
non-deprived
D
FLAG-Gaf-1b
HA-GABARAPL2
Merge
deprived
E
FLAG-Gaf-1b
HA-LC3B
Merge
non-deprived
F
FLAG-Gaf-1b
HA-LC3B
Merge
7µm
deprived
G
Number of aggregates per cell
***
0h
2h
H
Number of aggregates per cell
***
0h
2h
I
Number of aggregates per cell
***
0h
2h
J
2min
20min
40min
50min
70min
80min
90min
120min
140min
180min
20µm

2.10.3 Gaf-1b knock-down induces autophagosomes

A wrong assumption is that increased numbers of autophagosomes in cells correspond to increased autophagic activity [83]. Autophagy is a dynamic process and the autophagosome is an intermediate structure. The number of autophagosome at a timepoint defines a function of the balance between the rate of their generation and the rate of their maturation to autolysosomes. Therefore, the observed accumulation of autophagosomes is the result of either autophagy induction or suppression of the downstream steps in the autophagic pathway [83]. LC3 undergoes an ubiquitin-like posttranslational modification which converts the C-terminally truncated cytosolic form-I of LC3, to its lipidated membrane bound form-II [99, 100]. Induction of autophagy was shown to stimulate this conversion and association of LC3 with autophagosomal and pre-autophagosomal membranes was found to depend on form-II, thus LC3 is a reliable autophagosomal marker [83, 98].

Here, we were interested whether Gaf-1b was involved in the upstream or downstream path of the dynamic autophagosome formation pathway. HeLa cells were transfected with siRNA to down-regulate Gaf-1b. Prior to cell lysis, the cells were preincubated for two hours in 100 nM Bafilomycin 1A which inhibited the conversion of autophagosomes to autolysosomes. The expression of LC3 form-I and LC3 form-II was analysed by immunoblotting. Our preliminary data showed that the expression of LC3 form-I was slightly increased in Gaf-1b knock-down cells (Figure 2.24 A and B). Interestingly, the LC3 form-II signal was strongly increased in Gaf-1b down-regulated cells compared to nonsense transfection. The addition of Bafilomycin 1A to cells transfected with nonsense siRNA induced an increased signal of LC3 form-II to almost the same level as in Gaf-1b down-regulated cells. In contrast, application of Bafilomycin 1A showed only a sparse effect of an increased LC3-II signal in Gaf-1b down-regulated cells. This preliminary result indicated a function of Gaf-1b downstream of the autophagosome formation. We suggested that Gaf-1b induced the conversion of autophagosomes to autolysosomes as the LC3-II signal in Gaf-1b down-regulated cells was comparable with those of Bafilomycin 1A treated cells of the nonsense cells. In addition, Bafilomycin 1A did not have an effect on Gaf-1b down-regulated cells.

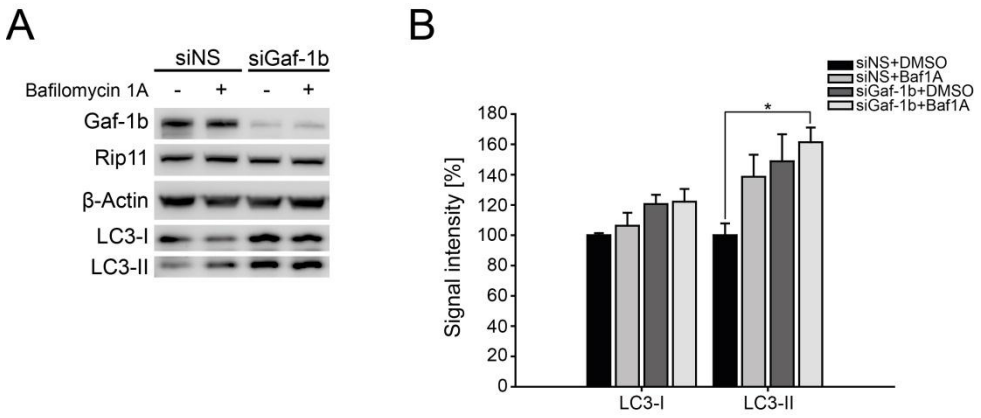

Figure 2.24: Gaf-1b knock-down induce autophagosomes

(A) HeLa cells were transfected with nonsense or Gaf-1b siRNAs for 48 hours. Cells were treated for two hours with DMSO or 100 nM Bafilomycin 1A prior to solubilization, cell lysate was separated on a 12% Bis-Tris gel and blotted onto PVDF membrane. Immunoblot was analysed with the following antibodies: anti-Gaf-1b C for Gaf-1b and Rip11, anti-β-actin and anti-LC3A. The Gaf-1b siRNA efficiently down-regulated Gaf-1b. In Bafilocmycin 1A treated nonsense cell, LC3 is increased compared to DMSO control cells. Downregulation of Gaf-1b showed a higher amount of LC3-I and LC3-II compared to nonsense cells and Bafilomycin 1A treated cells did not differ from DMSO control cells. (B) Quantification of data shown in (A). Error bars indicate mean ± SEM, *p>0.05, Tukey test. Baf1A, Bafilomycin 1A; NS, nonsense.

3. Discussion

3.1 Gaf-1b interacts with calsyntenin-1

Calsyntenin-1 was shown to function in the transport of kinesin-1-dependent post-Golgi vesicular carriers to axonal growth cones [176]. There exist two distinct, non-overlapping calsyntenin-1 transport packages, the calsyntenin-1/APP/BACE1 and the calsyntenin-1/Rab11 organelles [178]. Calsyntenin-1 was shown to be an essential element for sheltered anterograde transport of APP in the organelles containing calsyntenin-1, APP, and BACE1. It functions as a cargo-docking molecule and protects APP from premature proteolytic degradation by ADAM10 and BACE1 during its transport into the cell periphery [177]. The second organelle population of calsyntenin-1 was suggested to be involved in the endosomal recycling pathway as proteins of the endosomal recycling pathway were found in these organelles, such as Rab11, syntaxin 13 and TfR. Different studies reported that Rab11 is localized to the TGN, post-Golgi vesicles and recycling endosomes. These studies further implicated a function of Rab11 in controlling the polarized sorting of various proteins in the recycling-endosomal pathway [140-144]. We showed here that Gaf-1b, a splice variant of the Rab11-family interacting protein Rip11 [168], specifically and selectively interacts with calsyntenin-1, which indicates a potential function of calsyntenin-1 in the recycling-endosomal pathway.

We demonstrated a specific interaction between the calsyntenin-1 cytoplasmic domain and Gaf-1b by using a set of co-immunoprecipitation experiments from HeLa cells. An interaction of Gaf-1b with the cytoplasmic segment of calsyntenin-1 is reasonable because Rab11-FIPs are cytosolic proteins which are predominantly membrane-bound and are localized to the cytosolic face of endosomal recycling compartments, presumably through their interaction with GTP-Rab11 or through their C2 phosphoplipid-binding domain [153]. Interaction experiments implicated the acidic stretch or the very C-terminus of calsyntenin-1 as the binding domain for Gaf-1b because we showed that the cytoplasmic segment of calsyntenin-1 proximal to the transmembrane domain including the KBS1 motif is not involved in the binding to Gaf-1b. Furthermore, Gaf-1b does not interact with calsyntenin-3. Calsyntenin-3 lacks the very C-terminus, including the KBS2 motif and most of the acidic stretch compared to calsyntenin-1 [170]. Finally, we demonstrated that the cytoplasmic segment of calsyntenin-1 is necessary and alone sufficient for the binding to Gaf-1b. Acidic amino acid clusters are typically involved in high capacity and low affinity binding of Ca^{2+} and calsyntenin-1 has been demonstrated to bind calcium with low affinity but high capacity [169]. It was reported that amino acid clusters exist that are involved in protein-protein interaction. For instance, PACS-1, a cytosolic protein that controls the correct subcellular localization of integral membrane proteins, interacts with the cytosolic domains of proteins containing acidic clusters (e.g., furin, CI-MPR, PC6B and Nef) [220]. Therefore, the acidic stretch of calsyntenin-1 may be responsible for the direct interaction of Gaf-1b and calsyntenin-1. Cloning of additional calsyntenin-1 deletion and point mutant constructs is required to fully understand and map in detail the site of interaction.

We showed that calsyntenin-1 specifically interacts with Gaf-1b but not with Rip11, although Rip11 is an alternative splice variant of Gaf-1b that lacks the 565 amino acid splice insert. Thus, we expected that the splice insert may be crucial for the interaction to calsyntenin-1. However, the splice insert of Gaf-1b is necessary, but alone not sufficient for the interaction with calsyntenin-1 because truncation mutants consisting of the splice insert alone did not interact with calsyntenin-1. Hence, additional N- or C-terminal sequences of Gaf-1b are involved in the interaction. Two major domains on Gaf-1b were reported to contribute to protein-protein interactions, the Rab11/25 binding domain (RBD) located at

the C-terminus and the C2 domain located at the N-terminus. The RBD is responsible for Rab11 binding [157]. It was shown for FIP2, which belongs to class I FIPs, that its endosomal membrane association depends only on the RBD [204], while others demonstrated that both the N-terminal C2 domain and the RBD are necessary for directing Rip11 to endosomal membranes [165]. Based on the fact that the C2 domain serves as a protein-phospholipid and protein-protein binding module [153], we suggested that the C2 domain contributes to the interaction between Gaf-1b and calsyntenin-1 because it contains the protein-protein binding module, while the RBD is rather involved in membrane association and Rab11 binding. Interestingly, we showed that truncation mutants of Gaf-1b lacking the C-terminus and splice insert are able to associate with calsyntenin-1 and the binding assays revealed the C2 domain of Gaf-1b as the binding domain for calsyntenin-1. The phospholipid binding property of the C2 domain can be calcium-dependent or calcium-independent. For example, the C2 domain of cytosolic phospholipase A_2 ($cPLA_2$) translocates to the nuclear envelope upon Ca^{2+} influx [221, 222]. Therefore, the interaction between Gaf-1b and calsyntenin-1 may be Ca^{2+}-dependent because calsyntenin-1 also possesses a calcium-binding feature by means of its acidic stretch. Finally, we suggest that Gaf-1b is C-terminally bound to membranes through the association with GTP-Rab11 and that the splice insert of Gaf-1b is necessary to facilitate a conformation by which the N-terminus of Gaf-1b can interact with calsyntenin-1 (Figure 14.1). This would explain why calsyntenin-1 did not interact with Rip11, although Rip11 also possesses a C2 domain at the N-terminus. Crystal structure analysis would give an insight in the binding conformation of Gaf-1b and calsyntenin-1.

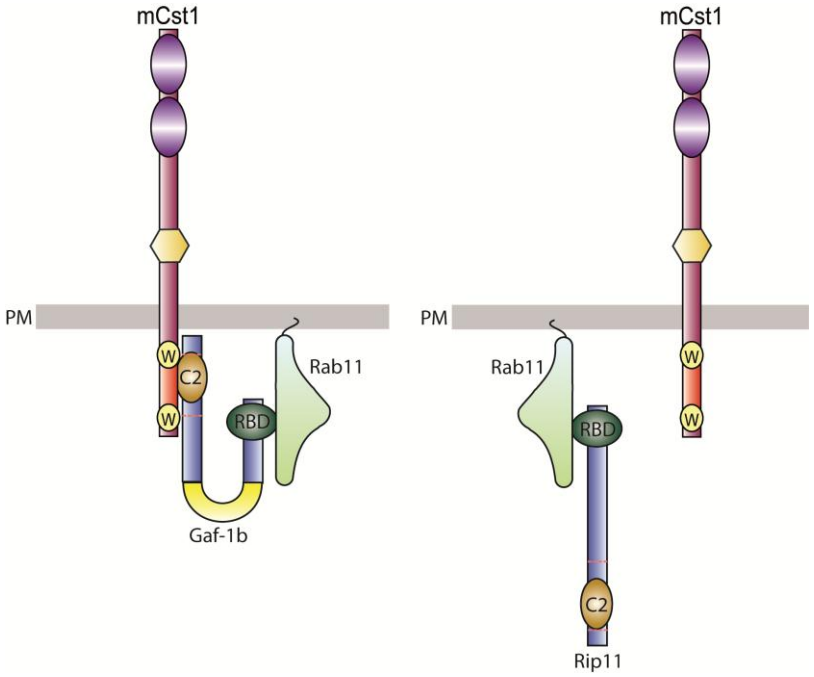

Figure 14.1: Model of the calsyntenin-1-Gaf-1b-Rab11 complex.
Rab11 is membrane-associated and bound to Rab11-FIPs. Gaf-1b compared to Rip11 possesses an additional 565 amino acid splice insert which leads to a conformational change of Gaf-1b. This conformational change allows Gaf-1b to interact with calsyntenin-1, whereas Rip11 does not have the ability to adapt such a conformation. Cst1, calsyntenin-1.

FIP2 is able to interact with Rab11 to form a heterotetrameric complex, arranged in a Rab11-$(FIP2)_2$-Rab11 conformation [151]. Furthermore, FIP2, Rip11 and FIP3 can interact with each other indicating a hetero-binding ability [152]. Therefore, we wondered whether Gaf-1b and Rip11 would also form such a heterotetrameric complex with Rab11 and whether such a complex would interfere with the interaction of Gaf-1b and calsyntenin-1. Indeed, Gaf-1b did not interact with calsyntenin-1 anymore in HeLa cells that were triple-transfected with Rip11, Gaf-1b and calsyntenin-1. Instead, Gaf-1b was found to be readily associated with Rip11. This data suggest that binding of Rip11 to Gaf-1b perturbs the interaction between Gaf-1b and calsyntenin-1. Given the fact that Gaf-1b and Rip11 belong to the class I FIPs, we suggest that Gaf-1b forms a heterotetrameric complex with Rip11 in a Rab11-Gaf-1b-Rip11-Rab11 manner. The result of this complex is that Gaf-1b is not able anymore to adopt the conformation that is required for its interaction with calsyntenin-1 (Figure 14.2). In this situation, Rip11 sequesters Gaf-1b from calsyntenin-1. Therefore, only a homodimerized complex of Gaf-1b is able to interact with calsyntenin-1.

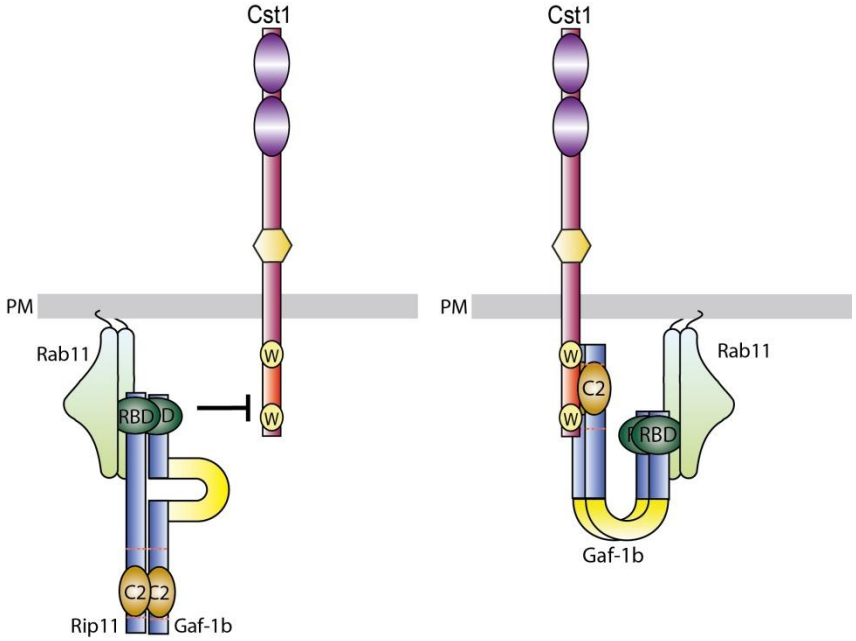

Figure 14.1: Model of the heterotetrameric complex of Gaf-1b, Rip11 and Rab11 in relation to calsyntenin-1 binding. Gaf-1b and Rip11 form a heterotetrameric complex with the membrane bound Rab11. In this complex Gaf-1b cannot interact with calsyntenin-1 because Rip11 hinders Gaf-1b to adopt the conformation where it is able to interact with calsyntenin-1. Only homodimeric complexes of Gaf-1b allow a conformational change of Gaf-1b to interact with calsyntenin-1. Cst1, calsyntenin-1.

3.2 Gaf-1b is associated with the TGN

Kinesin-1 is a plus-end directed microtubule-dependent motor protein and has been localized to Golgi/TGN membranes [22, 223]. Kinesin-1 is involved in Golgi-to-ER as well as TGN-to-plasma membrane transport [22, 224]. Kinesin-1 interacts with various cargo docking proteins. The KHC tail and the KLC1 TPR domains are responsible for cargo interaction and this interaction mechanism can be direct or indirect [225]. We recently identified KLC1 as an interaction partner of calsyntenin-1 [171]. The two conserved WDDS motifs (KBS1 and KBS2) in the cytoplasmic moiety of calsyntenin-1 were shown to be involved in the direct interaction with the TPR domains of KLC1. Additionally, we demonstrated that APP exits the TGN in association with calsyntenin-1 in tubulovesicular organelles in a kinesin-1-dependent manner [176] and that these vesicles are transported anterogradely along axons [171, 177].

We showed here that mouse and human Gaf-1b also interact with KLC1. This interaction is probably mediated by a KBS-like motif located in the splice insert of Gaf-1b. Sequence comparison across all known calsyntenins family members revealed a consensus of KBS as L/M-D/E-W-D-D-S [171]. Mouse and human Gaf-1b contain a KBS-like motif, P-E-W-D-D-T at position 632-637 and P-E-W-D-N-T at position 540-545, respectively. One KBS motif is sufficient for an interaction with KLC1 because it was demonstrated that truncation mutants of calsyntenin-1 lacking one KBS motif or calsyntenin-3, which contains only one KBS motif, were able to interact with KLC1 [171]. Therefore, this KBS-like motif in Gaf-1b may also be sufficient for the interaction with KLC1. Additionally, we showed in triple-transfected HeLa cells with Gaf-1b, calsyntenin-1 and KLC1 that all three proteins were able to interact simultaneously with each other. It was suggested that one KLC1 is able to bind two calsyntenin-1 [176]. Therefore, one KLC1 could interact simultaneously with one calsyntenin-1 and one Gaf-1b molecule. To verify the KBS-like motif in Gaf-1b as the binding segment for KLC1, additional binding assays with selected point mutations in the KBS-like motifs of Gaf-1b should be performed.

Another interesting feature of the Gaf-1b/calsyntenin-1/KLC1 complex is its subcellular distribution upon overexpression of these proteins. Overexpression of calsyntenins and KLC1 induces stacked ER and Golgi membranes, strictly speaking calsyntenin-1 and KLC1 produce ER stacks, while calsyntenin-3 and KLC1 induce Golgi stacks [176]. We observed ER whorls positive for calsyntenin-1 and KLC1 in triple-transfected HeLa cells with Gaf-1b, calsyntenin-1 and KLC1 but with the intriguing observation that the subcellular distribution pattern of Gaf-1b was completely altered. The usually vesicular staining pattern of Gaf-1b shifts to a TGN staining pattern. Notably, the ER whorls were devoid of Gaf-1b, instead Gaf-1b was accumulated in the TGN where it colocalized with KLC1, but not with calsyntenin-1. This observation led us to the assumption that Gaf-1b may be involved in biosynthetic sorting events at the TGN as it was shown for Rab11. Rab11 was reported to associate with the TGN and with TGN-derived secretory vesicles in PC12 cells [145]. Overexpression of dominant-negative (i.e. inactive) Rab11S25N disrupts the delivery of vesicular stomatitis virus (VSV) G protein to the basolateral cell surface in baby hamster kidney cells [226]. Rab11 may also regulate the targeting of rhodopsin to the apical surface of polarized epithelial cells because rhodopsin has been detected in Rab11-positve TGN-derived vesicles of Xenopus retina cell-free extracts [227]. We suggest that the TGN exit of Gaf-1b organelles is calsyntenin-1- and KLC1-dependent because blockage of TGN exit of calsyntenin-1 disrupts Gaf-1b trafficking and results in its accumulation at the TGN. The biosynthetic sorting may probably not be the major function of Gaf-1b but rather the transport of proteins to the recycling endosome and from there to the plasma membrane. Under

normal conditions, endogenous Gaf-1b sparsely colocalized with the TGN in HeLa cells. Gaf-1b may cycle between the endosomal recycling compartment and TGN to direct newly synthetized proteins from the TGN to recycling endosomes in collaboration with calsyntenin-1. It remains to note that Gaf-1b colocalized to a quite high extent with the TGN marker syntaxin 6 in dendrites of mouse hippocampal neurons and immunoisolation of Gaf-1b organelles showed that various TGN proteins were contained in Gaf-1b organelles, such as syntaxin 6, syntaxin 16, VAMP4 and mVPS45. These data support the assumption that Gaf-1b/Rab11 is recruited to the TGN, leaves the TGN in a calsyntenin-1-dependent manner and is involved in the tethering of TGN-derived tubules to recycling endosomes.

3.3 Gaf-1b is transported in TGN-derived calsyntenin-1 organelles along axons

Using organelle immunoisolation and proteomics, we lately found that axons contained at least two distinct, non-overlapping calsyntenin-1-containing transport packages, one is characterized by the presence of APP and early-endosomal markers, the other with recycling-endosomal markers including Rip11/Gaf-1b [178]. We confirmed the previous observation that Gaf-1b is transported in calsyntenin-1 organelles which are destined for recycling endosomes by inspecting the protein content of isolated Gaf-1b organelles. These organelles contained calsyntenin-1, TGN markers, recycling-endosomal markers, such as Rab11, syntaxin 13 and TfR. They are devoid of APP, BACE1 and Rab5, which are characteristic for the other calsyntenin-1-containing transport pathway. Colocalization assays showed sparse overlapping of Gaf-1b and APP in dendrites, whereas Gaf-1b colocalized well with calsyntenin-1, TfR, syntaxin 13, and syntaxin 6. Additionally, co-immunoprecipitation experiments resulted in the absence of an interaction between Gaf-1b and APP. These data support the fact that Gaf-1b and APP are transported in spatially distinct calsyntenin-1-containing vesicles to different destinations and that they carry out different functions associated with calsyntenin-1 at distinct locations. In summary, we suggest that a population of calsyntenin-1 exits the TGN via interaction with kinesin-1 and Gaf-1b, travels along microtubules and that Gaf-1b/Rab11 mediates tethering of TGN-derived vesicles to recycling endosomes, from where calsyntenin-1 might deliver proteins and lipids to the plasma membrane. This concept is based on the observation that firstly, full-length calsyntenin-1 is stable in recycling endosomes [177]. Secondly, the interaction of calsyntenin-1 and Gaf-1b provides an explanation of how calsyntenin-1 might be recruited to and maintained in recycling endosomes. Thirdly, TGN-derived tubules containing calsyntenin-1 docked at and seemed to fuse with endosomal organelles containing syntaxin 13 [228].

3.4 Gaf-1b is associated with the endosomal recycling compartment and interacts with endosomal recycling markers

Rip11 belongs to the class I Rab11-FIPs [163-165] and Gaf-1b was recently identified as an alternative splice variant of Rip11 [168]. Further, Rip11 was shown to interact with Rab11 in a GTP-dependent manner [165], whereas it has not been reported yet about a direct interaction between Gaf-1b and Rab11. Although it was expected that Gaf-1b also interacts with Rab11 in a GTP-dependent fashion because it possesses all the necessary binding domains for Rab11 like Rip11, we still aimed towards verifying this interaction. Indeed, we showed in GST pull-down experiments from mouse brain homogenate and from cell lysate of Gaf-1b-transfected HeLa cells that Rab11 bound to Rip11 and

Gaf-1b in a GTP-dependent manner [205]. All Rab11-FIPs specifically interact with GTP-bound Rab11, except for FIP2. FIP2 was shown to interact with both GDP- and GTP-bound Rab11 [204]. Different Rab effector proteins do not only interact with one specific Rab GTPase. For example, RCP was shown to interact with Rab11 and Rab4 [156] but RCP binds to Rab11 with a much higher affinity indicating a function of RCP associated with Rab11 rather than with Rab4 [157]. Rab4 was also found in Gaf-1b immunoisolates, therefore we wondered whether Gaf-1b also interacts with other Rab-GTPases. We showed in GST pull-downs that Gaf-1b and Rip11 exclusively interact with GTP-bound Rab11, but not with Rab4 and Rab5. This result supports other studies that Rip11 exclusively interacts with Rab11 [152, 206]. Additionally, we observed a higher binding affinity of Rip11 with Rab11 compared to Gaf-1b with Rab11 in GST pull-downs. Rab11 was pulled down by Rip11 with higher efficiency than Gaf-1b from mouse brain homogenate and from transfected HeLa cells. As the method used here is not adequate for quantitative analysis. Quantitative statements should be interpreted with care in this regard. Protein transfection and protein transfer onto PVDF, especially for the high molecular weight protein Gaf-1b, were not always reproducibly constant. Other methods to examine quantitatively the binding affinity of Rip11 and Gaf-1b to Rab11 should be performed, such as titration experiments or isothermal titration calorimetry. Alternative methods to test whether Gaf-1b and Rip11 compete for binding to Rab11 would be the competition assay, where one of the two proteins is allowed to interact to immobilized Rab11 followed by addition of different amounts of the second protein and quantification by Sypro Ruby staining. These methods require the expression and purification of recombinant full-length proteins, a feat which might be difficult for the high molecular weight protein Gaf-1b.

After showing the interaction between Gaf-1b and Rab11, the question arose whether calsyntenin-1 is also linked to the Gaf-1b-Rab11 complex. Indeed, we demonstrated in GST pull-down experiments that calsyntenin-1 and Gaf-1b were pulled down by GTP-bound Rab11. But calsyntenin-1 did not bind to activated Rab11 in the absence of Gaf-1b, indicating that Gaf-1b links calsyntenin-1 to Rab11. The identification of the tripartite complex consisting of calsyntenin-1, Gaf-1b and Rab11 support our previous findings that calsyntenin-1 may function in recycling endosomes and provides an explanation how calsyntenin-1 is recruited to and maintained in recycling endosomes. In addition, this complex links Rab proteins to another motor protein, namely kinesin-1. Rab proteins were reported to interact with several motor proteins and are implicated in vesicle transport. For example, Rab4 was demonstrated to interact with KIF3, a kinesin-2 family member [229], and Rab11 with myosin Vb [230]. Rab6 is involved in regulating the movement of vesicles and organelles along microtubules through the direct interaction with Rabkinesin-6 [131, 134]. Hence, these data support the fact that Rab GTPases are not only involved in membrane docking and fusion, but they also play a role in recruitment of motor proteins and regulation of organelle motility [154]. In addition, this findings support the assumption that different Rab11-FIPs form mutually exclusive complexes with Rab11 which target Rab11 to different membrane trafficking pathways [155].

In non-polarized cells, syntaxin 13 is localized to sorting endosomes and tubulovesicular recycling endosomes in which it is involved in early endosome trafficking and in endosomal recycling of plasma membrane components [120, 121]. In neurons, syntaxin 13 is also found in tubular sorting and recycling endosomes, where it colocalizes with TfR. Syntaxin 13 is associated with recycling endosomes which are localized in both dendrites and axons [62] and syntaxin 13 was shown to be implicated in neurotransmitter receptor trafficking at dendritic spines [122-124]. Here, we found a potential interaction between calsyntenin-1 and syntaxin 13. We have previously shown that the transmembrane domain of syntaxin 13 is necessary for the interaction with calsyntenin-1 because

deletion mutants of syntaxin 13 lacking the transmembrane segment did not interact with full-length calsyntenin-1 in immunoprecipitation experiments (data not shown). The transmembrane segment of syntaxins is necessary for the formation of the stable four-helix bundle and for maintaining their function [107, 231]. We abolished the assumption that calsyntenin-1 and syntaxin 13 interact through their transmembrane domain because the cytosolic calsyntenin-1, which lacks the transmembrane domain and the extracellular moiety, still interacted with syntaxin 13. Further, we isolated a complex comprising of calsyntenin-1, Gaf-1b and syntaxin 13 from triple-transfected HeLa cells. On note, Gaf-1b did not directly interact with syntaxin 13, suggesting that calsyntenin-1 physically links Gaf-1b to a SNARE complex containing syntaxin 13. It was shown that both Gaf-1b and Rip11 interact with γ-SNAP [168, 232]. Three mammalian forms of SNAPs have been identified and referred to as α-, β-, and γ-SNAP. α-SNAP and γ-SNAP are widely distributed, while β-SNAP is brain-specific and highly homologous to α-SNAP [233]. α- and β-SNAP bind to the *cis*-SNARE complex and recruit NSF which leads to ATP hydrolysis in order to dissociate the SNARE complex, while the function of γ-SNAP remains unclear. Altogether, these data point to intriguing interactions between Rab-associated proteins and SNARE complexes and suggest that calsyntenin-1 and Gaf-1b may provide a physical link between these. This complex may be involved in appropriate and specific targeting, tethering and fusion of vesicles destined for recycling endosomes.

We speculate that calsyntenin-1 and Gaf-1b interact with a SNARE complex composed of syntaxin 13 and other SNAREs. This assumption is supported by our observation that all components of the previously described syntaxin 13 SNARE complex including VAMP2, SNAP-25 and β-SNAP [120] were found in organelles immunoisolated with anti-calsyntenin-1 or anti-Gaf-1b antibodies [178]. It was also shown that calsyntenin-1 did also co-immunoprecipitate syntaxin 6 besides syntaxin 13, and a tertiary complex consisting of calsyntenin-1, syntaxin 13 and syntaxin 6 could be isolated from transfected cells [228]. This supports our assumption of a tethering and fusion protein complex consisting of SNARE proteins, Rab11, Gaf-1b and calsyntenin-1. However, one should note that SNAREs are often involved in intermolecular interactions that may not be true *in vivo* interactions [234]. Besides calsyntenin-1, also APP was co-immunoprecipitated with syntaxin 6 and syntaxin 13 from mouse brain membranes [228]. Further experiments are needed to examine whether these interactions are of physiological relevance or whether the interaction of SNAREs with other proteins present in the same organelle is unspecific. Although distinct experiments indicated a specific interaction between calsyntenin-1, syntaxin 13 and syntaxin 6, the interactions shown here need to be handled with care. Liposome fusion assays combined with *in vitro* interaction studies need to be performed to understand the interaction of the complex consisting of syntaxin 13, syntaxin 6, Rab11, Gaf-1b and calsyntenin-1.

Our studies indicate that TGN-derived tubules containing calsyntenin-1 and Gaf-1b are transported along microtubules in a kinesin-1-dependent manner, docked at and fused with endosomal organelles containing syntaxin 13 [228] and Rab11. Based on the fact that calsyntenin-1 did not interact with Rip11, we suggest that Rip11 and Gaf-1b recruit Rab11 to distinct membrane subdomains and therefore specify distinct transport routes at recycling endosomes to the plasma membrane. Indeed, it has been speculated that at the endosomal recycling compartment, specific proteins are packed into distinct transport packages, a process that could be achieved by different Rab11-FIP complexes [157]. Thus, our proposed syntaxin 13-calsyntenin-1-Gaf-1b-Rab11 complex may be contained in one vesicle population, while other vesicle types may contain other FIPs and Rab11. Different FIPs compete for Rab11 interaction, and overexpression of one of the various FIPs sequester Rab11, which results in a notable inhibitory effect on a variety of Rab11-dependent

trafficking processes [155]. Thus, Gaf-1b and Rip11 may compete for Rab11 to form distinct vesicles at the recycling endosome. Co-expression of Gaf-1b and Rab11 resulted in a shift of the vesicular staining pattern of Rab11 from the cytoplasm to the plasma membrane, where it colocalized with Gaf-1b [203]. Co-overexpression of Rip11 and Gaf-1b showed a diffuse staining pattern of Rip11 in the cytoplasm and Rip11 was found at the plasma membrane, where it colocalized with Gaf-1b. This data indicate enhanced trafficking of Gaf-1b- and Rab11-containing vesicles from the recycling-endosomal compartment to the plasma membrane. In addition, it is possible that Gaf-1b caused dissociation of Rip11 from endosomal recycling membranes because Gaf-1b sequestered Rab11 from Rip11 [203]. Calsyntenin-1 may function as a regulator of the activity of Rab11 and Gaf-1b in phospholipid recycling because we observed an interesting phenomenon upon co-overexpression of calsyntenin-1 and Gaf-1b in HeLa cells. High expression of Gaf-1b and calsyntenin-1 in HeLa cells resulted in an alteration of the cell shape and extensive outgrowth of the plasma membrane. The extreme outgrowth of plasma membrane protrusions suggests that both proteins are involved in the delivery of proteins and/or lipids to the plasma membrane. Additionally, we showed colocalization of Gaf-1b and calsyntenin-1 in dendrites, axons and axonal growth cones [177]. Thus, we assumed a function of calsyntenin-1 and Gaf-1b/Rab11 in regulating plasma membrane expansion, cytoskeleton rearrangement and/or receptor recycling in axonal growth cones or spine growth at postsynaptic sites. Myosin Vb was shown to bind to recycling endosomes through the interaction with Rab11 and its effector Rab11-FIP2 and to regulate the trafficking of AMPA receptors to the plasma membrane [149]. CASY-1, the *C. elegans* orthologue of calsyntenins, was shown to be involved in AMPA receptor-associated learning and memory processes [235]. SNAREs, Rab GTPases and the exocyst complex have been reported to be implicated in neurite outgrowth regulation [236-238]. These data suggest a function for calsyntenins and Gaf-1b at synapses.

The intriguing phenomenon of plasma membrane outgrowth led us to the assumption that this may be the result of RhoA or Cdc42 misregulation. RhoA, Rac1 and Cdc42 belong to the Rho family of small GTPases and are involved in regulating cytoskeletal organization, vesicular transport, morphogenesis, polarity, migration and cell adhesion. The actin cytoskeleton is crucial for molecular organization of the plasma membrane as well as for the regulation of cell architecture, such as the dynamics of cellular protrusions [239]. Rac1 and Cdc42 were identified as key regulators in protrusion formation of lamellipodia and filopodia, respectively, and RhoA have been shown to be involved in stress fiber formation [240]. Additionally, RhoA, Rac1 and Cdc42 regulate distinct features of axonal and dendritic outgrowth during development and regeneration [241, 242]. It was reported that Cdc42 and Rac1 induce neurite outgrowth, whereas RhoA suppresses it [65]. Therefore, we wondered whether Gaf-1b may influence the actin filament regulating proteins Cdc42 and RhoA. We down-regulated Gaf-1b in HeLa cells with siRNA and analysed the expression of Cdc42 and RhoA on Western blot. Preliminary immunoblot data showed an increase of Cdc42 and RhoA when Gaf-1b is down-regulated in HeLa cells. We also observed the formation of robust stress fibers in Gaf-1b down-regulated HeLa cells, whereas in siRip11-transfected cells, we also observed stress fiber formation but to a lesser extent compared to siGaf-1b transfected cells. Insterestingly, siRip11-transfected HeLa cells showed a slight decrease of RhoA and Cdc42 expression. We can speculate that Gaf-1b and Rip11 are related to Rho GTPases in a way they may regulate the expression or distribution of these molecules. But the underlying mechanism of this interaction is not clear because we still have too less information. Additionally, these are preliminary data which were not quantitatively assessed, therefore further experiments have to be established and are required to confirm our preliminary findings.

3.5 Gaf-1b has a minor effect on receptor recycling

Gaf-1b was shown to localize to recycling endosomes and interact with the recycling-endosomal marker Rab11. Rab11 and Rab11-FIPs play a crucial role in receptor recycling through the endosomal recycling compartment. Rab11, RCP and Rip11 were demonstrated to be implicated in recycling of the TfR [153, 157, 163]. Additionally, FIP2 and RCP are also involved in internalization and recycling of epidermal growth factor receptor [158, 243]. In order to answer the question whether Gaf-1b was also involved in receptor recycling, we analysed the expression level of TfR, EGFR and Erbs in Gaf-1b or Gaf-1b/Rip11 down-regulated HeLa cells on Western blot. Interestingly, we showed that only a minor part of TfR, EGFR and Erbs (at most 20%) were affected in its recycling by the downregulation of Gaf-1b or of both Gaf-1b and Rip11. The minor decrease of the receptor signal may indicate a missorting of the receptors from sorting endosomes to the degradative pathway instead of the recycling pathway. Peden *et al*., 2004, showed that the RCP-Rab11 complex regulates the sorting of TfR from the degradative to recycling pathway. In contrast to our findings, it was shown that Rip11 knock-down in HeLa cells increased plasma membrane levels of TfR, but the cellular TfR levels remained the same [163]. Additionally, Tf-uptake was increased in Rip11 down-regulated cells. We observed a slight decrease of TfR levels in the cell and no significant difference at the plasma membrane. Our data also showed no remarkable effect on the Tf-uptake in Rip11 down-regulated cells (data not shown). This discrepancy is hardly to explain. They used another siRNA mixture to down-regulate Rip11 as well as another transfection procedure. They showed a downregulation of Rip11 of about 90% with Lipofectamine 2000 transfection, whereas we used Hiperfect to transfect cells with siRNA because we experienced that Lipofectamine 2000 transfection was less efficient compared to Hiperfect transfection. Since both results for Rip11 knock-down are similar, the discrepancy is presumably not due the different performance of the experimental setup. We have shown that the siRNA of Rip11 down-regulates both Rip11 and Gaf-1b simultaneously and very efficiently, but other authors never considered that the Rip11 siRNA also affect the expression of Gaf-1b. Therefore, results with Rip11 siRNA should be interpreted with care and Gaf-1b should be implied in the result.

Here we showed that Gaf-1b and Gaf-1b/Rip11 downregulation in HeLa cells only slightly decreased the protein level of the ErbB family of RTKs (EGFR, Erb3 and Erb4) in the cell and at the plasma membrane. FIP2 was shown to be involved in the internalization and recycling of EGFR and the interaction is mediated by the EH domain containing protein, Reps1, which is a substrate for EGF receptor [243]. Among the Rab11-FIPs, FIP2 was reported to be unique because it contains multiple EH domain binding NPF motifs. FIP2 contains three NPF motifs and the second NPF (NPF2) motif was shown to interact with EH domain of Reps1 with highest affinity. The other two NPF motifs are flanked with negatively charged residues and this may reduce the affinity of the NPF1 and NPF3 for Reps1 binding because their interaction with the electronegative binding site of Reps1 is not favorable [243]. We found on the Gaf-1b sequence two NPF motifs in the splice insert domain. Thus, this prompted us to investigate whether Gaf-1b may also be involved in EGFR recycling. Adjacent to the second NPF motif in the Gaf-1b sequence, there are also negatively charged residues which may reduce the binding affinity to Reps1. Hence, Gaf-1b may only weakly interact with the Reps1/EGFR complex.

Altogether, our results indicated that the main function of Gaf-1b probably does not comprise receptor recycling which could explain the minor effects observed during this study. Other Rab11-FIPs

were shown to play important roles in receptor recycling events. This supports the fact that different Rab11-FIPs form mutually exclusive complexes with Rab11 [155].

3.6 Gaf-1b is involved in the autophagic pathway

We identified Gaf-1b as an interaction partner of calsyntenin-1 and we suggested that Gaf-1b is implicated in endosomal recycling. The fact that Gaf-1b only showed a partial overlap with Rab11 in immunocytostaining indicated a function of Gaf-1b which is independent of Rab11. So far less is known about Gaf-1b. Therefore, we performed a yeast two-hybrid screen in order to identify new interaction partners of Gaf-1b. In this screen we identified GABARAPL2 as a novel interaction partner of Gaf-1b and verified the binding with co-immunoprecipitation, GST pull-down and Far-Western blotting. GABARAPL2 is a small globular ubiquitin-like modifier protein of the MAP1LC3A/Atg8 family. In mammals, at least seven Atg8 orthologues have been identified. Based on amino acid sequence homology, there are two subgroups, namely the LC3 subfamily (LC3A, LC3B and LC3C) and the GABARAP subfamily (GABRAP, GABARAPL1, GABARAPL2 and GABARAPL3) [96]. In our study, we also tested the interaction of Gaf-1b with the other Atg8 orthologues, GABARAPL1, LC3A and LC3B. We showed that Gaf-1b specifically and directly interacted with GABARAPL1 and GABRAPL2, but not with LC3A and LC3B. Additionally, Rip11 was not able to interact with both GABARAPL1 and GABARAPL2 suggesting that the splice insert of Gaf-1b was responsible for the interaction. Indeed, we tested different Gaf-1b truncation mutants for the interaction with GABARAPL2 and it resulted that the interaction was dependent on the splice insert of Gaf-1b. Additionally, we showed in co-immunostaining experiments of HeLa cells co-transfected with Gaf-1b and either GABARAPL1 or GABARAPL2 that both proteins partially overlapped with Gaf-1b. Our entire binding and colocalization assay indicated that Gaf-1b binds with a higher affinity to GABARAPL1 compared to GABARAPL2. GABARAPL1 exhibits 93% and 86% sequence identity with GABARAPL3 and GABARAP, respectively, while it only displays 61% sequence identity with GABARAPL2 [186, 187, 195]. We suggested that Gaf-1b could also interact with the other GABARAP subfamily members based on the fact that GABARAPL1 bound with higher affinity to Gaf-1b than GABARAPL2 and that the sequence identity is much higher to other GABARAP subfamily members than GABARAPL2. Recently, a study about proteomic analysis of the MAP1LC3/Atg8 family interaction network implicated an interaction partner overlap between GABARAP subfamily members. It was reported that approximately 18% of the analysed GABARAP subfamily interaction proteins interact simultaneously with GABARAP, GABARAPL1 and GABARAPL2 [244]. In order to gain more insight into the function of Gaf-1b, the interaction of Gaf-1b with the other GABARAP subfamily members should be tested.

Autophagy plays an essential role as a physiological system for cellular homeostasis. Autophagosomes are formed in response to environmental stress and are maturated to autolysosomes. Autophagosomes undergo substantial remodeling on the way to the maturation to autolysosomes, which includes heterotypic fusion with early and late endocytic organelles before they fuse with lysosomes for degradation. Although, extensive studies of the autophagic pathway were performed in the last decade, further investigations are still needed to understand the molecular machinery that governs this maturation process [102]. We showed here that Gaf-1b partially associated with membranes of the autophagosomal pathway, such as late endosomes, autophagosomes and lysosomes. When HeLa cells were co-transfected with Gaf-1b and either with LC3B, GABARAPL1 or GABARAPL2 and then autophagy was induced by starvation, we observed an

accumulation of Gaf-1b in large, perinuclear, aggregated structures positive for LC3B, GABARAPL1 or GABARAPL2. Upon starvation vesicular structures of Gaf-1b and LC3B, GABARAPL1 or GABARAPL2 in the periphery were decreased, instead a small amount of larger aggregates were observed, indicating fusion of the small vesicles to the larger aggregates. This large aggregates may be autophagosomes because LC3B is regarded as the typical marker for autophagosomes and it was reported that upon starvation, large aggregated structures positive for LC3B were observed [83, 98]. Several studies implicated SNAREs and Rab GTPases in the autophagic pathway. In yeast, SNAREs (such as Vam3p, Vam7p, Vti1p), NSF and the core class C vacuolar protein sorting (Vps) tethering complex were shown to play a role in fusion of autophagosomes with vacuoles [245, 246]. Behrends *et al.* (2010) suggested that Atg8 controls localized Rab activation and vesicle dynamics because Atg8 interacts with multiple Rab GTPase regulatory proteins. Deficiency in Ypt7p, the yeast Rab7 orthologue, has been correlated with impaired fusion process of autophagosomes and vacuoles [179]. In HeLa cells, it was demonstrated that Rab7 is required for the maturation of late autophagic vacuoles and fusion with lysosomes [104, 105]. Rab11 was also shown to be implicated in autophagy because autophagy induction in K562 cells promotes fusion of Rab11-associated multivesicular bodies with LC3-labelled autophagosomes forming large hybrid organelles, termed as amphisome [106]. Inhibition of Rab11 function by overexpression of the Rab11 dominant-negative mutant, Rab11S25N, impaired the fusion of MVBs with the autophagosomes, indicating that Rab11 function is crucial for the generation of the hybrid organelle. These data indicate that Gaf-1b could be involved in the membrane dynamic or fusion during autophagosome maturation. Based on the facts that (a) the C2 domain of the class I Rab11-FIPs has been shown to preferably associate with and (b) even to recruit Rab11-FIPs to phosphatidylinositol-(3,4,5)-trisphosphate [153] and (c) autophagosome nucleation starts with synthesis of phosphatidylinositol-(3,4,5)-trisphosphate [86], we suggested that the C2 domain of Gaf-1b may target Gaf-1b to autophagosomal membranes. Additionally, the fact that Gaf-1b interacted with kinesin-1 motor indicated a possible function of Gaf-1b in perinuclear-to-peripheral positioning of autophagosomal structures.

Several studies showed a relation of GABARAP subfamily members and autophagy. It was demonstrated that GABARAPL1 localizes to autophagic vacuoles upon inhibition of lyosomal enzyme activity in MCF7 and HEK293 cells [192]. GABARAPL1 accumulates in punctuated structures in the cytoplasm upon starvation in wild-type mouse embryonal fibroblasts (MEFs), while in Atg4B deficient MEFs this effect is abolished [193]. For GABARAPL2 it was reported that the membrane-bound form-II of GABARAPL2 is upregulated and relocalized to LC3-positive structures upon starvation [98]. However, the exact role of GABARAPL1 and GABARAPL2 in the autophagic process remains to be elucidated. Mutational study of Atg4A suggest a function of GABARAP subfamily members in later stages of autophagosome biogenesis [199]. Atg4A is a cysteine protease and is required for the first processing step of MAP1LC3 family members during their post-translation modification. Atg4A specifically recognizes and cleaves GABARAP and GABARAPL2 [98]. Weidberg *et al.*, 2010, suggested that members of the GABARAP subfamily are implicated in the regulation of the sealing process required for closure of isolation membranes because accumulation of incomplete enclosed autophagosomal membranes were observed in HeLa cells expressing the dominant-negative mutant of Atg4A under starvation condition. GABARAPL1 and GABARAPL2 might also have a regulatory function in fusion processes during autophagosome maturation due to their homology to Atg8, the interaction with NSF and their function in SNARE priming [195]. It was shown that GABARAPL1 and GABARAPL2 only localized to autophagosomal membranes after starvation [213]. In contrast, it was demonstrated that Gaf-1b was found partially associated to LC3-labelled membranes already prior to

starvation which could indicate a role of Gaf-1b in the recruitment or transport of GABARAPL1 and GABARPL2 to autophagosomes upon starvation [213].
Typical for the MAP1LC3 family members, LC3 undergoes an ubiquitin-like posttranslational modification which converts the C-terminally truncated cytosolic form-I of LC3 to its lipidated membrane bound form-II [99, 100]. Induction of autophagy was shown to stimulate this conversion and association of LC3 with autophagosomal and pre-autophagosomal membranes was found to depend on form-II, thus establishing LC3 as a reliable autophagosomal marker [83, 98]. We showed here in preliminary experiments an interesting effect on the LC3 form-II expression in Gaf-1b down-regulated cells. The LC3 form-II signal was strongly increased in Gaf-1b down-regulated cells compared to nonsense transfection. The addition of Bafilomycin 1A to siNonsense transfected cells induced an increased signal of LC3 form-II to almost the same level as in Gaf-1b down-regulated cells. Bafilomycin 1A primarily inhibits the acidification of lysosomes which affects the degradation and it was also reported to inhibit autophagosome-lysosome fusion [247, 248]. In contrast, application of Bafilomycin 1A showed only a sparse effect of an increased LC3-II signal in Gaf-1b down-regulated cells. This result indicates a function of Gaf-1b downstream of the autophagosome formation. We suggest that Gaf-1b induces the conversion of autophagosomes to autolysosomes as the LC3-II signal in Gaf-1b down-regulated cells is comparable with those of Bafilomycin 1A treated cells of the nonsense cells. In addition, Bafilomycin 1A did not have an effect on Gaf-1b down-regulated cells. A general misunderstanding in autophagy is the belief that increased numbers of autophagosomes in cells correspond to increased autophagic activity [83]. Autophagy is a dynamic process and the autophagosome is an intermediate structure. The number of autophagosome at a timepoint defines a function of the balance between the rate of their generation and the rate of their maturation to autolysosomes. Therefore, the observed accumulation of autophagosomes is the result of either autophagy induction or suppression of the downstream steps in the autophagy pathway [83]. In our case we suggested that Gaf-1b may play a role in the downstream steps of the autophagosome formation. Further experiments verifying our findings are needed. For instance, it would be essential to test the effect of LC3-II expression in down-regulated Gaf-1b cells under starvation condition and other pharmacological drugs inhibiting the upstream (e.g., LY294002, Wortmannin) or downstream pathway (e.g., vinblastine, noccodazole) of autophagy should be tested.
In summary our data demonstrated a direct relation between endosomal organelles in the autphagic pathway. On one site, Gaf-1b is a direct interaction partner of Rab11 and it was shown that Rab11 is required for the generation of the hybrid organelle, the amphisomes. On the other site, Gaf-1b was identified as a direct binding partner of GABARAPL1 and GABARAPL2, thus this interaction links Gaf-1b to the autophagosomal pathway. Gaf-1b may recruit MVBs masked with Rab11 and GABARAPL1 and GABARAPL2 to autophagosomal membrane to induce the fusion of MVBs with lysosomes.

3.7 Gaf-1b is essential for cell viability

Gaf-1b was shown to be involved in distinct cellular processes. A role of Gaf-1b was speculated in the secretory and recycling pathway because Gaf-1b was found at the TGN, in vesicles trafficking along axons and at recycling endosomes. Together with calysntenin-1 and kinesin-1, Gaf-1b may transport specific proteins and/or lipids from the TGN through the endsosomal recycling compartment to the plasma membrane. Finally, we found a link between endosomal organelles and the autophagic pathway, where Gaf-1b may play an important role as a regulator of the fusion process

of the MVBs and autophagosome. Gaf-1b is localized to different organelles and seemed be a multifunctional regulator in cellular processes. We have shown that Gaf-1b was essential for cell viability because long-term downregulation of Gaf-1b in HeLa cells or neurons was lethal for these cells. Regulated endocytic recycling is essential for cells to maintenance their function and it is involved in processes, such as cytokinesis, cell adhesion, morphogenesis, cell fusion, learning and memory [33]. Autophagy is also involved in important cellular processes. It was shown to be crucial in fate decision because it is involved in specific cytosolic rearrangement required for death, proliferation and differentiation during embryogenesis and postnatal development [86]. Therefore, dysfunction of endocytic recycling as well of autophagy may severely impair cell functions or may even be lethal for cells. We showed that Gaf-1b is involved in both processes and impairment of Gaf-1b affects both processes. Even though Rip11 is splice variant of Gaf-1b, Rip11 was not able to take over or compensate the function of Gaf-1b in Gaf-1b knock-down cells. Additionally, we have shown in our research that Gaf-1b and Rip11 carry distinct features, although they just differ in the splice insert. Thus, Gaf-1b plays an important role in maintaining cell viability.

4. Material and Methods

4.1 Antibodies and Reagents

4.1.1 Affinity-purified antibodies

Rabbit polyclonal antibodies R85 and R140 were generated against murine calsyntenin-1 as described by Konecna *et al.*, 2006. R140 antibodies were raised against two peptides at the very C-terminus of calsyntenin-1: EGGPGDGQNATRQLEWDD and DGQNATRQLEWDDSTLSY. R85 antibodies were generated against the N-terminal cadherin domain corresponding to the residues 43-295. Both antibodies R140 and R85 were affinity-purified.

For affinity purification, 500 µg of each antigen were separated by SDS-PAGE and transferred onto Immobilon-P polyvinylidene difluoride (PVDF) membrane (Millipore, Zug, Switzerland) at 60 V for 2 h in a Criterion Blotter wet transfer chamber (BioRad, Reinach, Switzerland). Membrane containing the antigen of interest was cut into pieces and membrane pieces were stripped to remove weakly bound antigen (5 min in water, 5 min 0.2 M NaOH, 5 min in water), then soaked in methanol and air-dried for 15 min. 1.5 ml of serum were incubated overnight at 4°C, then the pieces were washed in phosphate-buffered saline (PBS, 137 mM NaCl, 2.5 mM KCl, 7 mM $Na_3HPO_4 \cdot H_2O$, 1.45 mM KH_2PO_4), pH 7.4, containing 0.1% Tween-20. Antibody were eluted twice in elution buffer (500 mM NaCl, 0.5% Tween-20, 100 mM glycine·HCl, pH 2.5) for 2 minutes and immediately neutralized in 0.15 volumes of 1 M Tris-Cl, pH 8.0. Concentrations were measured with an UV spectrometer and calculated with following formula [IgG] (mg/ml) = (1.55·A280)–(0.76·A260). Antibodies were stored in aliquots at –80°C and used at a concentration of 1-2 µg/ml for immunofluorescence and 0.5 µg/ml for immunoblotting. In this study we used affinity-purified R140 2nd and 3rd boost and R85 10th and 12th boost.

4.1.2 Purchased antibodies

Purchased antibodies were from **Abcam** (Cambridgeshire, EGFR phospho S1047 [Ab24918; m; WB 1:200], TGN46 [Ab16052; rb; ICC 1:500]), **Affinity Bioreagents** (Golden, CO, USA; BACE1 [PA1-757; rb; WB 1:500 – 1:1,000]), **Amersham** (Zurich, Switzerland, anti-GST [27-4577-01; g; WB 1:2,000]), **Clontech** (Saint-Germain-en-Laye, France, anti-GFP [632459; rb; WB 1:1,000]), **Chemicon** (Lucerne, Switzerland; APP [MAB348; m; WB 1:4,000], MAP2 [MAB3418; m; WB 1:10,000, ICC 1:750]), **Invitrogen** (Basel, Switzerland; Rab11 [71-5300; rb], TfR [13-6800; m; WB 1:1,000; ICC 1:500]), **Qiagen** (Hombrechtikon, Switzerland, anti-$(His)_4$ [34670; m; 1:2,000]), **Santa Cruz Biotechnology** (Nunningen, Switzerland; calnexin [Sc-11397; rb; WB 1:1,000], Cdc42 (P1) [Sc-87; rb; WB 1:200], EEA1 [Sc-6415; g; WB 1:200; ICC 1:200], EGFR 1005 [Sc-03; rb; WB 1:200], ErB-3 (C-17) [sc-285; rb; WB 1:200], ErB-4 (C-18) [sc-283; rb; WB 1:100], Rab-5 [Sc-46692; m; WB 1:200], Rac1 (C-14) [Sc-217; rb; WB 1:200], RhoB (119) [Sc-180; rb; WB 1:200], *anti*-HA [Sc-805; rb; WB 1:1,000, ICC 1:200], *anti*-myc A14 [Sc-789; rb; WB 1:5,000; ICC 1:200], Grp78 N-20 [Sc-1050; g; WB 1:1,000]), **Sigma-Aldrich** (Buchs, Switzerland; ADAM10 [A2726; rb; WB 1:500 – 1:1,000], APP [A8717; rb; WB 1:4,000; ICC 1:1,000], α-tubulin [T9026; m; WB 1:20,000], β-actin [A5316; m; WB 1:6,000], anti-FLAG M2 [F1804; m; WB 1:1,000; ICC 1:500], GABARAPL2 [SAB2100874; rb; WB 1:1,000; ICC 1:500], LC3A [L8793; rb; WB 1:2,000; ICC 1:500], Rab7 [R4779; rb; WB 1:500], *anti*-myc [M4439; m; WB 1:5,000]), **Synaptic Systems** (Göttingen, Germany; syntaxin 13 [110132; rb; WB 1:2,000; ICC 1:1,000], syntaxin 16 [110162; rb; 1:8,000], syntaxin 6 [110062; rb; WB 1:4,000; ICC

1:500], VAMP2 [104211; m; WB 1:10,000; ICC 1:1,000], VAMP4 [136002; rb; WB 1:2,000], mVPS45 [137002; rb; 1:300]), **Stressgen** (Zurich, Switzerland; syntaxin 13 [VAM-SV026; m; WB 1:2,000]), **BD Biosciences** (Allschwil, Switzerland; GM130 [610822; m; WB 1:2,000, ICC 1:200], Mint-2 [M76120; m; WB 1:2,000], Rab11 [610656; m; WB 1:2,000], Rab4 [610888; m; WB 1:2,000], syntaxin 6 [610635; m; WB 1:5,000], syntaxin 4 [610439; m; WB 1:1,000], TGN38 [610898; m; WB 1:500]), **Roche** (Basel, Switzerland; *anti*-GFP [1814460; m; WB 1:2,000], *anti*-HA 12CA5 [1583816; m; WB 1:5,000; ICC 1:5,000], *anti*-HA HiAffi [1867423; rt; ICC 1:600]), **Thermo scientific** (Waltham, USA, anti-FLAG [PA1-984B; rb; WB 1:1,000; ICC 1:500]) and **Zymed** (San Francisco, USA; anti-myc 9E10 [13-2500; m; WB 1:10,000; ICC 1:500]).

Fluorescent secondary antibodies (AlexaFluor488-, AlexaFluor647-, Cy3-, FITC- and Cy5-conjugated) were obtained from Jackson ImmunoResearch Laboratories (West Grove, PA, USA) and were diluted 1:400 for immunofluorescence. Horseradish peroxidase (HRP)-conjugated secondary antibodies (WB 1:20,000) were purchased from Kirkegaard & Perry Laboratories (Gaithersburg, MD, USA) and Chemicon (Lucerne, Switzerland).

4.1.3 Provided antibodies

The polyclonal rabbit antibodies αGaf1b A [0.1 mg/ml; rb; ICC 1:200], αGaf1b B [0.86 mg/ml; rb; WB 1:2,000; ICC 1:200] and αGaf1b C [0.5 mg/ml; rb; WB 1:2,000; ICC 1:200] were a kind gift of Mitsuo Tagaya (Tokyo University of Pharmacy and Life Science). αGaf1b A, αGaf1b B and αGaf1b C antibodies were raised against amino acids 221-520, amino acids 403-636 and amino acid 524-653 of Gaf-1b, respectively. αGaf1b B was generated against the splice insert of Gaf-1b [168]. Additional antibodies were kindly provided by Dr. Jack Rohrer (University of Zurich, Zurich, Switzerland; LAMP1 [rt; WB 1:1,000]), Dr. Rytis Prekeris (University of Colorado, Aurora, CO, USA; Rip11 [rb; ICC 1:200] [165], Dr. Markus Plomann (Center for Biochemistry and Molecular Medicine, Cologne, Germany; EHD3 [rb; ICC 1:300]) and Dr. Vance Lemmon (University of Miami, FL, USA; L1 [rb; WB 1:4,000]).

4.1.4 Reagents

All pharmacological inhibitors were purchased from AppliChem (Axonlab, Baden, Switzerland), Tocris Cookson Inc (Missouri, USA) and Sigma-Aldrich (Buchs, Switzerland). The following stock solutions were prepared and stored at -20°C. Bafilomycin A1 (200 µM stock solution in DMSO, used at 100 nM), chloroquine (1.5 mM stock solution in H_2O, used at 10 µM), leupeptin (10 mM stock solution in H_2O, used at 10 µM), pepstatin A (1 mg/ml stock solution in methanol:acetic acid (9:1), used at 5 µM) and wortmannin (100 µM stock solution in DMSO, used at 100 nM). Phalloidin-FITC was purchased from Sigma-Aldrich (Buchs-Switzerland).

4.2 Constructs

The constructs calsyntenin-1 wt, EGFP-calsyntenin-1_wt, EGFP-calsyntenin-1_cyto, EGFP-calsyntenin-1_906ΔC, EGFP-calsyntenin-1_WW (point mutation in the KBS1 and KBS2 were generated by replacing the conserved tryptophan residues (aa W903 and aa W972) with alanine), calsyntenin-1-myc, calsyntenin-3-myc, HA-KLC1 and RFP-KLC1 have been described previously [171, 176]. All the calsyntenins constructs contain the mouse calsyntenin cDNAs and were cloned in pcDNA3.1(-) (Invitrogen, Basel, Switzerland). HA-Stx13 was provided by Martin Steuble (University of Zurich, Switzerland). HA-Stx13 wt were generated by insertion of the mouse syntaxin 13 cDNA (aa 1-274) into pcDNA3.1(-)-HA, which contains a N-terminal HA-tag inserted into the BamHI and EcoRI restriction sites [249]. The HA-tag was previously ligated into pcDNA3.1(-) (Invitrogen) through BamHI and EcoRI sites. Rip11-EGFP was a gift from Rytis Prekris (University of Colorado, Aurora, CO, USA) and has been described previously [165]. Rab4a, Rab4aQ72L, Rab5a, Rab5aQ79L, Rab11a, Rab11aQ70L and Rab11aS25N in pEGFP-C3 plasmids (Clontech) were kindly provided by Marino Zerial (MPI, Dresden, Germany) and Ari Helenius (ETH Zurich, Switzerland). To generate GST-fusion protein of Rab GTPases, Rab sequences were amplified by PCR and cloned into the BamHI and NotI sites of pGEX-6P1 [205]. Human FLAG-Gaf1b was a kind gift from Mitsuo Tagaya (Tokyo University of Pharmacy and Life Science, Tokio, Japan) and has been described previously [168]. To construct FLAG-Gaf-1b truncation mutants, fragments of Gaf-1b were PCR amplified using the primers listed in Table 4.1 and inserted into BglII and XbaI restriction sites of pFLAG-CMV2. cDNA of murine Gaf-1b and Rip11 were generated by RT-PCR from brain polyA-RNA. Murine Gaf-1b and Rip11 were PCR amplified and inserted into XbaI and NotI restriction sites of pBluescript (SK+). Mouse Rip11-mEGFP and Gaf-1b-mEGFP constructs were generated by restriction of Rip11 or Gaf-1b from pBluescript (SK+) and inserted into pmEGFP-N3 through the BglII and KpnI restriction sites. Rip11-mCherry and Gaf-1b-mCherry constructs were obtained by PCR amplification of mCherry and replacement of mEGFP on Rip11-mEGFP or Gaf-1b-mEGFP by mCherry through KpnI and NotI sites. All cDNA clones of GABARAPL1, GABARAPL2, LC3A and LC3B were purchased from imaGenes (Nottingham, UK). HA-fusion constructs of GABARAPL1, GABARAPL2, LC3A and LC3B were generated by PCR amplification of the individual cDNA and inserted into the EcoRI and XhoI sites of pcDNA3.1(-)-HA. To generate GST-fusion protein of GABARAPL1, GABARAPL2, LC3A and LC3B, the corresponding cDNA sequences were amplified by PCR and cloned into BamHI and NotI sites of pGEX-6P1 [213].

Table 4.1: Oligonucleotides of human Gaf-1b truncation mutants.

Construct name	Oligo name	Sequence
FLAG-Gaf-1b_ΔC	Gaf1b_BglII_for	5'-GGCCAGATCTGATCGATATGGCCCTGGTG
	Gaf1b_insR_Xba	5'-GGCCTCTAGACTAGGCACTGGGCTGTGGC
FLAG-Gaf-1b_ΔN	Gaf1b_ins_BglII_for	5'-GGCCAGATCTGAGTGCCTCGAGGGCCAGCC
	Gaf1b_XbaI_rev	5'-CACCCGGGATCCTCTAGACTATTT
FLAG-Gaf-1b_ΔC2	Gaf1b_ΔC2d_BglII_for	5'-GGCCAGATCTAACGCAGTGGTACAAG
	Gaf1b_XbaI_rev	5'-CACCCGGGATCCTCTAGACTATTT
FLAG-Gaf-1b_ins	Gaf1b_ins_BglII_for	5'-GGCCAGATCTGAGTGCCTCGAGGGCCAGCC
	Gaf1b_insR_Xba	5'-GGCCTCTAGACTAGGCACTGGGCTGTGGC
FLAG-Gaf-1b_522ΔC	Gaf1b_BglII_for	5'-GGCCAGATCTGATCGATATGGCCCTGGTG
	Gaf1b_C2dΔ525_XbaI_rev	5'-GGCCTCTAGACTAGGGTTTCTGAGTC
FLAG-Gaf-1b_489ΔC	Gaf1b_BglII_for	5'-GGCCAGATCTGATCGATATGGCCCTGGTG
	Gaf1b_489ΔC _XbaI_rev	5'-CCGGTCTAGACTAGTGGTGGTGGAAGAGACC

FLAG-Gaf1b_435ΔC	Gaf1b_BglII_for	5'-GGCCAGATCTGATCGATATGGCCCTGGTG
	Gaf1b_435ΔC _XbaI_rev	5'-GGCCTCTAGACTAGGCCAGGACTTTAGCCTG
FLAG-Gaf1b_381ΔC	Gaf1b_BglII_for	5'-GGCCAGATCTGATCGATATGGCCCTGGTG
	Gaf1b_381ΔC_XbaI_rev	5'-GGCCTCTAGACTAGCCCGAGATGGAGCTGC
FLAG-Gaf1b_327ΔC	Gaf1b_BglII_for	5'-GGCCAGATCTGATCGATATGGCCCTGGTG
	Gaf1b_327ΔC_XbaI_rev	5'-GCGCTCTAGACTAGTAGGTCCTCTTATGGGTG
FLAG-Gaf1b_273ΔC	Gaf1b_BglII_for	5'-GGCCAGATCTGATCGATATGGCCCTGGTG
	Gaf1b_273ΔC_XbaI_rev	5'-GGCCTCTAGACTACAGCGAGGTGTTGGACTG
FLAG-Gaf1b_219ΔC	Gaf1b_BglII_for	5'-GGCCAGATCTGATCGATATGGCCCTGGTG
	Gaf1b_219ΔC_XbaI_rev	5'-GGCCTCTAGACTACTTCATCTTGTCCCTGATC
FLAG-Gaf1b_194ΔC	Gaf1b_BglII_for	5'-GGCCAGATCTGATCGATATGGCCCTGGTG
	Gaf1b_194ΔC_XbaI_rev	5'-GGCCTCTAGACTACAGGTTGTTGCGCGTGAAC
FLAG-Gaf1b_169ΔC	Gaf1b_BglII_for	5'-GGCCAGATCTGATCGATATGGCCCTGGTG
	Gaf1b_169ΔC_XbaI_rev	5'-GGCCTCTAGA CTACAGCTTGTACCACTGCGTG
FLAG-Gaf1b_C2	Gaf1b_BglII_for	5'-GGCCAGATCTGATCGATATGGCCCTGGTG
	Gaf1b_C2d_XbaI_rev	5'-GGCCTCTAGACTACTGCGTGTGCT

4.3 siRNA and shRNA constructs

4.3.1 siRNA

The siRNA oligonucleotides for human Rip11 (Rip11_hum) and human Rab11a (Rab11a_hum) as well as the negative control (nonsense) sequences were described previously [157, 250-252]. Additional siRNAs to down-regulate human Rip11 and Gaf-1b were designed and selected siRNAs (Table 4.2) were ordered from Microsynth (Balgach, Switzerland).

The siRNAs were generated according to the instructions of the siRNA user guide of the Tuschl Lab (www.rockefeller.edu/labheads/tuschl/sirna.html) and to the protocol from Nature [253]. The most efficient silencing was obtained with siRNA duplexes composed of 21 nucleotide sense and antisense strands, paired in a manner to have a 2-nucleotide 3' overhang according to Tuschl's user guide. siRNA sequences were selected with TT in the overhang. We searched for the 23-nt sequence motif AA(N19)TT or NA(N21) (N, any nucleotide) with a G/C-content of about 50% (or 30-70%) to design a siRNA duplex. The sequence of the sense siRNA corresponds to (N19)TT or N21, in the latter case the 3' end of the sense siRNA was converted to TT.

Table 4.2: Sequence of siRNA

Name	Sequence (sense)
NS_2	5'-ACAUCUCUACGCCACCAGGTT
NS_3	5'- UUCUCCGAACGUGUCACGUTT
siGaf_3_hum	5'-GUGAUCAGUGUGUGGGAGATT
siGaf_4_hum	5'-GAGCUAGUGGAGGAUGCCATT
siGaf_5_hum	5'-CCCUGUCACUCAAAGAGCUTT
siRip11_hum	5'-GCGUAGUGCUCAGGCUAAATT
sisRip11_1_hum	5'-ACCCAGUCCCCACCCCGUGTT
sisRip11_2_hum	5'-CUCAGAAACCCAGUCCCCATT
Rab11a_hum	5'-UGUCAGACAGACGCGAAAATT

4.3.2 shRNA

shRNA for mouse Gaf-1b and Rip11 were designed according to the instructions of the TRC RNAi consortium (Broad institute, www.broadinstitute.org/rnai/public/) and Ambion (Invitrogen, Zug, Switzerland) and the guideline described in [254]. The shRNA duplexes were designed to contain a HpaI and XbaI restriction sites at the end for the insertion of the shRNA in an expression plasmid. The sense strands start with one or two G, followed by 19-21 nucleotide sense strands and the reverse complement strands with TTTTT in the overhang. The sense and the reverse complement strands are linked by a linker of about 6 nucleotides. The linker was designed to contain a XhoI restriction site for cloning control. A G-nucleotide is inserted if the target strand does not start with a G. Therefore, the sense strands adopt such a form T-(G)-N(19-21)-CTCGAG-N(19-21)-TTTTT and the reverse complement antisense strands CTAGAAAAA-N(19-21)-CTCGAG-N(19-21)-(C)-A. shRNA target sequences were searched by the search tool or siRNA Target Finder tool from TRC RNAi consortium or Ambion, respectively. shRNA with a G/C-content of 30-52% and starting with a G-nucleotide were searched. Homology and specificity of the sequences were tested by NCBI's program blastn and the specificity server of the Griffith University. The blastn parameters were adjusted according to the Nature's protocol [254]. Sequences were selected which contained at least 2 missmatches (not at position 1 and 19) for 19 nucleotide sequences. For 21 nucleotide sequences, at least 3 missmatches

were necessary where two of them should be in position 3-19. The selected shRNA are listed in Table 4.3. All the oligonucleotides were purchases from Microsynth. shRNA oligonucleotide were annealed by mixing 9 µl of the forward oligo and 9 µl of the reverse oligo with 2 µl of 10x annealing buffer (Invitrogen, 1 M NaCl, 10 mM EDTA, 100 mM Tris-Cl pH 8.0) and running a PCR program where the reaction was heated to 95°C and slowly cooled down to 20°C in 2 h 30 min. The shRNA was inserted into XbaI and HpaI restriction sites of the mCherry-U6-pMCV1.4 vector. Note, the plasmid vector was not dephosphorylated prior to ligation. mCherry-U6 on pCMV-Transfer A was restricted at KpnI and PmeI sites and inserted into pMCV1.4 through KpnI and Klenow treated XhoI site to obtain mCherry-U6-pMCV1.4. Cloning of shRNA was more difficult than other recombinant proteins, therefore restriction control and sequencing of the whole construct was important.

Table 4.3.: shRNA construct

Construct name	Oligo name	Sequence
mCherry-U6-shNS	shNS_for	5'-T**GGGCATACCGCCCCGGGAT**TTCAAGAGA**ATCCCGGGGCGGTATGCCC**TTTTT
	shNS_rev	5'-CTAGAAAAA**GGGCATACCGCCCCGGGAT**TCTCTTGAA**ATCCCGGGGCGGTATGCCC**A
mCherry-U6-shRip11_5	shRip11_5_mus_for	5'-T**GAAACAAGCTACGCAAGTCCT**TTCTCGAG**AGGACTTGCGTAGCTTGTTTC**TTTTT
	shRip11_5_mus_rev	5'-CTAGAAAAA**GAAACAAGCTACGCAAGTCCT**CTCGAGAA**AGGACTTGCGTAGCTTGTTTC**A
mCherry-U6-shRip11_8	shRip11_8_mus_for	5'-T**GAATCCAAGGAGCCAACTCAG**TTCTCGAG**CTGAGTTGGCTCCTTGGATTC**TTTTT
	shRip11_8_mus_rev	5'-CTAGAAAAA**GAATCCAAGGAGCCAACTCAG**CTCGAGAA**CTGAGTTGGCTCCTTGGATTC**A
mCherry-U6-shGaf-1b_3	shGaf-1b_3_mus_for	5'-T**GCCGACATAGCACTAAATTCT**TTCTCGAG**AGAATTTAGTGCTATGTCGGC**TTTTT
	shGaf-1b_3_mus_rev	5'-CTAGAAAAA**GCCGACATAGCACTAAATTCT**CTCGAGAA**AGAATTTAGTGCTATGTCGGC**A
mCherry-U6-shGaf-1b_4	shGaf-1b_4_mus_for	5'-T**GCCGACATAGCACTAAATTCT**TTCTCGAG**AGAATTTAGTGCTATGTCGGC**TTTTT
	shGaf-1b_4_mus_rev	5'-CTAGAAAAA**GCCGACATAGCACTAAATTCT**CTCGAGAA**AGAATTTAGTGCTATGTCGGC**A

4.4 Molecular cloning

4.4.1 PCR and RT-PCR

Polymerase chain reactions (PCR) were performed with the Expand High Fidelity™ system (Roche diagnostics, Mannheim, Germany) using the Biometria T3 Thermocycler (Goettingen, Germany). A general PCR set up and PCR program is shown in Table 4.4 and 4.5, respectively.

The mouse coding sequence of Gaf-1b and Rip11 was amplified by RT-PCR. The polyA-RNA template from mouse hippocampus was isolated according to the TRI Reagent® protocol from Sigma-Aldrich. The ThermoScript™ RT-PCR System (Invitrogen, Basel, Switzerland) was used for cDNA synthesis following the manufacturer's protocol. 10% of the cDNA synthesis reaction was applied for PCR amplification.

Table 4.4: PCR setup

Components	1x reactions
10x reaction buffer	5 µl
dNTP's (10 mM)	1 µl
Forward Oligo (10 µM)	1 µl
Reverse Oligo (10 µM)	1 µl
Template	50 ng
Taq-polymerase (3.5 U/µl)	1 µl
DMSO	1 µl
ddH_2O	add to 50 µl

Table 4.5: PCR program

Stage	Time (sec)	Temperature (°C)	Cycles
Initial denaturation	300	95	1
Denaturation	30	95	25
Annealing	30	50-60	
Elongation	90	72	
Final extension	300	72	1

4.4.2 Purification of PCR products

PCR products were purified from dNTP's, DNA polymerases and primers using the NucleoSpin® Extract II kit (Machery-Nagel, Düren, Germany) according to the manufacturer's manual.

4.4.3 Restriction digest

Restriction enzymes and 10x restriction buffers were purchased from Promega (Madison, USA), New England BioLabs (New England) or Roche (Basel, Switzerland). Sample mixture of analytical or preparative digest was prepared according to Table 4.6. Analytical and preparative digests were performed for two hours or overnight at 37°C.

Table 4.6: Analytical and preparative digest

Analytical digest		Preparative digest	
DNA	300-500ng	DNA	2-5 µg
10x restriction buffer	1 µl	10x restriction buffer	3 µl
enzyme 1 (10-20 U/µl)	0.5 µl	enzyme 1 (10-20 U/µl)	1 µl
enzyme 2 (10-20 U/µl)	0.5 µl	enzyme 2 (10-20 U/µl)	1 µl
ddH_2O	add to 10 µl	ddH_2O	add to 30 µl

Acceptor plasmids were dephosphorylated for 1-2 hours at 37°C with 2 µl alkaline phosphatase (Roche, Basel, Switzerland) after restriction digest.

4.4.4 Agarose gel electrophoresis

DNA samples were mixed with 6x DNA loading buffer (30% glycerol, 0.25% bromphenol blue, 0.25% xylene cyanol) and were separated against known size markers (Smart Ladder, Eurogentech) by agarose gel electrophoresis in TAE (40 mM Tris-acetate, 1 mM EDTA, pH 8.0) at 80-100V. The concentration of agarose (Eurogenetic) was 1% and Ethidium bromide was added to a final concentration of 5 µg/ml. The DNA was visualized under UV illumination and images were taken using digital gel imaging system (UVI-tec).

4.4.5 Gel extraction

The DNA band of interest was cut out of the agarose gel using a sterile razor blade. DNA was isolated from the agarose gel using the NucleoSpin® Extract II kit (Machery-Nagel, Düren, Germany) following the manufacturer's manual.

4.4.6 Ligation

Inserts were ligated into the vector at a molar ratio of vector:insert of 1:3. Ligation reactions were performed in a volume of 10 µl containing 1 µl 10x ligation buffer (Roche diagnostics, Mannheim, Germany) and 1 µl T4 ligase (Fermentas) and incubated at 4°C overnight. Alternatively, the Takara DNA ligation kit (Takara Bio Inc, Shiga, Japan) was used. Reaction mix composed of 1 µl vector, 4 µl insert and 5 µl Takara ligation mix were incubated at 16°C for 30 minutes.

4.4.7 Preparation of competent *E.coli* cells

A preculture of *E.coli* XL1-blue or DH5α was grown in 4 ml LB medium (1% bacto tryptone, 0.5% yeast extract, 1% NaCl) over night at 37°C. 400 ml LB medium were inoculated with the 4 ml overnight preculture and cells grown for approximately two hours at 37°C with shaking at 220 rpm until an OD_{600} of 0.375. The cultures were distributed into eight prechilled 50 ml Sarstedt tubes and chilled on ice for 5 minutes. Cells were centrifuged for 7 minutes at 1,600 x g and 4°C (Sorvall RT6000D). The supernatant was removed and each pellet was resuspended in 10 ml ice-cold $CaCl_2$ solution (60 mM $CaCl_2$, 15% glycerol, 10 mM PIPES, pH 7.0). The resuspended cells were centrifuged for 5 minutes at 1,100 x g and 4°C (Sorvall RT6000D) and the supernatant was discarded. Each pellet was again resuspended in 10 ml ice-cold $CaCl_2$ solution and cells were incubated on ice for one hour, followed by centrifugation for 5 minutes at 1,100 x g and 4°C (Sorvall RT6000D). Pellets were resuspended in 2 ml ice-cold $CaCl_2$ solution. The final cell suspensions were pooled and distributed in 200 µl aliquots into prechilled sterile Eppendorf tubes and frozen immediately at -80°C.

For GST-fusion protein expression, 50 ml of LB medium were inoculated with a single colony of *E.coli* BL-21 and incubated at 37°C with shaking at 220 rpm until the cells reached an OD_{600} of 0.38. Cells were centrifuged for 15 minutes at 2,500 x g and 4°C (Sorvall RT6000D). Cells were resuspended in 10 ml ice-cold transformation solution (1% tryptone, 0.5% yeast extract, 0.5% NaCl, 10% PEG, 5% DMSO, 50 mM $MgCl_2$, pH 6.5) and immediately used for transformation.

4.4.8 Transformation of recombinant plasmid into competent *E.coli* XL1-blue or DH5α

Recombinant plasmids were transformed into competent *E.coli* XL1-blue or DH5α. 5 ng of recombinant plasmid were added to 100 µl competent cells and chilled on ice for 30 minutes. Then the cells were heatshocked at 42°C for 45 seconds in a water bath and incubated for another 15 minutes on ice. 400 µl fresh LB medium without antibiotics was added and the cell suspension was incubated for one hour at 37°C to allow the expression of the resistance gene. The incubation time in LB medium without antibiotics is dependent on the antibiotic resistance of the constructs. Cells were then dispersed onto LB agar plates (1% bacto, 0.5% yeast extract, 1% NaCl, 1.5% agar) containing the appropriate antibiotics. The plates were incubated at 37°C overnight and stored at 4°C. Positive colonies were picked and transferred into 3 ml fresh LB medium containing the appropriate antibiotics and incubated in a shaking incubator at 200 rpm overnight at 37°C.

4.4.9 Transformation of competent *E.coli* BL-21

Freshly prepared competent *E.coli* BL-21 were mixed with 10 ng of the pGEX-6P-1 construct and chilled on ice for 45 minutes. Cells were heatshocked for 2 minutes at 42°C in a water bath and incubated on ice for 5 minutes. 100 µl of the transformed cells were mixed with 100 µl LB medium, followed be incubation for 15 minutes at 37°C. Cells were plated onto LB agar plates containing 100 µg/ml ampicillin and grown overnight at 37°C.

4.4.10 Isolation and purification of DNA from *E.coli* cells

The QIAprep® Spin Miniprep Kit (Qiagen, Hilden, Germany) or the NucleoSpin® Plasmid QuickPure kit (Machery-Nagel, Düren, Germany) was used to isolate DNA from small scale (2-5 ml) overnight cultures. For purification of large scale and endotoxin-free transfection grade plasmid DNA, the EndoFree® Plasmid Maxi kit (Qiagen, Hilden, Germany) was used. The isolation was performed according to the manufacturer's instructions. Small and large scale plasmid isolations yield approximately 400 µg and 1-2 mg plasmid DNA, respectively.

4.5 Cell biological methods

4.5.1 Heterologous cell culture

HeLa, HEK293T, Cos7, NG108 or H4 cells were grown in 10 cm dishes (Nunc Inc., Roskilde, Denmark) in 10 ml Dulbecco's Modified Eagle Medium (DMEM, Invitrogen, Basel, Switzerland) supplemented with 5 mM glutamine, 4.5 g/l Glucose, 1 mM sodium pyruvate and 10% fetal calf serum or fetal bovine serum at 37°C and 10% CO_2. For immunocytochemistry, round 18 mm glass coverslips (Menzel, Braunschweig, Germany) were coated with 50 µg/ml poly-L-lysine (PLL, Sigma-Aldrich, Buchs, Switzerland) and cells were plated on the glass coverslips at an appropriate density. For Western blot analysis, cells were cultured in 6-well or 12-well culture dishes (Nunc Inc., Roskilde, Denmark), washed twice in ice-cold PBS and lysed for 30 min in IP buffer (1% Triton X-100, 150 mM NaCl, 5 mM EDTA, 1 mM Na_3VO_4, 5 mM NaF, 50 mM Tris-Cl, pH 8.0) supplemented with protease inhibitor cocktail (Roche, Basel, Switzerland) under constant shaking. Lysates were centrifuged at 20,000 x g and the pellet was discarded. The protein concentration was determined with the BCA™ protein assay kit (Pierce, Rockford, USA) and proteins were chloroform-methanol precipitated [255] for subsequent separation by PAGE.

4.5.2 Neuron cell culture

Primary hippocampal or cortical neurons were prepared from embryonic E18 NMRI mice and cultured on top of an astroglia feeder layer [256]. Cells were cultured in Neurobasal medium supplemented with B27 and 5 mM glutamine containing antibiotics (penicillin/streptomycin) and grown at 37°C in a humidified incubator containing 10% CO_2. Glass coverslips or 12-well culture dishes were coated with 0.5 mg/ml PLL o/n at 37°C and 10% CO_2. Coverslips were then extensively washed 3 times with sterile ddH_2O prior to the addition of the cell suspension. Cortical neurons cultured in 12-well culture dishes at a density of 100,000-150,000 cells/well were used for biochemical analysis. Low density (about 5,000-10,000 cells/coverslip) hippocampal neurons on glass coverslips were used for immunocytochemistry. For Western blot analysis, neurons (10-14 DIV) were washed twice with ice-cold PBS and lysed for 30 min in IP buffer. Cell lysates were centrifuged at 20,000 x g and the pellet was discarded. The protein concentration was determined with the BCA™ protein assay kit and proteins were chloroform-methanol precipitated for subsequent separation by PAGE.

4.5.3 Transfection of adherent heterologous cells with Polyethylenimine or Lipfectamine™ 2000

HeLa and Cos7 cells were transfected with polyethylenimine (PEI) [257] or with Lipofectamin™ 2000 (Sigma-Aldrich, Buchs, Switzerland).

PEI (1 mg/ml) was dissolved in ddH_2O, adjusted to pH 7.0 with HCl and stored at -20°C. Cells were usually transfected at a cell confluency of about 60% and 80% for immunocytochemistry and for western blot analysis, respectively. DNA and PEI were separately diluted in 150 mM NaCl where a DNA:PEI ratio of 1:3-1:4 was used. The DNA and PEI solutions were combined, mixed and incubated for no longer than 10 min at RT. The final volume of the DNA/PEI mixture was 10% of the volume of the culture medium used for transfection. The mixture was distributed drop wise onto the cells and incubated at 37°C and 10% CO_2. After 4 h the medium was replaced by fresh medium and the cells were put back onto the incubator. Transfected cells were used for experiments 24 h - 48 h post-transfection.

For Lipofectamine™ 2000 (Invitrogen) transfection, cells were usually transfected at a cell confluency of about 80%-90%. DNA and Lipofectamine™ 2000 were separately diluted in Opti-MEM®

and incubated for 5 min at RT. The amount of DNA and Lipofectamine™ 2000 used for transfections was determined according to the instructor's manual. The diluted DNA and Lipofectamine™ 2000 solution were combined, mixed and incubated for at least 20 min at RT. The combined solution was distributed drop wise onto the cells and incubated at 37°C and 10% CO_2. After 4 h – 6 h the medium was aspirated, fresh medium was added and the cells were put back onto the incubator. Transfected cells were used for experiments 24 h - 48 h post-transfection.

4.5.4 Transfection of siRNA in adherent heterologous cells

For small interfering RNA knock-down experiments HeLa cells were plated out in 12-well plates and the cells were transfected at a cell confluency of about 40%-60% using Hiperfect transfection reagent (Qiagen) according to the manufacturer's recommendations. At least two siRNA targeting the same protein were pooled to reduce off-target effects [254]. 15 nM siRNA was diluted in 100 µl DMEM without serum and 6 µl Hiperfect was added. The mixture was incubated for 5-10 minutes at RT and then drop wise distributed to the cells. The same transfection protocol was repeated after 24 hours. After 48 hours the cells were lysed in IP buffer (1% TritonX-100, 150 mM NaCl, 5 mM EDTA, 1 mM Na_3VO_4, 5 mM NaF, 50 mM Tris-Cl, pH 8.0), supplemented with protease inhibitor cocktail (Roche). The protein concentration was determined with the BCA™ protein assay kit (Pierce, Rockford, USA). For Western analysis 30 µg proteins were chloroform-methanol precipitated and subsequently separated by PAGE.

4.5.5 Amaxa nucleofection

Amaxa nucleofection was used to efficiently transfect shRNA plasmid in high density or low density mouse neurons for immunocytochemistry or Western blot analysis. Cells were transfected with the Amaxa® Mouse Neuron Nucleofector® Kit purchased from Lonza (Visp, Switzerland) which requires the Amaxa Nucleofector® I device from Amaxa Biosystems (Geithersburg, USA). The nucleofection program was determined according the protocol previously described in [258].

For immunocytochemistry, hippocampal neurons were prepared as usual in 12-well plates with feeder glia cells and wax dots. Glass coverslips were coated with 0.5 mg/ml PLL o/n at 37°C and 10% CO_2. 500 µl and 3.5 ml DMEM/nucleofection were pre-equilibrated in 25 ml tubes. 15 ml falcon tubes containing 500,000 hippocampal neurons (500,000 cells/nucleofection) were centrifuged at 800 rpm for 5 minutes and the supernatant was aspirated. Cells were resuspended in 100 µl nucleofector solution (room temperature) and carefully mixed by pipetting 10 times up and down. 20 µg shRNA was added and the tubes were flicked several times. The cell/DNA suspension was transferred into cuvette and the program O-05 was selected. 500 µl of the pre-equilibrated media were added to the cell suspension and the cell suspension was transferred with the provided pipet to the 3.5 ml pre-equilibrated media and carefully mixed. 100 µl of the cell suspension (25,000 cells/coverslips) were distributed to each glass coverslip. After 2 hours the glass coverslips were transferred to neurobasal media supplemented with B27 and 5 mM glutamine containing antibiotics (penicillin/streptomycin) with feeder glia cells. After 48 hours Ara-C was added to suppress glia growth.

Amaxa nucleofection for Western blot analysis was similar to the protocol for immunocytochemistry analysis. 24-well plates were coated with 0.5 mg/ml PLL o/n at 37°C and 10% CO_2. 500 µl and 700 µl DMEM/nucleofection were pre-equilibrated in 25 ml tubes. 7 million cortical neurons were used for one transfection. Cells were centrifuged, resuspended in 100 µl nucleofector solution, mixed and 5 µg shRNA was added. The program X-03 was selected. 500 µl of the pre-equilibrated media were added to the cell suspension and the cell suspension was transferred with the

provided pipet to the 700 µl pre-equilibrated media and carefully mixed. 1 ml of the cell suspension was added to the wells of the 24-well dishes. After 2 hours the media was changed to neurobasal media, after 24 hours the media was replaced by new neurobasal media and the media change was repeated after 48 hours in addition of Ara-C.

4.5.6 Immunocytochemistry

For immunofluorescence analysis in heterologous cell lines, cells were washed with PBS and fixed with 4% paraformaldehyde (PFA, 4% sucrose in PBS pH 7.4) for 10 minutes at room temperature, with ice-cold methanol for 2 minutes or with PFA for 5 minutes and subsequently with methanol for 5 minutes. PFA fixation solution containing 0.01% (v/v) glutaraldehyde was used for visualization of the cytoskeleton. The cells were incubated in blocking solution (10% FCS, 0.1% glycine and 0.1% saponin in PBS) for 1 hour at room temperature. Staining with primary antibodies was performed in antibody incubation buffer (3% FCS in PBS containing 0.1% saponin) overnight at 4°C according to the dilutions indicated in section 4.1.2 and 4.1.3. Cells were washed 3 times for at least 10 minutes with 1 ml PBS at RT. The secondary antibody labelled with FITC, Cy3 or Cy5 fluorophores were used at a dilution of 1:400 and incubated with the cells for 1 hour at RT. Cells were then washed 3 times with PBS and mounted in Vectashield medium (Vector Laboratories Burlingame, Ontario, Canada).

Hippocampal neurons for immunocytochemistry were processed similar to heterologous cell lines. To stain two antibodies of the same species, we converted one antibody into another species. Usually, a rabbit antibody (R140 or αGaf1b B or C) was converted into a goat. In this case the neurons were first labelled with the first primary antibody (R140 or αGaf1b B or C), washed and incubated with the goat *anti*-rabbit Fab fragments (1:10) for 1 hour according to the manufacturer's manual (Jackson Immunoresearch, PA, USA). After extensive washing of 3 times for 20 minutes, cells were incubated with the second primary antibody for 2-4 hours, followed by incubation with *anti*-goat Cy3- and *anti*-rabbit FITC-conjugated secondary antibodies (Jackson Immunoresearch, PA, USA) for 1 hour. Two control experiments were performed to confirm the specificity of this approach. First, it was shown that FITC-conjugated *anti*-rabbit secondary antibody was not immunoreactive in the presence of primary rabbit antibody masked with the goat Fab fragments. This control served to define the confocal settings during imaging and image processing. Second, the staining patterns of double-labeled cultures were shown to be identical to immunostainings of the respective antibodies alone [259].

Images were captured with a confocal laser microscope (Leica confocal laser scanning microscope TCS-SP2 or TCS-SP5) controlled by Leica confocal software (Leica, Heerbrugg, Switzerland). Images were captured with a 63x or 40x oil immersion objectives with a numerical aperture (NA) of 1.4 or 1.25, respectively. For direct comparison of signal intensities between control and treated cells, exposure times, on- and offset values, averaging and pinhole settings were kept constant. Images were further processed and analysed by the following programs: Adobe Photoshop CS4 (Adobe Systems Inc., San Jose, CA, USA), ImageJ (http://rsb.info.nih.gov/ij/), Imaris 7 (Bitplane), Leica LAS AF Lite (Leica) or Metamorph (Molecular Devices).

Quantification of colocalizations were performed by ImageJ software with the RG2B colocalization plug-in. Images were imported into ImageJ, despeckled, auto-thresholded and the number of particles for each channel counted using the "analyse particles" function. The mask output files for the green and the red channels were imported into Adobe Photoshop CS4 and assembled as two-color RGB files. The RGB images were analysed using the "RG2B colocalization" plug-in in ImageJ. The number of colocalized particles was counted from the resulting colocalization output file

using the “analyse particles” function. The percentage of colocalization was calculated as the ratio of colocalized particles versus the total number of particles counted in the red or the green channel.

4.5.7 Starvation experiment

HeLa cells were washed three times with Hank’s Buffered Salt Solution supplemented with Mg^{2+} and Ca^{2+} ($HBSS^{++}$, 137 mM NaCl, 5.4 mM KCl, 0.25 mM $Na_2HPO_4 \cdot 2H_2O$, 0.44 mM KH_2PO_4, 1.3 mM $CaCl_2 \cdot H_2O$, 1.0 mM $MgSO_4 \cdot 7H_2O$, 4.2 mM $NaHCO_3$, pH 7.1) 18-26h post-transfection and starved for 2 hours in $HBSS^{++}$ at 37°C and 10% CO_2. Control cells for nonstarving condition were also washed with $HBSS^{++}$ and incubated for 2 hours in DMEM at 37°C and 10% CO_2. Cells were then subsequently fixed according to section 4.5.6 for immunocytochemistry or lysed in lP buffer for Western blot analysis. Analysis and quantification of autophagosomal structures were analysed in Imaris 7. Accumulated structures with a diameter higher than 2 µm were defined as autophagosomal structures and manually counted.

4.6 Biochemical methods

4.6.1 SDS-PAGE

The protein samples were boiled in reducing 1x Lämmli buffer (50% glycerol, 10.3% SDS, bromphenolblue, 100 mM DTT, 350 mM Tris-Cl, pH 6.8) for 5 minutes at 95°C. 7.5%, 10% or 12.5% polyacrylamide gels were cast according to Sambrook *et al.*, 1989. The samples were electrophoretically separated under constant current of 25 mA per gel in running buffer (25 mM Tris-Cl, 192 mM glycine and 0.1% SDS). Alternatively, protein samples were dissolved in Tricine-SDS or LDS sample buffers freshly supplemented with 100 mM DTT and purchased from Invitrogen. Samples were separated on either 10-20% NuPage Tricine, 4-12% NuPage Bis-Tris gradient gels or 12% NuPage Bis-Tris gels using Tricine-SDS or MOPS-SDS running buffers (Invitrogen, Basel, Switzerland). The protein samples were separated under constant current of 30 mA per gel.

4.6.2 Coomassie brilliant blue staining

The gels were incubated in Coomassie brilliant blue staining solution (0.25% Coomassie brilliant blue, 25% MeOH, 7.5% AcOH) for 30 minutes and destained in 15% AcOH for 1-2h. PVDF membranes were stained with Coomassie brilliant blue staining solution for 1 minute and washed with 10% MeOH/7% AcOH solution.

4.6.3 Silver staining

Gels were fixed for 30 minutes in fixation solution (10% AcOH, 30% EtOH). Proteins were reduced and cross-linked for 10 minutes in reducing and cross-linking solution (30% EtOH, 6.8% NaAc, 0.2% $Na_2S_2O_3 \cdot 5H_2O$, 0.25% glutaraldehyde) and subsequently washed 3 times in H_2O for 2 minutes. Gels were stained for 15 minutes in silver staining solution (0.2% $AgNO_3$, 0.02% formaldehyde), rinsed with H_2O and incubated in development solution (2.5% Na_2CO_3, 0.01% formaldehyde) until the staining appeared. The development was stopped by washing 3 times with H_2O and incubation for 5-10 minutes in 3% AcOH.

4.6.4 Immunoblotting

Proteins separated by SDS-PAGE were transferred onto PVDF membranes (Millipore, Zug, Switzerland) at 20V for one gel and 30V for 2 gels overnight or at 60V for 4 hours for self-casted gels in a Criterion™ blotter (Bio-Rad, Reinach, Switzerland) wet transfer chamber. NuPage gels were run at 23V overnight or at 60V for 4 hours. The transfer buffer contained 25 mM Tris-Cl, 192 mM glycine, pH 8.3 supplemented with 20% methanol. Prior to blotting, PVDF membranes were activated by incubation in MeOH for 15 sec. After Blotting, the membranes were blocked in methanol for 10 seconds and air dried for at least 15 min. The membranes were incubated with primary antibodies in TBS-Tween (TBST; 150 mM NaCl, 50 mM Tris-Cl, pH 7.5, 0.1% (v/v) Tween-20) containing 5% Roche Blocking reagent (Roche diagnostics, Mannheim, Germany) at a dilution indicated in section 4.1.2 and 4.1.3 for 2-4 hours at RT or o/n at 4°C. Blots were washed 3 times with TBST and then incubated in secondary antibodies conjugated to HRP (GαRPOD (1:20,000) and GαMPOD (1:20,000)) for 1 hour at RT. Membranes were developed with a chemiluminescent substrate Chemiglow (Witec AG, Littau, Switzerland) and imaged on a ChemiImager 5500 (Alpha Innotech Corporation, San Leandro, USA). In order to re-probe PVDF membranes, membranes were washed with H_2O, stripped with 0.5 M NaOH for 10 min, extensively washed with H_2O again and equilibrated with TBST prior to the addition of the next primary antibody.

4.6.7 GST Pull-down

GST-fusion proteins of RabGTPases, GABARAPL1, GABARAPL2 and LC3A were expressed and purified as described [205, 213].

GST-RabGTPase pull-downs were previously described in [205]. Proteins from the -80°C freezer or HeLa cell lysates were cleared for 15 minutes at 18,000 x g at 4°C prior to use. 50 µl of glutathione sepharose 4B (GE Healthcare, UK) bead suspension were washed twice with pull-down buffer 1 (1% TritonX-100, 4.5 mM $MgCl_2$, 150 mM NaCl, 8 mM EDTA, 50 mM Tris-Cl, pH 7.5). 5-10 µg GST and GST-fusion proteins were coupled to the beads by incubation 400 µl PD1 for 1 hour at 4°C under constant rotation. Beads were washed with ice-cold PD1 and equilibrated to PD2 (1% TritonX-100, 10 mM $MgCl_2$, 150 mM NaCl, 8 mM EDTA, 50 mM Tris-Cl, pH 7.5). 1 mM GTP or 1 mM GDP (Sigma-Aldrich, Buchs, Switzerland) was dissolved in 100 µl PD2 buffer and added to the beads for additional incubation of 30 minutes at 37°C. Beads were once washed with PD2 buffer, then 200 µg HeLa cell lysate in 500 µl PD2 buffer supplemented with 100 µM GTP or GDP was added to the beads and incubated for 1 hour at 4°C. Beads were washed with PD2 buffer, followed by protein elution from the beads with Lämmli buffer.

GST-GABARAPL1, GST-GABARAPL2 or GST-LC3A pull-downs were previously described in [213]. 10 µg purified GST-fusion proteins was incubated with 50 µl glutathione sepharose 4B bead suspension in 500 µl IP buffer (1% TritonX-100, 150 mM NaCl, 5 mM EDTA, 1 mM Na_3VO_4, 5 mM NaF, 50 mM Tris-Cl, pH 7.4) supplemented with protease inhibitor cocktail (Roche diagnostics, Mannheim, Germany) for 2 hours at 4°C at constant rotation. Beads were washed with IP buffer and then incubated with 400 µg (in a volume of 200 µl) HeLa cell lysates transfected with FLAG-Gaf-1b for 2 hours at 4°C. Beads were extensively washed with IP buffer and bound proteins were eluted with Lämmli buffer.

4.6.8 Immunoprecipitation

HeLa cells were cultivated in 6-well plates. Cells were transfected with PEI or Lipofectamine™ 2000 according to the description in section 4.5.3. Cells were washed with ice-cold PBS and lysed in IP buffer (1% TritonX-100, 150 mM NaCl, 5 mM EDTA, 1 mM Na_3VO_4, 5 mM NaF, 50 mM Tris-Cl, pH 7.4) supplemented with protease inhibitor cocktail. Cell lysate were centrifuged at 20,000 x g for 30 minutes. 100-200 µg protein was incubated with 3 µg affinity purified IgGs for 2 h at 4°C under end-over-end rotation. Protein complexes were captured by the addition of 17 µl protein A- or G-Sepharose beads (Amershan Bioscience, Uppsla, Sweden) for 1 hour at 4°C. Beads were washed four times with IP buffer and then proteins were eluted from the beads with Lämmli buffer. Immunoprecipitation of 14 DIV cortical neurons cultured at a density of 100,000 cells/cm^2 was performed the same way as for HeLa cells.

4.6.9 Subcellular fractionation

Differential centrifugation was used to produce the V1 membrane fraction which was previously described [201, 202]. P6 or P8 mouse brains were homogenized in homogenization buffer (HSE-buffer; 320 mM sucrose, 5 mM EDTA, 1 mM Na_3VO_4, 5 mM NaF, 10 mM HEPES, pH 7.4), supplemented with protease inhibitor cocktail, using a glassteflon homogenizer at 900 rpm with 12 strokes. The homogenate was centrifuged at 12,500 x g for 10 minutes (SS-34) to remove cell debris, nuclei, and mitochondria. The supernatant (S1) was kept and the pellet was resuspended and centrifuged for another 10 minutes at 12,000 x g. The post-nuclear supernatant (PNS) was obtained by combining the resulting supernatant (S1') with S1. Different centrifugation steps of the PNS were

performed to produce three vesicle fractions. First, V0 were achieved at 40,000 x g (Ti50, Beckman) after 40 minutes centrifugation. Second, V1 was obtained at 120,000 x g (Ti50, Beckman) after 1 hour centrifugation and third, V2 was achieved at 250,000 x g (Ti50, Beckman) after 1 hour centrifugation. The V0 fraction comprises of light mitochondria, ER- and Golgi-derived membranes, while V1 and V2 pellets contain heavy and light microsomal vesicles.

4.6.10 Immunoprecipitation from solubilized brain membrane fraction

In order to perform immunoprecipitation from V1 fractions, V1 pellets were resuspended and lysed for 30 minutes at 4°C in IP buffer supplemented with protease inhibitor cocktail. Cell lysates were centrifuged at 200,000 x g (TLA100.3, Beckman) for 30 minutes. V1 lysates were pre-cleared with 20 µl protein A-Sepharose beads for 1 hour at 4°C under constant rotation and the resulting supernatant (150-270 µg protein) was incubated with 4 µg affinity purified IgG for 2 hours at 4°C. Protein A-Sepharose beads were pre-blocked in IP buffer containing 5% ovalalbumine for 1 hour at 4°C. Antigen-antibody complexes were coupled to 10 µl pre-blocked protein A-Sepharose beads for 1h at 4°C. Beads were washed four times with IP buffer and proteins were eluted with Lämmli buffer.

4.6.11 Immunoisolation of vesicular organelles

The V1 pellet was washed in homogenization buffer (320 mM sucrose, 5 mM EDTA, 10 mM HEPES, pH 7.4) supplemented with protease inhibitor cocktail, centrifuged at 120,000 x g, resuspended in IB buffer (320 mM sucrose, 5 mM EDTA, PBS, pH 7.4) and stirred at 4°C for 1 h. 100 µl magnetic Dynabeads M-280 protein A (Invitrogen, Basel, Switzerland) were washed twice with wash buffer (0.1‰ BSA, PBS, pH 7.4), incubated with 20 µg IgG for 40 minutes at 4°C under constant rotation, washed twice in wash buffer, incubated once in elution buffer (0.1% TritonX-100, 20 mM Tris-Cl, pH 7.4) for 10 minutes and washed four times in IB buffer. V1 inputs were adjusted to 0.5 mg/ml with IP buffer and incubated with IgG-pre-coated beads for 2 hours at 4°C. Beads with immunoisolated organelles were washed 10 times with 1.5 ml IB buffer, once with 20 mM Tris-Cl, pH 7.4, and subsequently incubated in 50 µl elution buffer for 30 minutes at RT. For comparative Western blot analysis, 10 µg protein from input and 40 µl eluate were resolved on 4-12% NuPage Bis-Tris gels.

4.6.12 Biotinylation experiments

Biotinylation of surface proteins was carried out on cultured HeLa cells in 12-well plates. 48 hours prior the biotinylation experiment HeLa cells were transfected with 15 nM siRNA with Hiperfect twice according to section 4.5.4. For all reactions, Sulfo-NHS-SS-biotin (Pierce, Rockford, USA) was dissolved in $HBSS^{++}$ pH 8.0 at a concentration of 1 mg/ml just prior to use. Cells were washed twice with 2 ml $HBSS^{++}$ pH 8.0 and 0.5 ml biotin in $HBSS^{++}$ pH 8.0 was added for 15 minutes at 4°C. Residual biotin was quenched with 100 mM Tris-Cl pH 8.0 for 2 minutes at 4°C. Cells were immediately lysed in 310 µl IP buffer/well and the lysate was cleared by centrifugation at 20,000 x g and 4°C for 30 minutes. 250 µl lysate (~50 µg) was adjusted to 400 µl with IP buffer and added to 50 µl Streptavidin beads (Pierce, Rockford, USA) for 2 h at 4°C under constant rotation. Beads were washed three times with IP buffer. Bound proteins were eluted from the beads with Lämmli buffer. Unbound samples were precipitated by chloroform-methanol precipitation protocol, dissolved in Lämmli buffer and analysed by Western blot.

4.6.13 Yeast two-hybrid screen

The yeast two-hybrid screen using human Gaf-1b as bait was performed by Dualsystems Biotech AG (Zürich, Switzerland). Gaf-1b was PCR amplified and inserted into the bait vector pMyc-LexA. Human fetal brain cDNA library subcloned into the prey vector pACT2 was used as prey library. The bait construct was cotransformed with the prey library into the *S. cerevisae* strain NMY32 [MATa trp1 leu2 his3 ade2 LYS2::lexA-HIS3 ade2::lexA-ADE2 URA3::lexA-lacZ]. Transformants were selected on SD-trp-leu-his-ade medium supplemented with 5 mM 3-aminotriazole. Positive hits were tested for β-galactosidase activity using a pellet Xgal assay. Library plasmids from clones that showed β-galactosidase activity were isolated and characterized by sequencing. The identity of the cDNA inserts was determined by BLAST searches.

4.7 Statistics

Data was expressed as the mean from at least three independent experiments ± standard error mean (SEM). For expressing significant differences across two data sets or more than two data sets which are parametric, a two-tailed paired t-test or Annova with Post-hoc Tukey test was performed, respectively. For non-parametric data sets Mann-Whitney Rank Sum test or Kruskal-Wallis test was used (Sigmaplot 11.0, Systat Software, Inc.).

5. References

1. De Matteis, M.A. and A. Luini, *Exiting the Golgi complex.* Nat Rev Mol Cell Biol, 2008. **9**(4): p. 273-84.
2. Dancourt, J. and C. Barlowe, *Protein sorting receptors in the early secretory pathway.* Annu Rev Biochem, 2010. **79**: p. 777-802.
3. Bonifacino, J.S. and B.S. Glick, *The mechanisms of vesicle budding and fusion.* Cell, 2004. **116**(2): p. 153-66.
4. Szul, T. and E. Sztul, *COPII and COPI traffic at the ER-Golgi interface.* Physiology (Bethesda), 2011. **26**(5): p. 348-64.
5. Winder, S.J. and K.R. Ayscough, *Actin-binding proteins.* J Cell Sci, 2005. **118**(Pt 4): p. 651-4.
6. Anitei, M. and B. Hoflack, *Bridging membrane and cytoskeleton dynamics in the secretory and endocytic pathways.* Nat Cell Biol, 2012. **14**(1): p. 11-9.
7. Desai, A. and T.J. Mitchison, *Microtubule polymerization dynamics.* Annu Rev Cell Dev Biol, 1997. **13**: p. 83-117.
8. Dammermann, A., A. Desai, and K. Oegema, *The minus end in sight.* Curr Biol, 2003. **13**(15): p. R614-24.
9. Kirchhausen, T., *Three ways to make a vesicle.* Nat Rev Mol Cell Biol, 2000. **1**(3): p. 187-98.
10. Bonifacino, J.S. and J. Lippincott-Schwartz, *Coat proteins: shaping membrane transport.* Nat Rev Mol Cell Biol, 2003. **4**(5): p. 409-14.
11. Braakman, I. and N.J. Bulleid, *Protein folding and modification in the mammalian endoplasmic reticulum.* Annu Rev Biochem, 2011. **80**: p. 71-99.
12. Vedrenne, C. and H.P. Hauri, *Morphogenesis of the endoplasmic reticulum: beyond active membrane expansion.* Traffic, 2006. **7**(6): p. 639-46.
13. High, S., *Protein translocation at the membrane of the endoplasmic reticulum.* Prog Biophys Mol Biol, 1995. **63**(2): p. 233-50.
14. Zanetti, G., et al., *COPII and the regulation of protein sorting in mammals.* Nat Cell Biol, 2012. **14**(1): p. 20-8.
15. Schweizer, A., et al., *Identification, by a monoclonal antibody, of a 53-kD protein associated with a tubulo-vesicular compartment at the cis-side of the Golgi apparatus.* J Cell Biol, 1988. **107**(5): p. 1643-53.
16. Wada, I., et al., *SSR alpha and associated calnexin are major calcium binding proteins of the endoplasmic reticulum membrane.* J Biol Chem, 1991. **266**(29): p. 19599-610.
17. Singer-Kruger, B., et al., *Partial purification and characterization of early and late endosomes from yeast. Identification of four novel proteins.* J Biol Chem, 1993. **268**(19): p. 14376-86.
18. Belden, W.J. and C. Barlowe, *Erv25p, a component of COPII-coated vesicles, forms a complex with Emp24p that is required for efficient endoplasmic reticulum to Golgi transport.* J Biol Chem, 1996. **271**(43): p. 26939-46.
19. Appenzeller-Herzog, C. and H.P. Hauri, *The ER-Golgi intermediate compartment (ERGIC): in search of its identity and function.* J Cell Sci, 2006. **119**(Pt 11): p. 2173-83.
20. Wilson, C., et al., *The Golgi apparatus: an organelle with multiple complex functions.* Biochem J, 2011. **433**(1): p. 1-9.
21. Presley, J.F., et al., *ER-to-Golgi transport visualized in living cells.* Nature, 1997. **389**(6646): p. 81-5.
22. Lippincott-Schwartz, J., et al., *Kinesin is the motor for microtubule-mediated Golgi-to-ER membrane traffic.* J Cell Biol, 1995. **128**(3): p. 293-306.
23. Brownhill, K., L. Wood, and V. Allan, *Molecular motors and the Golgi complex: staying put and moving through.* Semin Cell Dev Biol, 2009. **20**(7): p. 784-92.
24. Ladinsky, M.S., et al., *Golgi structure in three dimensions: functional insights from the normal rat kidney cell.* J Cell Biol, 1999. **144**(6): p. 1135-49.
25. Horton, A.C. and M.D. Ehlers, *Dual modes of endoplasmic reticulum-to-Golgi transport in dendrites revealed by live-cell imaging.* J Neurosci, 2003. **23**(15): p. 6188-99.
26. Sengupta, D. and A.D. Linstedt, *Control of organelle size: the Golgi complex.* Annu Rev Cell Dev Biol, 2011. **27**: p. 57-77.
27. Emr, S., et al., *Journeys through the Golgi--taking stock in a new era.* J Cell Biol, 2009. **187**(4): p. 449-53.
28. Pelham, H.R., *Traffic through the Golgi apparatus.* J Cell Biol, 2001. **155**(7): p. 1099-101.
29. Griffiths, G., et al., *The dynamic nature of the Golgi complex.* J Cell Biol, 1989. **108**(2): p. 277-97.
30. Sandvig, K. and B. van Deurs, *Transport of protein toxins into cells: pathways used by ricin, cholera toxin and Shiga toxin.* FEBS Lett, 2002. **529**(1): p. 49-53.
31. Pfeffer, S.R., *Entry at the trans-Face of the Golgi.* Cold Spring Harb Perspect Biol, 2011. **3**(a005272).
32. Farquhar, M.G. and G.E. Palade, *The Golgi apparatus (complex)-(1954-1981)-from artifact to center stage.* J Cell Biol, 1981. **91**(3 Pt 2): p. 77s-103s.

33. Grant, B.D. and J.G. Donaldson, *Pathways and mechanisms of endocytic recycling.* Nat Rev Mol Cell Biol, 2009. **10**(9): p. 597-608.
34. Doherty, G.J. and H.T. McMahon, *Mechanisms of endocytosis.* Annu Rev Biochem, 2009. **78**: p. 857-902.
35. Hansen, C.G. and B.J. Nichols, *Exploring the caves: cavins, caveolins and caveolae.* Trends Cell Biol, 2010. **20**(4): p. 177-86.
36. Mayor, S. and R.E. Pagano, *Pathways of clathrin-independent endocytosis.* Nat Rev Mol Cell Biol, 2007. **8**(8): p. 603-12.
37. Morrissette, N., E. Gold, and A. Aderem, *The macrophage--a cell for all seasons.* Trends Cell Biol, 1999. **9**(5): p. 199-201.
38. Ungewickell, E. and D. Branton, *Assembly units of clathrin coats.* Nature, 1981. **289**(5796): p. 420-2.
39. McPherson, P.S., *Proteomic analysis of clathrin-coated vesicles.* Proteomics, 2010. **10**(22): p. 4025-39.
40. Ritter, B., et al., *Molecular mechanisms in clathrin-mediated membrane budding revealed through subcellular proteomics.* Biochem Soc Trans, 2004. **32**(Pt 5): p. 769-73.
41. Ford, M.G., et al., *Curvature of clathrin-coated pits driven by epsin.* Nature, 2002. **419**(6905): p. 361-6.
42. Hinshaw, J.E., *Dynamin and its role in membrane fission.* Annu Rev Cell Dev Biol, 2000. **16**: p. 483-519.
43. Wigge, P. and H.T. McMahon, *The amphiphysin family of proteins and their role in endocytosis at the synapse.* Trends Neurosci, 1998. **21**(8): p. 339-44.
44. Johnson, L.S., et al., *Endosome acidification and receptor trafficking: bafilomycin A1 slows receptor externalization by a mechanism involving the receptor's internalization motif.* Mol Biol Cell, 1993. **4**(12): p. 1251-66.
45. Waguri, S., et al., *Visualization of TGN to endosome trafficking through fluorescently labeled MPR and AP-1 in living cells.* Mol Biol Cell, 2003. **14**(1): p. 142-55.
46. van Weert, A.W., et al., *Transport from late endosomes to lysosomes, but not sorting of integral membrane proteins in endosomes, depends on the vacuolar proton pump.* J Cell Biol, 1995. **130**(4): p. 821-34.
47. Aniento, F., et al., *An endosomal beta COP is involved in the pH-dependent formation of transport vesicles destined for late endosomes.* J Cell Biol, 1996. **133**(1): p. 29-41.
48. Katzmann, D.J., G. Odorizzi, and S.D. Emr, *Receptor downregulation and multivesicular-body sorting.* Nat Rev Mol Cell Biol, 2002. **3**(12): p. 893-905.
49. Raiborg, C. and H. Stenmark, *The ESCRT machinery in endosomal sorting of ubiquitylated membrane proteins.* Nature, 2009. **458**(7237): p. 445-52.
50. Hurley, J.H. and P.I. Hanson, *Membrane budding and scission by the ESCRT machinery: it's all in the neck.* Nat Rev Mol Cell Biol, 2010. **11**(8): p. 556-66.
51. Mayor, S., J.F. Presley, and F.R. Maxfield, *Sorting of membrane components from endosomes and subsequent recycling to the cell surface occurs by a bulk flow process.* J Cell Biol, 1993. **121**(6): p. 1257-69.
52. Dunn, K.W., T.E. McGraw, and F.R. Maxfield, *Iterative fractionation of recycling receptors from lysosomally destined ligands in an early sorting endosome.* J Cell Biol, 1989. **109**(6 Pt 2): p. 3303-14.
53. Maxfield, F.R. and T.E. McGraw, *Endocytic recycling.* Nat Rev Mol Cell Biol, 2004. **5**(2): p. 121-32.
54. Hao, M. and F.R. Maxfield, *Characterization of rapid membrane internalization and recycling.* J Biol Chem, 2000. **275**(20): p. 15279-86.
55. Yamashiro, D.J., et al., *Segregation of transferrin to a mildly acidic (pH 6.5) para-Golgi compartment in the recycling pathway.* Cell, 1984. **37**(3): p. 789-800.
56. Hopkins, C.R., *Intracellular routing of transferrin and transferrin receptors in epidermoid carcinoma A431 cells.* Cell, 1983. **35**(1): p. 321-30.
57. Lin, S.X., G.G. Gundersen, and F.R. Maxfield, *Export from pericentriolar endocytic recycling compartment to cell surface depends on stable, detyrosinated (glu) microtubules and kinesin.* Mol Biol Cell, 2002. **13**(1): p. 96-109.
58. Lin, S.X., et al., *Rme-1 regulates the distribution and function of the endocytic recycling compartment in mammalian cells.* Nat Cell Biol, 2001. **3**(6): p. 567-72.
59. Ghosh, R.N., et al., *An endocytosed TGN38 chimeric protein is delivered to the TGN after trafficking through the endocytic recycling compartment in CHO cells.* J Cell Biol, 1998. **142**(4): p. 923-36.
60. Dotti, C.G. and K. Simons, *Polarized sorting of viral glycoproteins to the axon and dendrites of hippocampal neurons in culture.* Cell, 1990. **62**(1): p. 63-72.
61. Sampo, B., et al., *Two distinct mechanisms target membrane proteins to the axonal surface.* Neuron, 2003. **37**(4): p. 611-24.
62. Prekeris, R., D.L. Foletti, and R.H. Scheller, *Dynamics of tubulovesicular recycling endosomes in hippocampal neurons.* J Neurosci, 1999. **19**(23): p. 10324-37.
63. Horton, A.C. and M.D. Ehlers, *Neuronal polarity and trafficking.* Neuron, 2003. **40**(2): p. 277-95.

64. Foletti, D.L., R. Prekeris, and R.H. Scheller, *Generation and maintenance of neuronal polarity: mechanisms of transport and targeting.* Neuron, 1999. **23**(4): p. 641-4.
65. da Silva, J.S. and C.G. Dotti, *Breaking the neuronal sphere: regulation of the actin cytoskeleton in neuritogenesis.* Nat Rev Neurosci, 2002. **3**(9): p. 694-704.
66. Fukata, Y., T. Kimura, and K. Kaibuchi, *Axon specification in hippocampal neurons.* Neurosci Res, 2002. **43**(4): p. 305-15.
67. Dotti, C.G., C.A. Sullivan, and G.A. Banker, *The establishment of polarity by hippocampal neurons in culture.* J Neurosci, 1988. **8**(4): p. 1454-68.
68. Goslin, K. and G. Banker, *Experimental observations on the development of polarity by hippocampal neurons in culture.* J Cell Biol, 1989. **108**(4): p. 1507-16.
69. Goslin, K., et al., *Development of neuronal polarity: GAP-43 distinguishes axonal from dendritic growth cones.* Nature, 1988. **336**(6200): p. 672-4.
70. Baas, P.W., M.M. Black, and G.A. Banker, *Changes in microtubule polarity orientation during the development of hippocampal neurons in culture.* J Cell Biol, 1989. **109**(6 Pt 1): p. 3085-94.
71. Etienne-Manneville, S. and A. Hall, *Rho GTPases in cell biology.* Nature, 2002. **420**(6916): p. 629-35.
72. Nobes, C.D. and A. Hall, *Rho GTPases control polarity, protrusion, and adhesion during cell movement.* J Cell Biol, 1999. **144**(6): p. 1235-44.
73. Luo, L., *Actin cytoskeleton regulation in neuronal morphogenesis and structural plasticity.* Annu Rev Cell Dev Biol, 2002. **18**: p. 601-35.
74. Kreitzer, G., et al., *Three-dimensional analysis of post-Golgi carrier exocytosis in epithelial cells.* Nat Cell Biol, 2003. **5**(2): p. 126-36.
75. Bacallao, R., et al., *The subcellular organization of Madin-Darby canine kidney cells during the formation of a polarized epithelium.* J Cell Biol, 1989. **109**(6 Pt 1): p. 2817-32.
76. Wandinger-Ness, A., et al., *Distinct transport vesicles mediate the delivery of plasma membrane proteins to the apical and basolateral domains of MDCK cells.* J Cell Biol, 1990. **111**(3): p. 987-1000.
77. Tuma, P.L. and A.L. Hubbard, *Transcytosis: crossing cellular barriers.* Physiol Rev, 2003. **83**(3): p. 871-932.
78. Colman, D.R., *Neuronal polarity and the epithelial metaphor.* Neuron, 1999. **23**(4): p. 649-51.
79. Wisco, D., et al., *Uncovering multiple axonal targeting pathways in hippocampal neurons.* J Cell Biol, 2003. **162**(7): p. 1317-28.
80. Garrido, J.J., et al., *Identification of an axonal determinant in the C-terminus of the sodium channel Na(v)1.2.* Embo J, 2001. **20**(21): p. 5950-61.
81. Klionsky, D.J., *The molecular machinery of autophagy: unanswered questions.* J Cell Sci, 2005. **118**(Pt 1): p. 7-18.
82. Massey, A.C., C. Zhang, and A.M. Cuervo, *Chaperone-mediated autophagy in aging and disease.* Curr Top Dev Biol, 2006. **73**: p. 205-35.
83. Mizushima, N., T. Yoshimori, and B. Levine, *Methods in mammalian autophagy research.* Cell, 2010. **140**(3): p. 313-26.
84. Xie, Z. and D.J. Klionsky, *Autophagosome formation: core machinery and adaptations.* Nat Cell Biol, 2007. **9**(10): p. 1102-9.
85. Levine, B. and G. Kroemer, *Autophagy in the pathogenesis of disease.* Cell, 2008. **132**(1): p. 27-42.
86. Cecconi, F. and B. Levine, *The role of autophagy in mammalian development: cell makeover rather than cell death.* Dev Cell, 2008. **15**(3): p. 344-57.
87. Fader, C.M. and M.I. Colombo, *Autophagy and multivesicular bodies: two closely related partners.* Cell Death Differ, 2009. **16**(1): p. 70-8.
88. Rubinsztein, D.C., *The roles of intracellular protein-degradation pathways in neurodegeneration.* Nature, 2006. **443**(7113): p. 780-6.
89. Baehrecke, E.H., *Autophagic programmed cell death in Drosophila.* Cell Death Differ, 2003. **10**(9): p. 940-5.
90. Clarke, P.G., *Developmental cell death: morphological diversity and multiple mechanisms.* Anat Embryol (Berl), 1990. **181**(3): p. 195-213.
91. Mehrpour, M., et al., *Autophagy in health and disease. 1. Regulation and significance of autophagy: an overview.* Am J Physiol Cell Physiol, 2010. **298**(4): p. C776-85.
92. He, C. and D.J. Klionsky, *Regulation mechanisms and signaling pathways of autophagy.* Annu Rev Genet, 2009. **43**: p. 67-93.
93. Juhasz, G. and T.P. Neufeld, *Autophagy: a forty-year search for a missing membrane source.* PLoS Biol, 2006. **4**(2): p. e36.
94. Kabeya, Y., et al., *LC3, a mammalian homologue of yeast Apg8p, is localized in autophagosome membranes after processing.* EMBO J, 2000. **19**(21): p. 5720-8.

95. Mann, S.S. and J.A. Hammarback, *Molecular characterization of light chain 3. A microtubule binding subunit of MAP1A and MAP1B.* J Biol Chem, 1994. **269**(15): p. 11492-7.
96. Monastyrska, I., et al., *Multiple roles of the cytoskeleton in autophagy.* Biol Rev Camb Philos Soc, 2009. **84**(3): p. 431-48.
97. Tanida, I., et al., *HsAtg4B/HsApg4B/autophagin-1 cleaves the carboxyl termini of three human Atg8 homologues and delipidates microtubule-associated protein light chain 3- and GABAA receptor-associated protein-phospholipid conjugates.* J Biol Chem, 2004. **279**(35): p. 36268-76.
98. Kabeya, Y., et al., *LC3, GABARAP and GATE16 localize to autophagosomal membrane depending on form-II formation.* J Cell Sci, 2004. **117**(Pt 13): p. 2805-12.
99. Hanada, T., et al., *The Atg12-Atg5 conjugate has a novel E3-like activity for protein lipidation in autophagy.* J Biol Chem, 2007. **282**(52): p. 37298-302.
100. Fujita, N., et al., *The Atg16L complex specifies the site of LC3 lipidation for membrane biogenesis in autophagy.* Mol Biol Cell, 2008. **19**(5): p. 2092-100.
101. Berg, T.O., et al., *Isolation and characterization of rat liver amphisomes. Evidence for fusion of autophagosomes with both early and late endosomes.* J Biol Chem, 1998. **273**(34): p. 21883-92.
102. Eskelinen, E.L., *Maturation of autophagic vacuoles in Mammalian cells.* Autophagy, 2005. **1**(1): p. 1-10.
103. Ravikumar, B., et al., *Rab5 modulates aggregation and toxicity of mutant huntingtin through macroautophagy in cell and fly models of Huntington disease.* J Cell Sci, 2008. **121**(Pt 10): p. 1649-60.
104. Gutierrez, M.G., et al., *Rab7 is required for the normal progression of the autophagic pathway in mammalian cells.* J Cell Sci, 2004. **117**(Pt 13): p. 2687-97.
105. Jager, S., et al., *Role for Rab7 in maturation of late autophagic vacuoles.* J Cell Sci, 2004. **117**(Pt 20): p. 4837-48.
106. Fader, C.M., et al., *Induction of autophagy promotes fusion of multivesicular bodies with autophagic vacuoles in k562 cells.* Traffic, 2008. **9**(2): p. 230-50.
107. Jahn, R. and R.H. Scheller, *SNAREs--engines for membrane fusion.* Nat Rev Mol Cell Biol, 2006. **7**(9): p. 631-43.
108. Hong, W., *SNAREs and traffic.* Biochim Biophys Acta, 2005. **1744**(3): p. 493-517.
109. Hong, W., *SNAREs and traffic.* Biochim Biophys Acta, 2005. **1744**(2): p. 120-44.
110. Fasshauer, D., *Structural insights into the SNARE mechanism.* Biochim Biophys Acta, 2003. **1641**(2-3): p. 87-97.
111. Chen, Y.A. and R.H. Scheller, *SNARE-mediated membrane fusion.* Nat Rev Mol Cell Biol, 2001. **2**(2): p. 98-106.
112. Fasshauer, D., et al., *Conserved structural features of the synaptic fusion complex: SNARE proteins reclassified as Q- and R-SNAREs.* Proc Natl Acad Sci U S A, 1998. **95**(26): p. 15781-6.
113. Hanson, P.I., et al., *Structure and conformational changes in NSF and its membrane receptor complexes visualized by quick-freeze/deep-etch electron microscopy.* Cell, 1997. **90**(3): p. 523-35.
114. Weber, T., et al., *SNAREpins: minimal machinery for membrane fusion.* Cell, 1998. **92**(6): p. 759-72.
115. Rice, L.M. and A.T. Brunger, *Crystal structure of the vesicular transport protein Sec17: implications for SNAP function in SNARE complex disassembly.* Mol Cell, 1999. **4**(1): p. 85-95.
116. Mayer, A., W. Wickner, and A. Haas, *Sec18p (NSF)-driven release of Sec17p (alpha-SNAP) can precede docking and fusion of yeast vacuoles.* Cell, 1996. **85**(1): p. 83-94.
117. Sollner, T., et al., *SNAP receptors implicated in vesicle targeting and fusion.* Nature, 1993. **362**(6418): p. 318-24.
118. Sutton, R.B., et al., *Crystal structure of a SNARE complex involved in synaptic exocytosis at 2.4 A resolution.* Nature, 1998. **395**(6700): p. 347-53.
119. Poirier, M.A., et al., *The synaptic SNARE complex is a parallel four-stranded helical bundle.* Nat Struct Biol, 1998. **5**(9): p. 765-9.
120. Prekeris, R., et al., *Syntaxin 13 mediates cycling of plasma membrane proteins via tubulovesicular recycling endosomes.* J Cell Biol, 1998. **143**(4): p. 957-71.
121. McBride, H.M., et al., *Oligomeric complexes link Rab5 effectors with NSF and drive membrane fusion via interactions between EEA1 and syntaxin 13.* Cell, 1999. **98**(3): p. 377-86.
122. Park, M., et al., *Postnatal development of the dopaminergic neurons in the rat mesencephalon.* Brain Dev, 2000. **22 Suppl 1**: p. S38-44.
123. Park, M., et al., *Plasticity-induced growth of dendritic spines by exocytic trafficking from recycling endosomes.* Neuron, 2006. **52**(5): p. 817-30.
124. Park, M., et al., *Recycling endosomes supply AMPA receptors for LTP.* Science, 2004. **305**(5692): p. 1972-5.
125. Hirling, H., et al., *Syntaxin 13 is a developmentally regulated SNARE involved in neurite outgrowth and endosomal trafficking.* Eur J Neurosci, 2000. **12**(6): p. 1913-23.
126. Zerial, M. and H. McBride, *Rab proteins as membrane organizers.* Nat Rev Mol Cell Biol, 2001. **2**(2): p. 107-17.
127. Stenmark, H. and V.M. Olkkonen, *The Rab GTPase family.* Genome Biol, 2001. **2**(5): p. REVIEWS3007.

128. Leung, K.F., et al., *Rab GTPases containing a CAAX motif are processed post-geranylgeranylation by proteolysis and methylation.* J Biol Chem, 2007. **282**(2): p. 1487-97.
129. Prekeris, R., *Rabs, Rips, FIPs, and endocytic membrane traffic.* ScientificWorldJournal, 2003. **3**: p. 870-80.
130. Riederer, M.A., et al., *Lysosome biogenesis requires Rab9 function and receptor recycling from endosomes to the trans-Golgi network.* J Cell Biol, 1994. **125**(3): p. 573-82.
131. Echard, A., et al., *Interaction of a Golgi-associated kinesin-like protein with Rab6.* Science, 1998. **279**(5350): p. 580-5.
132. Fukuda, M. and T.S. Kuroda, *Slac2-c (synaptotagmin-like protein homologue lacking C2 domains-c), a novel linker protein that interacts with Rab27, myosin Va/VIIa, and actin.* J Biol Chem, 2002. **277**(45): p. 43096-103.
133. Sztul, E. and V. Lupashin, *Role of tethering factors in secretory membrane traffic.* Am J Physiol Cell Physiol, 2006. **290**(1): p. C11-26.
134. Hill, E., M. Clarke, and F.A. Barr, *The Rab6-binding kinesin, Rab6-KIFL, is required for cytokinesis.* Embo J, 2000. **19**(21): p. 5711-9.
135. Gorvel, J.P., et al., *rab5 controls early endosome fusion in vitro.* Cell, 1991. **64**(5): p. 915-25.
136. Bucci, C., et al., *The small GTPase rab5 functions as a regulatory factor in the early endocytic pathway.* Cell, 1992. **70**(5): p. 715-28.
137. Stenmark, H., *Rab GTPases as coordinators of vesicle traffic.* Nat Rev Mol Cell Biol, 2009. **10**(8): p. 513-25.
138. Sonnichsen, B., et al., *Distinct membrane domains on endosomes in the recycling pathway visualized by multicolor imaging of Rab4, Rab5, and Rab11.* J Cell Biol, 2000. **149**(4): p. 901-14.
139. Barbero, P., L. Bittova, and S.R. Pfeffer, *Visualization of Rab9-mediated vesicle transport from endosomes to the trans-Golgi in living cells.* J Cell Biol, 2002. **156**(3): p. 511-8.
140. Ullrich, O., et al., *Rab11 regulates recycling through the pericentriolar recycling endosome.* J Cell Biol, 1996. **135**(4): p. 913-24.
141. Wang, X., et al., *Regulation of vesicle trafficking in madin-darby canine kidney cells by Rab11a and Rab25.* J Biol Chem, 2000. **275**(37): p. 29138-46.
142. Goldenring, J.R., et al., *Enrichment of rab11, a small GTP-binding protein, in gastric parietal cells.* Am J Physiol, 1994. **267**(2 Pt 1): p. G187-94.
143. Wilcke, M., et al., *Rab11 regulates the compartmentalization of early endosomes required for efficient transport from early endosomes to the trans-golgi network.* J Cell Biol, 2000. **151**(6): p. 1207-20.
144. Ren, M., et al., *Hydrolysis of GTP on rab11 is required for the direct delivery of transferrin from the pericentriolar recycling compartment to the cell surface but not from sorting endosomes.* Proc Natl Acad Sci U S A, 1998. **95**(11): p. 6187-92.
145. Urbe, S., et al., *Rab11, a small GTPase associated with both constitutive and regulated secretory pathways in PC12 cells.* FEBS Lett, 1993. **334**(2): p. 175-82.
146. Satoh, A.K., et al., *Rab11 mediates post-Golgi trafficking of rhodopsin to the photosensitive apical membrane of Drosophila photoreceptors.* Development, 2005. **132**(7): p. 1487-97.
147. Lock, J.G. and J.L. Stow, *Rab11 in recycling endosomes regulates the sorting and basolateral transport of E-cadherin.* Mol Biol Cell, 2005. **16**(4): p. 1744-55.
148. Mammoto, A., et al., *Rab11BP/Rabphilin-11, a downstream target of rab11 small G protein implicated in vesicle recycling.* J Biol Chem, 1999. **274**(36): p. 25517-24.
149. Lapierre, L.A., et al., *Myosin vb is associated with plasma membrane recycling systems.* Mol Biol Cell, 2001. **12**(6): p. 1843-57.
150. Zhang, X.M., et al., *Sec15 is an effector for the Rab11 GTPase in mammalian cells.* J Biol Chem, 2004. **279**(41): p. 43027-34.
151. Jagoe, W.N., et al., *Crystal structure of rab11 in complex with rab11 family interacting protein 2.* Structure, 2006. **14**(8): p. 1273-83.
152. Wallace, D.M., et al., *The novel Rab11-FIP/Rip/RCP family of proteins displays extensive homo- and hetero-interacting abilities.* Biochem Biophys Res Commun, 2002. **292**(4): p. 909-15.
153. Lindsay, A.J. and M.W. McCaffrey, *The C2 domains of the class I Rab11 family of interacting proteins target recycling vesicles to the plasma membrane.* J Cell Sci, 2004. **117**(Pt 19): p. 4365-75.
154. Horgan, C.P. and M.W. McCaffrey, *The dynamic Rab11-FIPs.* Biochem Soc Trans, 2009. **37**(Pt 5): p. 1032-6.
155. Meyers, J.M. and R. Prekeris, *Formation of mutually exclusive Rab11 complexes with members of the family of Rab11-interacting proteins regulates Rab11 endocytic targeting and function.* J Biol Chem, 2002. **277**(50): p. 49003-10.
156. Lindsay, A.J., et al., *Rab coupling protein (RCP), a novel Rab4 and Rab11 effector protein.* J Biol Chem, 2002. **277**(14): p. 12190-9.

157. Peden, A.A., et al., *The RCP-Rab11 complex regulates endocytic protein sorting.* Mol Biol Cell, 2004. **15**(8): p. 3530-41.
158. Caswell, P.T., et al., *Rab-coupling protein coordinates recycling of alpha5beta1 integrin and EGFR1 to promote cell migration in 3D microenvironments.* J Cell Biol, 2008. **183**(1): p. 143-55.
159. Nedvetsky, P.I., et al., *A Role of myosin Vb and Rab11-FIP2 in the aquaporin-2 shuttle.* Traffic, 2007. **8**(2): p. 110-23.
160. Fan, G.H., et al., *Rab11-family interacting protein 2 and myosin Vb are required for CXCR2 recycling and receptor-mediated chemotaxis.* Mol Biol Cell, 2004. **15**(5): p. 2456-69.
161. Wang, Z., et al., *Myosin Vb mobilizes recycling endosomes and AMPA receptors for postsynaptic plasticity.* Cell, 2008. **135**(3): p. 535-48.
162. Hales, C.M., J.P. Vaerman, and J.R. Goldenring, *Rab11 family interacting protein 2 associates with Myosin Vb and regulates plasma membrane recycling.* J Biol Chem, 2002. **277**(52): p. 50415-21.
163. Schonteich, E., et al., *The Rip11/Rab11-FIP5 and kinesin II complex regulates endocytic protein recycling.* J Cell Sci, 2008. **121**(Pt 22): p. 3824-33.
164. Welsh, G.I., et al., *Rip11 is a Rab11- and AS160-RabGAP-binding protein required for insulin-stimulated glucose uptake in adipocytes.* J Cell Sci, 2007. **120**(Pt 23): p. 4197-208.
165. Prekeris, R., J. Klumperman, and R.H. Scheller, *A Rab11/Rip11 protein complex regulates apical membrane trafficking via recycling endosomes.* Mol Cell, 2000. **6**(6): p. 1437-48.
166. Chen, D., et al., *Gaf-1, a gamma -SNAP-binding protein associated with the mitochondria.* J Biol Chem, 2001. **276**(16): p. 13127-35.
167. Bitto, E., et al., *Structure and dynamics of gamma-SNAP: insight into flexibility of proteins from the SNAP family.* Proteins, 2008. **70**(1): p. 93-104.
168. Kawase, K., et al., *Gaf-1b is an alternative splice variant of Gaf-1/Rip11.* Biochem Biophys Res Commun, 2003. **303**(4): p. 1042-6.
169. Vogt, L., et al., *Calsyntenin-1, a proteolytically processed postsynaptic membrane protein with a cytoplasmic calcium-binding domain.* Mol Cell Neurosci, 2001. **17**(1): p. 151-66.
170. Hintsch, G., et al., *The calsyntenins--a family of postsynaptic membrane proteins with distinct neuronal expression patterns.* Mol Cell Neurosci, 2002. **21**(3): p. 393-409.
171. Konecna, A., et al., *Calsyntenin-1 docks vesicular cargo to kinesin-1.* Mol Biol Cell, 2006. **17**(8): p. 3651-63.
172. Araki, Y., et al., *Novel cadherin-related membrane proteins, Alcadeins, enhance the X11-like protein-mediated stabilization of amyloid beta-protein precursor metabolism.* J Biol Chem, 2003. **278**(49): p. 49448-58.
173. Hata, S., et al., *Alcadein cleavages by amyloid beta-precursor protein (APP) alpha- and gamma-secretases generate small peptides, p3-Alcs, indicating Alzheimer disease-related gamma-secretase dysfunction.* J Biol Chem, 2009. **284**(52): p. 36024-33.
174. Araki, Y., et al., *Coordinated metabolism of Alcadein and amyloid beta-protein precursor regulates FE65-dependent gene transactivation.* J Biol Chem, 2004. **279**(23): p. 24343-54.
175. Araki, Y., et al., *The novel cargo Alcadein induces vesicle association of kinesin-1 motor components and activates axonal transport.* Embo J, 2007. **26**(6): p. 1475-86.
176. Ludwig, A., et al., *Calsyntenins mediate TGN exit of APP in a kinesin-1-dependent manner.* Traffic, 2009. **10**(5): p. 572-89.
177. Steuble, M., et al., *Calsyntenin-1 vesicles shelter APP from proteolytic processing during anterograde axonal transport.* Biology Open, 2012.
178. Steuble, M., et al., *Molecular characterization of a trafficking organelle: dissecting the axonal paths of calsyntenin-1 transport vesicles.* Proteomics, 2010. **10**(21): p. 3775-88.
179. Kirisako, T., et al., *Formation process of autophagosome is traced with Apg8/Aut7p in yeast.* J Cell Biol, 1999. **147**(2): p. 435-46.
180. Xin, Y., et al., *Cloning, expression patterns, and chromosome localization of three human and two mouse homologues of GABA(A) receptor-associated protein.* Genomics, 2001. **74**(3): p. 408-13.
181. He, H., et al., *Post-translational modifications of three members of the human MAP1LC3 family and detection of a novel type of modification for MAP1LC3B.* J Biol Chem, 2003. **278**(31): p. 29278-87.
182. Mansuy-Schlick, V., et al., *Specific distribution of gabarap, gec1/gabarap Like 1, gate16/gabarap Like 2, lc3 messenger RNAs in rat brain areas by quantitative real-time PCR.* Brain Res, 2006. **1073-1074**: p. 83-7.
183. Wang, H., et al., *GABA(A)-receptor-associated protein links GABA(A) receptors and the cytoskeleton.* Nature, 1999. **397**(6714): p. 69-72.
184. Mansuy, V., et al., *GEC1, a protein related to GABARAP, interacts with tubulin and GABA(A) receptor.* Biochem Biophys Res Commun, 2004. **325**(2): p. 639-48.

185. Jacob, T.C., S.J. Moss, and R. Jurd, *GABA(A) receptor trafficking and its role in the dynamic modulation of neuronal inhibition.* Nat Rev Neurosci, 2008. **9**(5): p. 331-43.
186. Mohrluder, J., M. Schwarten, and D. Willbold, *Structure and potential function of gamma-aminobutyrate type A receptor-associated protein.* FEBS J, 2009. **276**(18): p. 4989-5005.
187. Paz, Y., Z. Elazar, and D. Fass, *Structure of GATE-16, membrane transport modulator and mammalian ortholog of autophagocytosis factor Aut7p.* J Biol Chem, 2000. **275**(33): p. 25445-50.
188. Amar, N., et al., *Two newly identified sites in the ubiquitin-like protein Atg8 are essential for autophagy.* EMBO Rep, 2006. **7**(6): p. 635-42.
189. Weiergraber, O.H., et al., *Ligand binding mode of GABAA receptor-associated protein.* J Mol Biol, 2008. **381**(5): p. 1320-31.
190. Chen, C., et al., *GEC1 interacts with the kappa opioid receptor and enhances expression of the receptor.* J Biol Chem, 2006. **281**(12): p. 7983-93.
191. Chen, C., et al., *Effects of C-terminal modifications of GEC1 protein and gamma-aminobutyric acid type A (GABA(A)) receptor-associated protein (GABARAP), two microtubule-associated proteins, on kappa opioid receptor expression.* J Biol Chem, 2011. **286**(17): p. 15106-15.
192. Chakrama, F.Z., et al., *GABARAPL1 (GEC1) associates with autophagic vesicles.* Autophagy, 2010. **6**(4).
193. Marino, G., et al., *Autophagy is essential for mouse sense of balance.* J Clin Invest, 2010. **120**(7): p. 2331-44.
194. Legesse-Miller, A., et al., *Isolation and characterization of a novel low molecular weight protein involved in intra-Golgi traffic.* J Biol Chem, 1998. **273**(5): p. 3105-9.
195. Sagiv, Y., et al., *GATE-16, a membrane transport modulator, interacts with NSF and the Golgi v-SNARE GOS-28.* EMBO J, 2000. **19**(7): p. 1494-504.
196. Elazar, Z., R. Scherz-Shouval, and H. Shorer, *Involvement of LMA1 and GATE-16 family members in intracellular membrane dynamics.* Biochim Biophys Acta, 2003. **1641**(2-3): p. 145-56.
197. Muller, J.M., et al., *Sequential SNARE disassembly and GATE-16-GOS-28 complex assembly mediated by distinct NSF activities drives Golgi membrane fusion.* J Cell Biol, 2002. **157**(7): p. 1161-73.
198. Nakatogawa, H., K. Oh-oka, and Y. Ohsumi, *Lipidation of Atg8: how is substrate specificity determined without a canonical E3 enzyme?* Autophagy, 2008. **4**(7): p. 911-3.
199. Weidberg, H., et al., *LC3 and GATE-16/GABARAP subfamilies are both essential yet act differently in autophagosome biogenesis.* EMBO J, 2010. **29**(11): p. 1792-802.
200. Steuble, M., et al., *Calsyntenin-1 and APP specify distinct endosomal compartments in the axonal growth cone.* Manuscript in preparation, 2008.
201. Morfini, G., et al., *Approaches to study interactions between kinesin motors and membranes.* Methods Mol Biol, 2001. **164**: p. 147-62.
202. Morfini, G., et al., *Regulation of kinesin: implications for neuronal development.* Dev Neurosci, 2001. **23**(4-5): p. 364-76.
203. Diep, T.M., *The Rab11-binding protein Gaf-1b is a novel interaction partner of calsyntenin-1.* Master Thesis (University of Zurich), 2007.
204. Lindsay, A.J. and M.W. McCaffrey, *Rab11-FIP2 functions in transferrin recycling and associates with endosomal membranes via its COOH-terminal domain.* J Biol Chem, 2002. **277**(30): p. 27193-9.
205. Serricchio, M., *Gaf-1b, a new member of the Rab11/25 interacting protein family, form a tripartite complex with calsyntenin-1 and Rab11.* Master Thesis (University of Zurich), 2008.
206. Hales, C.M., et al., *Identification and characterization of a family of Rab11-interacting proteins.* J Biol Chem, 2001. **276**(42): p. 39067-75.
207. de Figueiredo, P., et al., *Inhibition of transferrin recycling and endosome tubulation by phospholipase A2 antagonists.* J Biol Chem, 2001. **276**(50): p. 47361-70.
208. Hopkins, C.R., et al., *In migrating fibroblasts, recycling receptors are concentrated in narrow tubules in the pericentriolar area, and then routed to the plasma membrane of the leading lamella.* J Cell Biol, 1994. **125**(6): p. 1265-74.
209. Chardin, P., et al., *The mammalian G protein rhoC is ADP-ribosylated by Clostridium botulinum exoenzyme C3 and affects actin microfilaments in Vero cells.* EMBO J, 1989. **8**(4): p. 1087-92.
210. Paterson, H.F., et al., *Microinjection of recombinant p21rho induces rapid changes in cell morphology.* J Cell Biol, 1990. **111**(3): p. 1001-7.
211. Ueda, H., et al., *G protein betagamma subunits induce stress fiber formation and focal adhesion assembly in a Rho-dependent manner in HeLa cells.* J Biol Chem, 2000. **275**(3): p. 2098-102.
212. Künzli, T., *Interaction study of the adaptor protein Gaf-1b and production of replicant-deficient shRNA expressing Adenovirus.* Master Thesis (University of Zurich), 2010.

213. Redli, P., *GABARAPL1 and GABARAPL2 are two novel interaction partners of Gaf-1b.* Master Thesis (University of Zurich), 2010.
214. Sengupta, A., J.D. Molkentin, and K.E. Yutzey, *FoxO transcription factors promote autophagy in cardiomyocytes.* J Biol Chem, 2009. **284**(41): p. 28319-31.
215. Cann, G.M., et al., *Developmental expression of LC3alpha and beta: absence of fibronectin or autophagy phenotype in LC3beta knockout mice.* Dev Dyn, 2008. **237**(1): p. 187-95.
216. French, A.P., et al., *Colocalization of fluorescent markers in confocal microscope images of plant cells.* Nat Protoc, 2008. **3**(4): p. 619-28.
217. Bottger, G., B. Nagelkerken, and P. van der Sluijs, *Rab4 and Rab7 define distinct nonoverlapping endosomal compartments.* J Biol Chem, 1996. **271**(46): p. 29191-7.
218. Rohrer, J., et al., *The targeting of Lamp1 to lysosomes is dependent on the spacing of its cytoplasmic tail tyrosine sorting motif relative to the membrane.* J Cell Biol, 1996. **132**(4): p. 565-76.
219. Eskelinen, E.L., *Roles of LAMP-1 and LAMP-2 in lysosome biogenesis and autophagy.* Mol Aspects Med, 2006. **27**(5-6): p. 495-502.
220. Crump, C.M., et al., *PACS-1 binding to adaptors is required for acidic cluster motif-mediated protein traffic.* EMBO J, 2001. **20**(9): p. 2191-201.
221. Gijon, M.A., et al., *Role of phosphorylation sites and the C2 domain in regulation of cytosolic phospholipase A2.* J Cell Biol, 1999. **145**(6): p. 1219-32.
222. Perisic, O., et al., *Mapping the phospholipid-binding surface and translocation determinants of the C2 domain from cytosolic phospholipase A2.* J Biol Chem, 1999. **274**(21): p. 14979-87.
223. Johnson, K.J., E.S. Hall, and K. Boekelheide, *Kinesin localizes to the trans-Golgi network regardless of microtubule organization.* Eur J Cell Biol, 1996. **69**(3): p. 276-87.
224. Kreitzer, G., et al., *Kinesin and dynamin are required for post-Golgi transport of a plasma-membrane protein.* Nat Cell Biol, 2000. **2**(2): p. 125-7.
225. Kimura, T., et al., *Tubulin and CRMP-2 complex is transported via Kinesin-1.* J Neurochem, 2005. **93**(6): p. 1371-82.
226. Chen, W., et al., *Rab11 is required for trans-golgi network-to-plasma membrane transport and a preferential target for GDP dissociation inhibitor.* Mol Biol Cell, 1998. **9**(11): p. 3241-57.
227. Deretic, D., *Rab proteins and post-Golgi trafficking of rhodopsin in photoreceptor cells.* Electrophoresis, 1997. **18**(14): p. 2537-41.
228. Ludwig, A., *The Function of Calsyntenins in Intracellular Trafficking.* PhD Thesis (University of Zurich), 2008.
229. Imamura, T., et al., *Insulin-induced GLUT4 translocation involves protein kinase C-lambda-mediated functional coupling between Rab4 and the motor protein kinesin.* Mol Cell Biol, 2003. **23**(14): p. 4892-900.
230. Jordens, I., et al., *Rab proteins, connecting transport and vesicle fusion.* Traffic, 2005. **6**(12): p. 1070-7.
231. Zwilling, D., et al., *Early endosomal SNAREs form a structurally conserved SNARE complex and fuse liposomes with multiple topologies.* Embo J, 2007. **26**(1): p. 9-18.
232. Tani, K., et al., *Mapping of functional domains of gamma-SNAP.* J Biol Chem, 2003. **278**(15): p. 13531-8.
233. Peter, F., et al., *Alpha-SNAP but not gamma-SNAP is required for ER-Golgi transport after vesicle budding and the Rab1-requiring step but before the EGTA-sensitive step.* J Cell Sci, 1998. **111 (Pt 17)**: p. 2625-33.
234. Bethani, I., et al., *The specificity of SNARE pairing in biological membranes is mediated by both proof-reading and spatial segregation.* Embo J, 2007. **26**(17): p. 3981-92.
235. Ikeda, D.D., et al., *CASY-1, an ortholog of calsyntenins/alcadeins, is essential for learning in Caenorhabditis elegans.* Proc Natl Acad Sci U S A, 2008. **105**(13): p. 5260-5.
236. Shirasu, M., et al., *VAMP-2 promotes neurite elongation and SNAP-25A increases neurite sprouting in PC12 cells.* Neurosci Res, 2000. **37**(4): p. 265-75.
237. Huber, L.A., P. Dupree, and C.G. Dotti, *A deficiency of the small GTPase rab8 inhibits membrane traffic in developing neurons.* Mol Cell Biol, 1995. **15**(2): p. 918-24.
238. Vega, I.E. and S.C. Hsu, *The exocyst complex associates with microtubules to mediate vesicle targeting and neurite outgrowth.* J Neurosci, 2001. **21**(11): p. 3839-48.
239. Lin, L., et al., *Induction of filopodia-like protrusions by transmembrane agrin: role of agrin glycosaminoglycan chains and Rho-family GTPases.* Exp Cell Res, 2010. **316**(14): p. 2260-77.
240. Kaibuchi, K., S. Kuroda, and M. Amano, *Regulation of the cytoskeleton and cell adhesion by the Rho family GTPases in mammalian cells.* Annu Rev Biochem, 1999. **68**: p. 459-86.
241. Sebok, A., et al., *Different roles for RhoA during neurite initiation, elongation, and regeneration in PC12 cells.* J Neurochem, 1999. **73**(3): p. 949-60.
242. Hall, A. and G. Lalli, *Rho and Ras GTPases in axon growth, guidance, and branching.* Cold Spring Harb Perspect Biol, 2010. **2**(2): p. a001818.

243. Cullis, D.N., et al., *Rab11-FIP2, an adaptor protein connecting cellular components involved in internalization and recycling of epidermal growth factor receptors.* J Biol Chem, 2002. **277**(51): p. 49158-66.
244. Behrends, C., et al., *Network organization of the human autophagy system.* Nature, 2010. **466**(7302): p. 68-76.
245. Darsow, T., S.E. Rieder, and S.D. Emr, *A multispecificity syntaxin homologue, Vam3p, essential for autophagic and biosynthetic protein transport to the vacuole.* J Cell Biol, 1997. **138**(3): p. 517-29.
246. Ishihara, N., et al., *Autophagosome requires specific early Sec proteins for its formation and NSF/SNARE for vacuolar fusion.* Mol Biol Cell, 2001. **12**(11): p. 3690-702.
247. Klionsky, D.J., et al., *Does bafilomycin A1 block the fusion of autophagosomes with lysosomes?* Autophagy, 2008. **4**(7): p. 849-950.
248. Yamamoto, A., et al., *Bafilomycin A1 prevents maturation of autophagic vacuoles by inhibiting fusion between autophagosomes and lysosomes in rat hepatoma cell line, H-4-II-E cells.* Cell Struct Funct, 1998. **23**(1): p. 33-42.
249. Steuble, M., *Proteomic analysis of calsyntenin-1 organelles and their functional and structural characterization.* PhD Thesis (University of Zurich), 2008.
250. Wilson, G.M., et al., *The FIP3-Rab11 protein complex regulates recycling endosome targeting to the cleavage furrow during late cytokinesis.* Mol Biol Cell, 2005. **16**(2): p. 849-60.
251. Kappler, M., *Molekulare Charakterisierung des IAP Survivin in Weichteilsarkomen - Bedeutung für Prognose und Etablierung neuer Therapiestrategien.* PhD Thesis (Martin-Luther University, Halle-Wittenberg), 2005.
252. Wang, H.H., et al., *Activation of endothelial cells to pathological status by down-regulation of connexin43.* Cardiovasc Res, 2008. **79**(3): p. 509-18.
253. Meister, G. and T. Tuschl, *Mechanisms of gene silencing by double-stranded RNA.* Nature, 2004. **431**(7006): p. 343-9.
254. Birmingham, A., et al., *A protocol for designing siRNAs with high functionality and specificity.* Nat Protoc, 2007. **2**(9): p. 2068-78.
255. Wessel, D. and U.I. Flugge, *A method for the quantitative recovery of protein in dilute solution in the presence of detergents and lipids.* Anal Biochem, 1984. **138**(1): p. 141-3.
256. Banker, G.A., *Trophic interactions between astroglial cells and hippocampal neurons in culture.* Science, 1980. **209**(4458): p. 809-10.
257. Boussif, O., et al., *A versatile vector for gene and oligonucleotide transfer into cells in culture and in vivo: polyethylenimine.* Proc Natl Acad Sci U S A, 1995. **92**(16): p. 7297-301.
258. Zeitelhofer, M., et al., *High-efficiency transfection of short hairpin RNAs-encoding plasmids into primary hippocampal neurons.* J Neurosci Res, 2009. **87**(1): p. 289-300.
259. Yamazaki, T., D.J. Selkoe, and E.H. Koo, *Trafficking of cell surface beta-amyloid precursor protein: retrograde and transcytotic transport in cultured neurons.* J Cell Biol, 1995. **129**(2): p. 431-42.

Curriculum Vitae

TU-MY DIEP, born in Bern, Switzerland on 1st of May, 1982

Education

09/2007 - present	PhD student at the Department of Biochemistry, University of Zurich (ZNZ PhD program (Neuroscience Center Zurich)) Dissertation with the title "The Role of Gaf-1b in Intracellular Trafficking and Autophagy" under the supervision of Prof. Dr. Peter Sonderegger
10/2002 - 06/2007	University of Zurich (major subject: biochemistry, minor subject: chemistry and biology)
10/2001 - 10/2002	ETH Zurich (major subject: biology chemical track)
08/1997 - 08/2001	Gymnasium Kirchenfeld (MNG), Bern

Working experience

06/2006 – 02/2007	Employer:	University of Zurich
	Section:	Department of Biochemistry (Co-assistant)
09/2000 - 03/ 2002	Employer:	Diakonissenhaus Bern
	Section:	Home for the aged (Part-time nurse)

Diploma and Certificates

09/2007	Master of Science UZH in Biochemistry (Chemistry/Biophysics Track)
05/2007	Master thesis at Department of Biochemistry, University of Zurich, with the title "The Rab11-binding Protein Gaf-1b is a Novel Interaction Partner of Calsyntenin-1" under the supervision of Prof. Dr. Peter Sonderegger
06/2006	Bachelor of Science UZH in Biochemistry (Chemistry/Biophysics Track)
08/2001	Maturitätsdiplom Typ MNG

Advanced Training

05/2011	Wirtschafts-Know-how (University of Zurich)
10/2010	Adobe InDesign CS4: Module 2 Creating books (IT of University of Zurich)
10/2010	Adobe InDesign CS4: Module 1 Basics (IT of University of Zurich)
08/2009	Writing Research Papers for Neuroscientists (University of Zurich)
02/2009	Introduction to Adobe Illustrator CS3 (IT of University of Zurich)
05/2008	Labortierkunde Module 1: Introductory Course in Laboratory Animal Science (Institute of animal facility UZH)
01/2008	Practical course in 3D Light & Electron Microscopy (Center for Microscopy and Image Analysis UZH, EMEZ ETH Zurich, Light Microscopy Center ETH Zurich)

Acknowledgment

First of all, I would like to thank **Peter Sonderegger** for offering me the opportunity to perform my PhD thesis in his laboratory and to acquire a broad spectrum of technical knowledge. I thank him for guiding me through my PhD project, his interest, advice and support.

I thank my committee members **Uwe Konietzko** and **Jack Rohrer** who followed this thesis throughout and gave valuable advice for technical knowledge.

Thank to my former master thesis supervisor **Alexander Ludwig** who introduced me into my project and I am grateful for the discussions, his constant support and advice during the whole time of my PhD thesis. I also thank **Martin Steuble** for his collaboration on the calsyntenin-1 project, stimulating discussions, constructive criticism, valuable advice and support. I have benefited a lot from their experience and knowledge on calsyntenin and trafficking.

I would like to thank **Urs Ziegler** and his team in the ZMB for the initial training, help and advice in microscopy.

I am also thankful to **Beat Kunz** for lab management and for his efforts in running of our animal facility over the years.

I acknowledge all past and present members of the group for their contributions and for creating a friendly working atmosphere. I also would like thank the master students **Mauro Serricchio, Patrick Redli** and **Thomas Künzli**, who contributed important data to this PhD thesis. I thank my bench neighbours **Claudio Gisler** and **Philipp Schätzle** for their critical judgments on my work, for creating a great lab atmosphere and for becoming good friends of mine.

I gratefully thank **Emina Besic** for exciting discussions, for her support, for sharing a lot of good and some bad times during my study and PhD thesis inside and outside the lab and especially, for becoming my best friend and family.

Last but not least, I want to express my deep gratitude to my family and especially **Minh**, who accompanied me during the highs and lows of life and during my PhD studies, supported and encouraged me the whole time. I am also gratefully thankful to **Tu-Anh** and **Quoc Thanh**, who supported me all the time and made my education possible.